UNIVERSITÀ DEGLI STUDI DI PARMA

Dottorato di ricerca in Biochimica e Biologia Molecolare

XXVI ciclo: 2011 – 2013

Bioanalytical solutions to characterize human proteome of clinical interest: healthy newborns and their early infections

Coordinatore:
Chiar.mo Prof. Andrea Mozzarelli

Tutor:
Dott.ssa Barbara Pioselli

Dottoranda: Laura Tigli

SUMMARY

Early-onset sepsis (EOS), defined as a septic state manifested in the first three days of life, is one of the major causes of neonatal mortality and surviving infants are at increased risk for developing morbidities. Since the traditional methods for the diagnosis of sepsis (i.e. cultures of blood, urine, cerebrospinal fluid or bronchial fluid specimens) usually take 24 to 48 hours and clinical symptoms frequently manifest themselves in the absence of a positive culture, a faster and more unequivocal test for the differential diagnosis of infection and sepsis is needed. The main aim of the project was the investigation of saliva as a biological fluid reporting on health status of newborns, followed by the development of an innovative and noninvasive diagnostic method to differentiate bacterial from noninfectious causes of inflammation.

2-DE – MALDI-TOF/TOF and 1-DE – LC-(HR)MS/MS untargeted gel-based approaches were exploited for the characterization of the protein composition of whole saliva samples collected from healthy newborns within 48 hours after birth. The two approaches proved to be useful in providing complementary information: 2-DE was focused on the pH range 4 – 7 and most of the identified proteins have MW < 40 kDa, whereas 1-DE – LC-(HR)MS/MS analyses allowed to identify a number of proteins featuring basic pI and/or high molecular weight. As a whole, the gel-based analyses led so far, not surprisingly, to the identification of a number of proteins linked to epidermal tissue functions and, more interestingly, of a number of proteins usually highly expressed and involved in inflammatory processes, including annexin A1, glutathione S-transferase P, heat shock proteins, protein S100-A8 and -A9, probable evidence of a stressed condition especially in the early 24 hours after birth. As soon as enough samples collected from newborns affected by bacterial infection will be available, a comparison will be performed to highlight the overall alteration of physiological protein pattern as well as over- or under-expressed proteins. This will give new inputs to the development of innovative and noninvasive diagnostic methods for the early detection of EOS.

In parallel with the identification of a specific target protein (or a pattern of target proteins) through the gel-based discovery approach, targeted analyses were carried out with the aim of developing an analytical method based on liquid chromatography coupled to mass spectrometry to qualitatively and quantitatively assay C-reactive protein, calcitonin and its precursor procalcitonin, acute-phase proteins widely considered plasmatic markers of sepsis, within salivary samples. Different sample preparation conditions were tested for each of the above-mentioned proteins and MALDI-TOF-based peptide mapping was exploited to compare a classical workflow of digestion in aqueous solution with the more recently described digestion in mixed organic-aqueous solution. In both cases, proteotypic peptides were identified and an optimization of the chromatographic and mass spectrometric conditions for their quantification on a Q TRAP instrument operated in MRM mode was performed. The developed methods allowed to detect the proteins of interest in the low µg/ml range. However, preliminary experiments on salivary samples showed the presence of matrix effects that need to be further investigated. Whenever possible, MS^E experiments on Synapt G2-S were carried out to evaluate the applicability of a similar platform to high-throughput screening of the proteins of interest and their post-translational modifications within biological samples.

1. INTRODUCTION

1.1. SALIVA

WHOLE SALIVA

Whole saliva is a complex mixture found in the oral cavity mainly constituted by:

- the exocrine secretions of the three pairs of major salivary glands (parotid, submandibular and sublingual) (Figure 1-1) and the minor salivary glands (located throughout the oral cavity);
- the gingival crevice fluid (mixture of substances derived from blood);
- the transudate of the oral mucosa;
- mucous of the nasal cavity and the pharynx;
- desquamated epithelial and blood cells;
- non-adherent oral bacteria;
- as well as potential food residues and traces of other exogenous compounds (drugs, smoke residues and tooth paste) [1-3].

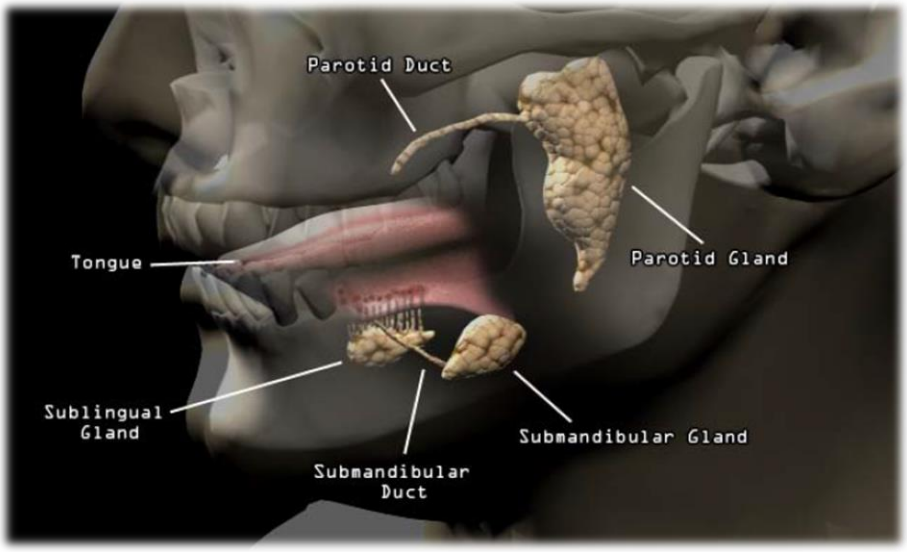

Figure 1-1. Location of the major salivary glands (parotid, submandibular and sublingual). From http://www.salimetrics.com

PRODUCTION OF SALIVA

Saliva produced by the salivary glands (Figure 1-2) consists approximately of 99% water and might also contain:

- a variety of electrolytes: sodium, potassium, calcium, chloride, magnesium, bicarbonate, phosphate;

- proteins and oligopeptides: enzymes, immunoglobulins and other antimicrobial factors, mucosal glycoproteins, albumin;
- nucleic acids;
- hormones: estradiol, progesterone, testosterone, DHEA, cortisol;
- glucose;
- nitrogenous products, such as urea and ammonia [1, 3].

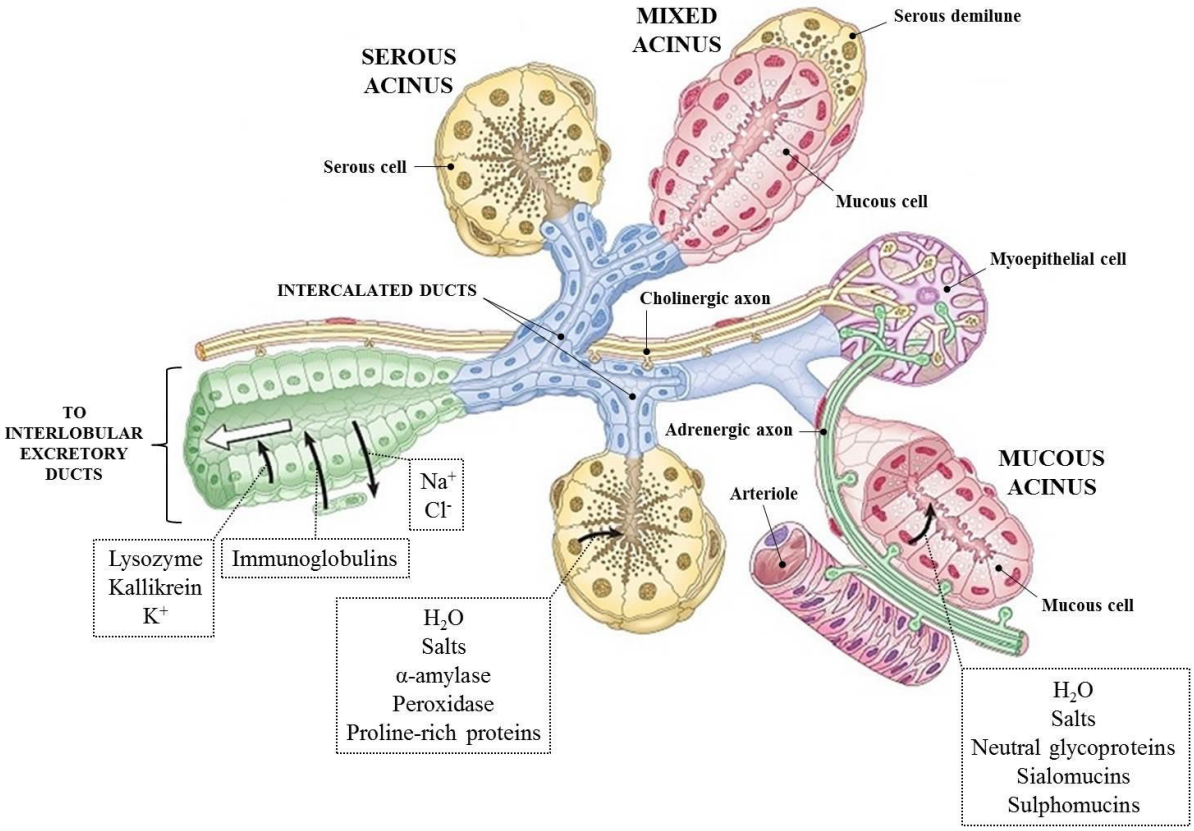

Figure 1-2. Scheme of a salivary gland. The primary secretion produced by the serous, mucous or mixed seromucous acini is further modified in the excretory ducts to produce saliva. Solid black arrows indicate the direction of transport of salivary components and the white arrow indicates the direction of salivary flow. Modified from Standring [4].

SALIVA AS A DIAGNOSTIC FLUID

Most of the organic compounds in whole saliva are hence produced locally by the salivary glands, but some molecules pass into saliva from blood. The transfer of biomolecules from blood into saliva can follow different pathways: diffusion, active transport, ultrafiltration, transudation from either the gingival crevicular fluid or the oral mucosa. This connection between saliva and blood makes saliva a potential diagnostic fluid that presents significant advantages over serum:

- ✓ easiness of sample collection;
- ✓ non-invasive collection procedure, well tolerated by patients;
- ✓ minimal risk of transmission of infections [1, 5-7].

Potential clinical applications are represented by:

- screening for oral and systemic diseases;
- treatment/outcome monitoring;
- environmental exposure monitoring.

Interest in saliva has increased over the past decade since it is widely accepted that it reflects oral and body's health status in a number of pathological conditions (HIV, cardiovascular disease, Sjögren's syndrome, cystic fibrosis, periodontitis, oral squamous cell carcinoma and others) [5, 8-11]. Nevertheless the lack of a deep knowledge of the biomolecules present in this complex fluid and the lack of understanding of their relevance in relationship to specific diseases, combined with the lack of high-sensitivity detection methods, are the major obstacles that frequently hinder its use as a diagnostic medium.

1.2. ACUTE INFLAMMATION

THE ACUTE-PHASE RESPONSE

The acute-phase response (APR) is the complex series of events, initiated in response to inflammatory stimuli (infection, injury or physical trauma), which aim to prevent tissue damage and restore the homeostasis of the organism (Figure 1-3) [12].

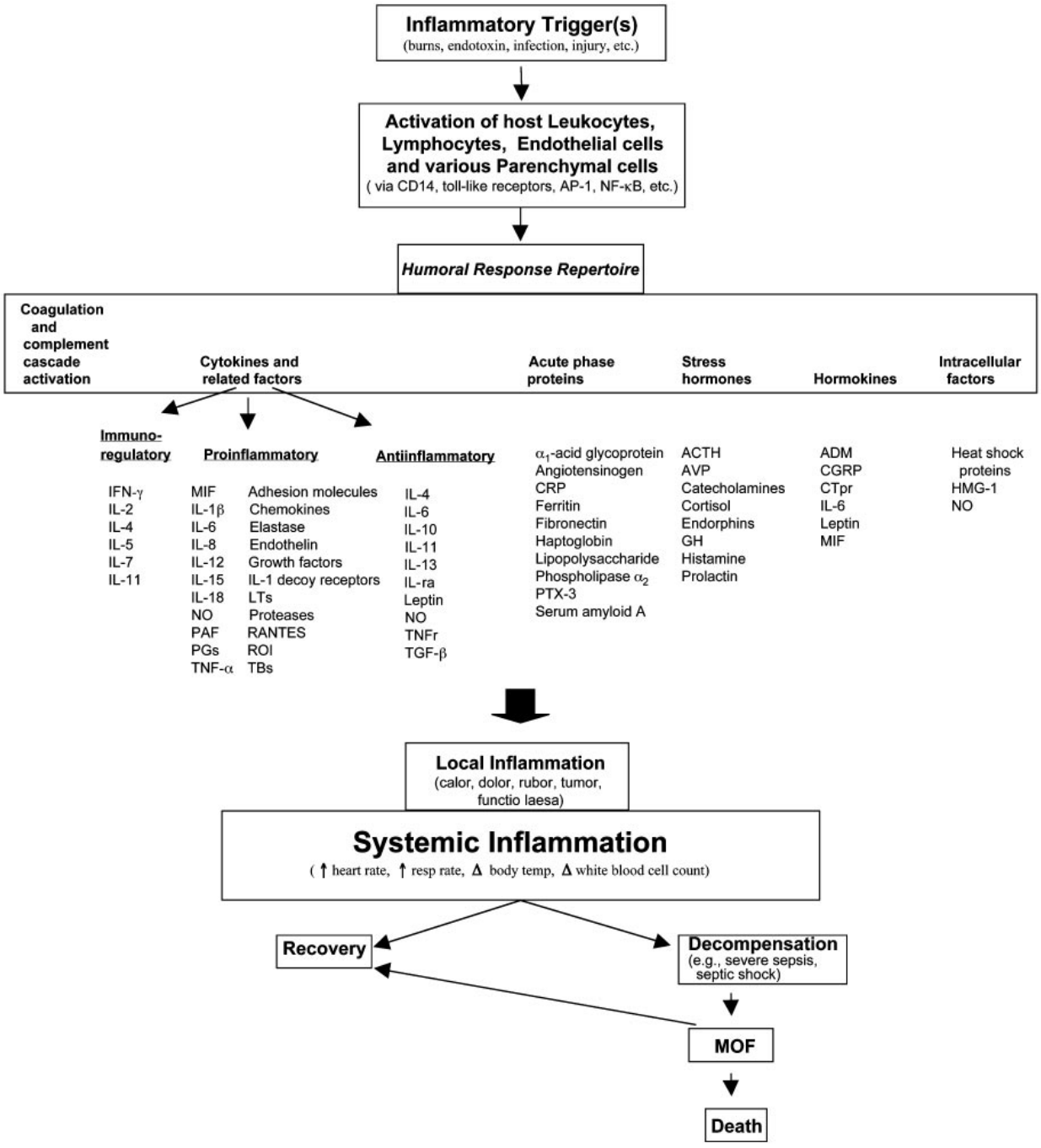

Figure 1-3. Scheme of the series of events triggered by an inflammatory stimulus. From Becker *et al.* [12].

The clinical signs of an ongoing acute-phase response are fever, alterations in the metabolism of many organs, leukocytosis and changes in the plasmatic concentrations of various proteins, known as the acute-phase proteins.

ACUTE-PHASE PROTEINS

Acute-phase proteins (APP) are those proteins whose plasmatic concentration varies by at least 25% during an acute-phase response in respect to the physiological values. Generally their concentration increases and therefore they are termed "positive" (e.g.: C-reactive protein, serum amyloid A, fibrinogen, complement factors, α-1-antitrypsin and many others), but there are also "negative" acute-phase proteins whose concentration decreases (e.g.: albumin, transferrin, transtyretin, antithrombin). The expression of the positive APPs is stimulated by cytokines, such as interleukins 1β, 6 and 8 (IL-1β, IL-6, IL-8), tumor necrosis factor α (TNF-α) and transforming growth factor β (TGF-β), which are released into the bloodstream by inflammatory cells. Positive acute-phase proteins are involved in different functions of the innate immunity [13, 14].
Upon infections of bacterial origin, circulating levels of C-reactive protein (CRP) and calcitonin precursors (CTpr), including procalcitonin (PCT), increase several thousand-fold (Figure 1-4). Moreover, this increase often correlates with the severity of the clinical condition and patient prognosis [15]. Therefore, measurement of acute-phase proteins in biological fluids is useful for the early diagnosis of infection and therapy monitoring [12, 16-19].

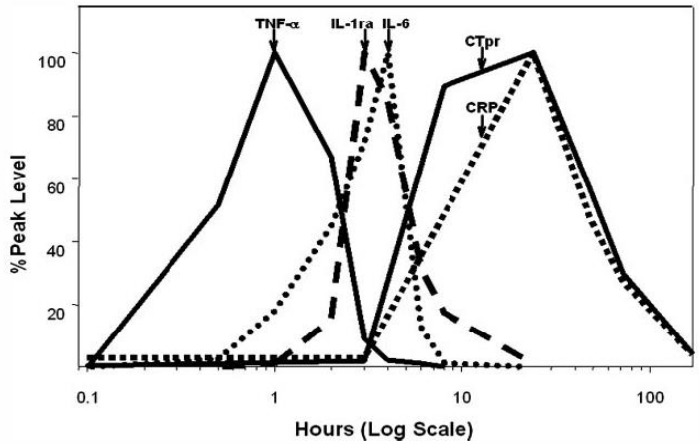

Figure 1-4. Diagram illustrating the response to one injection of endotoxin in human volunteers. Kinetics of some humoral markers of illness: tumor necrosis factor (TNF-α), interleukin-1 receptor antagonist (IL-1ra), interleukin-6 (IL-6), calcitonin precursors (CTpr) and C-reactive protein (CRP). From Becker *et al.* [12].

Calcitonin (CT)

Calcitonin is a peptide hormone constituted by 32 amino acids organized to form a single α-helix (Figure 1-5).

Figure 1-5. Cartoon of calcitonin structure. PDB code 2jxz.

CT is synthesized in thyroidal C-cells from pre-procalcitonin, a product of the expression of the CALC-1 gene, via a series of proteolytic cleavages. The immature form consists of 33 amino acids, ending with a glycine, which is finally cut by a protease to produce the mature form of the calcitonin peptide (Figure 1-6) [20].

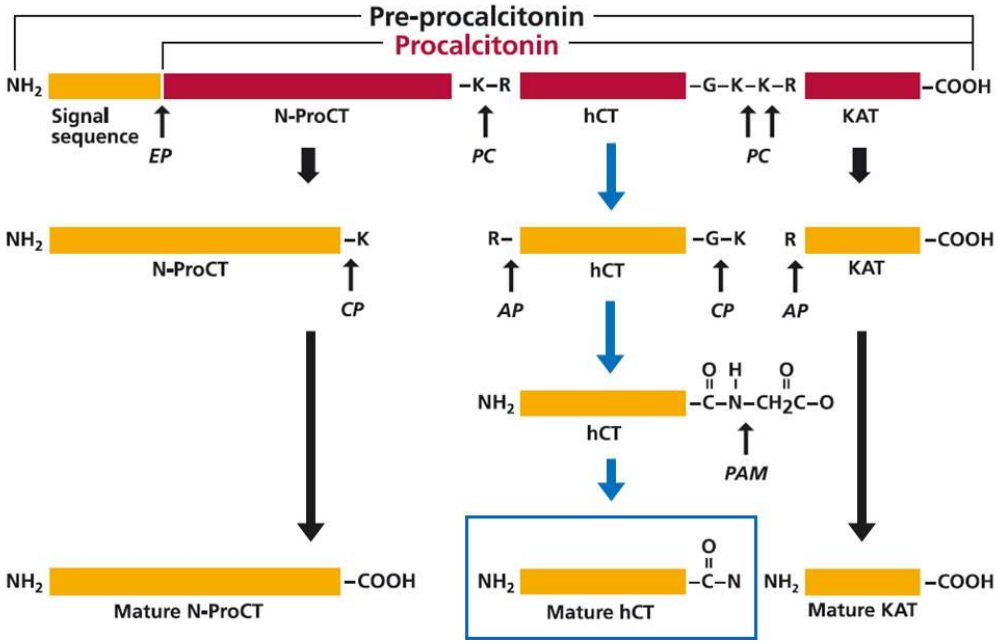

Figure 1-6. Synthesis of calcitonin in thyroidal C-cells. The synthetic pathway of human calcitonin is shown in blue. Pre-procalcitonin is a product of the expression of the CALC-1 gene. The N-terminal signalling sequence of pre-procalcitonin allows binding to the endoplasmic reticulum and cleavage by an endopeptidase to produce procalcitonin. Inside the C-cell, procalcitonin is cleaved into the three immature forms of N-ProCT, calcitonin and katacalcin. The immature calcitonin is further processed by an amino- and a carboxy- peptidase to produce the 32 amino acid peptide, which is amidated at the Pro32 by a peptidyl glycine amidating mono-oxygenase. N-ProCT = N-Procalcitonin, hCT = human Calcitonin, KAT = Katacalcin, EP = Endopeptidase, PC = Prohormone Convertase, CP = Carboxypeptidase, AP = Aminopeptidase, PAM = Peptidyl Glycine Amidating Mono-oxygenase. Modified from Maruna *et al.* [20].

Human CT presents two post-translational modifications: a disulfide bond between Cys residues 1 and 7 and an amidated proline at the C-terminus (residue 32). Both the N-terminal ring structure created by the disulfide bond and the post-translational amidation of Pro32 are essential for the full expression of the known functions of calcitonin. Calcitonin is a peptide hormone physiologically involved in the metabolism of calcium ions. It causes a rapid but short-lived drop in the levels of calcium and phosphate in blood by promoting their incorporation in the bones [12].

Procalcitonin (PCT)

Procalcitonin (PCT) is a protein composed by 116 amino acids (13 kDa), encoded by the CALC-1 gene. Cleavage of the primary transcript of the CALC-1 gene produces pre-PCT, which in turn undergoes further cleavage of an N-terminal signal sequence to produce PCT [21].
Procalcitonin is composed of three portions: the N-terminus (N-proPCT), the immature calcitonin (CT) and calcitonin carboxypeptide-1 (CCP-1, also known as katacalcin) (Figure 1-7). Known post translational modifications include a disulfide bond between Cys residues 60 and 66, glycosylation at a site located between the Cys residues, deamidation and enzymatic cleavage into the 3 – 116 amino acid protein [21].

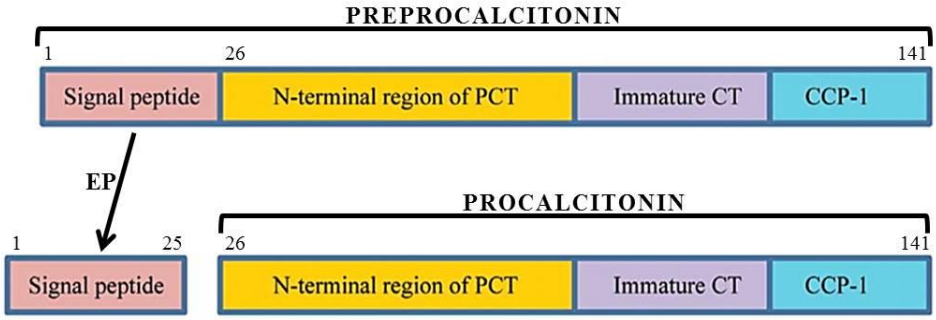

Figure 1-7. Scheme of procalcitonin synthesis from preprocalcitonin. EP = endopeptidase, PCT = procalcitonin, CT = calcitonin, CCP-1 = calcitonin carboxypeptide-1 (katacalcin). Modified from Jin *et al.* [16].

In healthy individuals PCT is physiologically expressed in thyroidal C-cells and post-translationally modified to produce calcitonin. In the presence of bacterial infection, PCT is expressed also in extra-thyroidal tissues (lung, liver, kidney, pancreas, adipose tissue, white blood cells), which lack the enzymes responsible for the post-translational modifications. Thus, high plasmatic levels of PCT and not CT are found in infected patients [15].
PCT expression appears to be stimulated both directly, via bacterial toxins, and indirectly, via inflammatory mediators such as IL-1, IL-6 and TNF-α. However, the functions of PCT synthetized in non-neuroendocrine tissues are still unclear. Current hypotheses point to a role of PCT in the neutralization of lipopolysaccharide molecules, in the modulation of NO synthesis and in pain-relieving mechanisms [12, 20-22].

C-reactive protein (CRP)

The product of the *CRP* gene is a protein of 224 amino acids (Figure 1-8), further processed into the mature form by cleavage of the signal peptide 1-18 [23].
CRP is a pentaxin, that is a protein composed of five identical protomers non-covalently associated and arranged symmetrically around a central pore (Figure 1-9). Each protomer consists of 206 amino acids (23 kDa) and is folded into two antiparallel β sheets with a flattened jellyroll shape. Since all the five protomers have the same orientation, the CRP pentamer has essentially two faces. On one side there are the recognition sites for phosphocholine (PCh), with a binding site on each protomer consisting of two

coordinated calcium ions adjacent to a hydrophobic pocket. On the opposite side of the CRP pentamer there is the effector site, involved in the binding of complement C1q and Fcγ receptors [14, 23-25].
Known post translational modifications include a disulfide bond between the two Cys residues 54 and 115 and the cyclization of the N-terminal glutamine forming the pyrrolidone carboxylic acid.

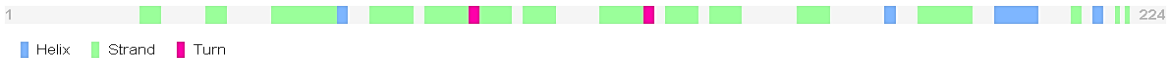

Figure 1-8. Secondary structure of CRP. From http://www.uniprot.org/uniprot/P02741

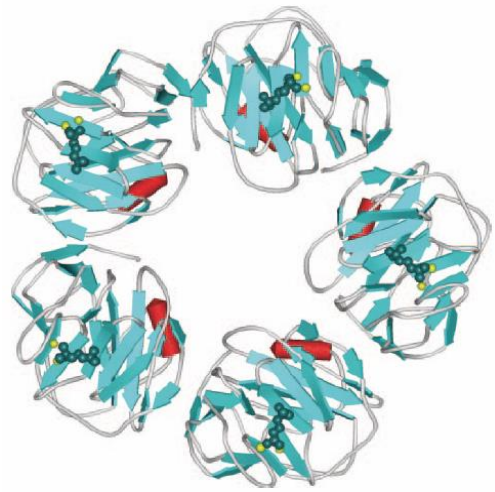

Figure 1-9. Cartoon of CRP structure. From Black *et al.* [23].

CRP owes its name to its ability to precipitate pneumococcal C-polysaccharide in the presence of calcium ions. CRP binds to phosphocholine and to a variety of other ligands, including phosphoethanolamine, chromatin, histones, fibronecting, small nuclear ribonucleoproteins, laminin and polycations. The main physiologic function of CRP is to recognize bacteria and damaged or apoptotic cells of the host and to mediate their elimination by recruiting the complement system and phagocytic cells. Ligand-bound CRP activates the classical complement pathway through direct interaction with C1q [23-25].
CRP is mainly synthetized by the liver during the acute phase response. IL-6 is the principal inducer of the CRP gene while IL-1, glucocorticoids and some other factors including complement activation products, act synergistically with IL-6 to enhance its effect. CRP concentrations rise within 12 hours and reach peak levels between 24 and 48 hours with a 1000-fold increase. CRP levels decline quite rapidly because its relatively short half-life of 18 hours [25]. Since rapid and marked increases in CRP concentrations occur in a variety of conditions (inflammation, infection, trauma, malignancies, and autoimmune disorders) CRP doesn't diagnose any specific disease.

1.3. BOTTOM-UP PROTEOMICS

Bottom-up proteomics is a well-known and widely used approach for protein identification and characterization. The two main bottom-up strategies, peptide mass fingerprinting (PMF) and peptide fragment fingerprinting (PFF), consist respectively on the acquisition of MS and MS/MS data of peptides originated by proteolytic cleavage with a specific enzyme. Peptides may be originated by digestion of single proteins (isolated by 2-DE approach or liquid chromatography) or by digestion of a complex mixture ("shotgun proteomics") (Figure 1-10).

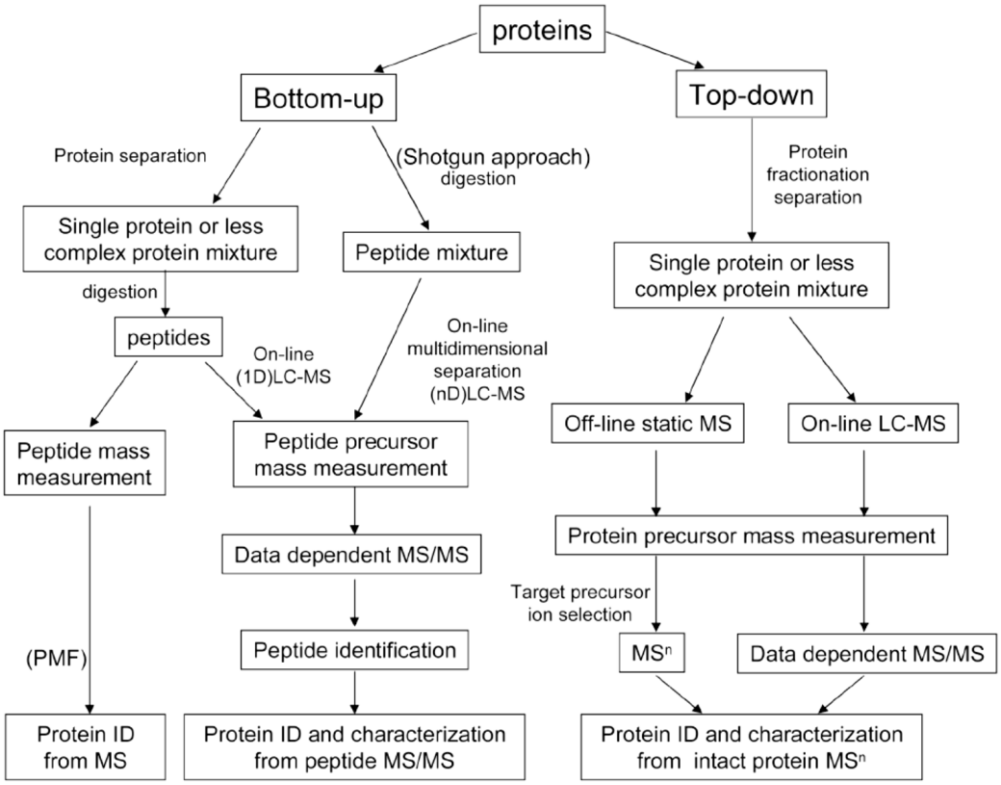

Figure 1-10. Scheme of the bottom-up and top-down strategies for protein identification and characterization. From Han *et al.* [26]**.**

Protein digestion

As previously mentioned, the key steps in bottom-up proteomics are protein digestion with proteases followed by mass spectrometric analysis. Trypsin is the most commonly used protease since it has a well-defined specificity: the peptide bonds are cleaved at the carboxyl side of lysine (Lys) and arginine (Arg) residues. The hydrolytic reaction is less likely to occur when Lys and Arg are followed by a proline and when an acidic residue is on either side of the cleavage site [27].

Trypsin shares the same mechanism of serine proteases (Figure 1-11 and Figure 1-12) [28].

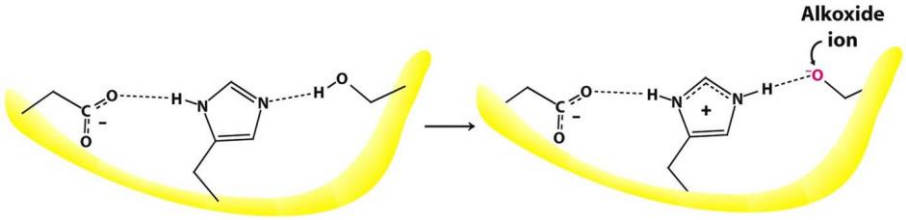

Figure 1-11. Scheme of trypsin active site. The catalytic triad is constituted by a serine (Ser), a histidine (His) and an aspartate (Asp). From Berg *et al.* [28].

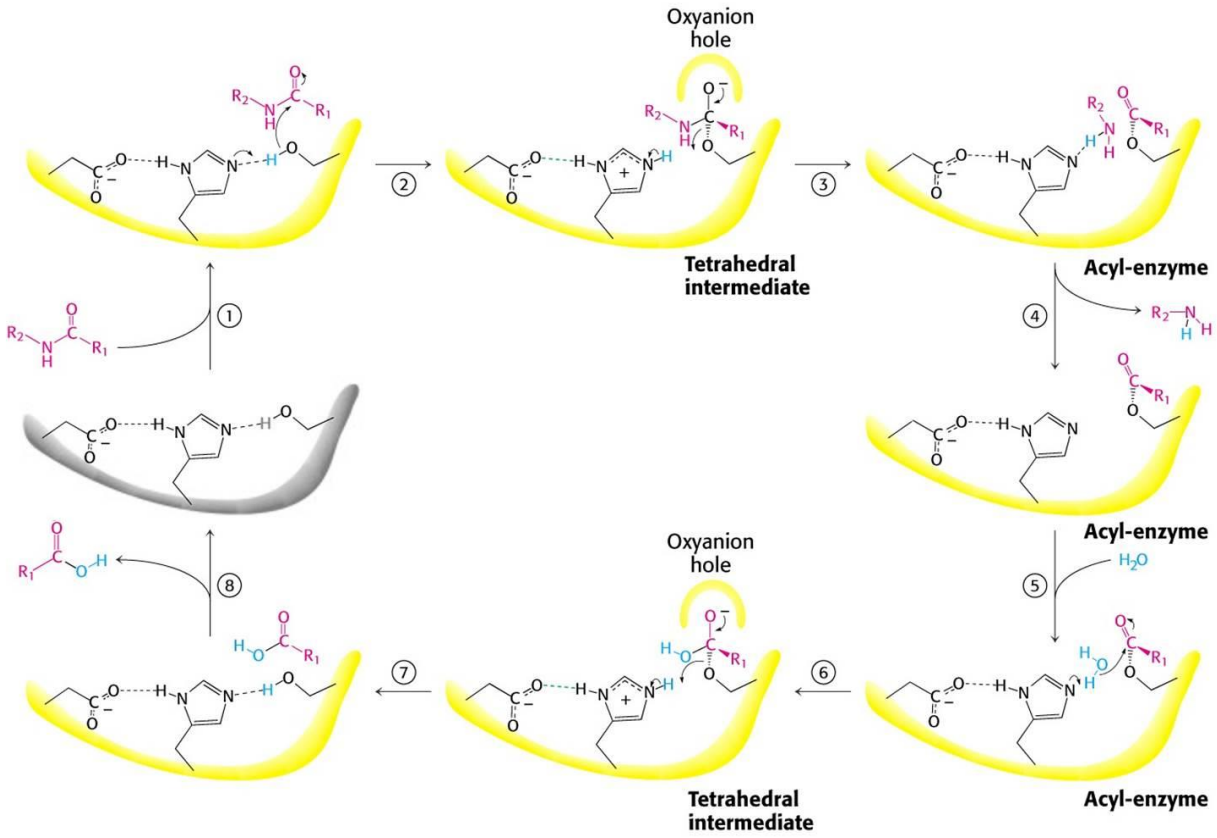

Figure 1-12. Scheme of the catalytic mechanism of serine proteases. The reaction proceeds through eight steps: (1) substrate binding, (2) nucleophilic attack of serine alkoxyde ion on the peptide carbonyl group, (3) collapse of the tetrahedral intermediate, (4) release of the amine component, (5) water binding, (6) nucleophilic attack of water on the acyl-enzyme intermediate, (7) collapse of the tetrahedral intermediate, (8) release of the carboxylic acid component. Modified from Berg *et al.* [28].

The main variables to be considered when performing a tryptic digestion experiment are:

- pH: the optimal range is 7.5 – 8.5;
- temperature: trypsin has a maximum activity at 37 °C;
- enzyme to protein ratio: it is usually recommended between 1:20 and 1:100;
- time: the optimal duration of the reaction has to be evaluated as it depends on the enzyme to substrate ratio and on the type of reaction buffer.

It has been shown that trypsin maintains its proteolytic activity and specificity in a variety of mixed organic-aqueous solvent systems, such as methanol–water, acetonitrile–water, 2-propanol–water, or acetone–water, even at high concentrations of organic solvent (60 – 80%) [29-31]. The main features of proteolysis in mixed organic-aqueous solution, compared to proteolysis in aqueous solution, are:

- high efficiency in terms of both rate of digestion and amino acid sequence coverage, probably due to the retention of activity of trypsin combined to the increased solvation and conformational changes of substrate proteins;
- tendency to produce a high number of peptides containing missed cleavages.

GEL-BASED APPROACHES

Mono-dimensional (1D-PAGE) and two-dimensional (2-DE) gel electrophoresis are gel-based separation techniques in bottom-up proteomics. Gel-based approaches feature some advantages and some drawbacks. Added information is available regarding the molecular weight (1D-PAGE) or both molecular weight and isoelectric point (2-DE) of the protein(s) prior to proteolysis. Furthermore, some post-translational modifications can be easily visualized on 2-DE gels. For example multiple phosphorylation states of a single protein appear as multiple spots on the same horizontal row since those molecules share nearly the same molecular weight but their isoelectric points differ. However gel-based approaches are time-consuming and labor-intensive, although a certain degree of automation is possible.

Two-Dimensional Electrophoresis analysis (2-DE)

Two-dimensional electrophoresis (2-DE) is a method for the analysis of complex protein mixtures which sorts proteins through two orthogonal separative dimensions: in the first dimension, isoelectric focusing (IEF), proteins are separated according to their isoelectric point (pI), and then in the second dimension, sodium dodecyl sulfate polyacrylamide gel electrophoresis (SDS-PAGE), proteins having the same pI are separated according to their molecular weight (Figure 1-13).

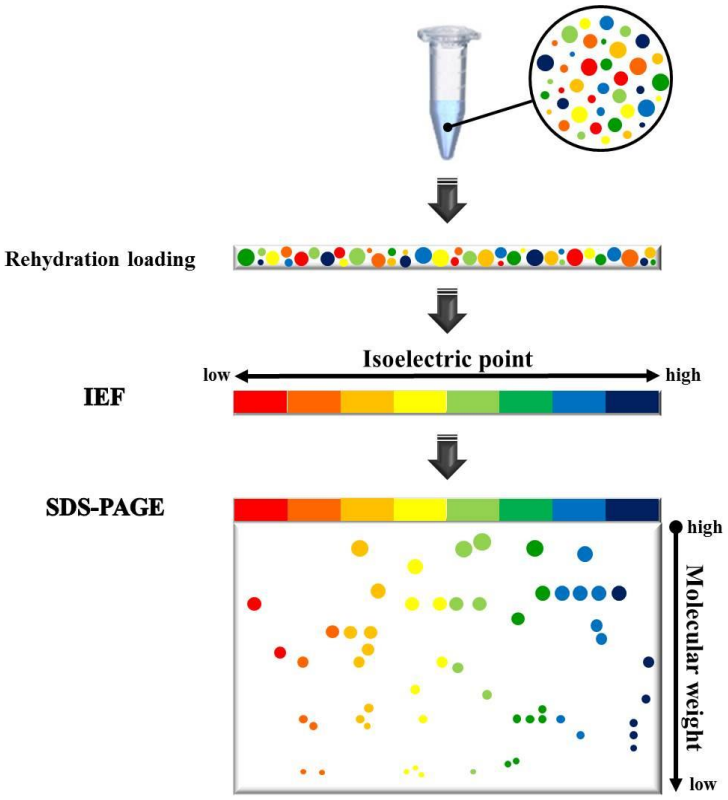

Figure 1-13. Scheme of the two orthogonal dimensions in 2-DE. After sample preparation proteins are loaded onto the IPG strip (rehydration loading in the picture) and separated according to their pI in the first dimension (IEF). The co-focalized proteins are then separated in the second dimension (SDS-PAGE) according to their molecular weight.

A 2-DE analysis goes through a number of steps that will be briefly discussed hereinafter [1, 10].

1. **Protein sample preparation**

   The sample preparation step is a key to the success of the whole 2-DE experiment and strongly depends on the aim of the research. The optimal preparation is to be determined empirically. Features of the proteins of interest, such as the solubility, size, charge, and isoelectric point, have an impact on sample preparation. Sample preparation can also help to reduce the complexity of a protein mixture when the interest is focused only on a subset of the proteins in the sample.

2. **IPG strip rehydration**

   Rehydration solutions generally contain:

   - ✓ a denaturant agent (urea and thiourea) that solubilizes and denatures proteins;
   - ✓ a non-ionic or zwitterionic detergent (CHAPS, Triton X-100, octyl-glucoside) that helps to solubilize hydrophobic proteins and minimizes protein aggregation;
   - ✓ a reducing agent (dithiothreitol, dithioerythritol, trybutylphosphine) to cleave disulphide bonds and maintain all proteins in their fully reduced state;
   - ✓ an ampholyte mixture, appropriate to the pH range of the IPG strip, to enhance sample solubility by minimizing protein aggregation due to charge-charge interactions and to improve conductivity across the immobilized pH gradient;
   - ✓ a tracking dye (bromophenol blue) to monitor the beginning of the IEF protocol.

   Rehydration solution may or may not include the sample.

3. **Sample loading**

   Basically there are two methods to load a sample onto an IPG strip for analytical analyses:

   - Rehydration loading.

     Sample is included in the rehydration solution. As the strip rehydrates, proteins in the sample are absorbed and distributed over the entire length of the strip. This method is the most commonly exploited since it carries some advantages: the general procedure is easy and it is suitable for loading not only large quantities of proteins but also diluted samples. There are two rehydration methods:

     - Passive rehydration.

       No electric field is applied during the rehydration step.
     - Active rehydration.

       A low voltage is applied (usually 20 – 120 V) to facilitate the entry into the strip of proteins featuring high molecular weights.
   - Cup loading.

     This method usually gives better results in analyses at basic pH ranges. Sample is applied via a sample cup at the anodic side of a previously rehydrated IPG strip. The limits of this procedure include the risk of formation of precipitates at the application point and problems of leakage.

4. IEF (first dimension)

The net charge of a protein is the sum of all the negative and positive charges of the side chains of its residues and the amino- and carboxyl- termini. The net charge can be positive, negative or equal to zero depending on the pH of the environment. The isoelectric point (pI) of a protein is the specific pH at which the net charge of the protein is zero. At pH values below its pI the protein carries a positive net charge, while at pH values above its pI the protein carries a negative net charge (Figure 1-14).

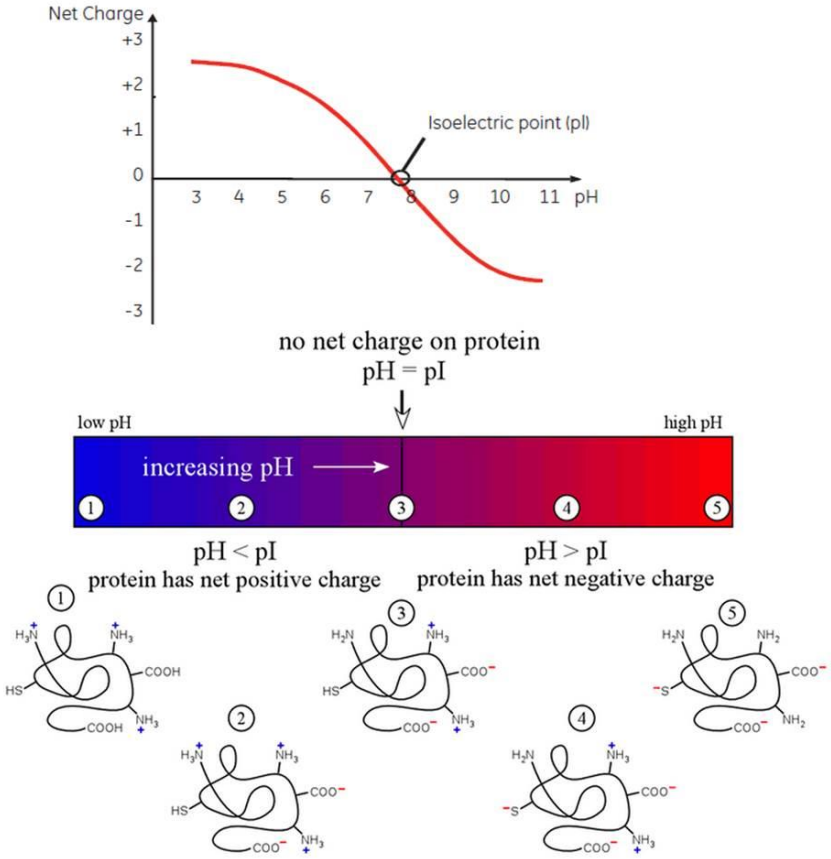

Figure 1-14. Plot of the net charge of an hypothetical protein versus the pH of the environment. The intercept with the x-axis, that is the pH at which the net charge is zero, represents the pI of the protein.

The first dimension in 2-DE is represented by isoelectric focusing (IEF) which is an electrophoretic method to separate proteins according to their isoelectric point (pI): each protein migrates through an immobilized pH gradient (IPG) under the influence of an electric field until its net charge becomes zero.

IPG strips are commercially available in a variety of pH ranges and lengths (

Figure 1-15.). The degree of resolution of the IEF separation is determined by a series of factors, including the slope of the pH gradient, the electric field strength applied and the length of the IPG strip.

	Strip Length				
	7 cm	11 cm	17 cm	18 cm	24 cm
IPG Strip Dimensions					
IPG strip length, cm	7.9	11.8	17.8	19.0	24.7
Gel length, cm	7.3	11.0	17.1	18.0	23.4
Strip width, mm	3.3	3.3	3.3	3.3	3.3
Linear pH Gradient Range					
Broad range	3–10 3–10 NL*	3–10 3–10 NL*	3–10 3–10 NL*	3–10 3–10 NL*	3–10 3–10 NL*
Narrow range	3–6, 4–7, 5–8, 7–10	3–6, 4–7, 5–8, 7–10	3–6, 4–7, 5–8, 7–10	3–6, 4–7, 5–8, 7–10	3–6, 4–7, 5–8, 7–10
Micro range	3.9–5.1, 4.7–5.9, 5.5–6.7, 6.3–8.3	3.9–5.1, 4.7–5.9, 5.5–6.7, 6.3–8.3	3.9–5.1, 4.7–5.9, 5.5–6.7, 6.3–8.3	3.9–5.1, 4.7–5.9, 5.5–6.7, 6.3–8.3	3.9–5.1, 4.7–5.9, 5.5–6.7, 6.3–8.3

When rehydrated, IPG strips will be approximately 0.5 mm thick. The gel composition for each IPG strip is 4%T/3%C. The anode (acidic) end of each IPG strip is indicated with a "+" symbol. Storage temperature is –20°C. Each package contains 12 IPG strips.

* NL, Nonlinear gradient.

Figure 1-15. Example of IPG strips commercially available. From BIO-RAD catalogue.

A typical IEF protocol generally proceeds through a series of steps. The main steps can be summarized as follows:

I. a low-voltage step to initiate desalting of the sample;
II. a progressive gradient to high voltage to mobilize the ions;
III. a high-voltage step to complete the isoelectric focusing: this step is generally performed through the application of a constant number of Volt-hours (Vh), with Vh being the integral of the Volts applied over the separation time;
IV. a low-voltage step to keep the proteins focalized.

Three processes mainly contribute to mass transfer in isoelectric focusing:

a) electrical migration of charged species: the establishment of a voltage gradient between two electrodes causes mass transfer between them;
b) diffusion: species move under a chemical potential gradient (e. g.: concentration gradient);
c) convection, which occurs as a result of diffusion or hydrodynamic transport (e. g.: electroendosmotic movement).

Those three mass transfer processes contribute to the net observable electrical current (I), which follows Ohm's law $V = I \bullet R$, where V is the voltage and R the resistance. The moving current is due to both ionic species, which move towards the oppositely charged electrode, and amphoteric molecules, that move under the influence of the electric field until they reach their steady state position in the IPG. The equilibrium current is the current generated by all the species as they diffuse around their equilibrium position. Therefore at constant voltage, the contribution of the moving current to the net current progressively decreases with time, whereas the equilibrium current is linearly proportional to the voltage.

5. Equilibration step

Proteins co-focalized at a given pI in the first dimension are prepared to be separated in the second dimension according to their molecular weight. The equilibration step usually consists of two phases:

- at first the IPG strip is incubated in SDS-PAGE running buffer (50 mM Tris-HCl, pH 8.8) containing urea, SDS, glycerol, DTT, tracking dye (bromophenol blue):
  - urea reduces electroendosmosis effects;
  - SDS denatures proteins;
  - glycerol both helps reducing electroendosmosis effects and improves transfer of proteins from the IPG strip to the SDS-PAGE gel;
  - DTT keeps the Cys residues in their reduced state;
  - bromophenol blue allows the monitoring of the electrophoresis;
- then iodoacetamide is added to alkylate sulfhydryl groups and thus prevent their oxidation during electrophoresis.

6. SDS-PAGE

In the second dimension (SDS-PAGE), proteins are separated according to their molecular weight (MW) in a polyacrylamide gel containing SDS. SDS is an anionic detergent that denatures proteins and wraps around their backbone at a constant ratio (1.4 g of SDS per 1 g of protein). Therefore the intrinsic electrical charge of the proteins in the sample does not influence their mobility in the gel since the anionic complexes formed carry a constant net negative charge per unit of mass.

Various types of polyacrylamide gel can be produced (Table 1-1):

- single percentage gels, which offer better resolution in a particular range of molecular weights. The most common is the 12%.
- gradient gels, which generally offer wider separation windows.

Table 1-1. Relationship between acrylamide concentrations and allowed separation ranges. From Berkelman *et al.* [32].

% Acrylamide in resolving gel	Separation Size Range (MW × 10^{-3})
Single percentage:	
5%	36–200
7.5%	24–200
10%	14–200
12.5%	14–100[1]
15%	14–60[1]
Gradient:	
5–15%	14–200
5–20%	10–200
10–20%	10–150

[1] The larger proteins fail to move significantly into the gel.

The most commonly used running buffers for SDS-PAGE are the Tris-Glycine Laemmli buffer and the Tris-Tricine buffer, with the latter being preferred when better resolution at low molecular weights (below 10 kDa) is required.

7. Visualization of proteins: staining methods

- Coomassie staining.

  The colloidal form of Coomassie dye (Figure 1-16), formulated in acidic buffer, binds to proteins through ionic interactions between the sulfonic acid groups and basic residues (arginine, lysine and histidine), but also Van der Waals forces and hydrophobic interactions are involved. The binding causes a spectral shift from the reddish-brown to the blue form of the dye. The difference between the two forms of the dye has its maximum at $\lambda = 595$ nm, which is therefore the optimal wavelength to measure the absorbance of the protein-dye complex.

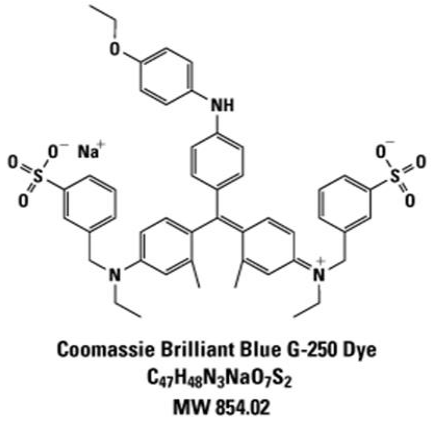

Figure 1-16. Chemical structure of Coomassie Brilliant Blue G-250 dye.

  Advantages: simpler and more quantitative than silver staining. Limits: about 50-fold less sensitive than silver staining, incompatible with surfactants.

- Silver staining.

  This is the most sensitive staining technique (sub ng). Basically the procedure consists in the deposition of metallic silver in correspondence of protein bands or spots in the gel. Silver ions of a silver nitrate solution interact and bind to certain protein functional groups. The strongest interactions occur with carboxylic acid groups (aspartate and glutamate), imidazoles (histidine), sulfhydryls (cysteine) and amines (lysine). Sensitizers and enhancers are used in the procedure to control the specificity and efficiency of the binding and the following reduction to metallic silver (staining development). Limits: complex and multistep process, high-purity reagents and precise timing are required for high-quality and reproducible results.

1.4. MASS SPECTROMETRY

Mass spectrometry is basically a two-step technique: it requires at first the ionization of the analyte and then the determination of its mass-to-charge ratio (m/z). Therefore, a mass spectrometer is essentially composed of two distinct parts: the ion source, the place where ionization and desolvation of the analytes actually take place, and the analyzer, where the ions are separated and their m/z ratio is measured (Figure 1-17).

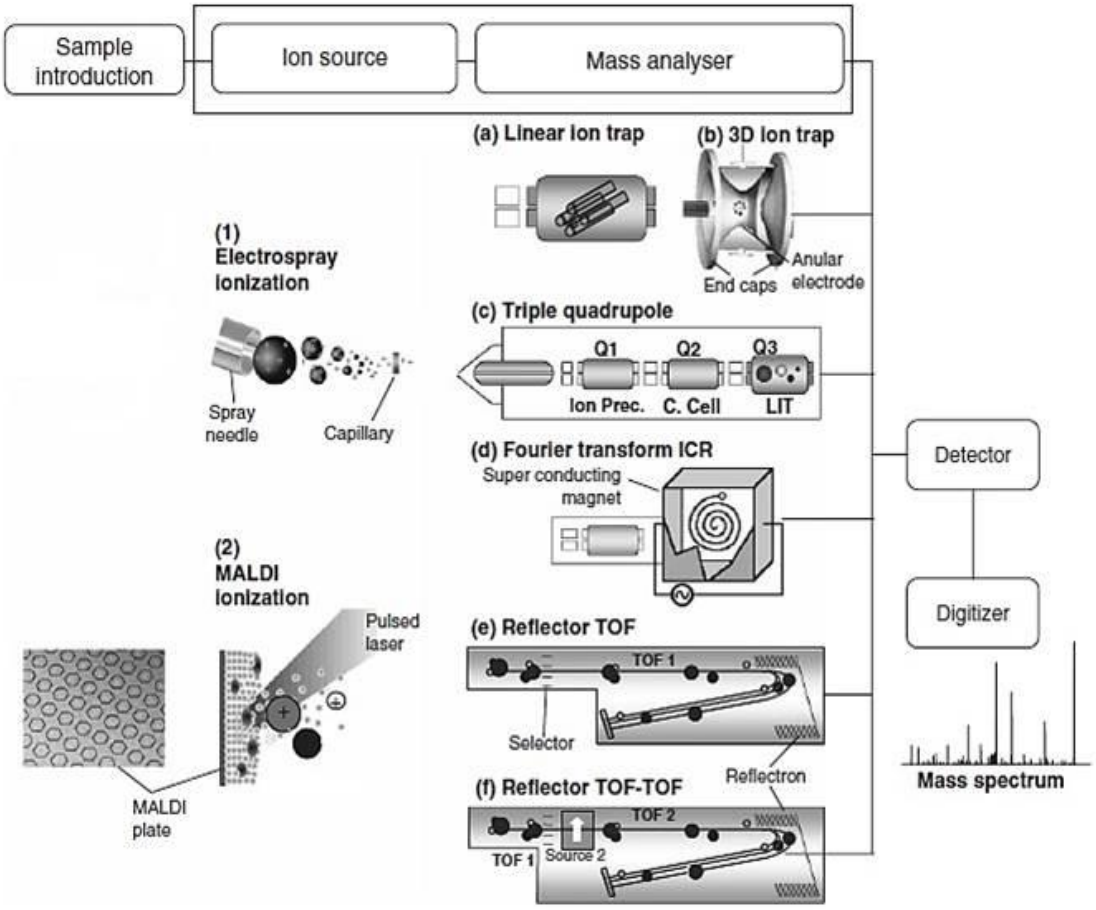

Figure 1-17. Scheme of the main components of a mass spectrometer: a sample introduction device, the ion source, the analyzer and the detector. As will be discussed later on, the traditional ionization sources for proteomics research are MALDI (Matrix-Assisted Laser Desorption/Ionization) and ESI (ElectroSpray Ionization). Different types of analyzers exist, some of which are usually employed with MALDI ion sources (e.g. TOF) and some others are normally coupled to ESI ion sources (e.g. ion traps or quadrupoles). From Cañas *et al.* [33].

SOFT IONIZATION SOURCES

The primary methods of choice for the ionization of large non-volatile and thermally labile molecules are matrix-assisted laser desorption/ionization (MALDI) and electrospray ionization (ESI).

MALDI

Introduced in 1988 principally by Karas and Hillenkamp, MALDI is suitable for mass spectrometric analysis of large, non-volatile and thermally-labile biomolecules such as proteins, oligonucleotides and synthetic polymers.
Typical MALDI analyses essentially require the mixing of the sample with an excess of a suitable matrix and the ionization of the analyte molecules by laser pulses. UV-MALDI instruments are usually endowed with nitrogen lasers emitting at 337 nm. The observed MALDI mass spectrum is a function of experimental variables which affect sensitivity and reproducibility: choice of matrix, physico-chemical properties of the analyte, matrix-analyte relative concentrations, method of spot preparation, laser characteristics and local environment [34, 35].

The currently proposed models of UV-MALDI action involve a two-step process: primary ionization, during or shortly after the laser pulse hits the matrix-analyte solid, followed by secondary ion-molecule reactions in the dense expanding plume of desorbed material.
Two different models can be considered to explain primary ionization [36, 37].

- The cluster model.
  Analytes are incorporated in the matrix in a charged state defined by the solution pH. These "preformed" ions need to be separated from their counterions to generate free ions. The period during and soon after the laser pulse is characterized by high energy and material density, which causes the rapid generation and emission of clusters with an excess of positive or negative charge. Subsequent desolvation, either “soft” (loss of neutral matrix) or “hard” (ejection of charged matrix), frees the ions in the gas phase (Figure 1-18).
- The photoexcitation/pooling model.
  This model proposes MALDI as the result of the combination of two processes: the migration of excitation energy in the matrix followed by pooling events, leading to matrix molecules with excitation states energetically sufficient for ionization.

Secondary events take place in the expanding plume as soon as primary ions are formed. Analyte ions are derived from primary matrix ions by charge transfer reactions:

- proton transfer:

$$mH^+ + A \leftrightarrow m + AH^+ \quad \text{and} \quad (m\text{-}H)^- + A \leftrightarrow m + (A\text{-}H)^-$$

- electron transfer:

$$m^+ + A \leftrightarrow m + A^+ \quad \text{and} \quad m^- + A \leftrightarrow m + A^-$$

- cation transfer (e.g.: $mNa^+ + A \leftrightarrow m + ANa^+$).

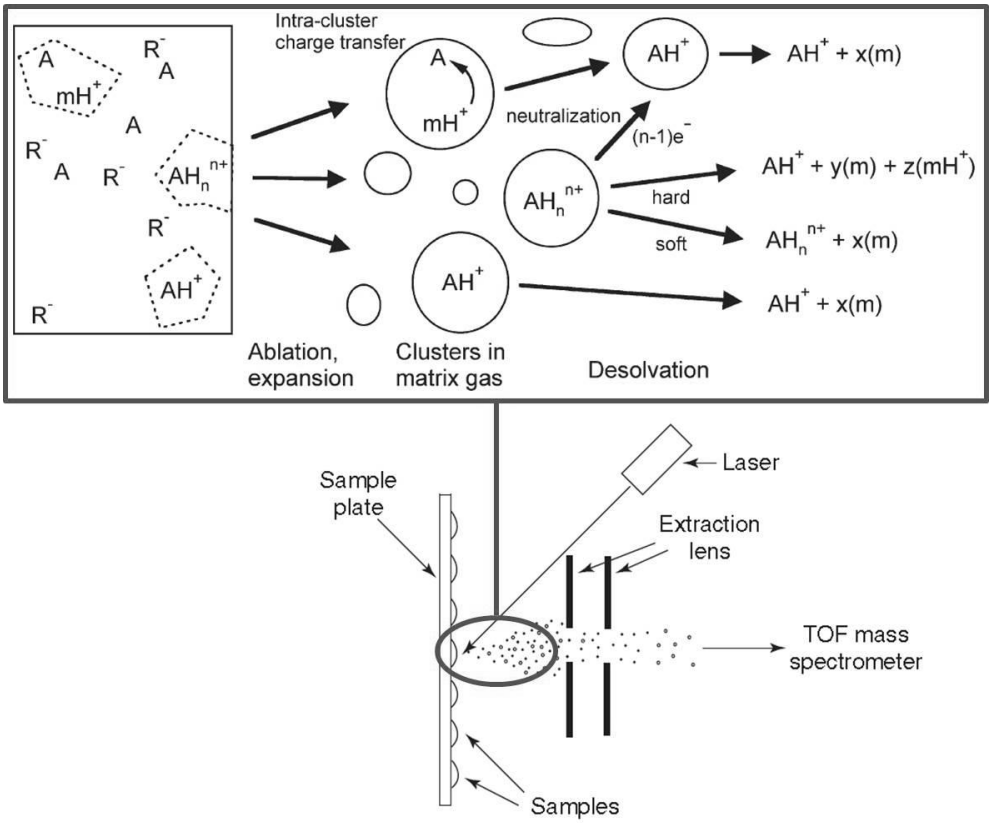

Figure 1-18. Scheme of the MALDI process. The cluster model of ion formation is represented in the upper box. m = matrix; A = analyte; R = generic counterion. Modified from Knochenmuss [37].

The roles of the matrix in MALDI are mainly two: it serves as a "solvent" for the analyte and it converts the photon energy absorbed from the laser beam into the excitation energy of the solid system. Therefore, the fundamental requirements that a matrix must meet can be summarized as follows:

- solubility in solvents compatible with the analyte
- ability to embed the analyte
- lack of chemical reactivity
- vacuum stability
- absorbance at the chosen laser wavelength
- molecular mass low enough to undergo sublimation
- ability to promote analyte ionization.

The selection of a suitable matrix depends on both the laser wavelength and the type of analyte. Common matrices used for UV-MALDI analyses of proteins and peptides are reported in Table 1-2.

Table 1-2. Common matrices used for UV-MALDI analyses of proteins and peptides.

MATRIX	STRUCTURE	Molecular weight	Solvent
α-Cyano-4-hydroxycinnamic acid (CHCA)	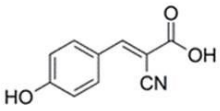	189.2	ACN/H_2O, acetone
2,5-Dihydroxybenzoic acid (DHB)	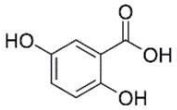	154.1	ACN, acetone
3,5-Dimethoxy-4-hydroxycinnamic acid (SA)	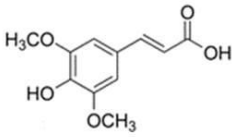	224.2	ACN/H_2O

The quality of the spectra strongly depends on sample preparation, although a good preparation for a given sample is to be determined empirically [38, 39].

The most common sample preparation techniques include:

- **Dried-droplet**. This is the original method for sample preparation and still the most widely used. A volume of saturated solution of matrix is mixed 1:1 with the sample solution, typically in a molar ratio of 1:1000 to 1:10000. The mixture is spotted on the MALDI target and allowed to dry. This method well tolerates the presence of salts and buffers.

  A variation of the classical dried-droplet method is the **vacuum-drying** crystallization method, in which the drop of mixed matrix and analyte solutions is rapidly dried in a vacuum chamber, giving rise to small-sized crystals with an increased sample homogeneity, thus offering improvements in mass accuracy and resolution.
- **Slow crystallization**. This method can be useful when samples contain non-volatile solvents or additives (e.g. glycerol, urea, DMSO), high salt concentrations, low protein concentrations. A few microliters of sample solution are mixed in a vial with about a tenfold volume of saturated matrix solution. The vial is left open in the dark for at least one hour to allow the formation of microcrystals. Then the supernatant is removed and the microcrystals are washed twice with cold aqueous solution. Finally, 1 µl of water is added to make a slurry of crystals which is applied on the sample plate and allowed to dry.
- **Fast-evaporation**. A drop of the matrix solution, prepared in a highly volatile solvent, is applied on the sample plate. The solvent is allowed to evaporate, leaving a thin homogeneous film of small crystals of matrix. Then a drop of the analyte solution is applied and allowed to dry. This method can improve the resolution and mass accuracy of MALDI measurements.
- **Overlayer**. The fast-evaporation method is exploited for the deposition of the first layer of small matrix-only crystals. A mixture of matrix and analyte solution is deposited on top of the first layer. This method offers good results particularly for proteins and mixtures of proteins or peptides.
- **Sandwich** (combination of fast-evaporation and overlayer methods). The first matrix layer is deposited on the sample spot in the fast-evaporation method. The application of a sample droplet

on top of it is followed by the deposition of a second layer of matrix, this time solubilized in a traditional solvent.

- **Quick and dirty**. A drop of analyte solution (0.1 – 10 mM) is spotted onto the sample plate, then a drop of matrix solution is added on top of it and the solutions are mixed thoroughly with a pipette before letting the mixture dry under an air or nitrogen steam.
- **Matrix-precoated target**. This method is fast since it consists in the straightforward addiction of a droplet of sample on a thin layer matrix-pre-coated plate.

Compared to other ionization techniques, MALDI is more tolerant to low concentrations of common contaminating species such as buffers, salts and detergents, that strongly interfere with the analyte desorption and ionization. However, when the concentration of contaminants is suspected to be high, a prior purification step is recommended.
The main drawbacks of the MALDI technique are the strong dependence on the sample preparation, the low shot-to-shot reproducibility and also a short sample lifetime.

ESI

Mainly developed by Fenn and co-workers and described in 1989, ESI is an ion source that works at atmospheric pressure. Unlike MALDI, in which the analyte ions are produced in a pulsed way from a solid sample, ions in ESI are produced continuously from a liquid-phase sample.

Ionization involves three major steps: droplet formation, droplet shrinkage and desorption of gas-phase ions (Figure 1-19) [34, 35].

- **Droplet formation.** The sample solution flows continuously through a stainless steel capillary tube whose tip is held at a high potential with respect to the walls of the surrounding atmospheric-pressure region. In the positive-ion mode of operation, the difference of potentials between the tip (positive voltage) and the nozzle (the counter-electrode placed at negative voltage) generates an electrostatic field that causes cations to migrate towards the counter-electrode. This tendency to migrate is counterbalanced by the surface tension of the solution, giving rise to the Taylor cone at the tip of the capillary. If the applied electric field is strong enough, the flux of solution extending from the cone breaks into a mist of fine droplets.
- **Droplet shrinkage.** Solvent evaporation, assisted by a flow of hot nitrogen, leads to droplet shrinkage and thus to the progressive increase of the charge density until the Rayleigh limit is reached. At this point, the repulsive coulombic forces exceed the droplet surface tension causing fission of the droplets into smaller and highly charged offspring droplets which in turn give rise to second-generation droplets.
- **Desorption of gas-phase ions.** Two mechanisms have been proposed to explain ion desorption from the droplets: the charge-residue model (CRM) and the ion-desorption model (IDM) [40, 41]. Briefly, according to the charge-residue model, the electrospray process generates droplets that contain only one solute molecule which is released as an ion when the solvent evaporates.
  According to the ion-desorption model, expulsion of the solvated ions into the gas phase happens when the droplets reach a small size (about 20 nm of diameter) and the charge density is high,

although less than the Rayleigh limit. Because of coulombic repulsion, the energy gain in the electric field at the surface of the droplet compensates for the energy required to enlarge the surface of the droplet very rapidly when the solvated ion is expelled.

It is generally believed that the ESI response depends on the nature of the analyte and in particular the ion-desorption model best applies to ions with significant surface activity whereas the charge-residue model applies largely to hydrophilic species.

The characteristic multiple charging of ions in ESI occurs via charge distribution from the surface of the final droplet to the available charge-retaining sites on the solute molecule.

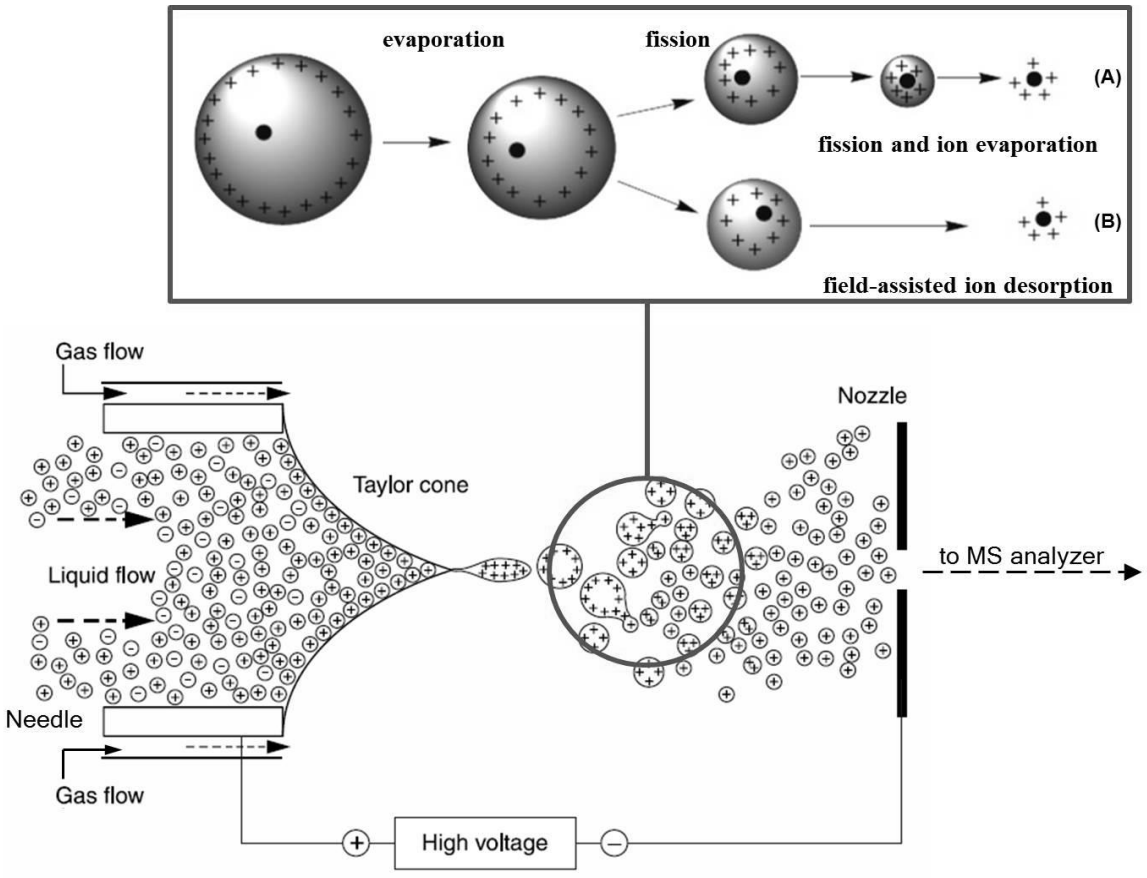

Figure 1-19. Scheme of the ESI process. The proposed mechanisms of formation of gas-phase ions are represented in the upper box: the charge-residue model (A) and the ion desorption model (B). Modified from Dass [34] and Westman-Brinkmalm *et al.* [42].

Radio frequency (rf), multipoles (quadrupoles, hexapoles, octapoles) or "ion funnels" are commonly placed between the ESI source and the mass analyser to improve ion transmission efficiency.

An additional source of energy, such as heat or a high-velocity annular flow of gas, is required when operating at high flow rates (0.2 to 1 ml/min) to disperse the liquid into fine droplets.

MASS ANALYZERS

All mass analyzers use static or dynamic electric and magnetic fields, alone or combined, to measure the m/z ratio of gas-phase ions.

Analyzers can be divided into two groups:

- beam analyzers: ions leave the source in a beam and pass through the analyzer to the detector;
- trapping analyzers: ions are trapped in the analyzer after being injected from the ion source or being formed in the analyzer itself.

Since there are different types of sources, a variety of mass analyzers has been developed. Their main features are reported in Table 1-3.

Table 1-3. Mass analyzers and their main features.

ANALYZER	Principle of separation	Pulsed / continuous	Resolution
Quadrupole (Q)	m/z (trajectory stability)	Continuous	Low
Time-of-flight (TOF)	velocity (flight time)	Pulsed	High
Linear ion trap (LIT)	m/z (resonance frequency)	Pulsed	Low
Orbitrap (OT)	m/z (resonance frequency)	Pulsed	Very high
Fourier-transform ion cyclotron resonance (FT-ICR)	m/z (resonance frequency)	Pulsed	Very high

The main characteristics to be considered when evaluating the performances of a mass analyzer are:

- **mass range**: the range of m/z values over which the analyzer can measure ions. It is expressed in Th or in u for an ion carrying an elementary charge (z = 1).
- **detection sensitivity**: the smallest amount of an analyte that can be detected at a certain defined confidence level
- **mass resolution (resolving power)**: the ability to distinguish between two ions of close masses. If M is the mass of an ion and ΔM the difference between the two ion masses, the mass resolution is defined as the ratio M/ΔM.
- **mass accuracy**: index of how close the experimentally measured mass (M_{exp}) is to the theoretical mass (M_{th}). It is usually expressed in parts-per-million: ppm = $[(M_{th} - M_{exp}) / M_{exp}] \cdot 10^6$. Mass accuracy is directly linked to the resolving power.
- **transmission**: the ratio between the number of ions reaching the detector and the number of ions entering the mass analyzer.
- **analysis speed (scan speed)**: the number of spectra acquired per unit of time. It is expressed in mass units per second (u s^{-1}) or millisecond (u ms^{-1}). Fast scan speed is desirable when

investigating rapidly changing events while slow scan speed is required in accurate mass measurement experiments.

It is worth keeping in mind that sensitivity, resolution, accuracy and scan speed are in some ways linked together.

The mass analyzers that were exploited in this work of thesis and their main applications are briefly described hereinafter.

Time-of-flight (TOF)

The time-of-flight analyzer consists of a field-free flight tube through which ions are separated on the basis of their velocities. The velocities of ions are an inverse function of the square root of their mass over charge values:

$$v = \sqrt{\frac{2\,q\,V}{m}}$$

The lower the m/z ratio of an ion, the faster the ion moves through the flight tube and reaches the detector. The time of flight of an ion, before reaching the detector, can be defined as:

$$t = \frac{L}{v} = L \cdot \sqrt{\frac{m}{2\,q\,V}}$$

The measured arrival times of all ions provide a time spectrum that is converted into a mass spectrum by calibrating the instrument.

Linear or reflector mode

Ions are accelerated out of the source region with inherent dispersion in time, space and velocity, reflecting the differences in the instant of ion formation, the location of the ion at the time of acceleration and the differences in initial kinetic energy.

Desorbed ions have inherent different initial velocities (v_0). Therefore, after a period of time, ions of the same m/z will have a spread in space (condition 1 in Figure 1-20). Operating in linear mode, the spread of velocity increases till the ions reach the detector (situation 2 in Figure 1-20), leading to peak broadening.

Improvement in resolution is possible operating in reflector mode. A reflectron is an energy-correcting device that minimizes the effects of spatial and kinetic energy spreads. It consists of grids and a series of ring electrodes, each with a progressively increasing repelling potential, commonly referred to as mirror. The mirror is placed at the end of the flight tube. Ions entering the mirror are slowed down (event 3 in Figure 1-20. and those with higher initial velocity will cover a longer distance before coming to rest: the shorter flight time is compensated by the extra time spent in the mirror. As a consequence, after reversing direction and after being reaccelerated into a second field-free region (situation 4 in Figure 1-20), ions with the same m/z ratio get to the detector simultaneously (point 5 in Figure 1-20) [42].

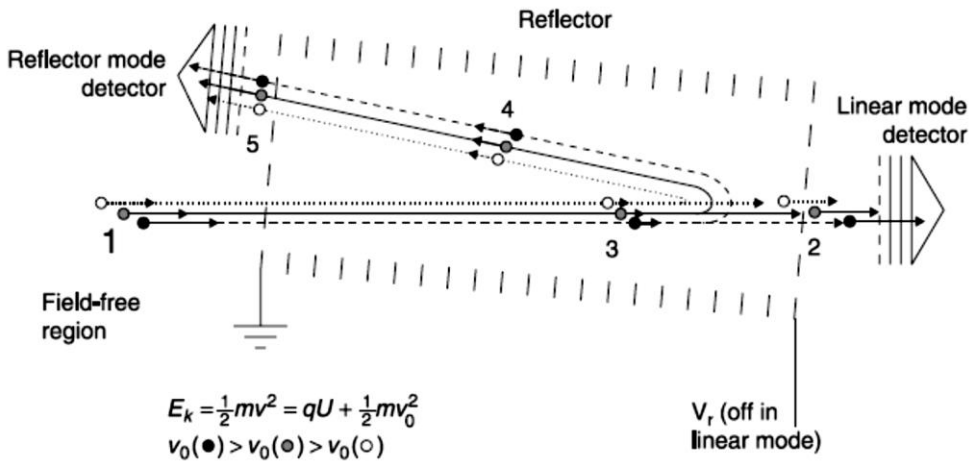

Figure 1-20. Scheme of the ion path in a TOF analyzer. From Westman-Brinkmalm *et al.* [42].

Time-of-flight analyzers have a number of attractive features: the potential of an unlimited mass range, high ion-transmission efficiency, high spectrum-acquisition rate, multiplex detection capability, simplicity in instrument design, ease of use and low cost [43, 44].

4800 MALDI-TOF/TOF (AB SCIEX)

The 4800 MALDI-TOF/TOF instrument and its main components are shown in Figure 1-21.

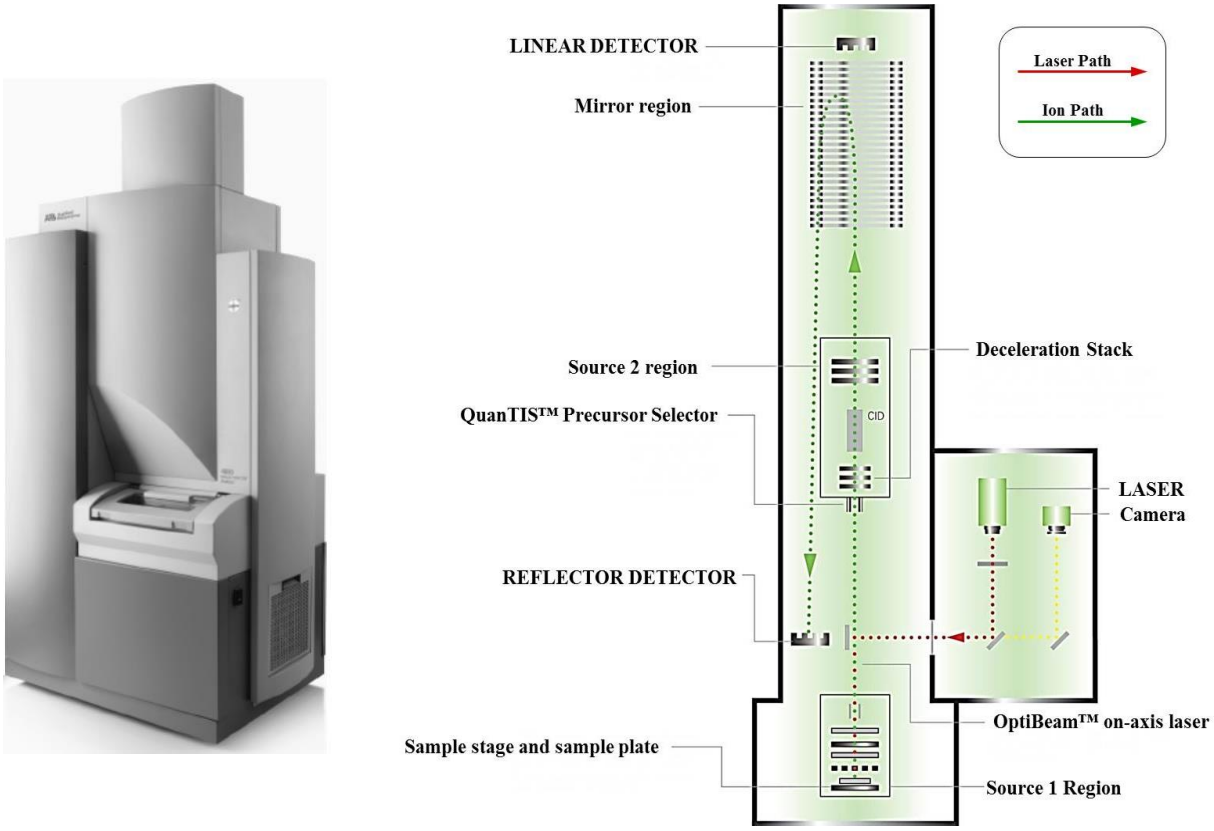

Figure 1-21. 4800 MALDI TOF/TOF instrument (AB SCIEX) and a schematic representation of its main components.

The 4800 MALDI TOF/TOF mass spectrometer allows fast, sensitive, high resolution and accurate MS analyses of biomolecules, including peptides, intact proteins, lipids, carbohydrates and oligonucleotides. The system can also perform MS/MS analyses for precise identification and characterization of these biomolecules.

The main components of the 4800 MALDI TOF-TOF mass spectrometer are:

- source region with on-axis UV-laser, which increases sensitivity in both MS and MS/MS modes
- TOF
- linear detector
- mirror region and reflector detector
- QuanTIS (Timed Ion Selector) Precursor Selector, CID cell and source 2 region for high-resolution MS/MS analyses.

Peptide mass fingerprinting (PMF)

MALDI-TOF-based peptide mass fingerprinting is a technique for protein identification. The process can be summarized as follows:

a) isolation of single proteins from complex mixtures by bi-dimensional electrophoresis (2-DE) or liquid chromatography;
b) digestion of the protein with a specific protease, usually trypsin;
c) acquisition of the MALDI-TOF spectrum which represents the "fingerprint" of the protein;
d) database search: identification of the unknown protein through the match of the experimental data with the theoretical peptide map of a protein present in the database. The identification is given with a score that greatly depends on sequence coverage and mass accuracy of the considered peptides [45].

Quadrupole (Q)

Quadrupole analyzers are composed of four parallel circular metallic rods (electrodes), arranged in a squared array. Separation of ions of different m/z values is accomplished through the principle of path stability in a high-frequency oscillating electric field, created by applying direct-current (DC) and radio-frequency (RF) potentials to those rods (Figure 1-22).

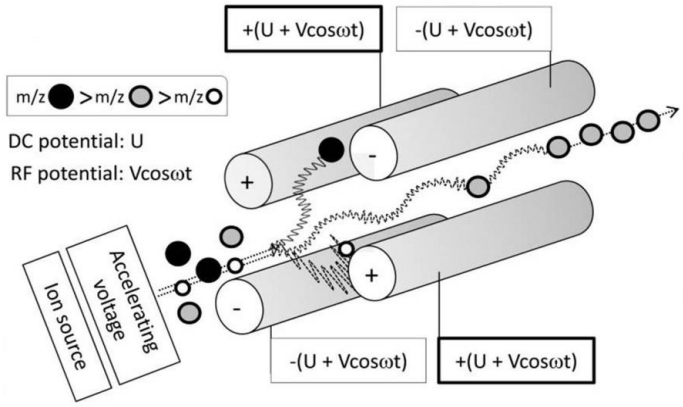

Figure 1-22. Scheme of a quadrupole analyzer. From Rubakhin *et al.* [46].

The field within the quadrupole is created by connecting electrically the opposite pairs of electrodes: one pair receives a superimposed positive DC potential (U) and a time-dependent RF potential ($V \cdot \cos\omega t$, where ω is the angular frequency of the applied RF voltage, V its amplitude and t the time), while the other pair of rods receives a negative DC potential (–U) and a RF potential of the same magnitude but out of phase by 180° (id est $-U - V\cos\omega t$).
Different experiments can be performed:

- if the DC is set to zero and only RF is applied, every ion trajectory is stable and all ions pass through the quadrupole.
- when a set of defined DC and RF potentials are applied, only the ions with a specific m/z ratio have stable trajectories and pass through the quadrupole. The duty cycle (i.e. the percentage of time in which a particular ion is getting through the quadrupole and reaching the detector) is very high.
- in the scanning mode, DC and RF potentials are varied simultaneously while keeping their ratio constant, allowing the ions with different m/z ratio to pass sequentially. In this instance, the duty cycle is low.

The main characteristics of a quadrupole mass filter are: high scan speeds, high transmission, sensitivity, unit mass resolution, independence on the initial energy distribution of ions, linear mass range and also low cost and mechanical simplicity [43, 44].

Quadrupole ion trap (QIT)

The quadrupole ion trap, also known as 3D ion trap, is the three-dimensional analogue of a quadrupole mass filter. Mass separation is achieved by storing the ions in the trapping space and by analyzing their motion in time, rather than in space.
The three-electrode structure of a QIT consists of a central ring electrode and two identical end-cap electrodes, each with a hyperbolic geometry (Figure 1-23). One of the end-cap electrodes has a small aperture through which an electron beam can be gated periodically into the trapping space. The opposite end-cap electrode has several openings for the ejection of ions towards the detector.

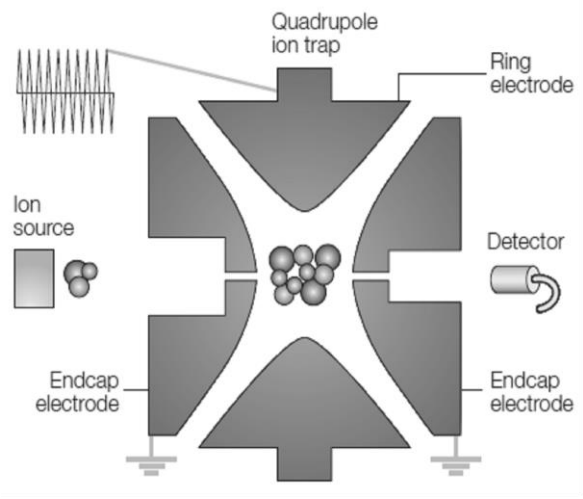

Figure 1-23. Scheme of a QIT analyzer.

The three-dimensional ion trapping field is created by applying a potential to the ring electrode and maintaining the end-cap electrodes at ground potential. Helium is introduced into the trap to cool the ions (reduction of the kinetic energy caused by collisions) and to focus them in the center of the trap.
The mass spectrum of the trapped ions is acquired using the mass-selective instability mode of analysis, also known as mass-selective axial ejection. Increasing the magnitudes of the DC and RF voltages and the frequency of the RF signal, either singly or in combination, forces ions of successively increasing m/z values to become sequentially unstable in the axial direction and thus be ejected out of the trap.
QIT mass analyzers have high scan speed and sensitivity and are compact, simple to operate and relatively low cost. On the other hand, their major drawbacks are poor resolution (unit), low dynamic range, poor ion-trapping efficiency [43, 44].

Quadrupole linear ion trap (LIT or LTQ)

A quadrupole linear ion trap, also known as two-dimensional ion trap, is identical in construction to the quadrupole analyzer, although its operational modes are similar to those of the quadrupole ion trap.
A LIT consists of two pairs of hyperbolic rods, connected electrically. The four parallel rods are segmented into three axial sections, with the central section about three times longer than the two end sections (Figure 1-24). Mass analysis of the trapped ions is performed by using the mass-selective instability mode with radial ejection of the trapped ions through the slit present along the length of one of the rods of the central section.

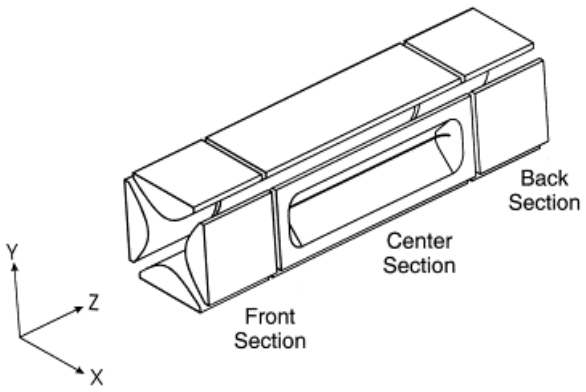

Figure 1-24. Scheme of a LIT analyser.

In comparison with a 3D ion trap, a LIT shows improved trapping efficiency, ion storage capacity, ion-ejection efficiency, scan speed and detection sensitivity [43, 44].

4000 TRAP (AB SCIEX)

The 4000 Q TRAP instrument and its main components are shown in Figure 1-25 and Figure 1-26.

Figure 1-25. The 4000 and 5500 QTRAP LC/MS/MS Systems (AB SCIEX).

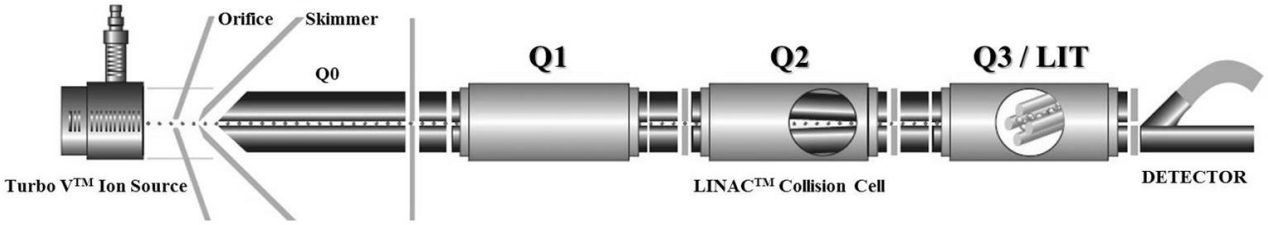

Figure 1-26. Scheme of the main components of the 4000 QTRAP mass spectrometer.

The main components of the 4000 QTRAP mass spectrometer are:

- Q0. High-pressure cell that performs collisional focusing to maximize the transmission of ions. Furthermore, in MS/MS or MS^3 experiments, ions can be trapped in Q0 while the Q3 is scanning ions, thus improving sensitivity and duty cycle.
- Q1.
- Q2 with LINAC Collision Cell. The LINAC high-pressure collision cell accelerates ions through the Q2 providing great sensitivity at reduced dwell times.
- Q3 Linear Ion Trap.

Q TRAP modes of operation

The Q TRAP mass spectrometer can be operated either in QqQ or LIT modes [47].
QqQ modes:

- Q1 MS (Q1). A full scan using the first quadrupole (Q1) as the mass filter for specific masses. The ion intensity is returned for every requested mass in the scan range. Used for target compound analysis.
- Q1 Multiple Ions (Q1 MI). A scan using the first quadrupole (Q1) as the mass filter. The ion intensity is returned for specific masses.
- Q3 MS (Q3). A full scan using the third quadrupole (Q3) as the mass filter. The ion intensity is returned for every requested mass in the scan range.
- Q3 Multiple Ions (Q3 MI). A scan using the third quadrupole (Q3) as the mass filter. The ion intensity is returned for specific masses. Used for target compound analysis.

- Product Ion (MS2). An MS/MS scan in which the first quadrupole is set to a fixed mass and the third quadrupole sweeps a mass range. An experiment that will search for all of the products of a particular precursor ion fragmenting in Q2.
- Precursor Ion (Prec). An MS/MS scan in which the third quadrupole is set to a fixed mass and the first quadrupole sweeps a mass range. A scan for the ion of a specific mass-to-charge ratio that is generating specific product ions.
- Neutral Loss (NL). An MS/MS scan in which both the first quadrupole and the third quadrupole are swept over a mass range using a fixed mass difference between them. A response will be observed if the ion chosen by the first analyzer fragments by losing or gaining the mass difference or neutral loss specified.
- Multiple Reaction Monitoring (MRM). Mode of operating a triple quadrupole instrument so that an ion of a given mass (Q1) must fragment or dissociate to give a product ion of specific mass (Q3) in order for a response to be detected. Used for very specific target compound analysis.

LIT modes for screening, confirmation and identification applications [47]:

- Enhanced MS (EMS). An MS full scan in which all the ions in the specified m/z range are trapped in LIT for a specified fill time prior to being scanned out and detected.
- Enhanced Multi-Charge (EMC). An MS scan in which multiply-charged ions are detected within the specified range. Singly-charged ions are of minimum intensity.
- Enhanced Resolution (ER). An MS scan in which ions within a 20 Da region are collected in LIT for a specified fill time and scanned out slowly for enhanced resolution. The ER scan is useful to determine charge states and isotopic patterns.
- Enhanced Product Ion (EPI). An MS/MS scan in which Q1 filters the parent ion that is fragmented in Q2. Fragment ions are trapped in LIT for a specified fill time prior to being scanned out. The EPI mode can be used to confirm the presence of the detected analyte by interpretation of fragment ions.
- MS/MS/MS (MS3). A scan in which product ions generated in Q2 are collected in LIT. Product ions of a specified m/z are isolated in LIT and further fragmented. The resulting fragment ions are trapped into LIT prior to being scanned out and detected.

MRM analyses of mixtures of peptides

Multiple reaction monitoring (MRM) is a specific and sensitive method to quantify target proteins within complex mixtures. The MRM process consists of a series of steps (**Errore. L'origine riferimento non è stata trovata.**):

1. ionization of the components of the digestion mixture;
2. Q1: selection of the proteotypic peptide of known m/z (precursor ion). A proteotypic peptide is a peptide unique to the protein of interest. When possible, to maximize the sensitivity of the analysis, it is better to choose a peptide showing high signal response;
3. Q2: fragmentation of the precursor ion with N_2;
4. Q3: selection of product ion with known m/z (transition). The term transition refers to the specific pair of m/z values associated to the precursor and fragment ions respectively;
5. acquisition of a spectrum of signal intensity as function of time;
6. quantitation of the protein of interest identified by the proteotypic peptide.

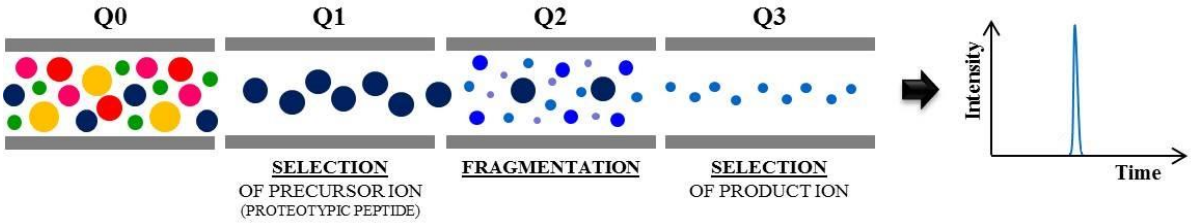

Figure 1-27. Scheme of a MRM analysis.

Orbitrap (OT)

The orbitrap analyzer is an electrostatic ion trap that exploits the Fourier transform to obtain mass spectra. The instrument is composed of an axial spindle-like central electrode and a coaxial barrel-like outer electrode, cut into two equal parts separated by a small slit. The outer electrode is at ground potential while an electrostatic potential is applied to the spindle-like electrode. Ions enter the orbitrap tangentially through the fissure between the two parts of the outer electrode. The trapped ions undergo rotation around the central electrode and harmonic oscillations along its length (Figure 1-28). The frequencies of the harmonic oscillations of the trapped ions, a function of their m/z values, are converted to mass spectra using fast FT [48, 49]. Characteristics of OT instruments are high accuracy and resolving power but relatively limited dynamic range [43, 44].

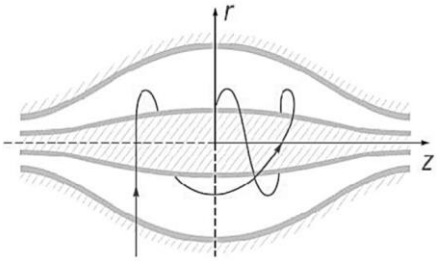

Figure 1-28. Scheme of an orbitrap analyzer.

LTQ-Orbitrap XL (Thermo Scientific)

LTQ-Orbitrap XL instrument and its main components are shown in Figure 1-29 and Figure 1-30.

Figure 1-29. LTQ-Orbitrap XL mass spectrometer (Thermo Scientific).

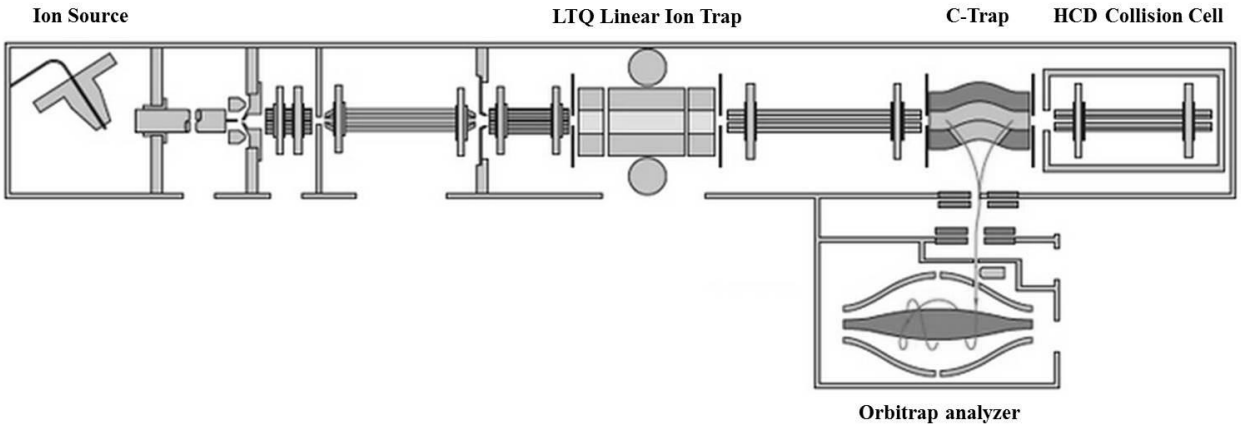

Figure 1-30. Scheme of the main components of the LTQ-Orbitrap XL mass spectrometer.

The characteristic components of the LTQ-Orbitrap XL mass spectrometer are:

- LTQ XL Linear Ion Trap. The ion trap can store, select and fragment ions (CID) before sending them to the Orbitrap. The trap also features Automatic Gain Control (AGC), which provides extended dynamic range and ensures that the Orbitrap is always filled with the optimum number of ions for all scans.
- Transfer octopole.
- C-trap (a gas-filled, curved, RF-only quadrupole). In the C-trap ions are accumulated and their energy is dampened using a bath gas (nitrogen). Radial ejection from the C-trap is the most recent device for injection of ion packets with narrow spatial and temporal distributions into the Orbitrap analyzer.
- HCD (Higher-energy Collision Dissociation) cell.
  The fragmentation process involves four major steps:
  1) precursor ion selection in the linear ion trap;
  2) ion fragmentation in the HCD collision cell;
  3) transfer of product ion back to the C-trap
  4) immediate ejection into the Orbitrap mass analyzer for accurate mass detection.
- Orbitrap analyzer.

Ion mobility spectrometer (IMS)

Ion mobility mass spectrometers are hybrid instruments that combine an ion mobility separation system with conventional MS systems. An ion mobility spectrometer (IMS) can also serve as a stand-alone ion detection system.

The operating principle of an IMS is based on the mobility of a gas-phase ion under both the positive influence of an electrical field gradient and a negative influence of a cross-flow of buffer gas. In these conditions, the mobility of an ion essentially depends on its mass, charge and collision cross section (shape): ion charges being equal, small and compact ions with small collision cross sections drift more quickly than large and extended ions with large collision cross sections (Figure 1-31).

Schematically, a typical ion mobility spectrometer consists of a reaction region and a drift region separated by an electrical shutter. Both regions contain a series of uniformly spaced electrodes that provide uniform electric field strength. Buffer gas is also circulated in the drift tube. Ion mobility is a property that results from the combined effect of ion acceleration by the electric field and retardation by collisions with the buffer gas. The resolution of an IMS is usually very low but can be increased by increasing the pressure of the buffer gas, connecting the ion source directly with the drift tube, increasing the length of the drift tube and increasing the electric field gradient of the drift tube [43, 44].

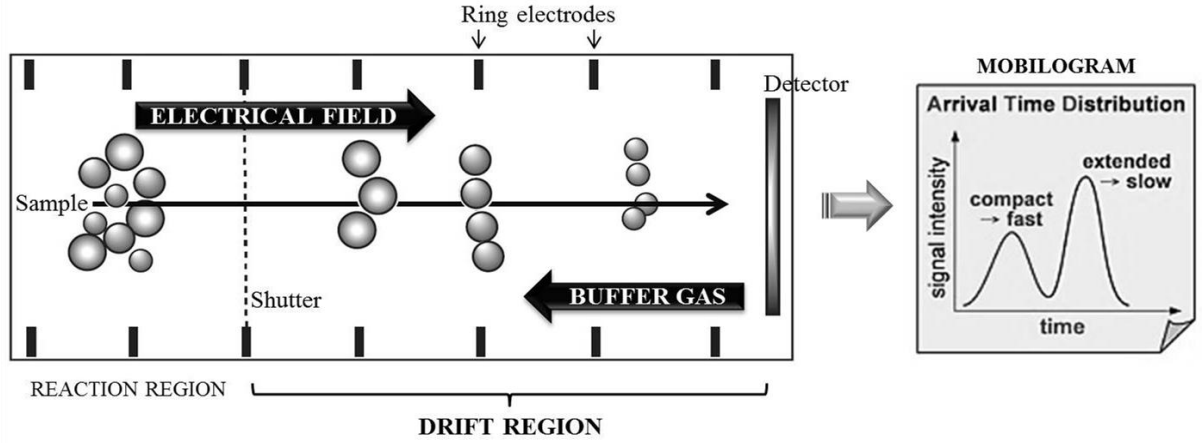

Figure 1-31. Scheme of an ion mobility mass spectrometer. Modified from Dass [43].

For more accurate mass analysis, an ion mobility spectrometer can be coupled with a quadrupole or TOF analyzer: the IMS serves as a separation device while the quadrupole or TOF operates as a detection device.

Synapt G2-S (Waters)

Synapt G2-S instrument and its main components are shown in Figure 1-32 and Figure 1-33.

Figure 1-32. Synapt G2-S mass spectrometer (Waters).

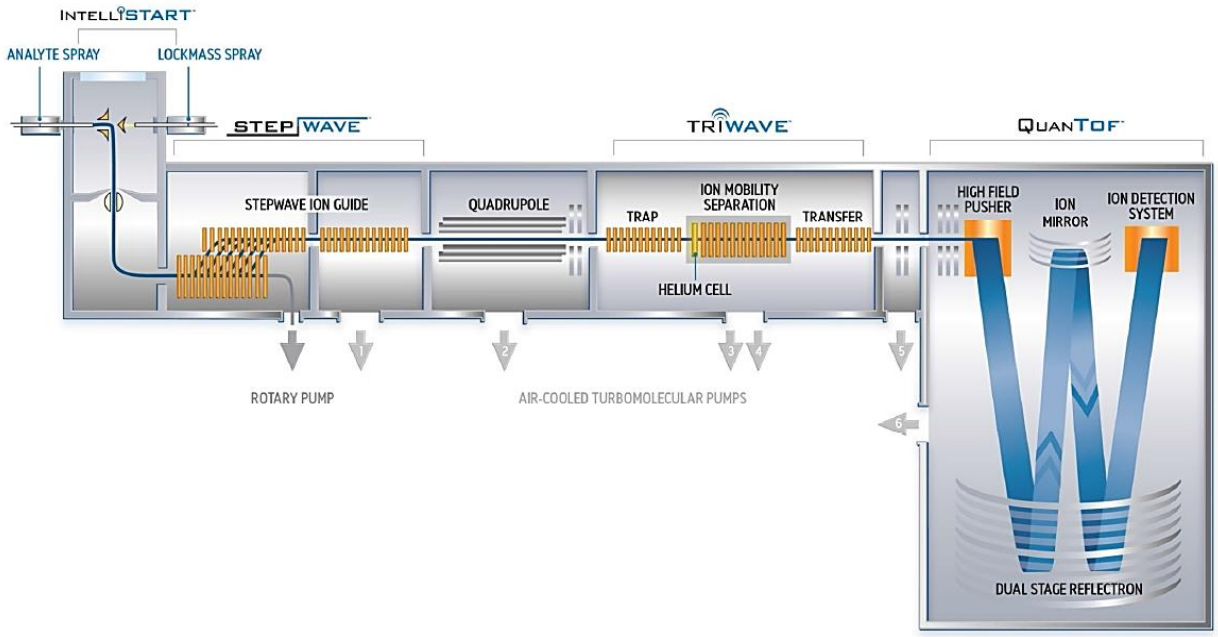

Figure 1-33. Main components of Synapt G2-S.

Characteristic features of the Synapt G2-S are:

- StepWave region.
  Thanks to its particular design, the StepWave transfers the ions from the ion source to the quadrupole analyzer with high efficiency while eliminating neutral contaminants. Therefore it increases signal intensity and minimizes background noise.
- TriWave region.
  It is essentially composed of three components: two TWIGs (Travelling Wave Ion Guides) with the ion mobility separation cell in between.
  - Trap T-Wave. This cell traps the ions prior to the ion mobility separation.
  - Ion Mobility Separation (IMS) T-Wave. This is the cell where separation of ions based on their mobility actually takes place. It is preceded by an helium cell that maximizes transmission of ions.
  - Transfer T-Wave. This cell transfers the ions coming from the IMS cell to the TOF analyzer.

  Both the Trap and Transfer T-Waves can be operated as collision cells.
- QuanTOF analyzer.
  The user can choose between different modes of operation of the QuanTOF:
  - sensitivity mode (“V path”)
  - resolution mode (“V path”)
  - high resolution mode (“W path”).

HDMS^E analysis

High definition mass spectrometry (HDMS) is the combination of high resolution mass spectrometry and high efficiency ion mobility. In HDMS^E experiments the IMS cell provides an extra dimension of ion separation while the transfer collision cell cycles between low and high collision energy states so that the

precursor and its fragment ions alternatively pass through and are detected (Figure 1-34). HDMS^E collects exact mass data for both precursor and fragment ions.

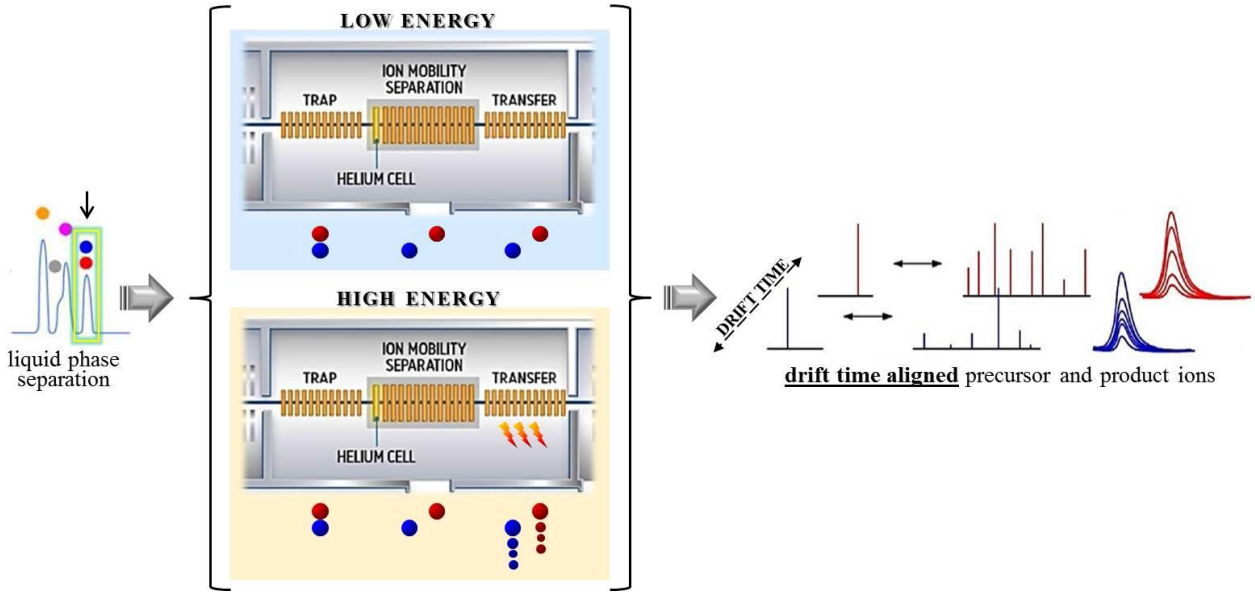

Figure 1-34. Scheme of High Definition MSE experiments (HDMSE) with Synapt G2-S.

Analyses of complex mixtures and structural investigations of gas-phase ions are possible thanks to the ability of the instrument to differentiate chimeric molecules (increased peak capacity) in a wide dynamic range with high accuracy and resolving power.

TANDEM MASS SPECTROMETRY

The term tandem mass spectrometry (also known as MS/MS) refers to the coupling of two or more mass spectrometers (tandem in-space) or stages of mass analysis (tandem in-time), with fragmentation occurring between them [50, 51].

Tandem in-space instruments.

The three steps of a MS/MS analysis (i.e. mass selection, fragmentation and mass analysis) are carried out in three discrete regions. Examples of tandem in-space instruments are the triple quadrupoles and the TOF-based instruments.

Tandem in-time instruments.

Mass selection, fragmentation and mass analysis are performed in the same region but in a temporal sequence. Examples of tandem in-time instruments are the Quadrupole Ion Trap, the Linear Ion Trap and the Fourier-transform ion-cyclotron resonance mass spectrometers.

The major contributions of tandem mass spectrometry are in the fields of:

- ✓ structure elucidation of unknown compounds
- ✓ identification of compounds in complex mixtures
- ✓ elucidation of fragmentation pathways
- ✓ quantification of selected compounds in complex samples.

Tandem mass spectrometers allow to perform various types of experiments (Figure 1-35):

A. **Product ion scanning.**

The purpose of this experiment is the generation of a fragment ion spectrum from an analyte of interest. The first analyzer (MS1) is set to a value that selects one specific precursor ion at a time. The selected ion undergoes CID in the collision cell and the resulting fragments are then analyzed by the second analyzer (MS2).

B. **Precursor ion scanning.**

This method is typically used to detect a specific subset of peptides in a complex mixture. MS2 is set to transmit only one specific fragment ion to the detector while MS1 is scanned to detect all the precursor ions that generate this fragment.

C. **Neutral loss scanning.**

Neutral loss scanning allows the detection of peptides that contain a specific functional group. In this experiment both analyzers scan in a synchronized manner so that the mass difference of the ions passing through MS1 and MS2 remains constant. The mass difference corresponds to a neutral fragment that is lost by the precursor ion in the collision cell.

D. **Multiple ion monitoring.**

This experiment allows the detection and quantification of a target analyte, with known fragmentation properties, in complex samples. MS1 filters a specific precursor ion and MS2 selects a specific fragment, characteristic for that precursor. Typically, the instrument cycles through a series of transitions (precursor-fragment pairs) and records the signal as a function of time, correspondent to the chromatographic elution.

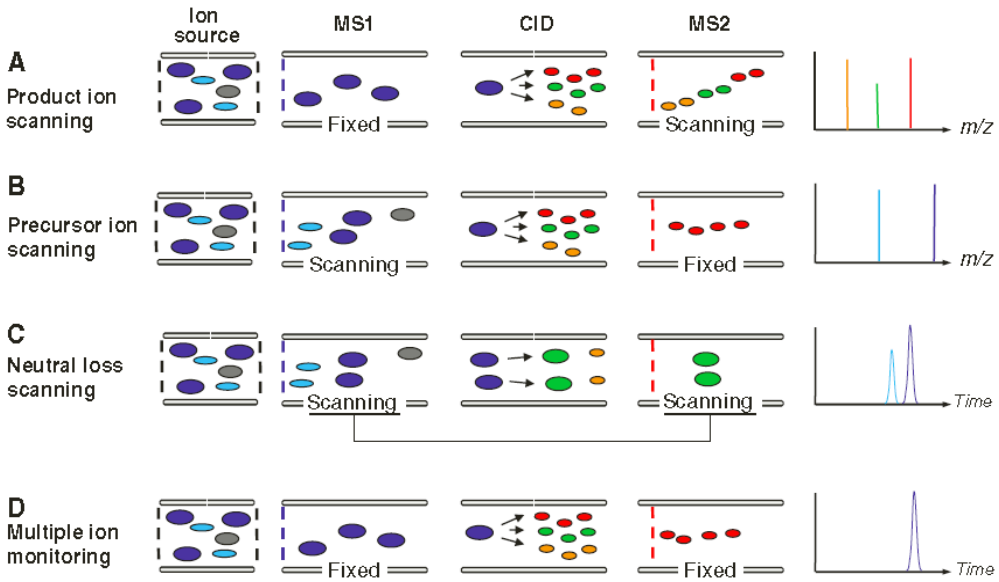

Figure 1-35. Scheme of various types of tandem mass experiments. From Domon [52].

Peptide fragmentation

The types of fragment ions observed in a MS/MS spectrum depend on many factors, including the primary sequence, the charge state, the amount of internal energy and how the energy was introduced.
Only fragments carrying at least one charge can be detected. If this charge is retained on the N-terminal fragment, the ion is classified as either *a*, *b* or *c*, otherwise, if the charge is retained on the C-terminal fragment, the ion type is either *x*, *y* or *z*, all with a subscript number indicating the number of residues in the fragment (
Figure 1-36.).

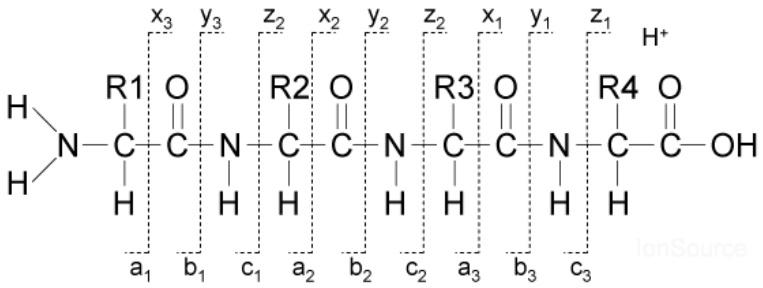

Figure 1-36. Nomenclature of the potential fragments of a precursor ion.

In low energy CID (i.e. collision-induced dissociation) a peptide carrying a positive charge fragments mainly along its backbone, generating predominantly *b* and *y* ions. In addition, *a**, *b** and *y** ions, with the star indicating loss of ammonia (-17 Da), are frequently observed when fragments contain R, K, N, or Q residues, while *a*°, *b*° and *y*° ions, with the ° indicating loss of water (-18 Da), are frequently observed when fragments contain S, T, E or D residues.

2. AIM OF THE WORK

Early diagnosis of infection is of paramount importance in neonatology clinical care units since it has a major impact on therapy management, clinical course and patient outcome. The traditional methods for the diagnosis of sepsis (i.e. cultures of blood, urine, cerebrospinal fluid or bronchial fluid specimens) usually take 24 to 48 hours. Furthermore, clinical symptoms frequently manifest themselves in the absence of a positive culture [53-55]. In view of the above diagnostic and therapeutic dilemmas, a more unequivocal test for the differential diagnosis of infection and sepsis is needed.

The main aim of the project was the investigation of saliva as a biological fluid reporting on health status of newborns followed by the development of an innovative and noninvasive diagnostic method to differentiate bacterial from noninfectious causes of inflammation.

Two parallel approaches were applied.

- Untargeted analysis to characterize the protein composition of whole saliva samples collected from healthy newborns within 48 hours after birth according to a precise study protocol approved by the local ethical committee. The comparison between healthy and unhealthy newborns will eventually highlight the alteration of whole saliva protein patterns as well as over or under-expressed proteins.

- Targeted analysis of acute-phase proteins widely considered plasmatic markers of sepsis, C-reactive protein, calcitonin and its precursor procalcitonin, to develop an analytical MS-based method to qualitatively and quantitatively assay them within salivary samples.

The bioanalytical platform has been applied to saliva samples. However, the developed methods and strategies can be adapted to other biological fluids.

3. RESULTS

3.1. UNTARGETED GEL-BASED APPROACHES

In this thesis, untargeted gel-based approaches were exploited to characterize the protein content of salivary samples collected from healthy newborns in their early 48 hours after birth. The comparison between healthy newborns and newborns affected by bacterial infection will be carried out at a later stage of the project. In particular the aims of this phase of the study were the description of the overall protein profile and the identification of the most abundant proteins, as well as the clarification of the differences, if present, occurring between samples collected in the first and in the second day of life. Both 2D-PAGE – MALDI-TOF/TOF and SDS-PAGE – LC-(HR)MS/MS analyses were performed in order to collect complementary information (Figure 3-1).
Results are showed in this section and discussed in paragraph 4.1.

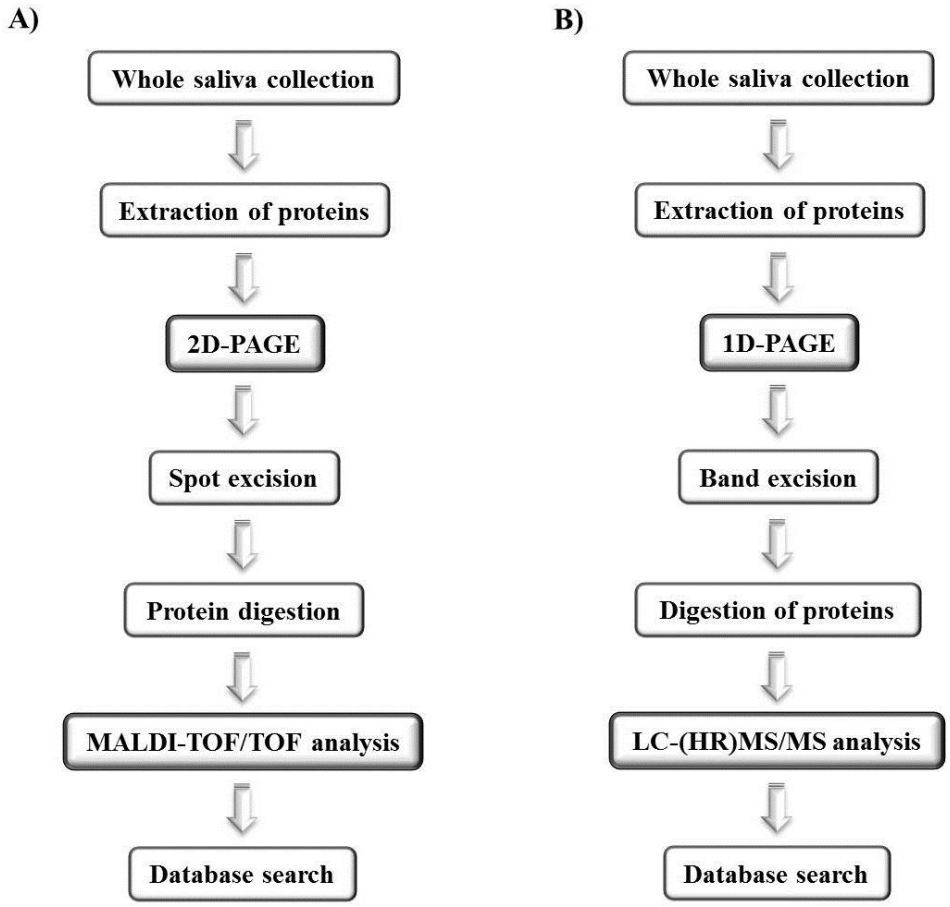

Figure 3-1. Scheme of the gel-based discovery approaches applied in this work of thesis: 2D-PAGE and MALDI-TOF/TOF (A) and 1D-PAGE and LC-(HR)MS/MS (B). 2-DE analyses were performed on both single samples and pooled samples.

2-DE – MALDI-TOF/TOF

To begin with, some of the collected salivary samples were analyzed individually to explore the intra- and inter-individual variability. Later, analyses of pooled samples were performed for a more comprehensive examination of the protein content in healthy newborns.

Single newborn analyses

Three newborns were individually analyzed (Table 3-1). For each newborn the sample collected within 24 hours after delivery (day 1) and the one collected between 24 and 48 hours after delivery (day 2) were analyzed separately and in duplicate, therefore four 2-DE gels were obtained for each newborn.

Table 3-1. Clinical data of newborns whose samples were individually exploited to perform 2-DE analyses.

NEWBORN	RACE	SEX	WEIGHT (g)	AGE (weeks)	DELIVERY	samplings	
						I	II
115	African	F	4800	40	spontaneous	19 hours	43 hours
516	Caucasian	M	3250	39	caesarean section	19 hours	43 hours
1396	Caucasian	F	2920	38	spontaneous	17 hours	41 hours

Each gel was at first stained with Bio-safe Coomassie Blue and then, after destaining, a Silver staining was performed (Figure 3-2).

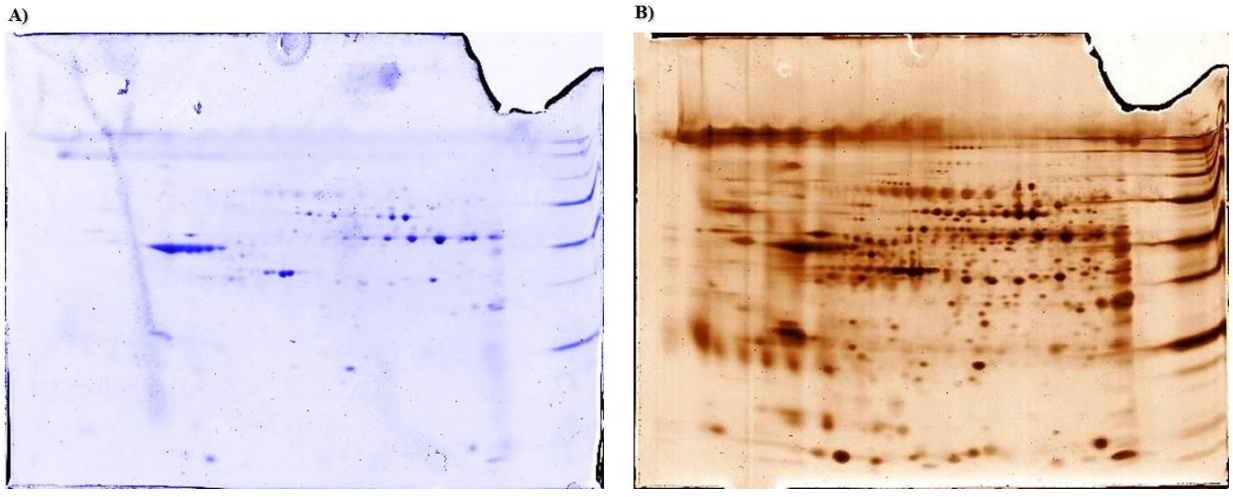

Figure 3-2. Example images of the same 2-DE gel stained at first with Bio-safe Coomassie Blue (A) and later with Silver staining (B). The difference in sensitivity between the two stains can be appreciated.

The images acquired after Coomassie and Silver staining were compared. As expected, the latter staining exhibited greater sensitivity (low ng): considering all the spots detected in the first and in the second day of the three newborns analyzed, an average of 105 spots were detected with Coomassie staining versus an average of 305 spots detected with the Silver staining. Therefore, almost the 65% of the total number of

spots detected are present in amounts included between the limits of detection of the two stains (0.5-10 ng).

The MALDI-TOF analysis of the digestion solutions of the excised spots led to define the identity of the most abundant proteins in the oral fluid samples: polymeric immunoglobulin receptor (PIGR), serum albumin, keratins and actins (Figure 3-3).

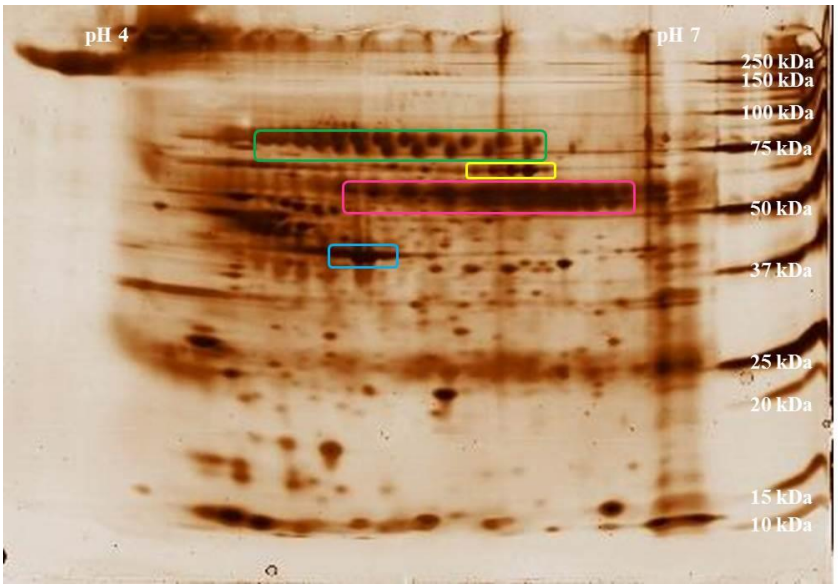

Figure 3-3. Image of a 2-DE gel showing the regions were most abundant proteins focalize: polymeric immunoglobulin receptor (PIGR), serum albumin, keratins and actins focalize in the gel regions marked in green, yellow, pink and blue respectively.

Pool analyses

Two distinct pools were created, merging respectively the extraction solutions of samples collected from six healthy newborns within 24 hours after delivery (day 1) and between 24 and 48 hours after delivery (day 2) (Table 3-2). Pools were created using the same amount of protein from each sample and a total protein quantity of 40 µg was loaded onto each IPG strip.

Table 3-2. Clinical data of newborns whose samples were pooled to perform 2-DE analyses of day 1 and day 2.

NEWBORN	RACE	SEX	WEIGHT (g)	AGE (weeks)	DELIVERY	samplings	
						I	II
1061/2013	Caucasian	F	3140	37	caesarean section	12 hours	33 hours
1062/2013	Caucasian	M	2790	38	spontaneous	11 hours	32 hours
1056/2013	Caucasian	M	4210	41	caesarean section	18 hours	39 hours
1588/2013	Caucasian	M	3640	40	spontaneous	14 hours	38 hours
1645/2013	Caucasian	F	4270	40	spontaneous	15 hours	39 hours
2201/2013	Caucasian	M	2620	38	caesarean section	7 hours	32 hours

The pool were analyzed separately and in duplicate, therefore four 2-DE gels were obtained (Figure 3-4).

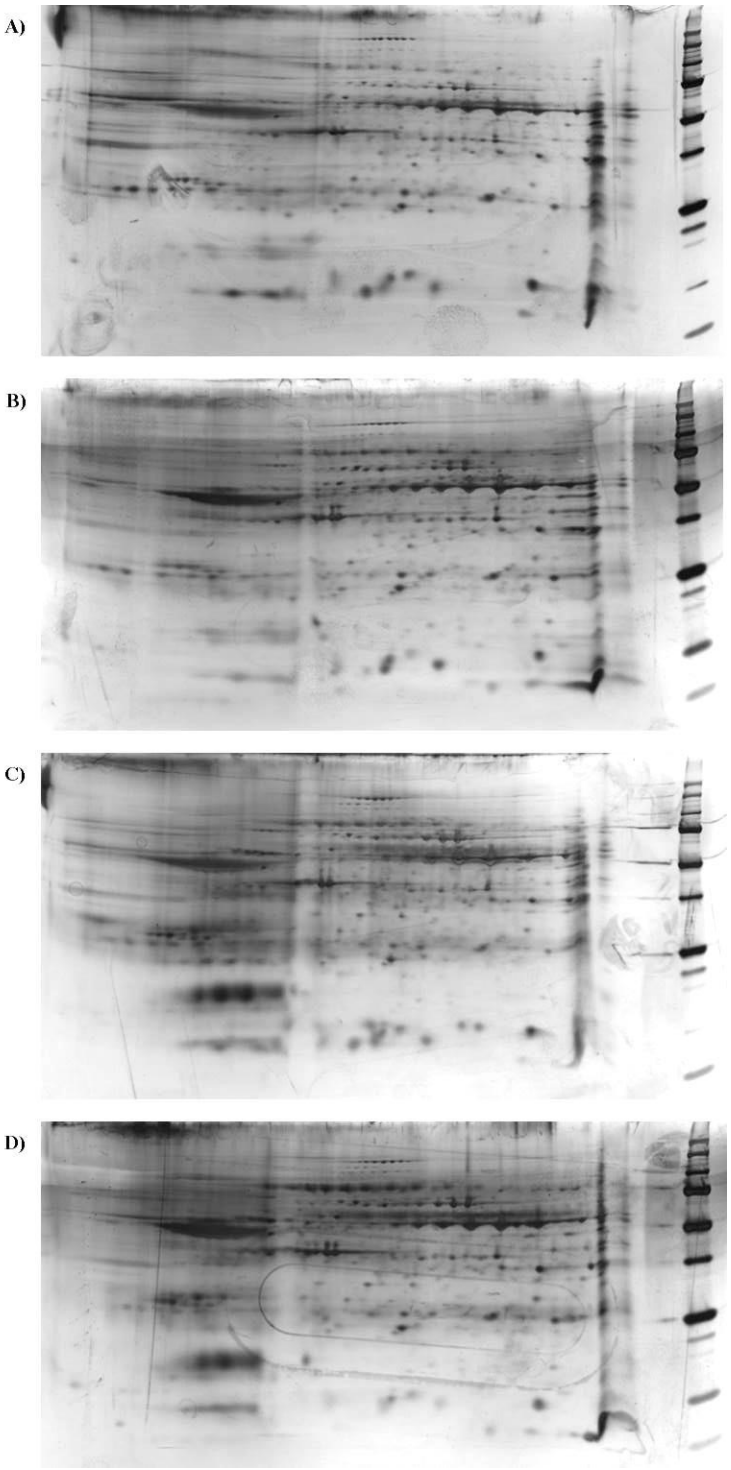

Figure 3-4. Images of the gels obtained from the 2-DE analysis of the pool (silver staining): A) and B) are technical replicates of the pool obtained from 6 samples collected from newborns within 24 hours after delivery (day 1), whereas C) and D) are technical replicates of the pool obtained from 6 samples collected from the same newborns between 24 and 48 hours after delivery (day 2).

Image analysis of the four gels was performed with PDQuest software (Figure 3-5). Gel C) in Figure 3-4 was taken as reference.

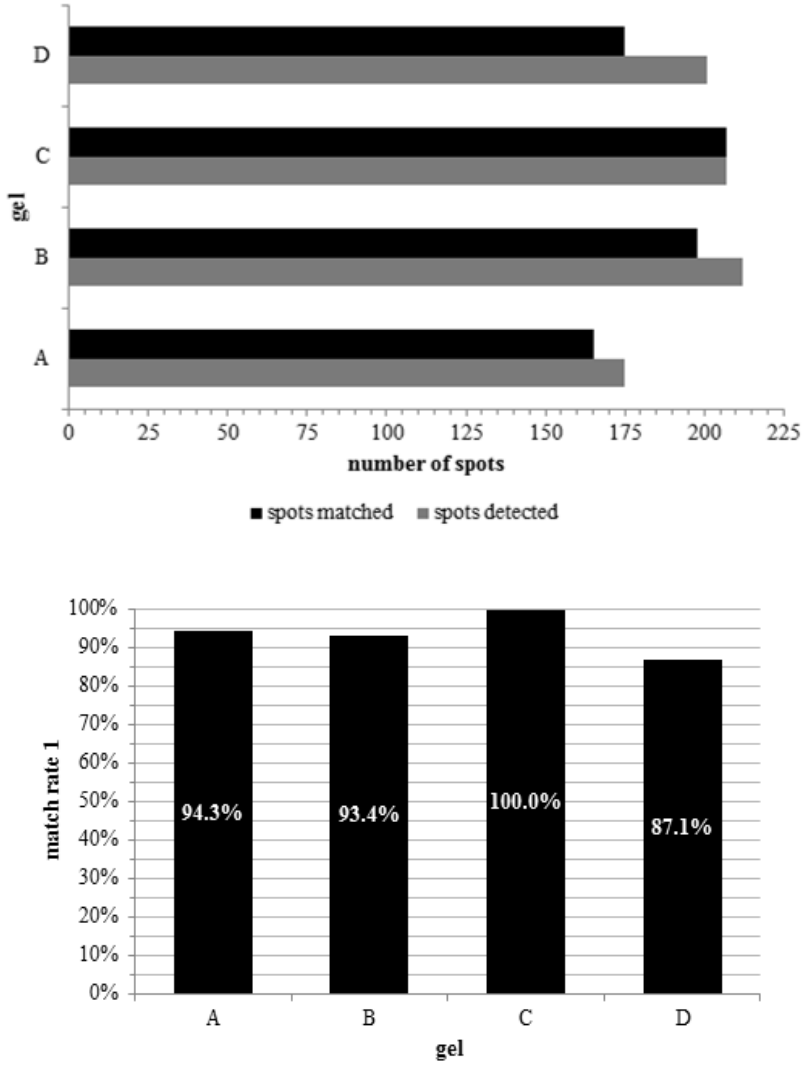

Figure 3-5. Image analysis of the pool. The upper schematic shows the relationship between the number of spots detected in each of the four gels and the number of spots matched with the gel taken as reference (gel C). The bottom schematic shows the match rate 1 value for each gel. A and B are technical replicates of day 1, whereas C and D are technical replicates of day 2.

Gel B and D, second technical replicate of day 1 and 2 respectively, were compared and a scatter plot was obtained, highlighting the matched spots whose intensity varied more than twofold up or down (Figure 3-6). Among the matched spots, protein S100-A8 (calgranulin-A), protein S100-A9 (calgranulin-B) and Heat shock protein beta-1 (Hsp27) were identified as proteins whose intensity in day 1 was more than twofold higher than in day 2.

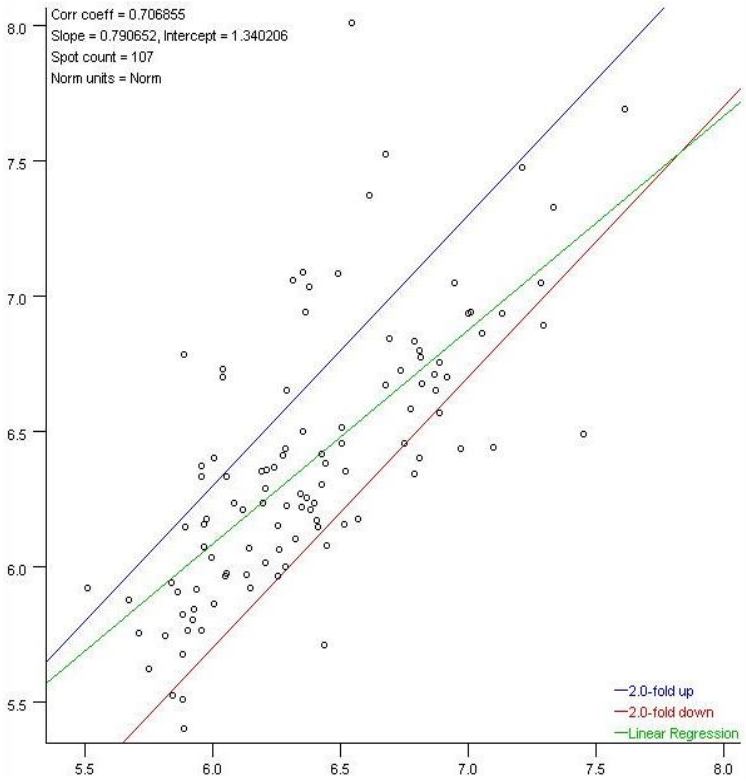

Figure 3-6. Comparison between day 1 and day 2. Scatter plot: x-axis = gel B and y-axis = gel D.

The identification of Hsp27 is reported as an example (Figure 3-7 and Figure 3-8).

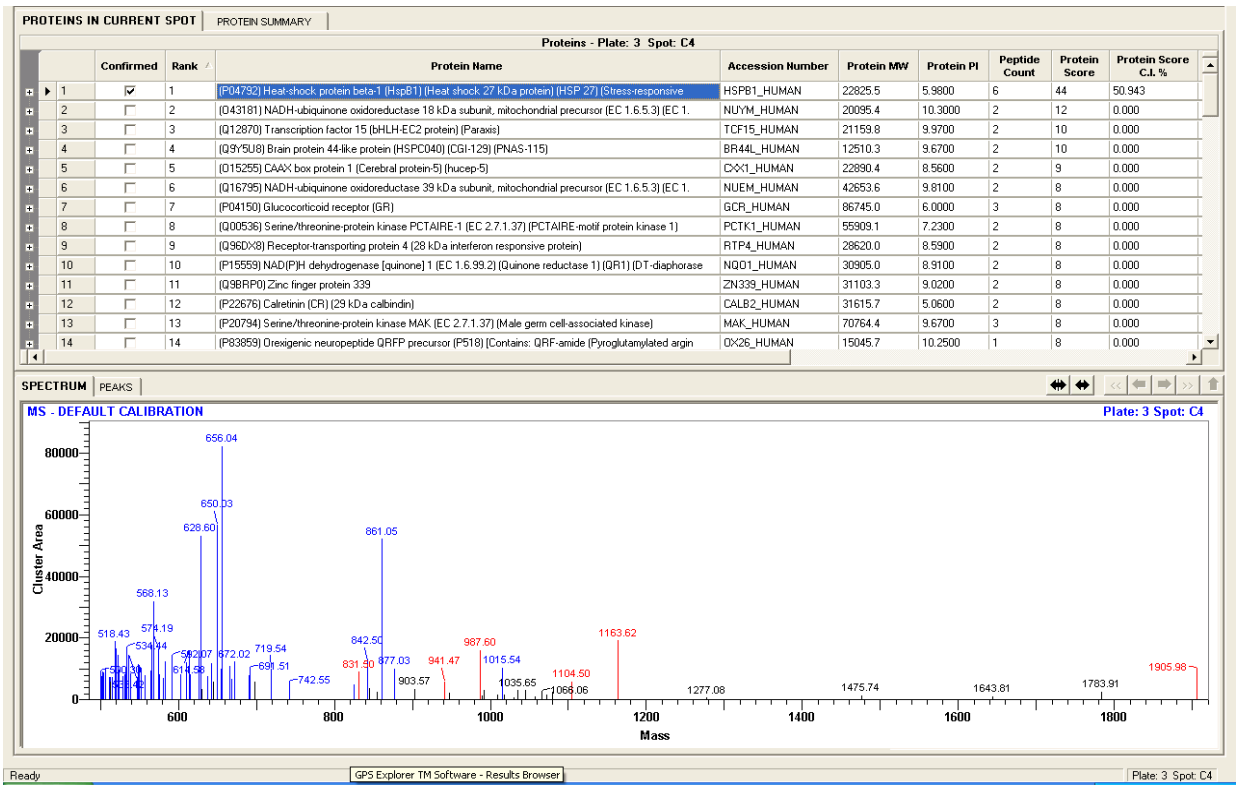

	Confirmed	Rank	Protein Name	Accession Number	Protein MW	Protein PI	Peptide Count	Protein Score	Protein Score C.I. %
1	☑	1	(P04792) Heat-shock protein beta-1 (HspB1) (Heat shock 27 kDa protein) (HSP 27) (Stress-responsive	HSPB1_HUMAN	22825.5	5.9800	6	44	50.943
2	☐	2	(O43181) NADH-ubiquinone oxidoreductase 18 kDa subunit, mitochondrial precursor (EC 1.6.5.3) (EC 1.	NUYM_HUMAN	20095.4	10.3000	2	12	0.000
3	☐	3	(Q12870) Transcription factor 15 (bHLH-EC2 protein) (Paraxis)	TCF15_HUMAN	21159.8	9.9700	2	10	0.000
4	☐	4	(Q9Y5U8) Brain protein 44-like protein (HSPC040) (CGI-129) (PNAS-115)	BR44L_HUMAN	12510.3	9.6700	2	10	0.000
5	☐	5	(O15255) CAAX box protein 1 (Cerebral protein-5) (hucep-5)	CXX1_HUMAN	22890.4	8.5600	2	9	0.000
6	☐	6	(Q16795) NADH-ubiquinone oxidoreductase 39 kDa subunit, mitochondrial precursor (EC 1.6.5.3) (EC 1.	NUEM_HUMAN	42653.6	9.8100	2	8	0.000
7	☐	7	(P04150) Glucocorticoid receptor (GR)	GCR_HUMAN	86745.0	6.0000	3	8	0.000
8	☐	8	(Q00536) Serine/threonine-protein kinase PCTAIRE-1 (EC 2.7.1.37) (PCTAIRE-motif protein kinase 1)	PCTK1_HUMAN	55909.1	7.2300	2	8	0.000
9	☐	9	(Q96DX8) Receptor-transporting protein 4 (28 kDa interferon responsive protein)	RTP4_HUMAN	28620.0	8.5900	2	8	0.000
10	☐	10	(P15559) NAD(P)H dehydrogenase [quinone] 1 (EC 1.6.99.2) (Quinone reductase 1) (QR1) (DT-diaphorase	NQO1_HUMAN	30905.0	8.9100	2	8	0.000
11	☐	11	(Q9BRP0) Zinc finger protein 339	ZN339_HUMAN	31103.3	9.0200	2	8	0.000
12	☐	12	(P22676) Calretinin (CR) (29 kDa calbindin)	CALB2_HUMAN	31615.7	5.0600	2	8	0.000
13	☐	13	(P20794) Serine/threonine-protein kinase MAK (EC 2.7.1.37) (Male germ cell-associated kinase)	MAK_HUMAN	70764.4	9.6700	3	8	0.000
14	☐	14	(P83859) Orexigenic neuropeptide QRFP precursor (P518) [Contains: QRF-amide (Pyroglutamylated argin	0X26_HUMAN	15045.7	10.2500	1	8	0.000

Figure 3-7. List of potential identifications from the analysis of the MALDI-TOF spectrum acquired.

Figure 3-8. Detail of the identification of Heat-shock protein beta-1. The upper table reports the amino acidic sequence of the identified peptides with the match errors between the observed and the calculated mass values. The table also reports for each peptide its position in the protein and the fixed/variable modifications (if present).

Another pool was analyzed merging the extraction solutions of samples collected from four healthy newborns on their second day after birth (Table 3-3).

Table 3-3. Clinical data of newborns whose samples were pooled to perform a 2-DE analysis of day 2.

NEWBORN	RACE	SEX	WEIGHT (g)	AGE (weeks)	DELIVERY	samplings	
						I	II
629	Caucasian	F	3250	40	spontaneous	15 hours	39 hours
1400	Caucasian	F	n. a.	40	spontaneous	8 hours	32 hours
1406	African	F	3880	39	spontaneous	6 hours	30 hours
1399	Caucasian	F	3250	38	caesarean section	4 hours	28 hours

Once again, the pool was created using the same amount of protein from each sample, but this time a total protein quantity of 100 µg was loaded onto the IPG strip and the 2-DE gel obtained was stained with Coomassie blue (Figure 3-9).

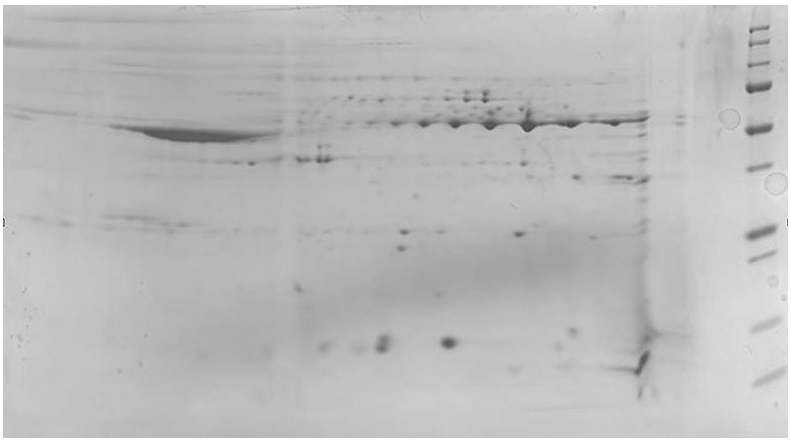

Figure 3-9. Coomassie staining of the 2-DE gel of the pool obtained from samples collected from four newborns on their second day after birth.

Overall, the identifications obtained from the MALDI-TOF analysis of digested protein spots are reported in Table 3-4.

Protein ID	MW (kDa)	pI	Coverage
14-3-3 protein sigma	27.8	4.68	10
Actin, cytoplasmic 1	41.7	5.29	73
Actin, cytoplasmic 2	41.8	5.31	23
Alpha-lactalbumin	14.1	4.70	47
Annexin A1	38.6	6.64	70
Apolipoprotein A-I	28.1	5.27	52
Fatty acid-binding protein, epidermal	15.0	6.82	80
Glutathione S-transferase P	23.2	5.44	74
Heat shock protein beta 1	22.0	5.98	25
Ig alpha-1 chain C region	37.7	6.08	55
Interleukin-1 receptor antagonist	17.1	5.42	46
Keratin, type I cytoskeletal 13	49.6	4.91	56
Keratin, type II cytoskeletal 4	57.3	6.25	75
Keratin, type II cytoskeletal 6C	59.9	8.14	12
Leukocyte elastase inhibitor	42.7	5.90	52
Peroxiredoxin-6	24.9	6.02	21
Polymeric immunoglobulin receptor	83.3	5.59	30
Protein S100-A8	10.7	6.57	21
Protein S100-A9	13.1	5.71	99
Serum albumin	66.5	5.67	78

Table 3-4. List of identifications obtained from the 2-DE – MALDI-TOF/TOF analyses of pooled samples. The identified proteins are reported in alphabetical order.

The main features of the identified proteins are summarized in the following charts (Figure 3-10 and Figure 3-11).

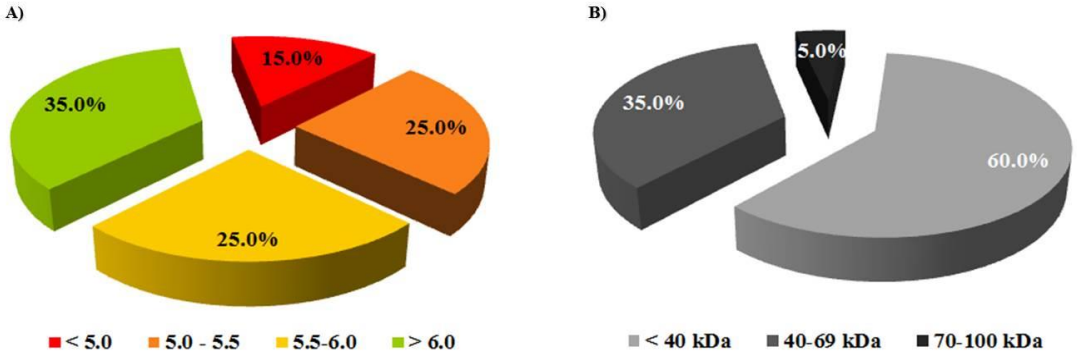

Figure 3-10. Pie charts summarizing the main characteristics of the identified proteins: molecular weight (A) and isoelectric point (B).

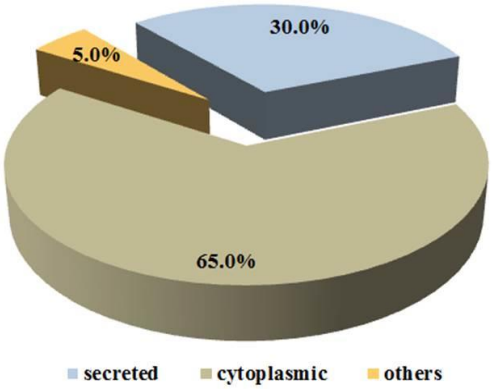

Figure 3-11. Pie chart summarizing the location of the identified proteins.

SDS-PAGE – LC-(HR)MS/MS

An experiment of mono-dimensional SDS-PAGE followed by band excision, tryptic digestion and LC-(HR)MS/MS analysis was performed to evaluate the feasibility of the method and its complementarity compared to the designed 2-DE – MALDI-TOF/TOF approach (Figure 3-12).

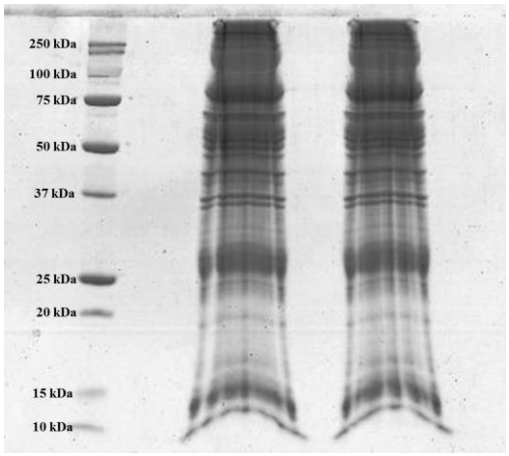

Figure 3-12. Image of a mono-dimensional SDS-PAGE gel. The sample was loaded in duplicate.

Identifications were obtained and a list is reported in Table 3-5. The main features of the identified proteins are summarized in the following charts (Figure 3-13 and Figure 3-14).

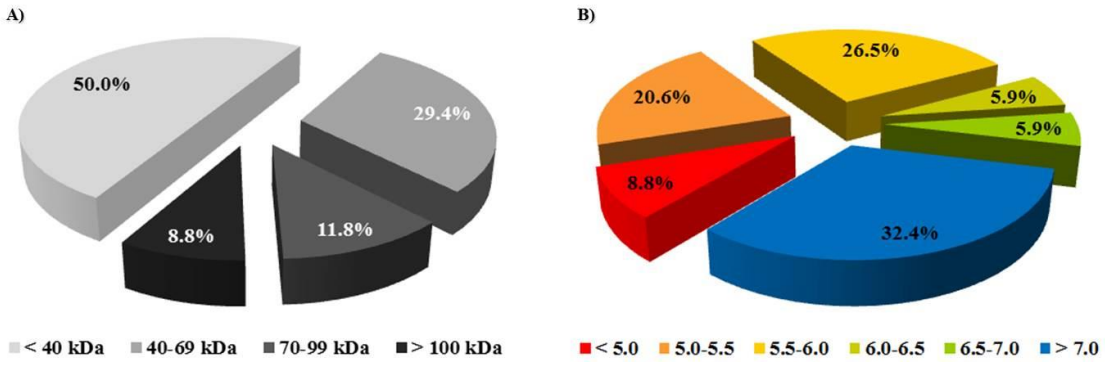

Figure 3-13. Pie charts summarizing the main characteristics of the identified proteins: molecular weight (A) and isoelectric point (B).

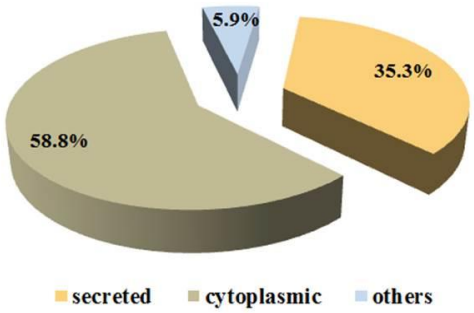

Figure 3-14. Pie chart summarizing the location of the identified proteins.

Protein ID	MW (Da)	pI	Peptide count	Coverage	Score
Deleted in malignant brain tumors 1 protein	260569	5.18	24	15.13	37.91
Alpha-2-macroglobulin-like protein 1	161004	5.50	30	10.73	48.07
Alpha-actinin-4	104788	5.27	41	21.41	84.95
Polymeric immunoglobulin receptor	83232	5.59	27	16.62	48.76
Lactotransferrin	78132	8.50	123	54.23	300.12
Protein-glutamine gamma-glutamyltransferase E	76584	5.61	37	25.83	76.94
Heat shock 70 kDa protein 1A/1B	70009	5.47	26	23.24	50.23
Serum albumin	69321	5.92	134	52.05	241.99
Cornulin 53 kDa (Squamous epithelial-induced stress protein)	53502	5.73	17	13.74	30.44
6-phosphogluconate dehydrogenase, decarboxylating	53106	6.80	18	18.63	42.99
Alpha-1-antichymotrypsin (SERPIN A3)	47621	5.33	17	18.91	29.94
Gamma-enolase	47239	4.91	12	13.59	19.07
Alpha-enolase	47139	7.01	42	42.86	89.38
Alpha-1-antitrypsin (SERPIN A1)	46707	5.37	12	16.27	18.06
Phosphoglycerate kinase 1	44586	8.30	15	16.55	38.74
Serpin B3	44537	6.35	11	15.90	22.93
Leukocyte elastase inhibitor (SERPIN B1)	42715	5.90	14	16.89	31.28
Fructose-bisphosphate aldolase A	39395	8.30	17	13.74	24.76
Mucin-7	39135	8.99	23	8.75	18.25
Annexin A1	38690	6.57	78	49.13	228.86
Annexin A2	38580	7.57	99	64.01	253.88
Macrophage-capping protein	38474	5.82	5	14.94	11.83
L-lactate dehydrogenase A chain	36665	8.44	11	19.88	19.36
Glyceraldehyde-3-phosphate dehydrogenase	36030	8.57	55	28.06	101.82
Malate dehydrogenase, mitochondrial	35481	8.92	12	19.53	22.02
Zinc-alpha-2-glycoprotein	34237	5.71	21	35.57	33.03
14-3-3 protein sigma	27757	4.68	45	39.11	98.96
Heat shock protein beta-1	22768	5.98	15	27.80	26.68
Peroxiredoxin-1	22096	8.27	6	14.07	1.92
Small proline-rich protein 3	18142	8.86	41	85.21	88.59
Alpha-lactalbumin	16214	4.83	23	28.17	58.79
Protein S100-A9 (Calgranulin-B)	13234	5.71	30	56.14	59.18
Cystatin-A	11000	5.38	10	37.76	23.64
Protein S100-A8 (Calgranulin-A)	10828	6.50	32	58.06	56.85

Table 3-5. List of identifications obtained from the SDS-PAGE – LC-(HR)MS/MS analysis of a single-newborn sample. The identified proteins are reported in decreasing order of molecular weight.

3.2. TARGETED ANALYSES

While waiting for the identification of a specific target protein (or a pattern of target proteins) through the gel-based discovery approach, the targeted analysis was focused on the development of an analytical method based on liquid chromatography coupled to mass spectrometry to qualitatively and quantitatively assay C-reactive protein, calcitonin and its precursor procalcitonin, acute-phase proteins widely considered plasmatic markers of sepsis.

In the following sections the results of the mass spectrometric characterization of hCT, hPCT and hCRP, are reported. The development of the most appropriate sample preparation conditions in order to accurately assay the above-mentioned proteins within biological samples is shown together with the progressive optimization of the chromatographic and mass spectrometric conditions used with the different analytical platforms. The general workflow of analysis is summarized in Figure 3-15.

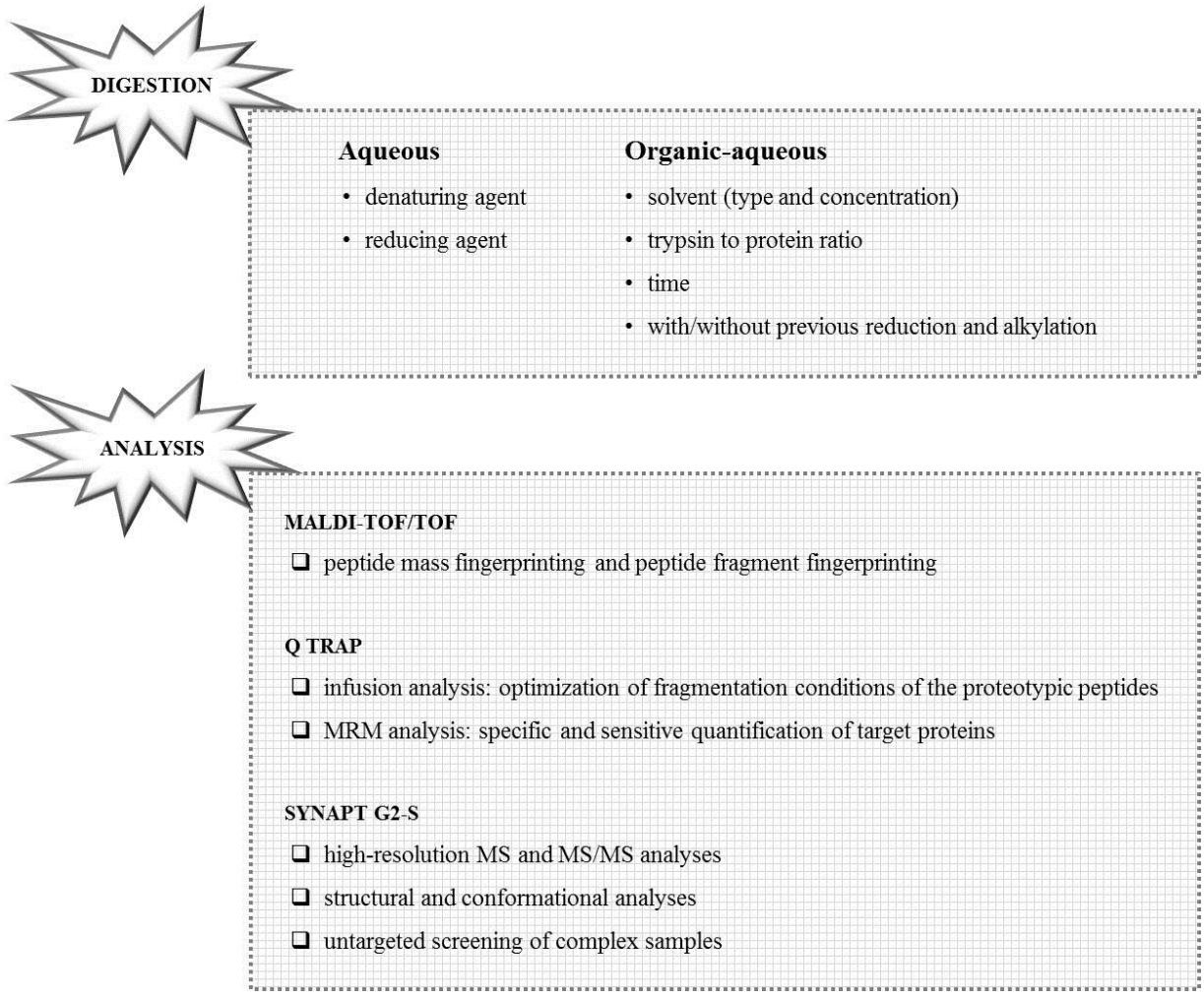

Figure 3-15. General workflow of analysis of human calcitonin, human procalcitonin and C-reactive protein applied in this thesis. The main variables explored in the aqueous or organic-aqueous digestion step are reported. The following MS analyses of the digestion solutions were carried out exploiting three different instruments (4800 MALDI-TOF/TOF, 4000 Q TRAP and Synapt G2-S) to gather complementary information on the proteins of interest.

MALDI-TOF-based peptide mass fingerprinting was exploited to compare different sample preparation conditions and in particular to test the feasibility of a mixed organic-aqueous digestion instead of a classical procedure in aqueous solution. MALDI-TOF/TOF spectra were also acquired in some cases to identify peptides whose signal was not expected on the basis of a theoretical tryptic cleavage, due to the presence of missed cleavages.

Q TRAP infusion analyses were performed to verify the ESI ionizability of the peptides of interest as multiply charged species and to figure out the optimal experimental conditions for the fragmentation of the proteotypic peptides, especially in the triple quadrupole mode, with a view to the subsequent MRM analyses.

Whenever possible, MS^E experiments were carried out to evaluate the applicability of a similar platform to high-throughput screening of the proteins of interest and their post-translational modifications within biological samples.

Results are showed in this section and discussed in paragraph 4.2.

TARGETED ANALYSES IN AQUEOUS SOLUTION

Human calcitonin

Analysis of the intact protein

Solubilization of the human calcitonin (hCT) standard at 1 mg/ml was performed in 20 mM ammonium bicarbonate. MALDI-TOF analysis was performed in order to characterize the standard solution prior to the tests of different sample preparations (Figure 3-16).

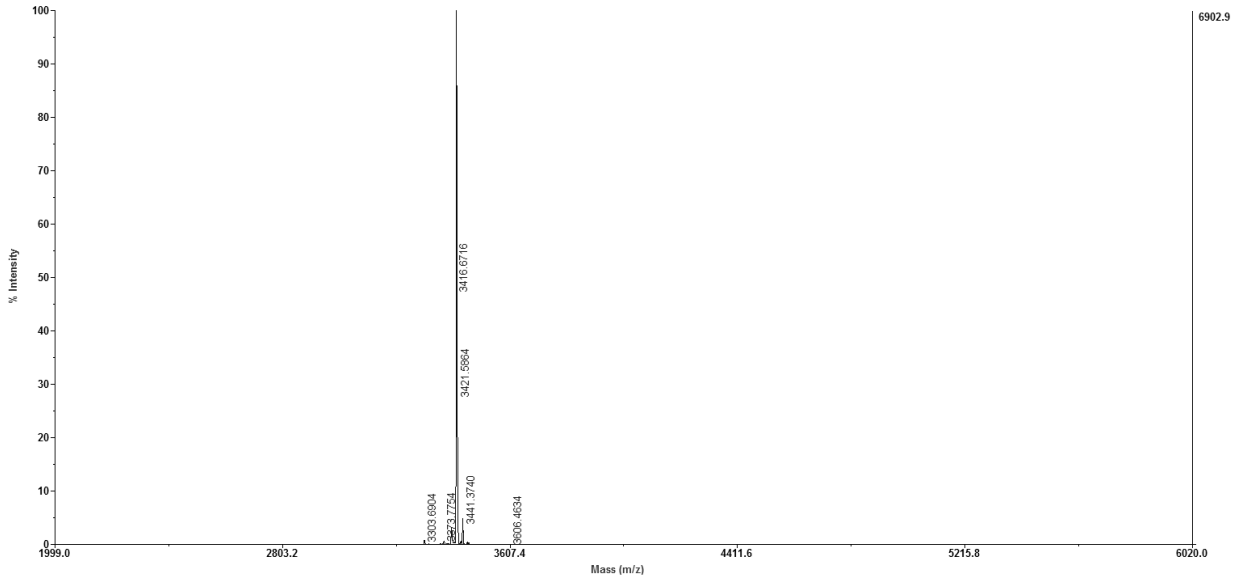

Figure 3-16. MALDI-TOF spectrum of human calcitonin standard.

Sequence	Length (aa)	Theoretical monoisotopic molecular weight	Experimental monoisotopic $[M+H]^+$
CGNLSTCMLGTYTQDFNKFHTFPQTAIGVGAP	32	3418.58	3416.6716

The theoretical monoisotopic molecular weight reported in the upper table was calculated on the basis of the amino acidic sequence, but because of the disulfide bond between cysteine 1 and 7 and the amidated C-terminal proline, the effective theoretical monoisotopic molecular weight of intact human calcitonin is 3415.5789 Da. Therefore, the experimental monoisotopic weight observed is in good agreement with the expected one.

Two different protein denaturation procedures were considered: a SDS-based denaturation and a urea/thiourea procedure.

SDS-based denaturation

Two different sample preparations were tested, one at 4 °C and the other at 37 °C.
Protocol 1:

- thawing of an aliquot of frozen hCT stock solution (1 mg/ml in 20 mM ammonium bicarbonate)

- denaturation and reduction in 0.1% SDS, 48 mM DTE; 5 minutes at 95 °C, then 1 hour at 4 °C
- alkylation in 100 mM IAA, 30 minutes at 4 °C in the dark
- sample desalting with GE Healthcare PD Mini-Trap G-10
- protein concentration in speed-vac to theoretical concentration of 0.1 mg/ml.

Protocol 2:

- thawing of an aliquot of frozen hCT stock solution (1 mg/ml in 20 mM ammonium bicarbonate)
- denaturation and reduction in 0.1% SDS, 48 mM DTT; 5 minutes at 95 °C, then 1 hour at 37 °C
- alkylation in 100 mM IAA, 30 minutes at 37 °C in the dark
- desalting with GE Healthcare PD Mini-Trap G-10 → elution at theoretical protein concentration of 48 µg/ml.

Neither of the two preparations gave satisfactory results in terms of yield of the alkylation reaction (data not shown).

Protein denaturation in urea and thiourea mixture

Sample preparation:

- protein denaturation in 20 mM ammonium bicarbonate, 6 M urea, 2 M thiourea
- reduction in 48.75 mM DTT, 30 minutes at 25 °C
- alkylation in 100 mM IAA, 30 minutes at 25 °C in the dark
- desalting with GE Healthcare PD Mini-Trap G-10.

MALDI-TOF ANALYSIS

The MALDI-TOF spectrum acquired shows that the reduction of the disulfide bond and the subsequent alkylation of the cysteine residues can be considered complete: most of the protein is in the bis-alkylated state and only a small fraction is in the mono-alkylated state (Figure 3-17).

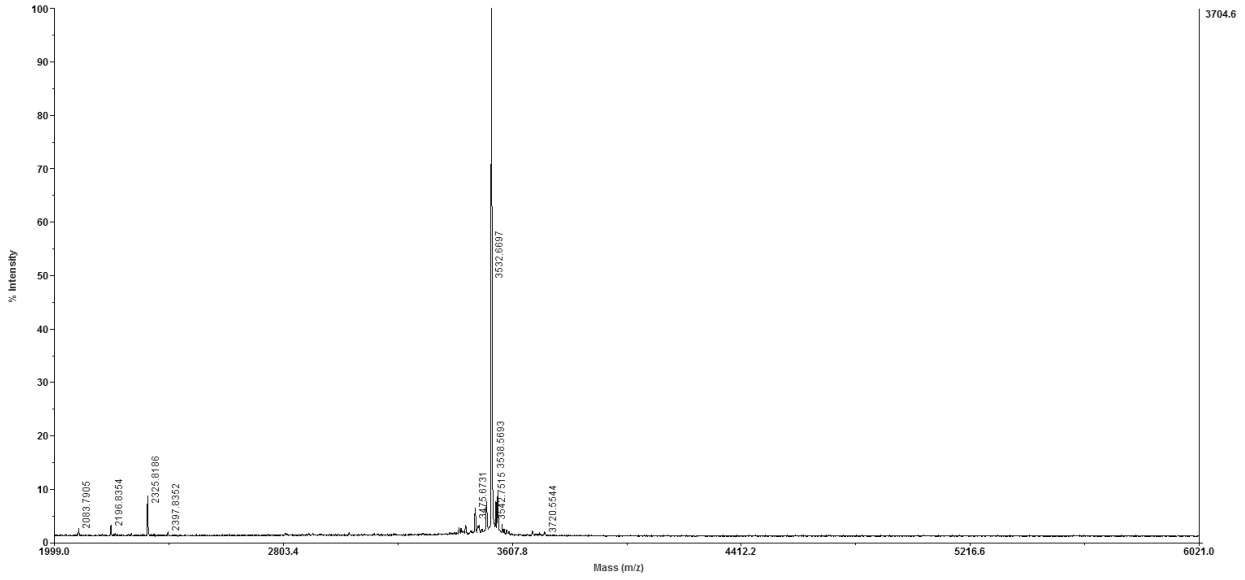

Figure 3-17. MALDI-TOF spectrum of intact hCT after the alkylation reaction.

Peptide	Length (aa)	Position	Theoretical monoisotopic molecular weight	Experimental monoisotopic $[M+H]^+$
Human calcitonin	32	1 – 32	3418.58	-
Mono-alkylated human calcitonin	32	1 – 32	3475.60	3475.6731
Bis-alkylated human calcitonin	32	1 – 32	3532.62	3532.6697

Q TRAP INFUSION ANALYSIS

The solution of intact hCT was infused in the Q TRAP and analyzed in EMS mode (Figure 3-18).

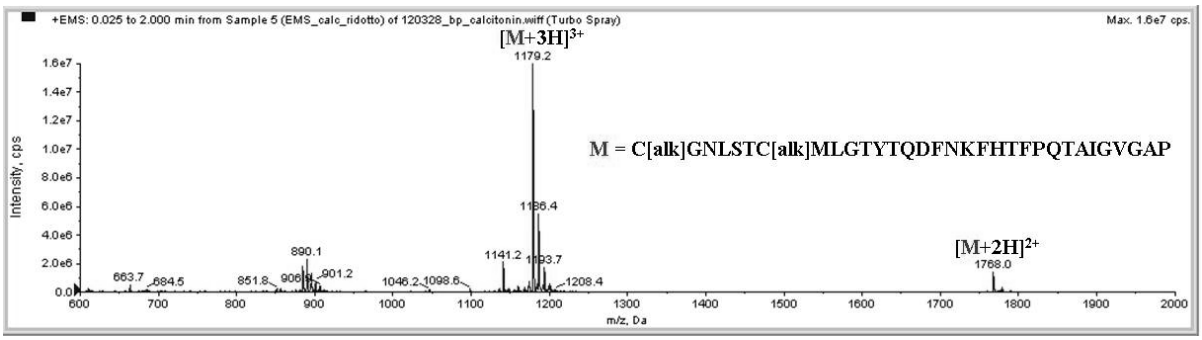

Figure 3-18. EMS spectrum of intact hCT after the alkylation reaction.

The m/z value of the most abundant ion in the full scan spectrum was compatible with the one expected for the triply-charged ion of the bis-alkylated intact protein. Therefore an ER spectrum was acquired, which confirmed the triply-charge state of the ion of interest (Figure 3-19).

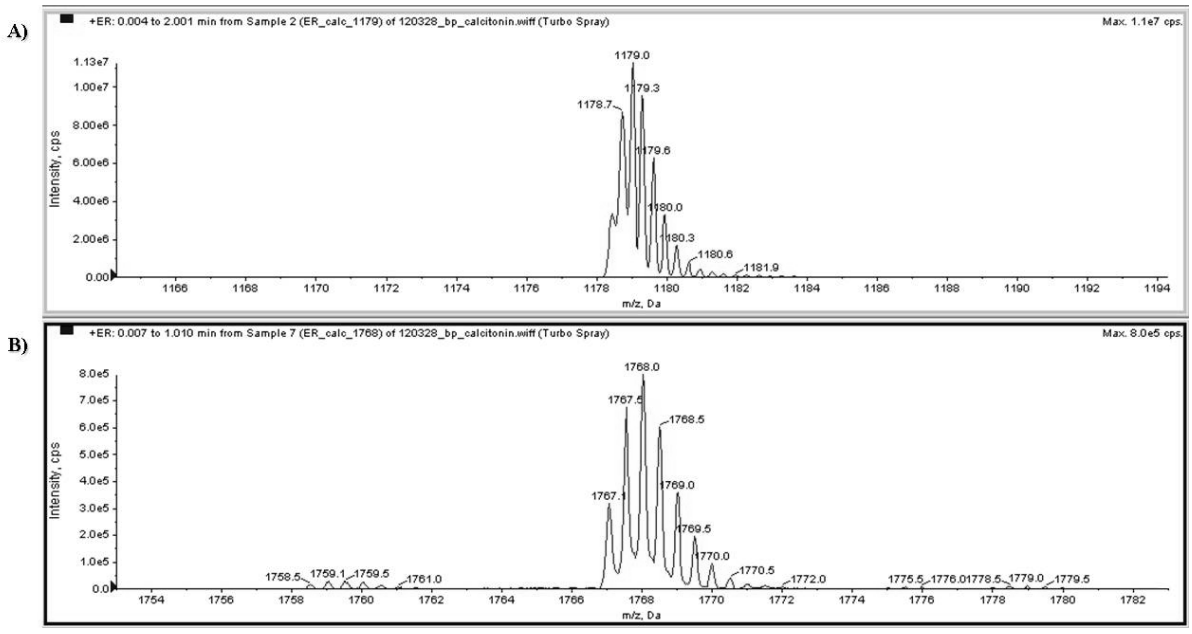

Figure 3-19. ER spectra of m/z 1179.0 (A) and 1768.0 (B), the triply- and doubly-charged ions of the bis-alkylated intact hCT respectively.

Intact hCT with alkylated Cys residues mainly ionizes in ESI as $[M+3H]^{3+}$ (m/z 1179.0).

EPI and MS2 fragmentation spectra were acquired for the triply-charged ion of the bis-alkylated intact protein (Figure 3-20 and Figure 3-21 respectively).

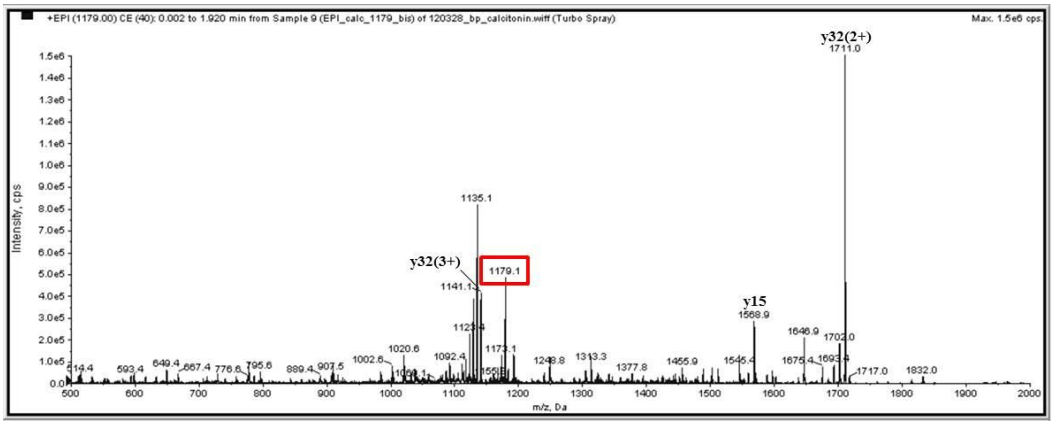

Figure 3-20. EPI spectrum of the triply-charged ion of the bis-alkylated intact hCT (m/z 1179.0). Applied CE = 40. The precursor ion is marked in red.

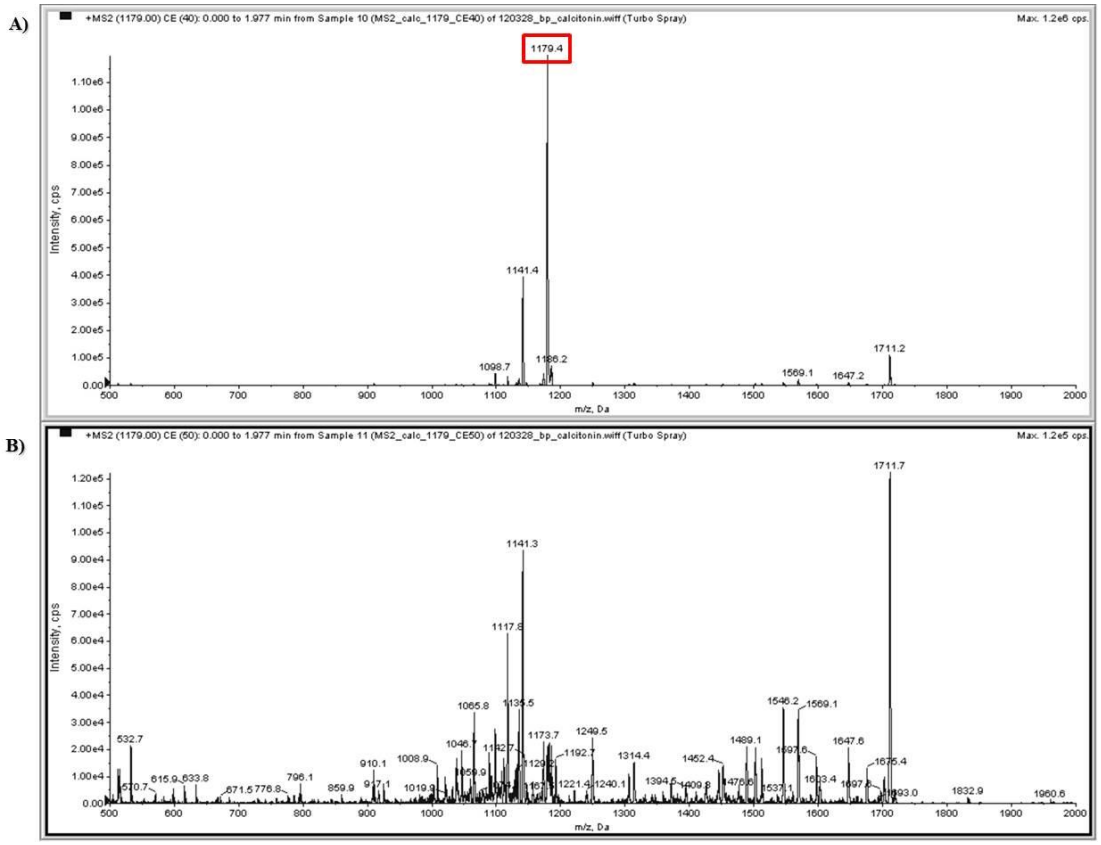

Figure 3-21. MS2 spectra of the triply-charged ion of the bis-alkylated intact hCT (m/z 1179.0). The applied CE values are 40 (A) and 50 (B) volts. The precursor ion is marked in red.

MRM ANALYSIS

The following transitions were analyzed:

m/z precursor ion (Q1)	m/z fragment ion (Q3)	Fragment ion
1179.0	1711.0	y32(2+)
1179.0	1569.0	y15(1+)
1179.0	1141.0	y32(3+)
1179.0	1249.0	y23(2+)
1179.0	910.0	y10(1+)

Linearity in the theoretical range of concentrations 0.4 – 50 µg/ml was tested and calibration curves were obtained (Figure 3-22).

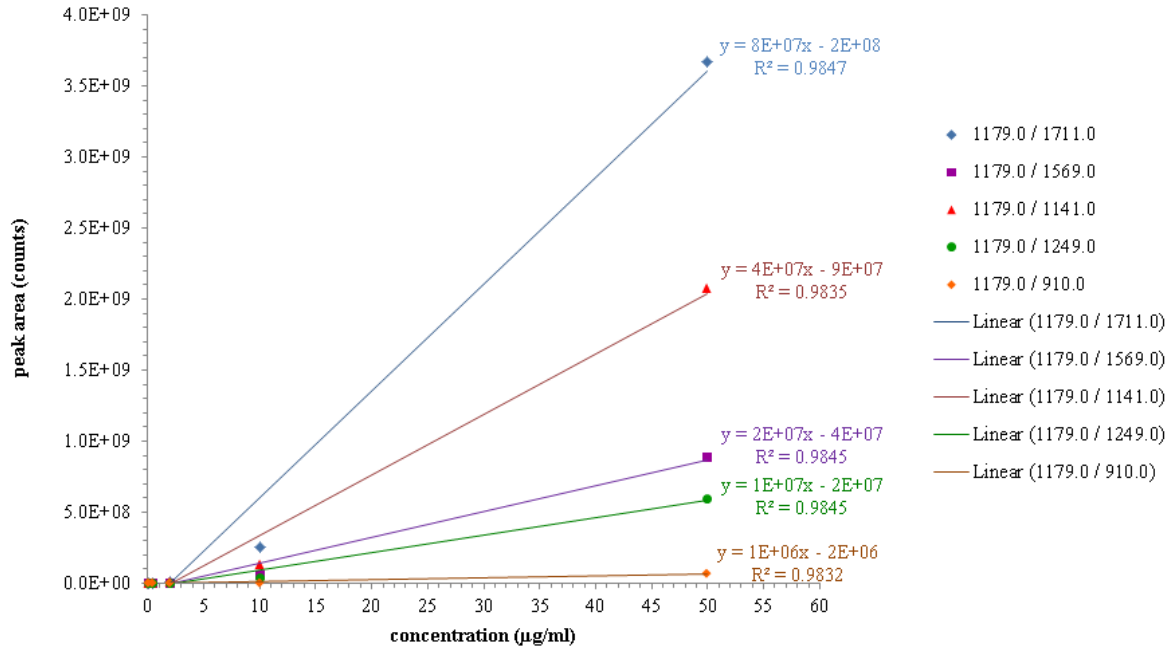

Figure 3-22. Calibration curves obtained for intact hCT.

R^2 values are ≥ 0.983 for each of the transitions analyzed.

Analysis of the digested protein

The peptides originated by a virtual tryptic digestion of hCT are reported in Table 3-6, together with their cleavage probabilities.

Position of cleavage site	Name of cleaving enzyme(s)	Resulting peptide sequence (see explanations)	Peptide length [aa]	Peptide mass [Da]	Cleavage probability
18	Trypsin	CGNLSTCMLGTYTQDFNK	18	1996.255	91.4 %
32	end of sequence	FHTFPQTAIGVGAP	14	1442.637	-

Table 3-6. Tryptic digestion of hCT: cleavage sites and cleavage probabilities. From http://web.expasy.org/peptide_cutter/

Two protocols of digestion in aqueous solution were tested for hCT, essentially differing in the denaturing step: the first protocol was based on SDS and thermal denaturation whereas the second protocol was based on urea and thiourea mixture.

Protein denaturation in SDS

Protocol based on SDS and thermal denaturation:

- denaturation and reduction in 100 mM NH4HCO3, 0.1% SDS, 9.5 mM TCEP, 5 minutes at 95 °C
- alkylation in 17 mM IAA, 30 minutes at 25 °C in the dark
- sample dilution 2x in 100 mM ammonium bicarbonate
- in-solution digestion: 16 hours at 37 °C with trypsin 1:25 (w/w)
- quenching of digestion by addition of 0.1% formic acid.

MALDI-TOF ANALYSIS

Desalting of the digestion solution of hCT prior to MALDI-TOF analysis was performed using a ZipTip C18 Pipette Tip. The MALDI-TOF spectrum of the digestion solution is characterized by the presence of signals which can be attributed to hCT peptides, although a large part of the protein remained intact (Figure 3-23).

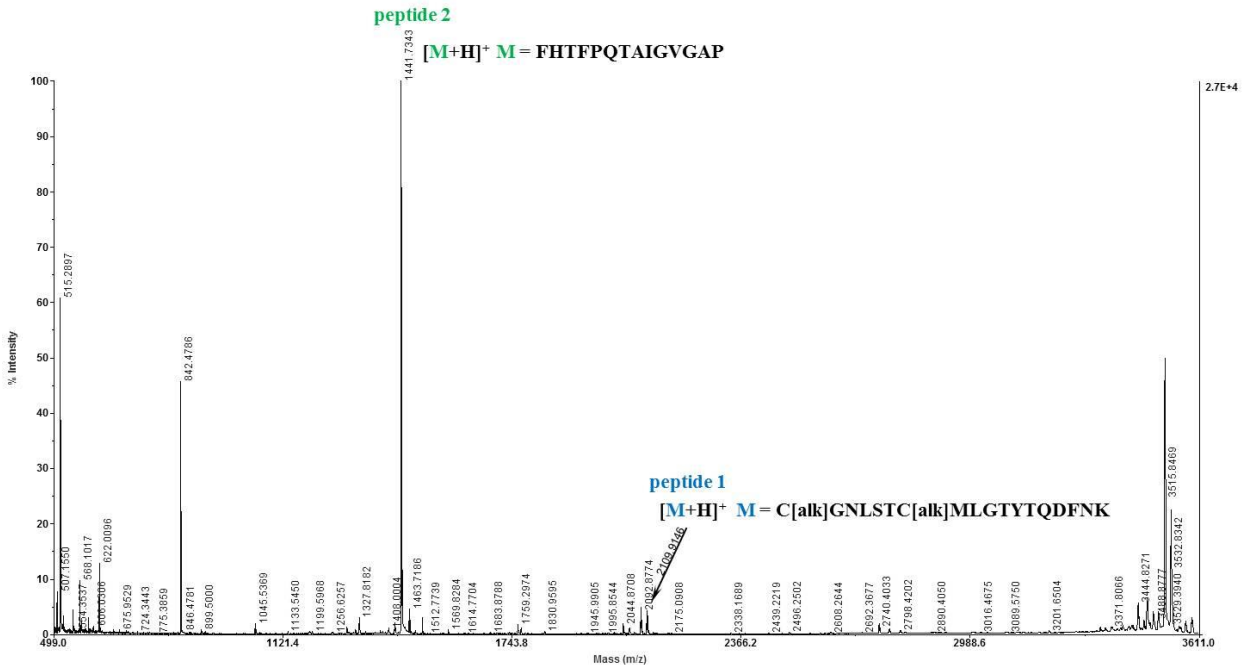

Figure 3-23. MALDI-TOF spectrum of the digestion solution of hCT.

Peptide sequence	Length (aa)	Position	Theoretical monoisotopic molecular weight	Experimental monoisotopic $[M+H]^+$
FHTFPQTAIGVGAP	14	19 – 32	1441.74	1441.7343
C[alk]GNLSTC[alk]MLGTYTQDFNK	18	1 – 18	2108.89	2109.9146
Bis-alkylated human calcitonin	32	1 – 32	3532.62	3532.8342

Sequence coverage = 100%

Protein denaturation in urea and thiourea mixture

Protein denaturation using urea and thiourea:

- denaturation in 20 mM NH4HCO3, 6 M urea, 2 M thiourea
- reduction in 48.75 mM DTT, 30 minutes at 25 °C
- alkylation in 100 mM IAA, 30 minutes at 25 °C in the dark
- desalting with GE Healthcare PD Mini-Trap G-10
- in-solution digestion: 15 hours at 37 °C with trypsin 1:50 (w/w)
- quenching of digestion by addition of 0.1% formic acid.

MALDI-TOF ANALYSIS

The MALDI-TOF spectrum of the digestion solution is characterized by the presence of signals which can be attributed to the two expected hCT peptides (Figure 3-24).

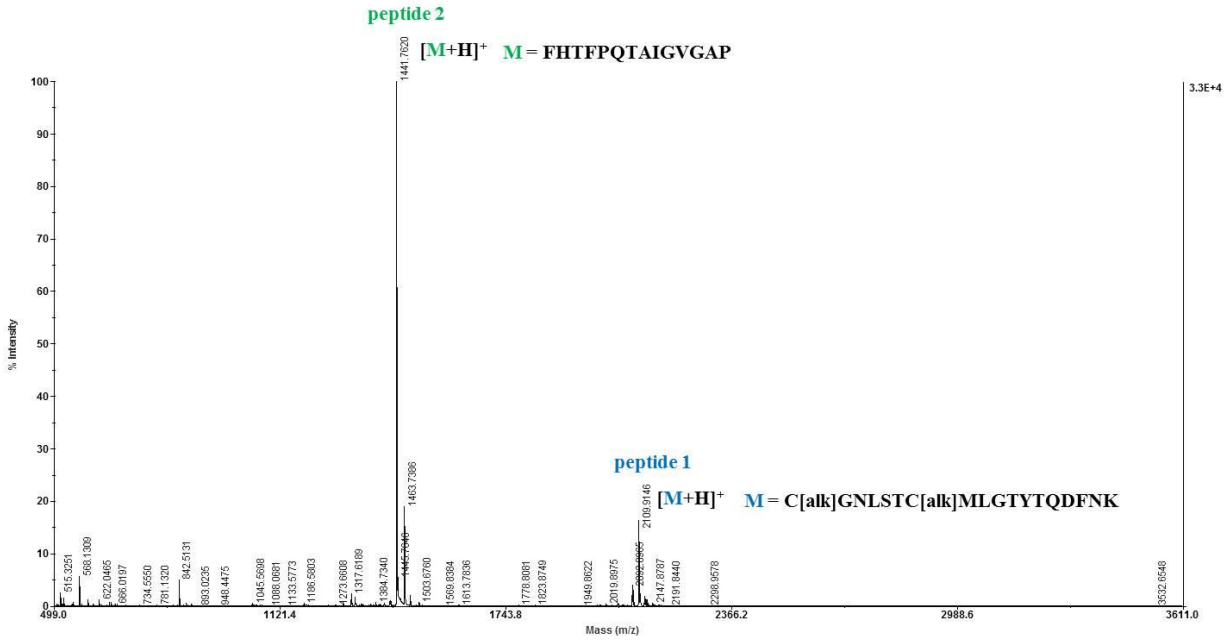

Figure 3-24. MALDI-TOF spectrum of the digestion solution of hCT.

Peptide	Length (aa)	Position	Theoretical monoisotopic molecular weight	Experimental monoisotopic $[M+H]^+$
FHTFPQTAIGVGAP	14	19 – 32	1441.74	1441.7620
C[alk]GNLSTC[alk]MLGTYTQDFNK	18	1 – 18	2108.89	2109.9146
Bis-alkylated human calcitonin	32	1 – 32	3532.62	3532.6548

Sequence coverage = 100%

QTRAP INFUSION ANALYSIS

The digestion solution of hCT was infused in the Q TRAP and analyzed in EMS and Q1 full scan modes (Figure 3-25).

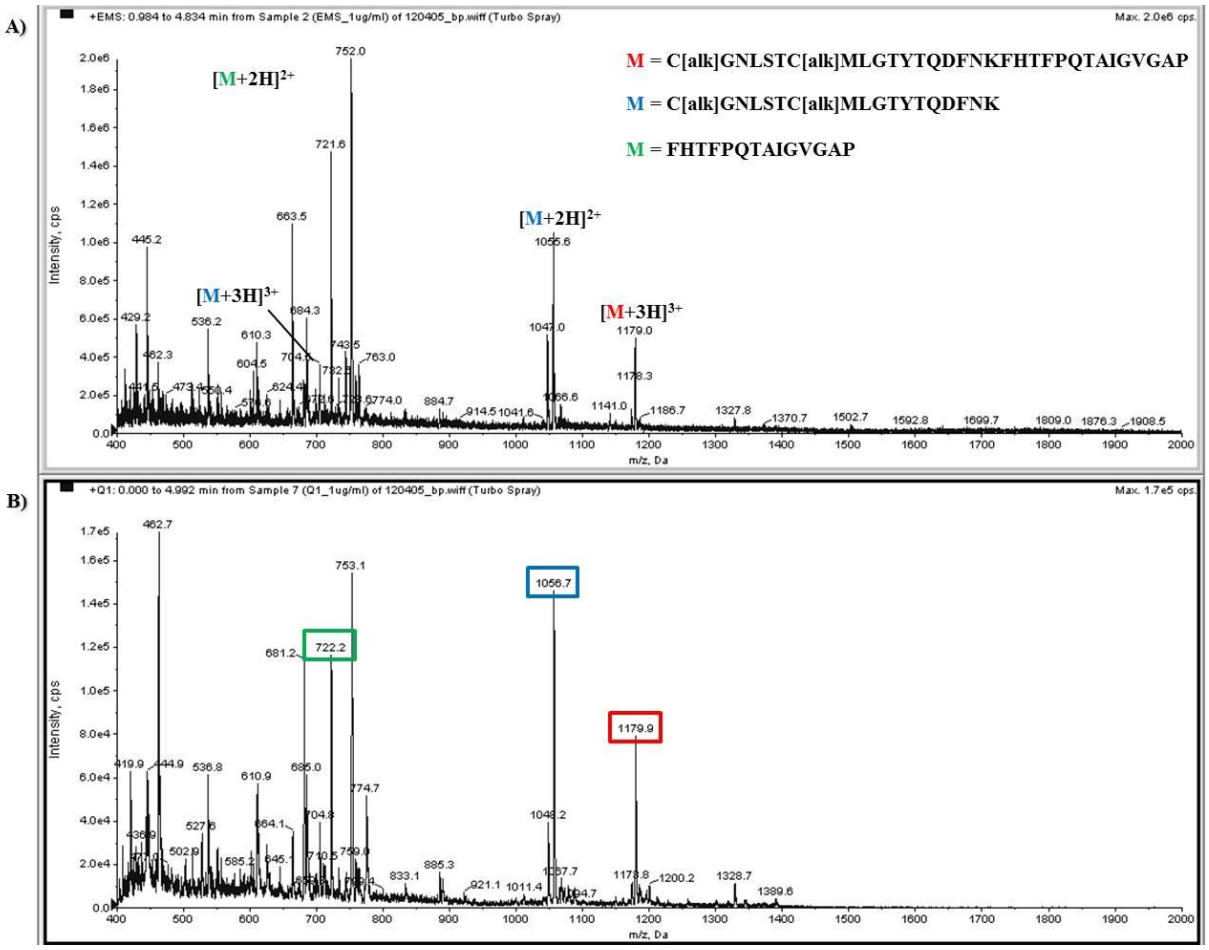

Figure 3-25. Comparison between the EMS spectrum (A) and the Q1 spectrum (B) of hCT digestion solution.

Tryptic digestion of hCT produces two peptides that mainly ionize in ESI as $[M+2H]^{2+}$:

- N-terminal peptide C[alk]GNLSTC[alk]MLGTYTQDFNK
- C-terminal peptide FHTFPQTAIGVGAP.

The ions of interest were analyzed in ER mode to verify their charge state (Figure 3-26).

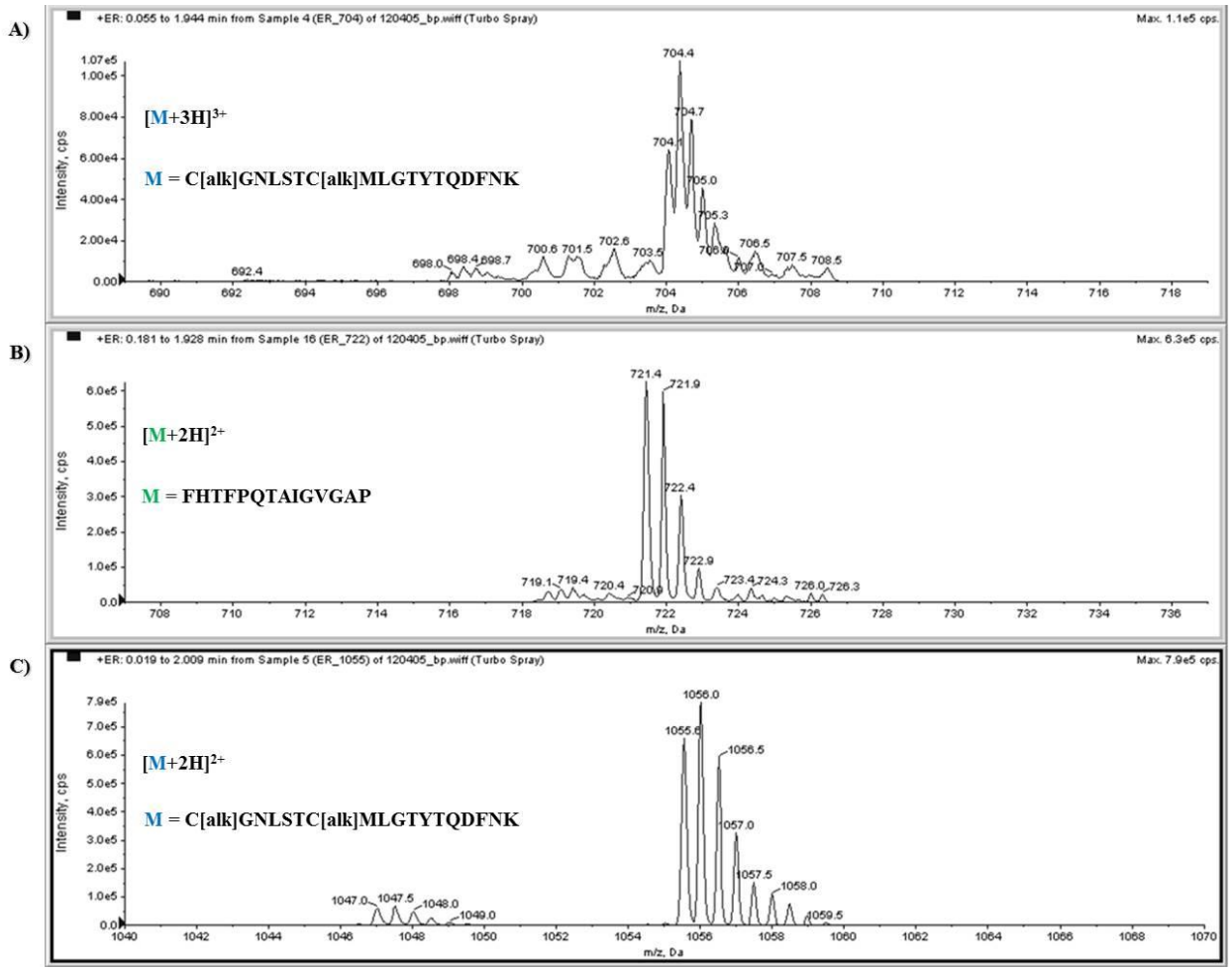

Figure 3-26. ER spectra of m/z 704.4 (A), 721.4 (B) and 1056.0 (C). A) and C) correspond respectively to the triply- and doubly-charged ions of the N-terminal peptide C[alk]GNLSTC[alk]MLGTYTQDFNK; B) corresponds to the doubly-charged ion of the C-terminal peptide FHTFPQTAIGVGAP.

EPI and MS2 fragmentation spectra were acquired for the two peptides originated by the tryptic digestion of hCT (Figure 3-27, Figure 3-29, Figure 3-31).

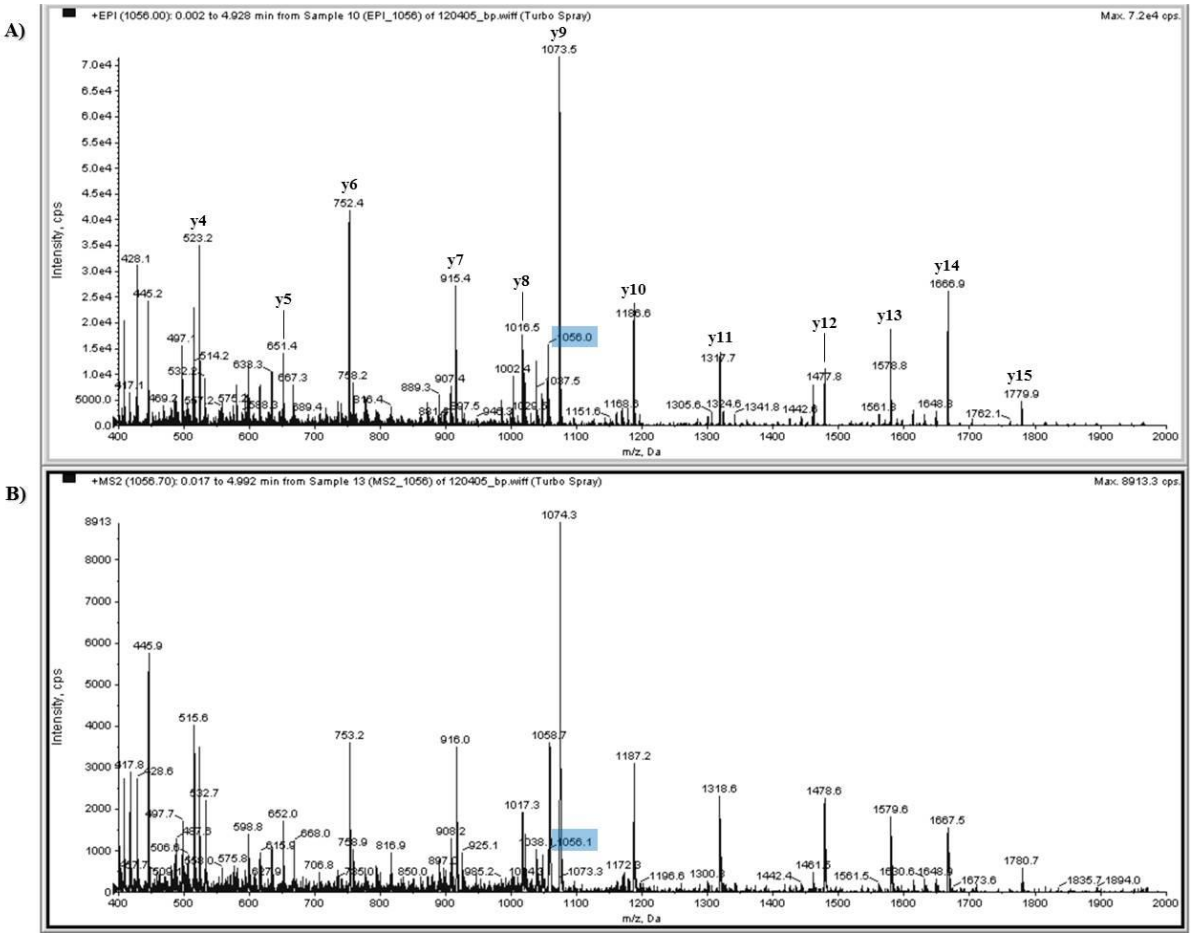

Figure 3-27. EPI (A) and MS2 (B) fragmentation spectra of calcitonin N-terminal peptide C[alk]GNLSTC[alk]MLGTYTQDFNK. The precursor ion is highlighted in blue.

Seq	#	B	Y	# (+1)
C	1	161.01706	2109.86149	18
G	2	218.03852	1949.85230	17
N	3	332.08145	1892.83084	16
L	4	445.16551	1778.78791	15
S	5	532.19754	1665.70385	14
T	6	633.24522	1578.67182	13
C	7	793.25440	1477.62414	12
M	8	924.29489	1317.61496	11
L	9	1037.37895	1186.57447	10
G	10	1094.40041	1073.49041	9
T	11	1195.44809	1016.46894	8
Y	12	1358.51142	915.42126	7
T	13	1459.55910	752.35794	6
Q	14	1587.61768	651.31026	5
D	15	1702.64462	523.25168	4
F	16	1849.71303	408.22474	3
N	17	1963.75596	261.15632	2
K	18	2091.85092	147.11340	1

Seq	#	B	Y	# (+2)
C	1	81.01246	1055.43468	18
G	2	109.52319	975.43009	17
N	3	166.54466	946.91935	16
L	4	223.08669	889.89789	15
S	5	266.60270	833.35586	14
T	6	317.12654	789.83984	13
C	7	397.13114	739.31601	12
M	8	462.65138	659.31141	11
L	9	519.19341	593.79117	10
G	10	547.70414	537.24914	9
T	11	598.22798	508.73841	8
Y	12	679.75965	458.21457	7
T	13	730.28348	376.68290	6
Q	14	794.31277	326.15906	5
D	15	851.82624	262.12978	4
F	16	925.36045	204.61630	3
N	17	982.38191	131.08210	2
K	18	1046.42940	74.06063	1

Figure 3-28. Fragment ion tables of calcitonin N-terminal peptide C[alk]GNLSTC[alk]MLGTYTQDFNK: theoretical monoisotopic mass values of singly- and doubly-charged b and y ions. From http://db.systemsbiology.net/proteomicsToolkit/

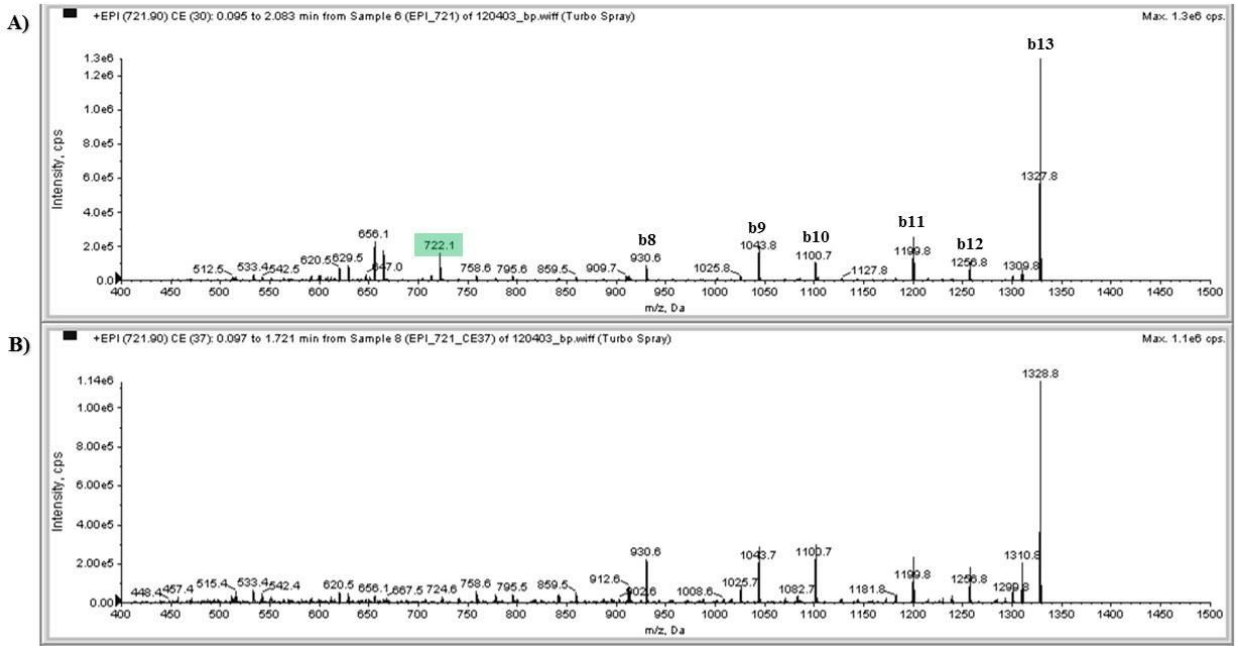

Figure 3-29. EPI fragmentation spectra of calcitonin C-terminal peptide FHTFPQTAIGVGAP. The applied CE values are 30 (A) and 37 (B). The precursor ion is highlighted in green.

Seq	#	B	Y	# (+1)
F	1	148.07628	1442.74327	14
H	2	285.13520	1295.67485	13
T	3	386.18287	1158.61594	12
F	4	533.25129	1057.56826	11
P	5	630.30405	910.49985	10
Q	6	758.36263	813.44709	9
T	7	859.41031	685.38851	8
A	8	930.44742	584.34083	7
I	9	1043.53148	513.30372	6
G	10	1100.55295	400.21965	5
V	11	1199.62136	343.19819	4
G	12	1256.64282	244.12978	3
A	13	1327.67994	187.10831	2
P	14	1424.73270	116.07120	1

Seq	#	B	Y	# (+2)
F	1	74.54208	721.87557	14
H	2	143.07153	648.34136	13
T	3	193.59537	579.81191	12
F	4	267.12958	529.28807	11
P	5	315.65596	455.75386	10
Q	6	379.68525	407.22748	9
T	7	430.20909	343.19819	8
A	8	465.72764	292.67435	7
I	9	522.26968	257.15579	6
G	10	550.78041	200.61376	5
V	11	600.31462	172.10303	4
G	12	628.82535	122.56882	3
A	13	664.34390	94.05809	2
P	14	712.87029	58.53953	1

Figure 3-30. Fragment ion tables of calcitonin C-terminal peptide FHTFPQTAIGVGAP: theoretical monoisotopic mass values of singly- and doubly-charged b and y ions. From http://db.systemsbiology.net/proteomicsToolkit/

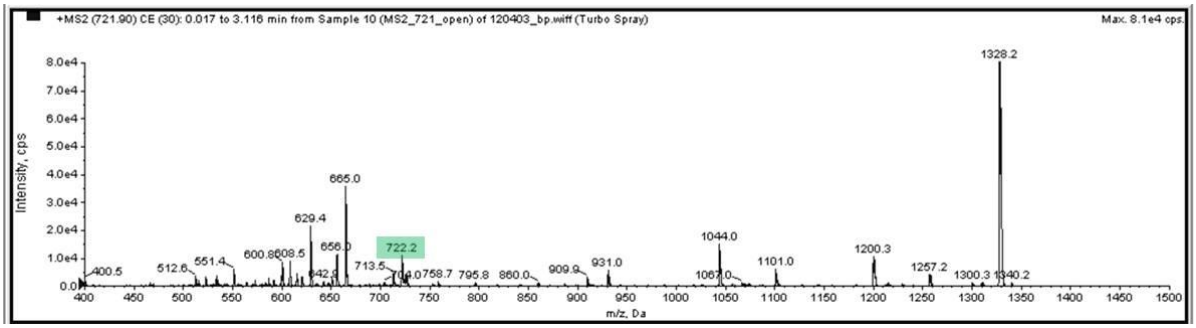

Figure 3-31. MS2 fragmentation spectrum of calcitonin C-terminal peptide FHTFPQTAIGVGAP. The precursor ion is highlighted in green.

MRM ANALYSIS

The following transitions were analyzed:

m/z precursor ion (Q1)	m/z fragment ion (Q3)	Fragment ion
721.9	**1328.2**	b13(1+)
721.9	**665.0**	b13(2+)
721.9	**629.4**	b5(1+)
1056.0	**1074.3**	y9(1+)
1056.0	**1187.2**	y10(1+)
1056.0	**753.2**	y6(1+)

Linearity in the theoretical range of concentrations 0.5 – 50 µg/ml was tested and calibration curves were obtained (Figure 3-32 and Figure 3-33).

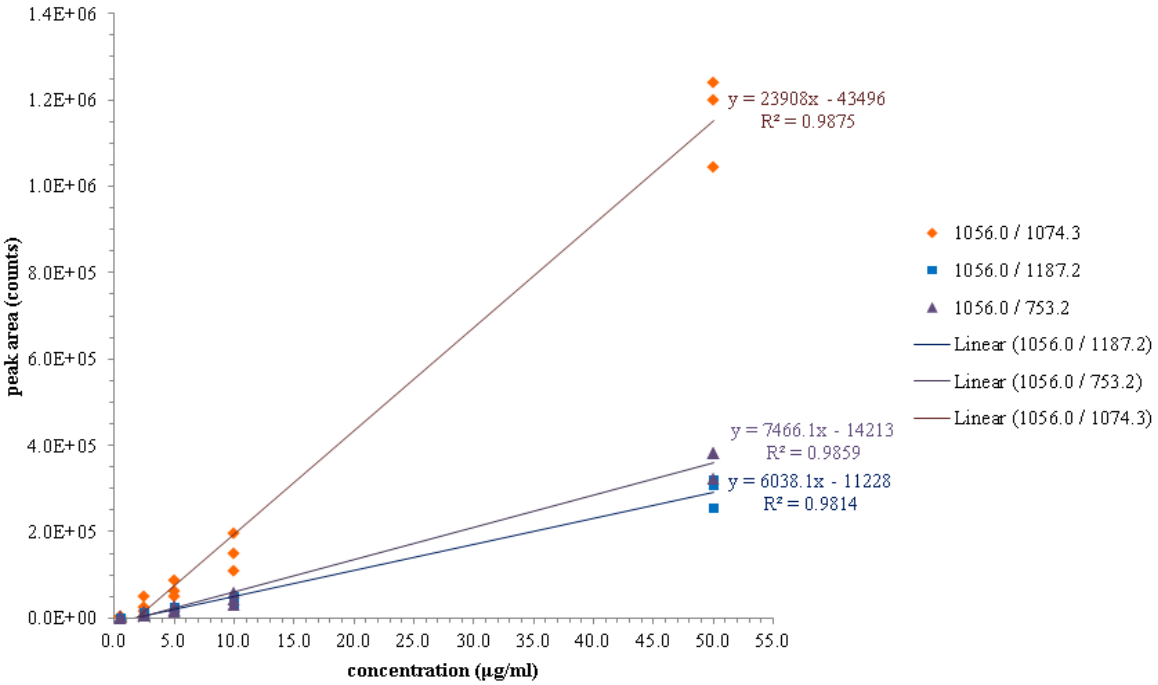

Figure 3-32. Calibration curves obtained for calcitonin N-terminal peptide C[alk]GNLSTC[alk]MLGTYTQDFNK.

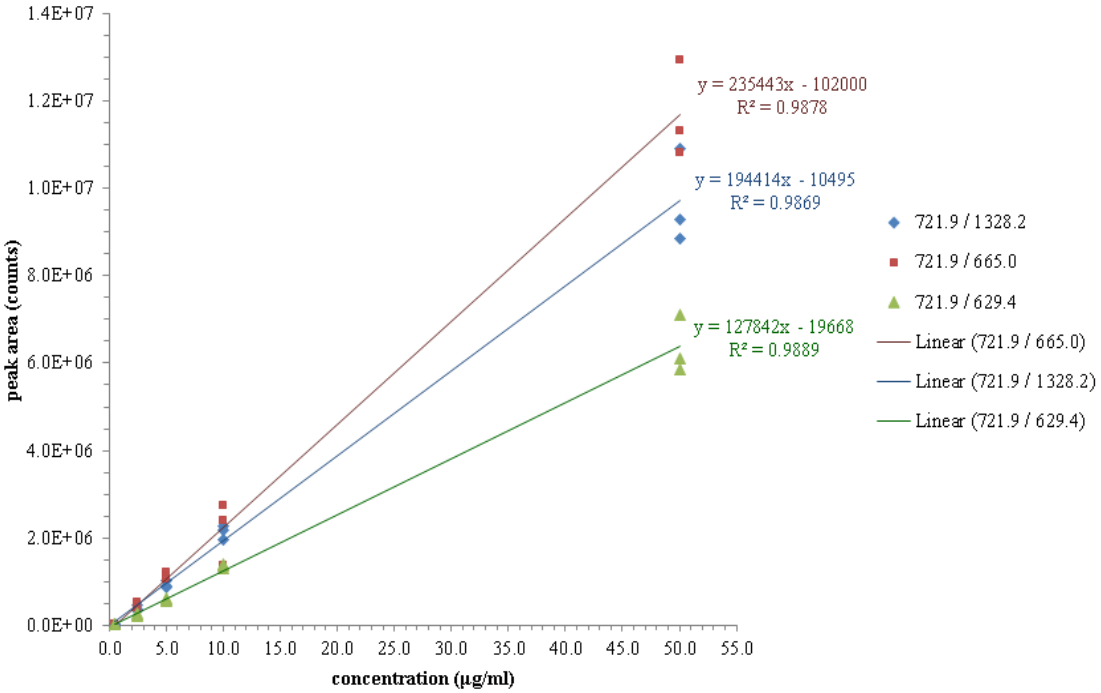

Figure 3-33. Calibration curves obtained for calcitonin C-terminal peptide FHTFPQTAIGVGAP.

R^2 values are ≥ 0.987 for each of the analyzed transitions of the C-terminal peptide FHTFPQTAIGVGAP.

Human procalcitonin

The peptides originated by a virtual tryptic digestion of hPCT are reported in Table 3-7, together with their cleavage probabilities.

Position of cleavage site	Name of cleaving enzyme(s)	Resulting peptide sequence (see explanations)	Peptide length [aa]	Peptide mass [Da]	Cleavage probability
4	Trypsin	APFR	4	489.575	100 %
23	Trypsin	SALESSPADPATLSEDEAR	19	1946.012	100 %
37	Trypsin	LLLAALVQDYVQMK	14	1604.968	91.2 %
47	Trypsin	ASELEQEQER	10	1218.243	78.4 %
56	Trypsin	EGSSLDSPR	9	946.969	100 %
58	Trypsin	SK	2	233.268	65 %
59	Trypsin	R	1	174.203	100 %
77	Trypsin	CGNLSTCMLGTYTQDFNK	18	1996.255	91.4 %
93	Trypsin	FHTFPQTAIGVGAPGK	16	1627.863	92.9 %
94	Trypsin	K	1	146.189	54.5 %
95	Trypsin	R	1	174.203	100 %
103	Trypsin	DMSSDLER	8	952.004	89.7 %
106	Trypsin	DHR	3	426.432	23.8 %
116	end of sequence	PHVSMPQNAN	10	1094.210	-

Table 3-7. Tryptic digestion of hPCT: cleavage sites and cleavage probabilities. From http://web.expasy.org/peptide_cutter/

Protein denaturation in SDS

Protocol based on SDS and thermal denaturation:

- thawing of the protein standard: 10 µg of hPCT lyophilized in 10 mM phosphate buffer
- solubilization in 100 mM ammonium bicarbonate
- buffer exchange to 100 mM ammonium bicarbonate with Micro Bio-Spin Chromatography Columns
- denaturation and reduction with 0.1% SDS and 9.5 mM TCEP, 5 minutes a 95 °C in the dark
- alkylation in 17 mM IAA, 30 minutes at 25 °C in the dark
- in-solution digestion with trypsin 1:20 (w/w), 16 hours at 37 °C
- detergent removal with Pierce Detergent Removal Spin Columns
- quenching of digestion by addition of 0.1% formic acid.

MALDI-TOF ANALYSIS

The MALDI-TOF spectrum is characterized by the presence of signals which can be attributed to the tryptic digestion of hPCT (Figure 3-34).

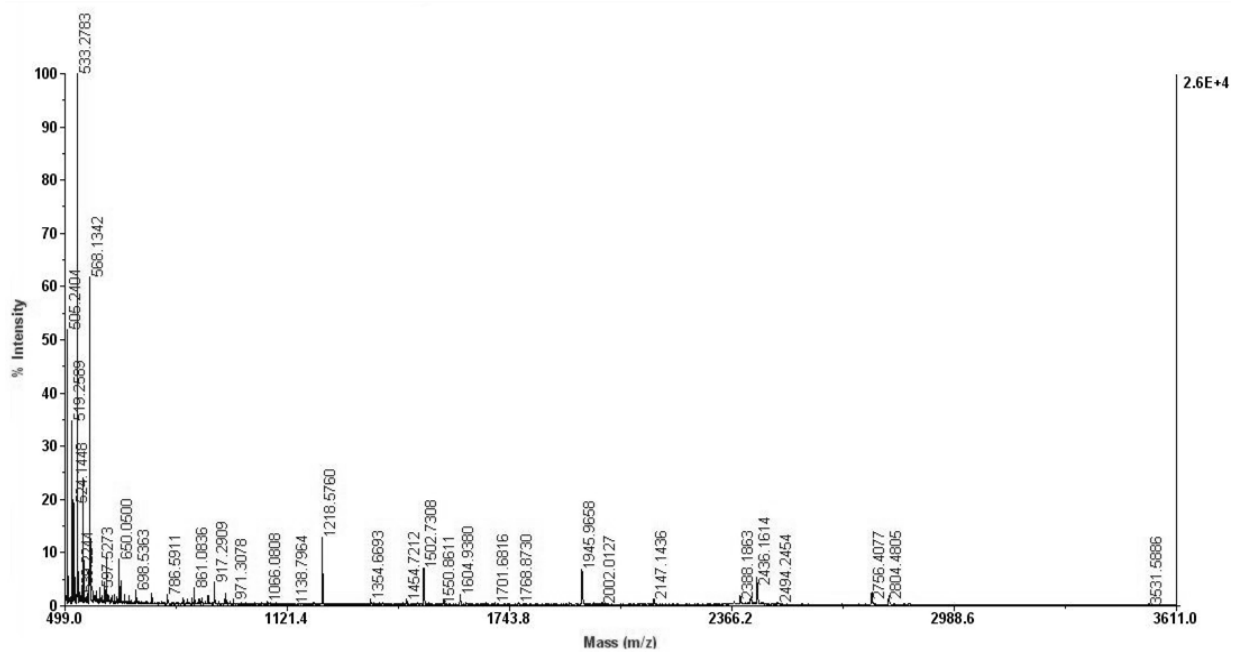

Figure 3-34. MALDI-TOF spectrum of digestion solution of hPCT.

Peptide sequence	Length (aa)	Position	Missed cleavages	Theoretical monoisotopic molecular weight	Experimental monoisotopic $[M+H]^+$
ASELEQEQER	10	38 – 47	-	1217.55	1218.5760
DH*R*PHVSMPQNAN	13	104 – 116	1	1501.68	1502.7308
LLLAALVQDYVQMK	14	24 – 37	-	1603.90	1604.9380
SALESSPADPATLSEDEAR	19	5 – 23	-	1944.89	1945.9658
ASELEQEQE*R*EGSSLDSPR	19	38 – 56	1	2145.98	2147.1436
DMSSDLE*R*DH*R*PHVSMPQNAN	21	94 – 116	2	2435.07	2436.1614

Sequence coverage = 62.9 %

Q TRAP INFUSION ANALYSIS

The digestion solution was subjected to ZipTip C18 purification and then diluted 2x prior to Q TRAP analysis. EMS and Q1 full scan spectra were acquired (Figure 3-35).

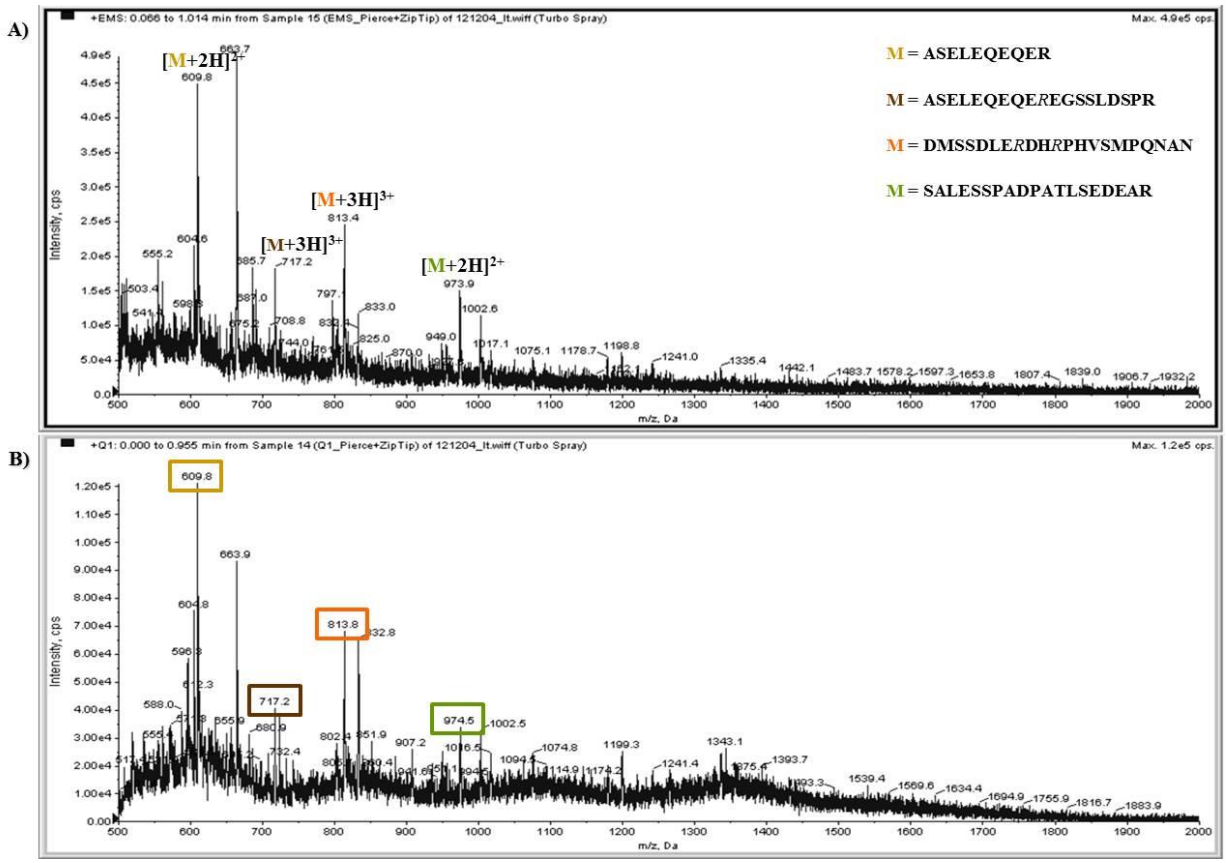

Figure 3-35. Comparison between the EMS spectrum (A) and the Q1 spectrum (B) of the digestion mixture.

Tryptic digestion of hPCT produces peptides that ionize in ESI as multiply-charged ions. The most intense signals in the EMS and Q1 full scan spectra are:

- $[M+2H]^{2+}$ of peptide ASELEQEQER;
- $[M+3H]^{3+}$ of peptide ASELEQEQEREGSSLDSPR;
- $[M+3H]^{3+}$ of C-terminal peptide DMSSDLERDHRPHVSMPQNAN;
- $[M+2H]^{2+}$ of peptide SALESSPADPATLSEDEAR.

The ions of interest were analyzed in ER mode to verify their charge state (Figure 3-36).

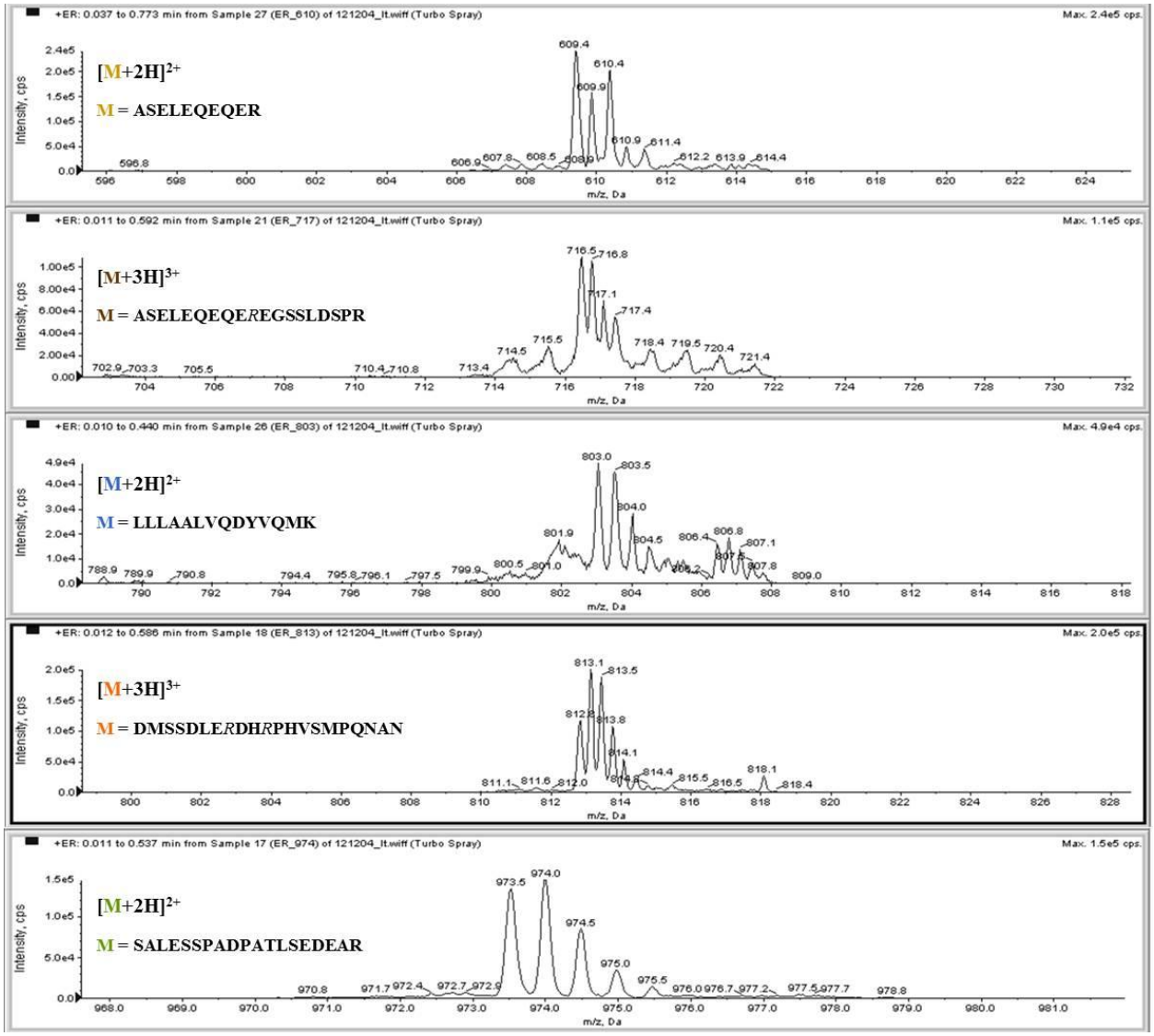

Figure 3-36. ER spectra of the multiply-charged peptides resulting from hPCT digestion.

Peptide ASELEQEQER and peptide SALESSPADPATLSEDEAR were selected for MS/MS experiments (data not shown):

- ❖ fragmentation of peptide ASELEQEQER produced y5, y6, y4, y7 and y8 fragment ions, listed in decreasing order of signal intensity;
- ❖ fragmentation of peptide SALESSPADPATLSEDEAR produced y10, y11, y13 and y14 fragment ions, listed in decreasing order of signal intensity.

Human C-reactive protein

The peptides originated by a virtual tryptic digestion of hCRP are reported in Table 3-8, together with their cleavage probabilities.

Position of cleavage site	Name of cleaving enzyme(s)	Resulting peptide sequence (see explanations)	Peptide length [aa]	Peptide mass [Da]	Cleavage probability
6	Trypsin	QTDMSR	6	736.798	100 %
7	Trypsin	K	1	146.189	89.1 %
13	Trypsin	AFVFPK	6	707.871	90.7 %
23	Trypsin	ESDTSYVSLK	10	1128.201	100 %
31	Trypsin	APLTKPLK	8	867.100	100 %
47	Trypsin	AFTVCLHFYTELSSTR	16	1875.129	100 %
57	Trypsin	GYSIFSYATK	10	1136.270	100 %
58	Trypsin	R	1	174.203	100 %
69	Trypsin	QDNEILIFWSK	11	1392.574	86.7 %
114	Trypsin	DIGYSFTVGGSEILFEVPEVTVAPVHICTSWESASGIVEFWVDGK	45	4859.438	51.9 %
116	Trypsin	PR	2	271.319	100 %
118	Trypsin	VR	2	273.335	100 %
119	Trypsin	K	1	146.189	83.4 %
122	Trypsin	SLK	3	346.427	82.6 %
123	Trypsin	K	1	146.189	83.7 %
188	Trypsin	GYTVGAEASIILGQEQDSFGGNFEGSQSLVGDIGNVNMWDFVLSPDEINTIYLGGPFSP NVLNWR	65	6994.675	100 %
191	Trypsin	ALK	3	330.428	100 %
206	end of sequence	YEVQGEVFTKPQLWP	15	1821.063	-

Table 3-8. Tryptic digestion of hCRP: cleavage sites and cleavage probabilities. From http://web.expasy.org/peptide_cutter/

Two different protein denaturation procedures were considered: a SDS-based denaturation and a urea/thiourea procedure.

Protein denaturation in urea and thiourea mixture

The first sample preparation procedure to be applied to hCRP was the one optimized for the digestion of hCT:

- denaturation in 20 mM NH_4HCO_3, 6 M urea, 2 M thiourea
- reduction in 48.75 mM DTT, 30 minutes at 25 °C
- alkylation in 100 mM IAA, 30 minutes at 25 °C in the dark
- desalting with GE Healthcare PD MiniTrap G-10 column
- in-solution digestion: 16 hours at 37 °C with trypsin 1:50 (w/w)
- quenching of digestion by addition of 0.1% formic acid.

MALDI-TOF ANALYSIS

The MALDI-TOF spectrum is characterized by the presence of signals which can be attributed to the tryptic digestion of hCRP (Figure 3-37).

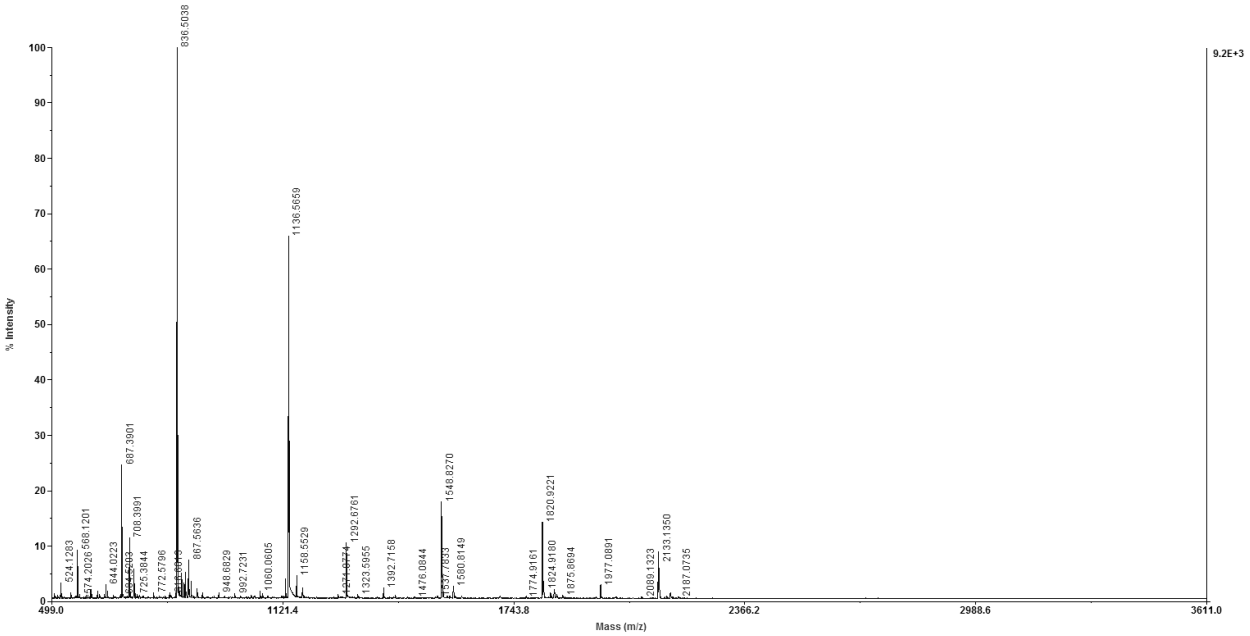

Figure 3-37. MALDI-TOF spectrum of digestion solution of hCRP.

Peptide sequence	Length (aa)	Position	Missed cleavages	Theoretical monoisotopic molecular weight	Experimental monoisotopic $[M+H]^+$
AFVFPK	6	8 – 13	-	707.40	708.3991
*K*AFVFPK	7	7 – 13	1	835.50	836.5038
ESDTSYVSLK	10	14 – 23	-	1127.53	1128.5327
GYSIFSYATK	10	48 – 57	-	1135.55	1136.5659
GYSIFSYAT*K*R	11	48 – 58	1	1291.66	1292.6761
*R*QDNEILIFWSK	12	58 – 69	1	1547.81	1548.8270
YEVQGEVFT*K*PQLWP	15	192 – 206	1	1819.91	1820.9221
AFTVCLHFYTELSSTR	16	32 – 47	-	1873.90	1874.8694
ESDTSYVSL*K*APLT*K*PLK	18	14 – 31	2	1976.08	1977.0891
AL*K*YEVQGEVFT*K*PQLWP	18	181 – 206	2	2132.13	2133.1350

Sequence coverage = 39.3%

Q TRAP INFUSION ANALYSIS

The digestion solution of hCRP was infused in the Q TRAP and analyzed in EMS and Q1 full scan modes (Figure 3-38).

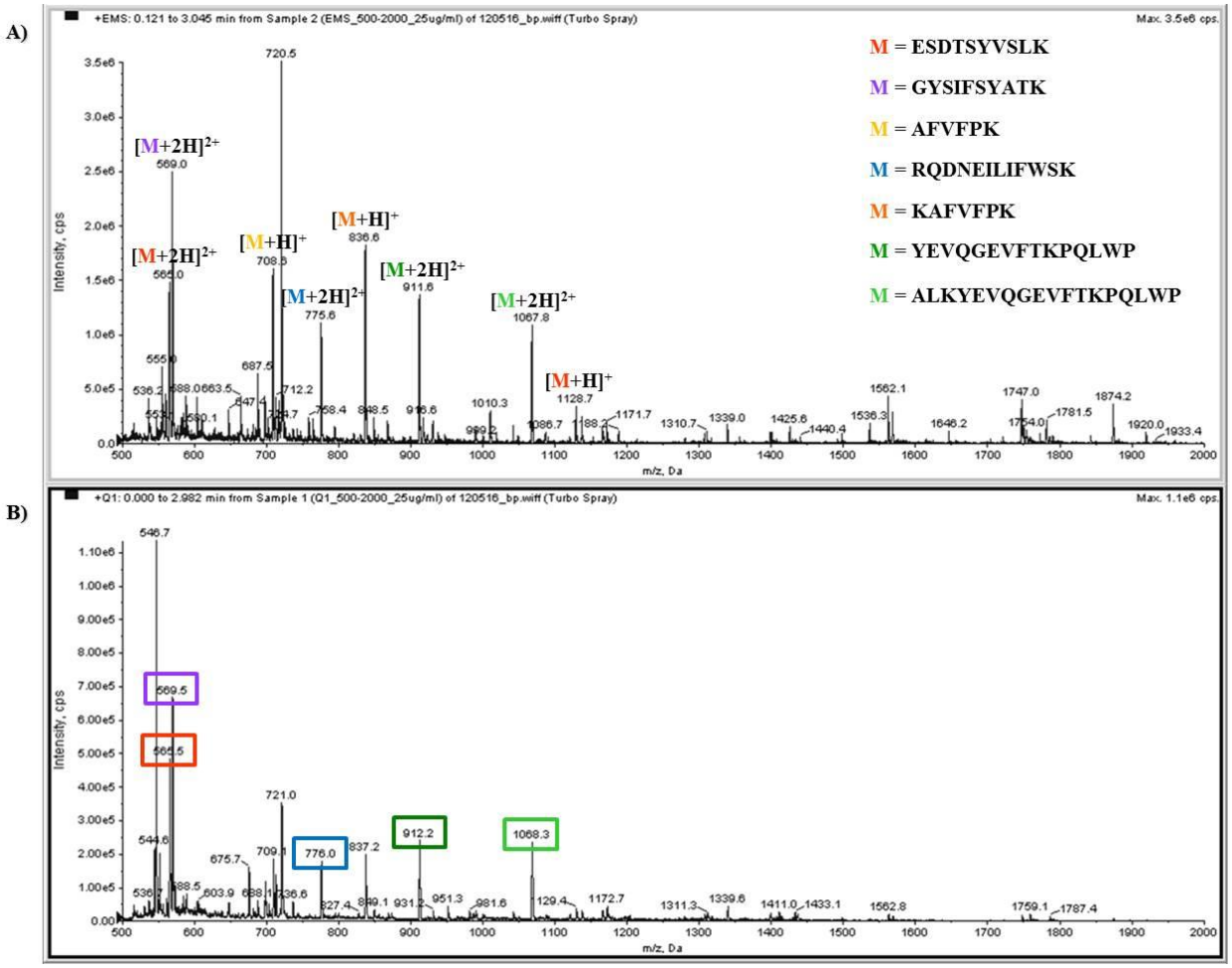

Figure 3-38. Comparison between the EMS spectrum (A) and the Q1 spectrum (B) of the digestion solution of hCRP.

Tryptic digestion of hCRP produces peptides that ionize in ESI as multiply-charged ions. The most intense signals in EMS and Q1 full scan spectra are:

- $[M+2H]^{2+}$ of peptide ESDTSYVSLK;
- $[M+2H]^{2+}$ of peptide GYSIFSYATK;
- $[M+2H]^{2+}$ of peptide RQDNEILIFWSK;
- $[M+2H]^{2+}$ of C-terminal peptide YEVQGEVFTKPQLWP;
- $[M+2H]^{2+}$ of C-terminal peptide AL*K*YEVQGEVFT*K*PQLWP.

The ions of interest were analyzed in ER mode to verify their charge state (Figure 3-39).

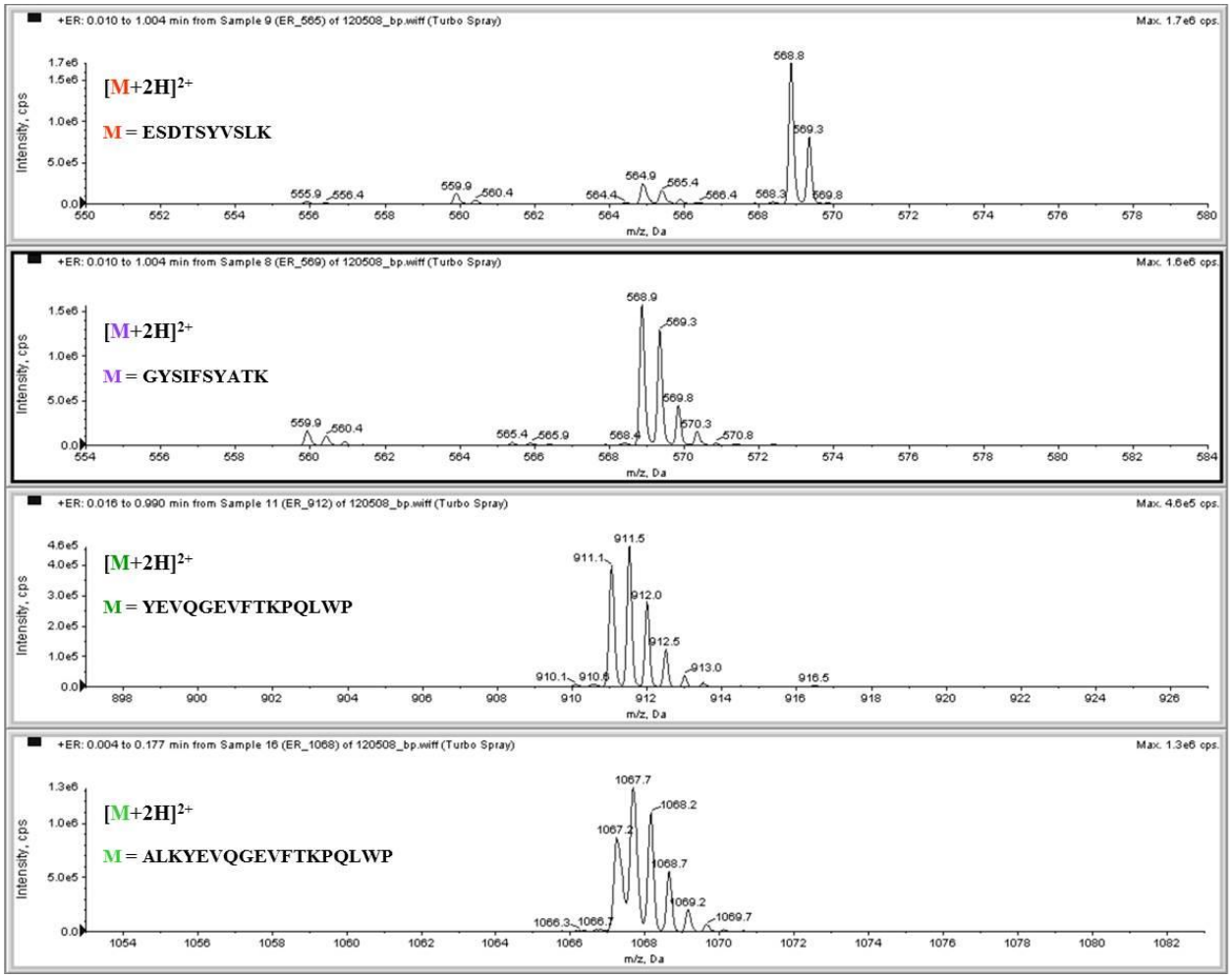

Figure 3-39. ER spectra of multiply-charged peptides resulting from hCRP digestion.

MS/MS ANALYSIS

Two peptides were selected for MS/MS analysis on the basis of their signal intensity in the Q1 full scan: peptide GYSIFSYATK and peptide ESDTSYVSLK. MS^E and MS2 spectra were acquired (Figure 3-40, Figure 3-41, Figure 3-43, Figure 3-44).

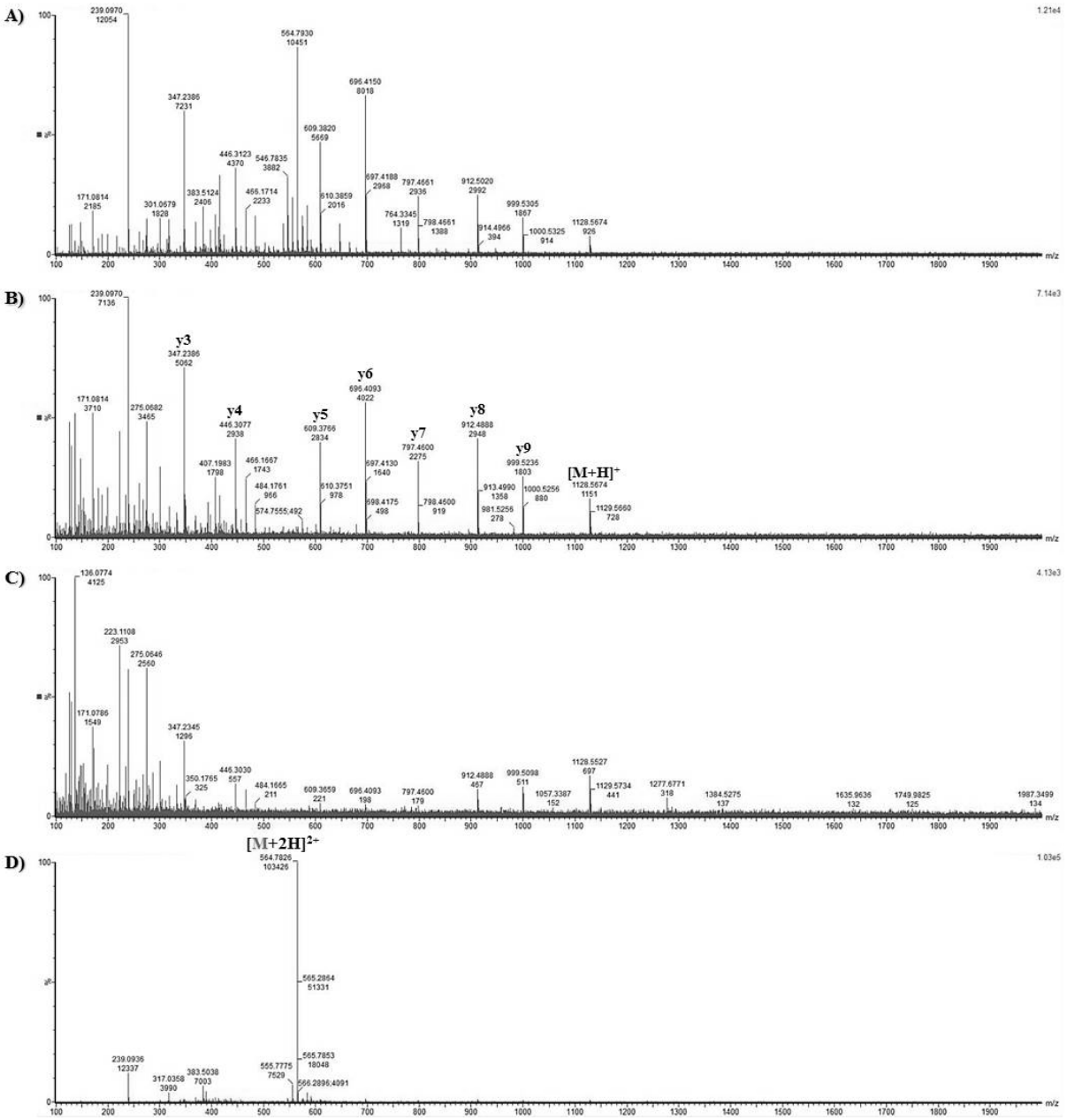

Figure 3-40. MS^E spectra of peptide ESDTSYVSLK. The low energy function is reported in (D). A wide range of CE values have been tested: 10 – 25 (A), 20 – 35 (B) and 30 – 45 (C).

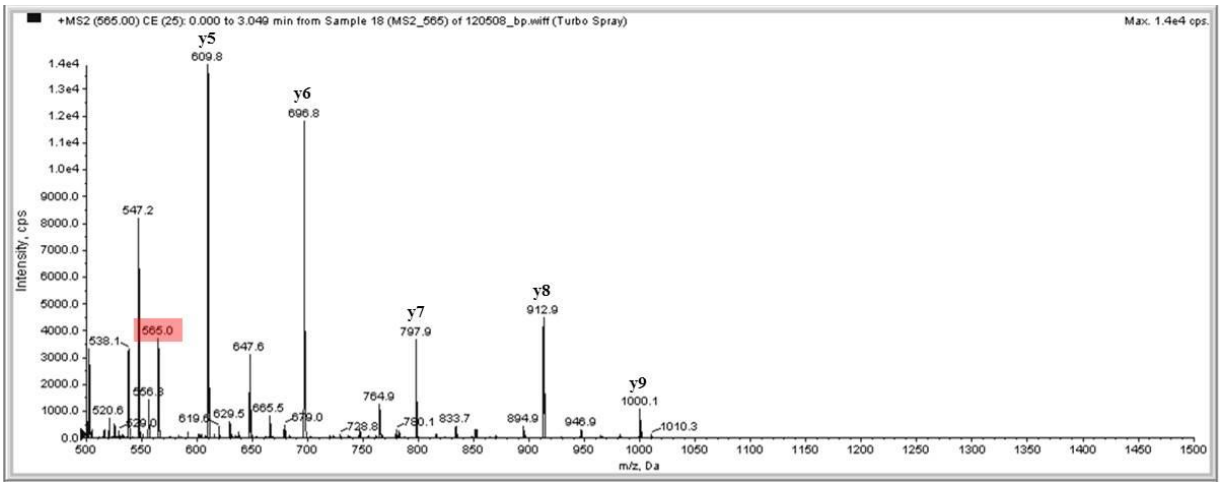

Figure 3-41. MS2 fragmentation spectrum of peptide ESDTSYVSLK. The precursor ion is highlighted in red.

Seq	#	B	Y	# (+1)
E	1	130.05046	1128.54250	10
S	2	217.08249	999.49991	9
D	3	332.10943	912.46788	8
T	4	433.15711	797.44094	7
S	5	520.18914	696.39326	6
Y	6	683.25247	609.36123	5
V	7	782.32088	446.29790	4
S	8	869.35291	347.22949	3
L	9	982.43697	260.19746	2
K	10	1110.53194	147.11340	1

Seq	#	B	Y	# (+2)
E	1	65.52917	564.77519	10
S	2	109.04518	500.25389	9
D	3	166.55865	456.73788	8
T	4	217.08249	399.22440	7
S	5	260.59851	348.70056	6
Y	6	342.13017	305.18455	5
V	7	391.66438	223.65289	4
S	8	435.18039	174.11868	3
L	9	491.72242	130.60267	2
K	10	555.76990	74.06063	1

Figure 3-42. Fragment ion tables of peptide ESDTSYVSLK: theoretical monoisotopic mass values of singly- and doubly-charged b and y ions. From http://db.systemsbiology.net/proteomicsToolkit/

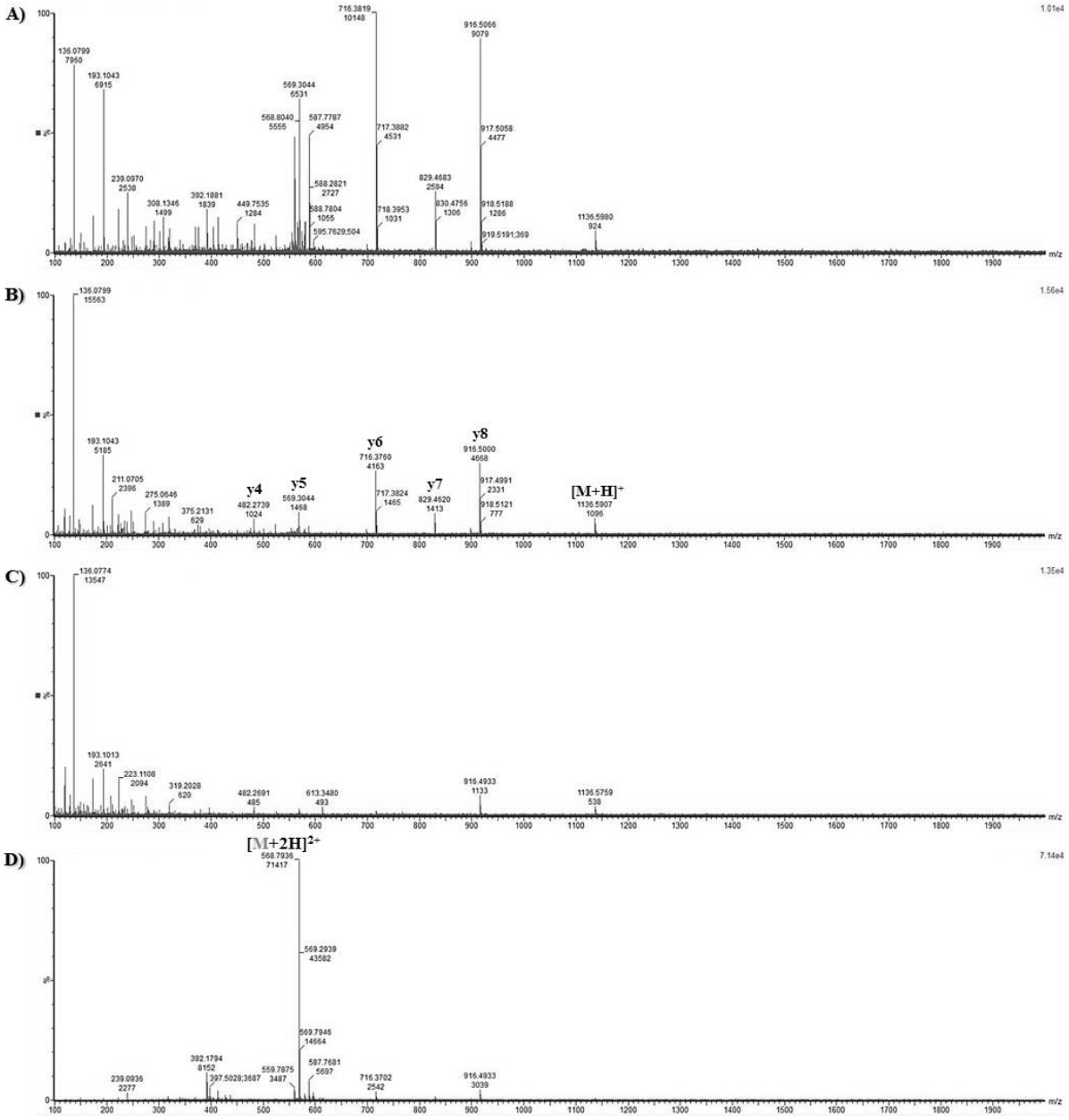

Figure 3-43. MS^{E} spectra of peptide GYSIFSYATK. The low energy function is reported in (D). A wide range of CE values have been tested: 10 – 25 (A), 20 – 35 (B) and 30 – 45 (C).

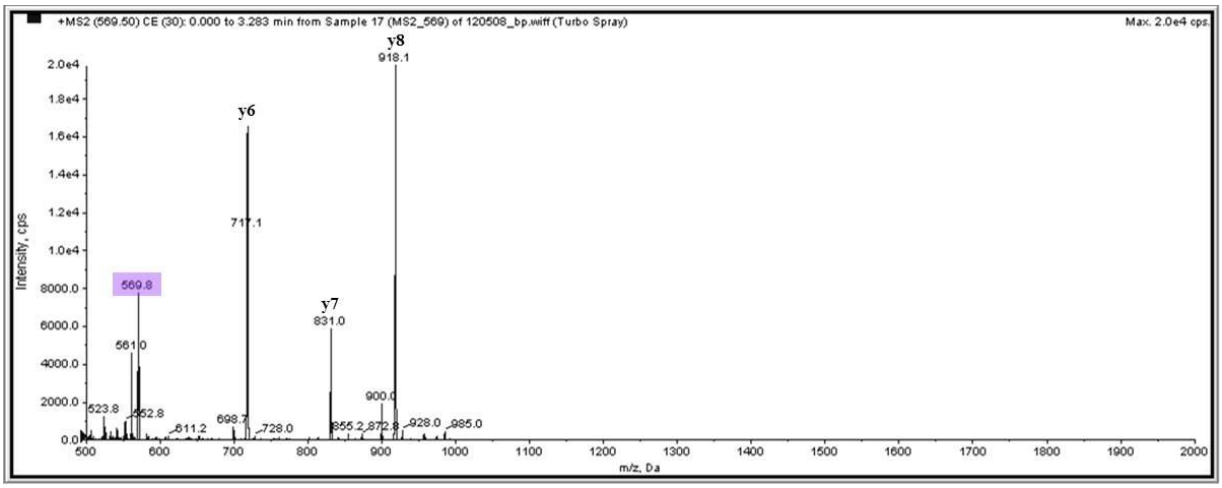

Figure 3-44. MS2 fragmentation spectrum of peptide GYSIFSYATK. The precursor ion is highlighted in purple.

Seq	#	B	Y	# (+1)
G	1	58.02933	1136.56284	10
Y	2	221.09266	1079.54138	9
S	3	308.12469	916.47805	8
I	4	421.20875	829.44602	7
F	5	568.27717	716.36196	6
S	6	655.30920	569.29355	5
Y	7	818.37252	482.26152	4
A	8	889.40964	319.19819	3
T	9	990.45732	248.16108	2
K	10	1118.55228	147.11340	1

Seq	#	B	Y	# (+2)
G	1	29.51860	568.78536	10
Y	2	111.05027	540.27462	9
S	3	154.56628	458.74296	8
I	4	211.10831	415.22695	7
F	5	284.64252	358.68491	6
S	6	328.15853	285.15071	5
Y	7	409.69020	241.63469	4
A	8	445.20875	160.10303	3
T	9	495.73259	124.58447	2
K	10	559.78007	74.06063	1

Figure 3-45. Fragment ion tables of peptide GYSIFSYATK: theoretical monoisotopic mass values of singly- and doubly-charged b and y ions. From http://db.systemsbiology.net/proteomicsToolkit/

MRM ANALYSIS

The following transitions were analyzed:

m/z precursor ion (Q1)	m/z fragment ion (Q3)	Fragment ion
565.0	**609.8**	y5(1+)
565.0	**696.8**	y6(1+)
565.0	**913.0**	y8(1+)
565.0	**797.9**	y7(1+)
569.8	**918.1**	y8(1+)
569.8	**717.1**	y6(1+)
569.8	**831.0**	y7(1+)

Linearity in the theoretical range of concentrations 2.5 – 50 µg/ml was tested and calibration curves were obtained (Figure 3-46).

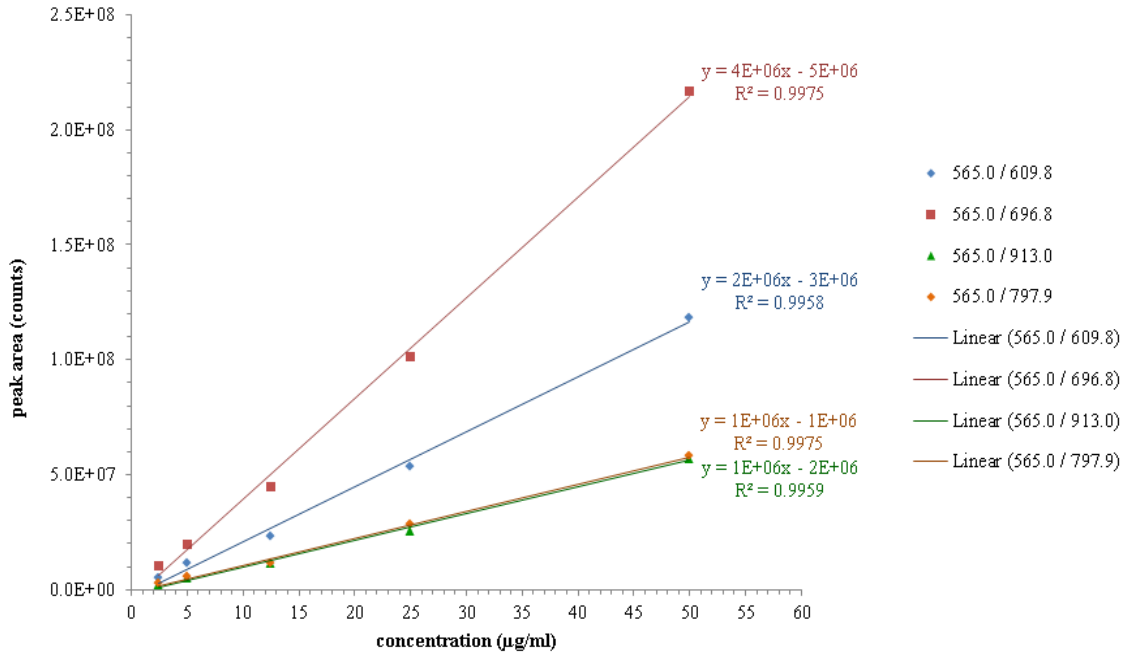

Figure 3-46. Calibration curves obtained for hCRP peptide ESDTSYVSLK.

R^2 values are ≥ 0.995 for each of the analyzed transitions of peptide ESDTSYVSLK.

Protein denaturation in SDS

Two different protocols have been tested, differing in the strategy exploited to reduce the detergent concentration prior to the digestion step:

- protocol 1: sample purification with Detergent Removal Spin Column
- protocol 2: sample dilution with reaction buffer.

Protocol 1:

- buffer exchange with Micro Bio-Spin Columns BIO-RAD (from 140 mM NaCl, 20 mM Tris-HCl, 2 mM CaCl2, 0.05% NaN3, pH 7.5 to 200 mM NH4HCO3)
- denaturation in 100 mM NH4HCO3, 0.1% SDS
- reduction in 9.5 mM TCEP, 1 hour at 55 °C in the dark
- alkylation in 17 mM IAA, 30 minutes at 25 °C in the dark
- Pierce Detergent Removal Spin Column → elution in 20 mM NH4HCO3
- in-solution digestion: 16 hours at 37 °C with trypsin 1:50 (w/w)
- quenching of digestion by addition of 0.1% formic acid.

MALDI-TOF ANALYSIS

The MALDI-TOF spectrum is characterized by the presence of signals which can be attributed to the tryptic digestion of hCRP (Figure 3-47).

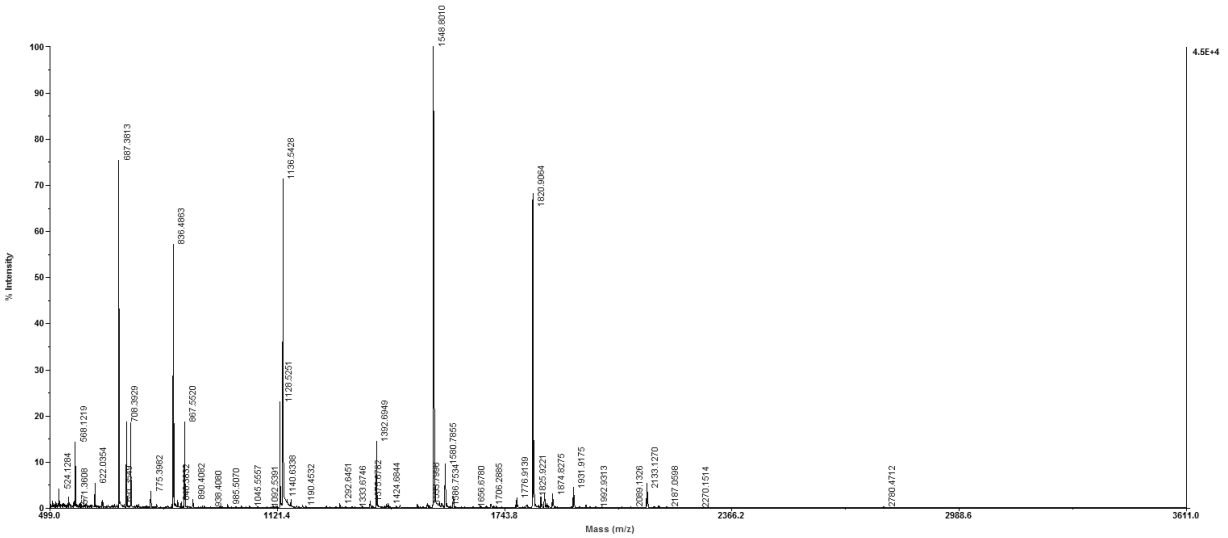

Figure 3-47. MALDI-TOF spectrum of digestion solution of hCRP.

Peptide sequence	Length (aa)	Position	Missed cleavages	Theoretical monoisotopic molecular weight	Experimental monoisotopic $[M+H]^+$
AFVFPK	6	8 – 13	-	707.40	708.3929
*K*AFVFPK	7	7 – 13	1	835.50	836.4863
APLT*K*PLK	8	24 – 31	1	866.56	867.5520
ESDTSYVSLK	10	14 – 23	-	1127.53	1128.5251
GYSIFSYATK	10	48 – 57	-	1135.55	1136.5428
GYSIFSYAT*K*R	11	48 – 58	1	1291.66	1292.6451
QDNEILIFWSK	11	59 – 69	-	1391.71	1392.6949
*R*QDNEILIFWSK	12	58 – 69	1	1547.81	1548.8010
YEVQGEVFT*K*PQLWP	15	192 – 206	1	1819.91	1820.9064
AFTVCLHFYTELSSTR	16	32 – 47	-	1873.90	1874.8275
AFTVC[alk]LHFYTELSSTR	16	32 – 47	-	1930.92	1931.9175
AL*K*YEVQGEVFT*K*PQLWP	18	181 – 206	2	2132.13	2133.1270

Sequence coverage = 39.3%

Protocol 2:

- buffer exchange with Micro Bio-Spin Columns BIO-RAD (from 140 mM NaCl, 20 mM Tris-HCl, 2 mM CaCl2, 0.05% NaN3, pH 7.5 to 100 mM NH4HCO3)
- denaturation and reduction in 100 mM NH4HCO3, 0.1% SDS, 9.5 mM TCEP, 5 minutes at 95 °C in the dark
- alkylation in 17 mM IAA, 30 minutes at 25 °C in the dark
- sample dilution 2x in 100 mM ammonium bicarbonate
- in-solution digestion: 16 hours at 37 °C with trypsin 1:25 (w/w)
- quenching of digestion by addition of 0.1% formic acid.

MALDI-TOF ANALYSIS

Desalting of the digestion solution of hCRP prior to MALDI-TOF analysis was performed using a ZipTip C18 Pipette Tip. The MALDI-TOF spectrum is characterized by the presence of signals which can be attributed to the tryptic digestion of hCRP (Figure 3-48).

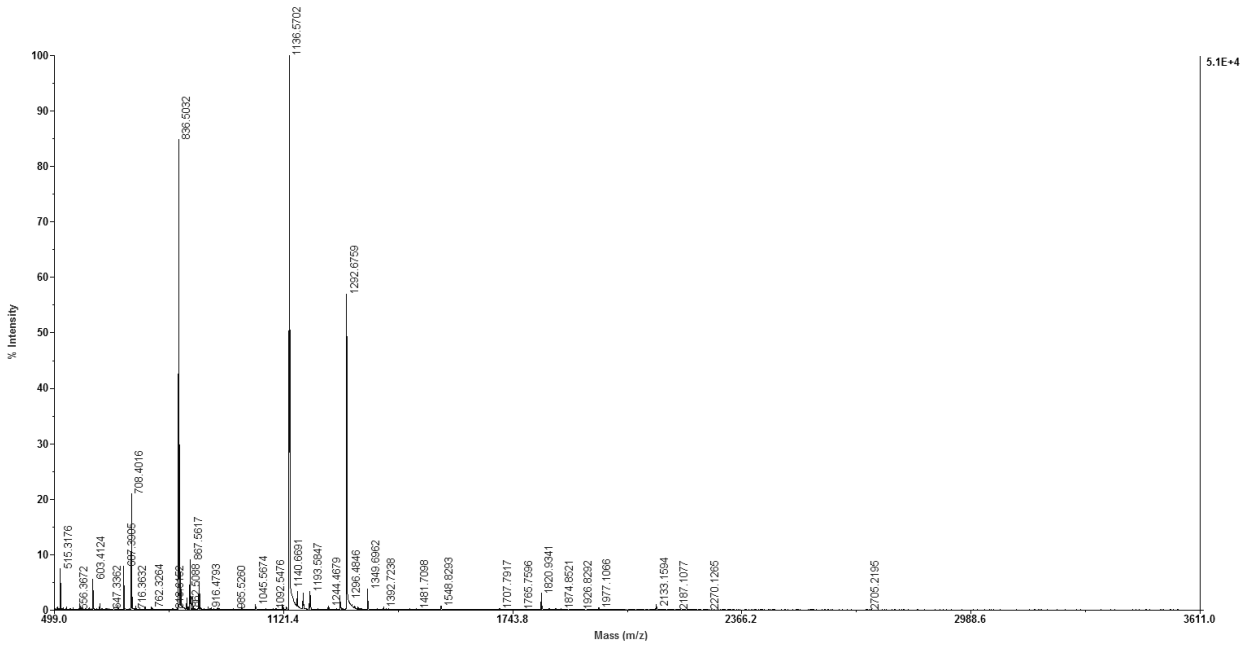

Figure 3-48. MALDI-TOF spectrum of digestion solution of hCRP.

Peptide sequence	Length (aa)	Position	Missed cleavages	Theoretical monoisotopic molecular weight	Experimental monoisotopic $[M+H]^+$
AFVFPK	6	8 – 13	-	707.40	708.4016
*K*AFVFPK	7	7 – 13	1	835.50	386.5032
APLT*K*PLK	8	24 – 31	1	866.56	867.5617
GYSIFSYATK	10	48 – 57	-	1135.55	1136.5702
GYSIFSYAT*K*R	11	48 – 58	1	1291.66	1292.6759
YEVQGEVFT*K*PQLWP	15	192 – 206	1	1819.91	1820.9341
ESDTSYVSL*K*APLT*K*PLK	18	14 – 31	2	1976.08	1977.1066
AL*K*YEVQGEVFT*K*PQLWP	18	181 – 206	2	2132.13	2133.1594

Sequence coverage = 26.2%

TARGETED ANALYSES IN ORGANIC-AQUEOUS SOLUTION

Human calcitonin

Digestion of the reduced and alkylated protein

Sample preparation:

- 20x dilution of the stock solution of CT 1 mg/ml with the mixed organic-aqueous solvent system
- reduction in 5 mM TCEP, 5 minutes at 25 °C in the dark
- alkylation in 17 mM IAA, 30 minutes at 25°C in the dark
- quenching of alkylation by addition of 5 mM DTT, 15 minutes at 25 °C
- in-solution digestion: 1 hour at 37 °C with trypsin 1:20 (w/w)
- quenching of digestion by addition of 0.1% formic acid.

The mixed organic-aqueous solvent systems tested are:

a) 60% ACN / 40% 20 mM ammonium bicarbonate
b) 80% ACN / 20% 20 mM ammonium bicarbonate
c) 60% methanol / 40% 20 mM ammonium bicarbonate
d) 80% methanol / 20% 20 mM ammonium bicarbonate.

MALDI-TOF ANALYSIS

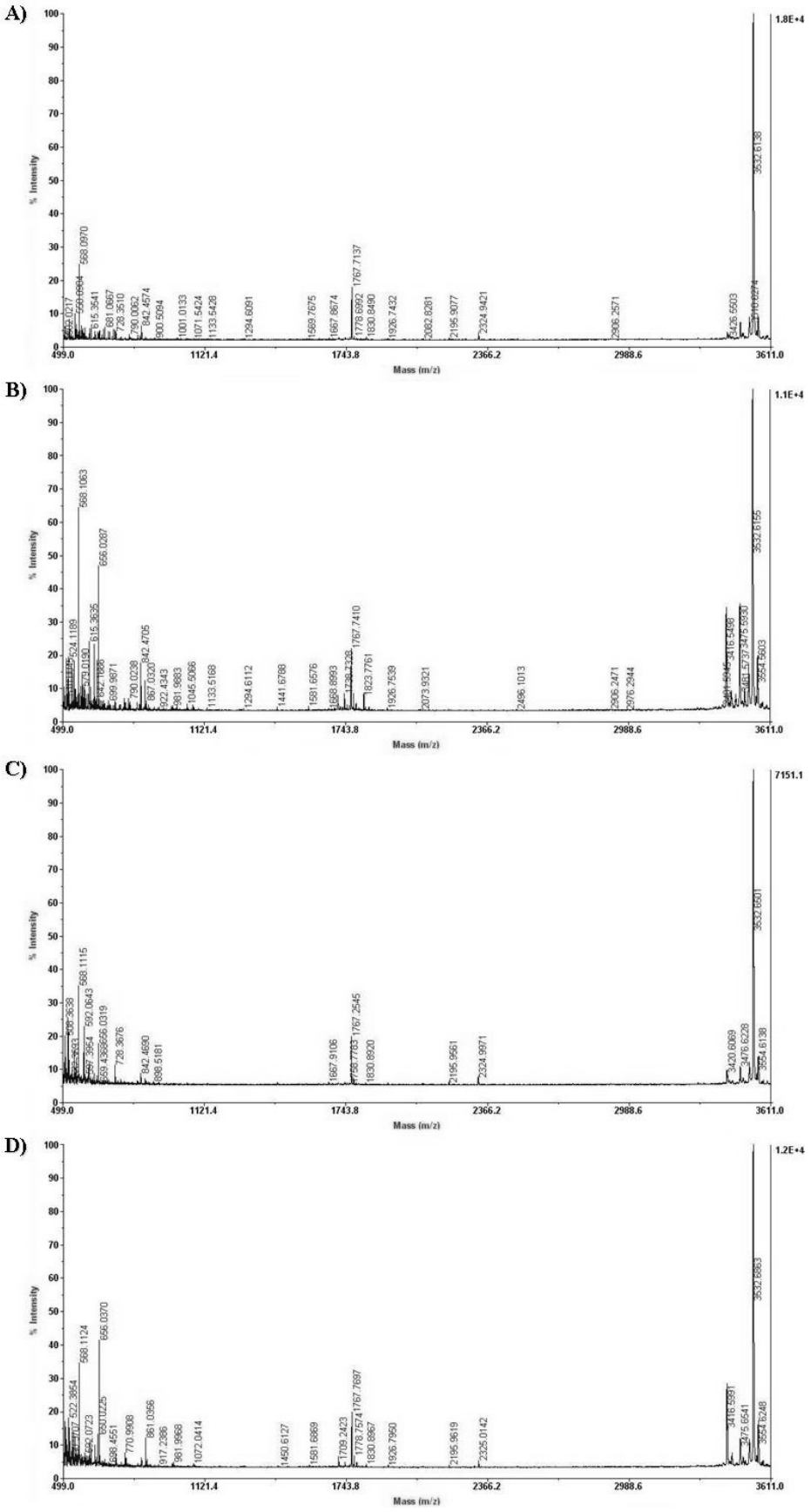

Figure 3-49. MALDI-TOF spectra of the digestion solution of hCT in 60% ACN (A), 80% ACN (B), 60% methanol (C) and 80% methanol (D).

In each of the solvent systems tested hCT essentially remains intact. Reduction of disulfide bonds and alkylation of Cys residues occurs to a variable extent depending on the type of organic solvent used and its concentration in the reaction mixture: the best results were obtained in the solvent system 60% ACN / 40% 50 mM ammonium bicarbonate (Figure 3-49). The results obtained suggest that in 60% ACN hCT adopts a conformation in which the Cys residues (N-terminal portion of the protein) are exposed to the solvent, whereas the unique cleavage site (Lys18) is hindered.

Taking into account this observation, a different sample preparation protocol was designed to verify whether a change in the ACN concentration in the reaction mixture just prior to the addition of trypsin could improve digestion yield by altering hCT conformation.

Sample preparation:

- 20x dilution of hCT stock solution 1 mg/ml with 60% ACN / 40% 50 mM ammonium bicarbonate
- reduction in 5 mM TCEP, 5 minutes at 25 °C
- alkylation in 17 mM IAA, 30 minutes at 25°C in the dark
- quenching of alkylation by addition of 5 mM DTT, 15 minutes at 25 °C
- 3x dilution of sample with 50 mM ammonium bicarbonate to reduce the ACN concentration to 20%
- split the solution in two aliquots
- in-solution digestion: 1 hour at 37 °C with trypsin 1:20 and 1:5 (w/w)
- quenching of digestion by addition of 0.1% formic acid.

MALDI-TOF ANALYSIS

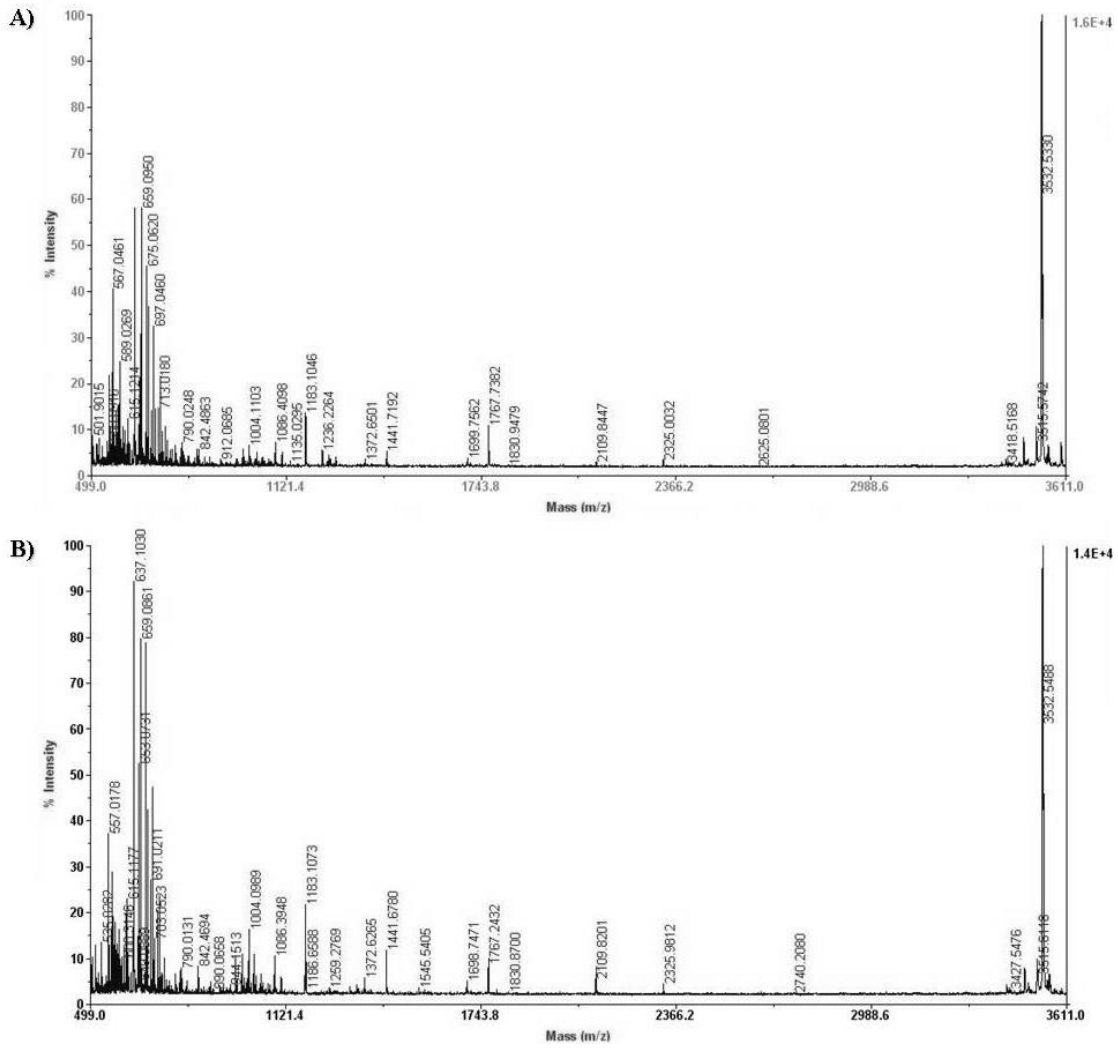

Figure 3-50. MALDI-TOF spectra of the digestion solutions of hCT in 20% ACN with trypsin to protein ratio 1:20 (A) and 1:5 (B).

Even though a large part of hCT is still undigested, the spectra of the digestion solutions of hCT in 20% ACN show signals of its two constituent peptides (m/z 1441.7 and 2109.8), which appear more intense when trypsin to protein ratio is increased from 1:20 to 1:5 (Figure 3-50). This result is an evidence of the change in hCT conformation produced by the reduction of the ACN concentration in the reaction solution: in this environment the cleavage site (Lys18) is more exposed to the action of the proteolytic enzyme, although longer times are required for the reaction to be complete.

Digestion in 60% ACN

Digestion of hCT in 60% ACN / 40% 50 mM ammonium bicarbonate with trypsin to protein ratio 1:5, without previous reduction of disulfide bonds and alkylation of Cys residues, was tested and monitored over time (15 – 90 minutes) (Figure 3-51).

Sample preparation:

- 20x dilution of the stock solution of CT 1 mg/ml with 60% ACN / 40% ammonium bicarbonate
- in-solution digestion with trypsin to protein ratio 1:5 (w/w) at 37 °C
- quenching of digestion by addition of 0.1% formic acid after 15, 30, 60 and 90 minutes.

MALDI-TOF ANALYSIS

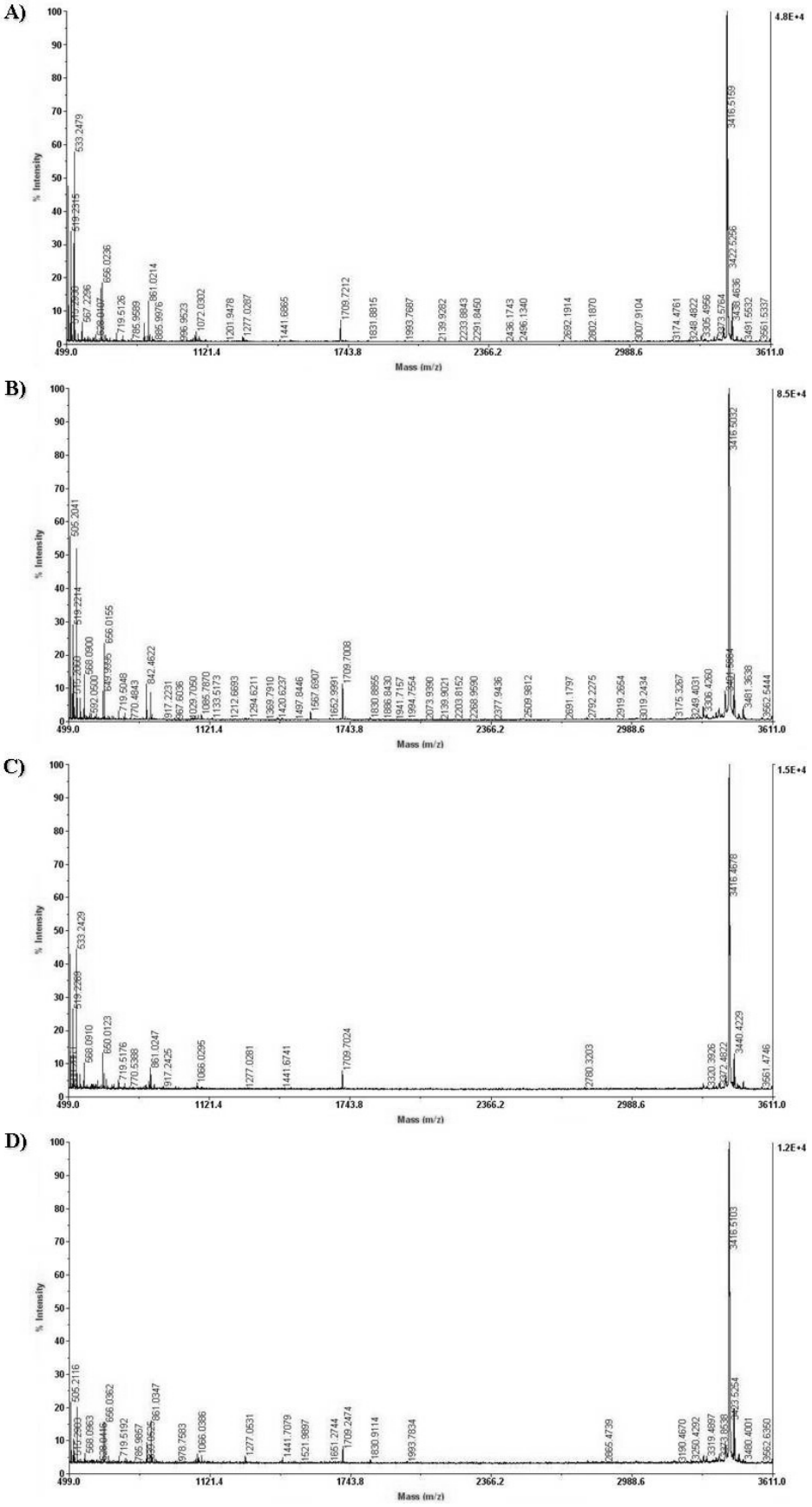

Figure 3-51. MALDI-TOF spectra of the digestion solutions of hCT in 60% ACN after 15 minutes (A), 30 minutes (B), 60 minutes (C) and 90 minutes (D).

Peptide	Length (aa)	Position	Theoretical monoisotopic molecular weight	Experimental monoisotopic $[M+H]^+$
Intact human calcitonin	32	1 – 32	3418.58	3416.5

The theoretical monoisotopic molecular weight reported in the upper table was calculated on the basis of the amino acidic sequence, but because of the disulfide bond between cysteine 1 and 7 and the amidated C-terminal proline, the effective theoretical monoisotopic molecular weight of intact human calcitonin is 3415.5789 Da. Therefore, the experimental monoisotopic weight observed is in good agreement with the expected one. hCT is essentially still undigested after 1 hour of reaction.

Q TRAP INFUSION ANALYSIS

The digestion solution of hCT after 1 hour of reaction was infused in the Q TRAP and analyzed in Q1 and EMS mode (data not shown). The m/z value of the most abundant ion in the full scan spectra was compatible with the one expected for the triply-charged ion of the intact protein. Therefore an ER spectrum was acquired, which confirmed the triply-charged state of the ion of interest (Figure 3-52).

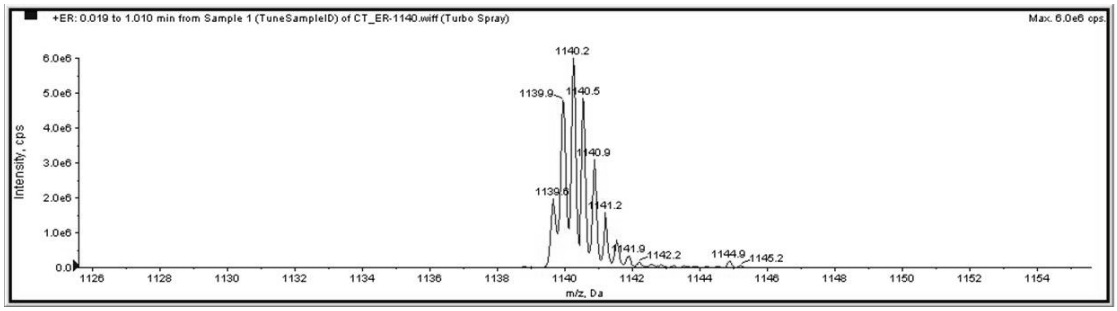

Figure 3-52. ER spectrum of m/z 1140.2, the triply-charged ion of intact hCT.

MS/MS ANALYSIS

MS/MS analysis of intact hCT was performed: MS^E, EPI and MS2 spectra were acquired (Figure 3-53, Figure 3-54, Figure 3-56).

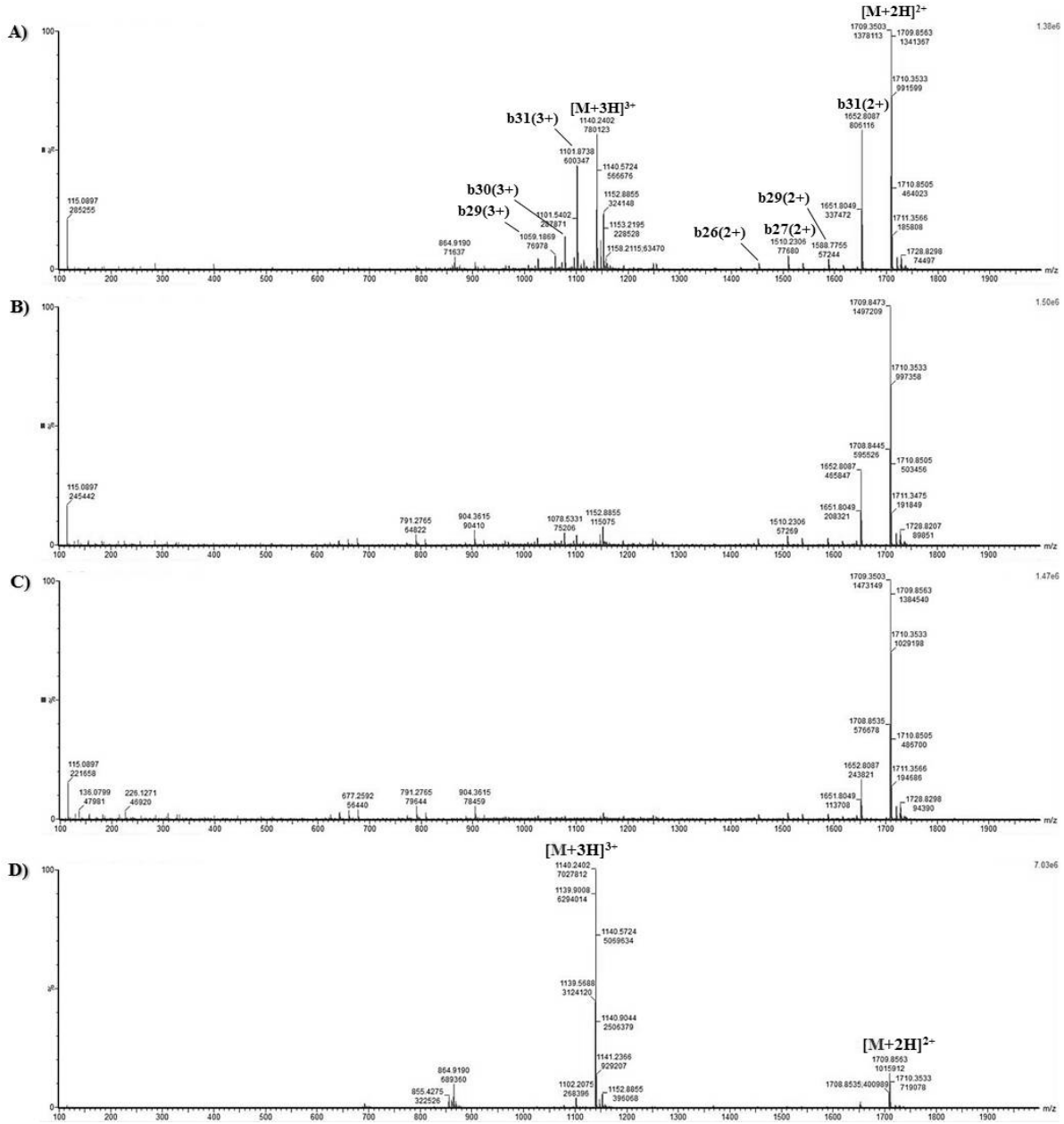

Figure 3-53. MS^E spectra of hCT. The low energy function is reported in (D). A wide range of CE values have been tested: 15 – 30 (A), 25 – 40 (B) and 30 – 45 (C).

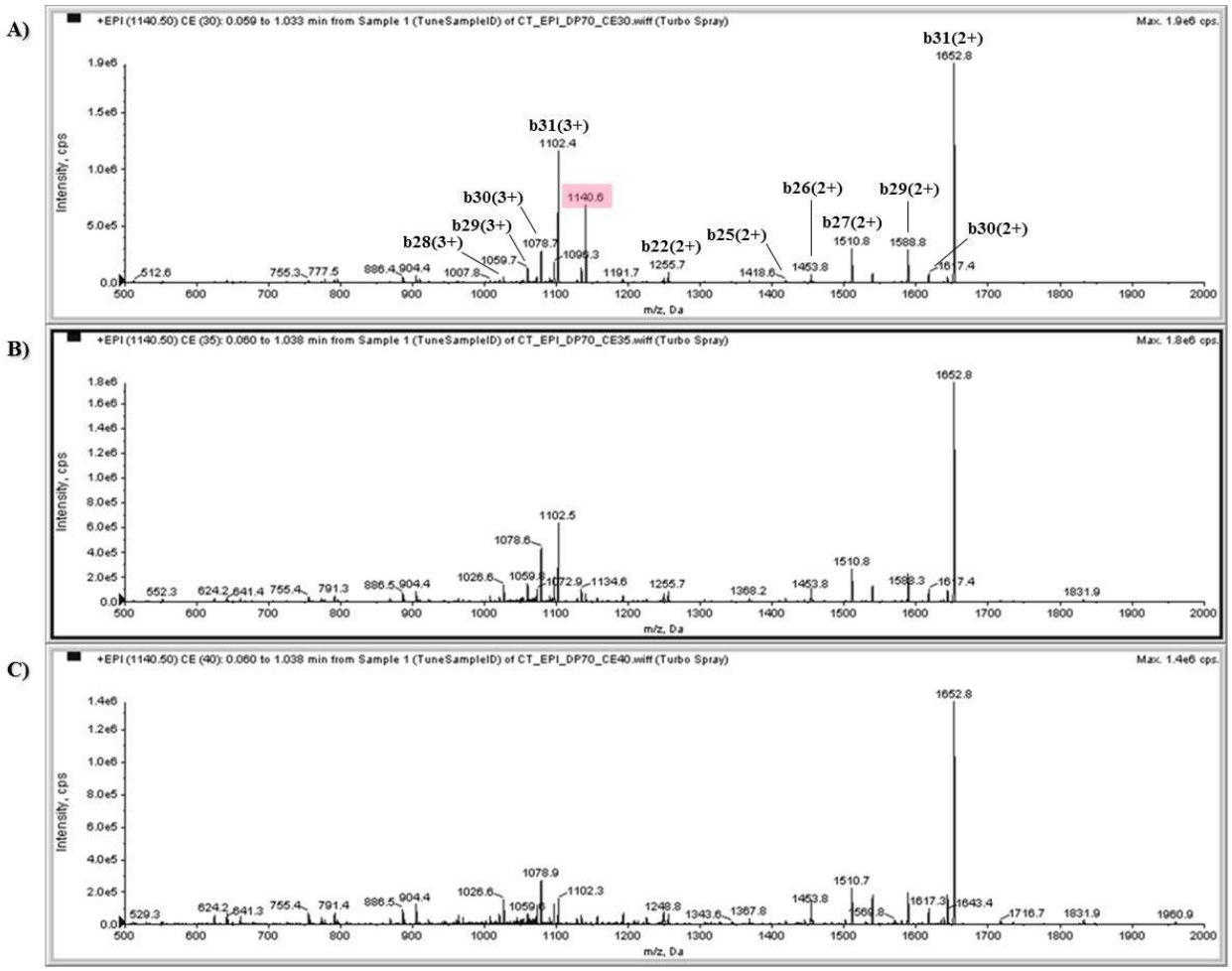

Figure 3-54. EPI fragmentation spectra of hCT. Increasing CE values were applied: 30 (A), 35 (B) and 40 (C). The precursor ion is highlighted in pink.

Seq	#	B	Y	# (+1)
C	1	104.01706	3418.58632	32
G	2	161.03852	3315.57713	31
N	3	275.08145	3258.55567	30
L	4	388.16551	3144.51274	29
S	5	475.19754	3031.42868	28
T	6	576.24522	2944.39665	27
C	7	679.25440	2843.34897	26
M	8	810.29489	2740.33979	25
L	9	923.37895	2609.29930	24
G	10	980.40041	2496.21524	23
T	11	1081.44809	2439.19377	22
Y	12	1244.51142	2338.14610	21
T	13	1345.55910	2175.08277	20
Q	14	1473.61768	2074.03509	19
D	15	1588.64462	1945.97651	18
F	16	1735.71303	1830.94957	17
N	17	1849.75596	1683.88116	16
K	18	1977.85092	1569.83823	15
F	19	2124.91934	1441.74327	14
H	20	2261.97825	1294.67485	13
T	21	2363.02593	1157.61594	12
F	22	2510.09434	1056.56826	11
P	23	2607.14710	909.49985	10
Q	24	2735.20568	812.44709	9
T	25	2836.25336	684.38851	8
A	26	2907.29047	583.34083	7
I	27	3020.37454	512.30372	6
G	28	3077.39600	399.21965	5
V	29	3176.46441	342.19819	4
G	30	3233.48588	243.12978	3
A	31	3304.52299	186.10831	2
P	32	3400.57575	115.07120	1

Seq	#	B	Y	# (+2)
C	1	52.51246	1709.79709	32
G	2	81.02319	1658.29250	31
N	3	138.04466	1629.78177	30
L	4	194.58669	1572.76031	29
S	5	238.10270	1516.21827	28
T	6	288.62654	1472.70226	27
C	7	340.13114	1422.17842	26
M	8	405.65138	1370.67383	25
L	9	462.19341	1305.15359	24
G	10	490.70414	1248.61155	23
T	11	541.22798	1220.10082	22
Y	12	622.75965	1169.57698	21
T	13	673.28348	1088.04532	20
Q	14	737.31277	1037.52148	19
D	15	794.82624	973.49219	18
F	16	868.36045	915.97872	17
N	17	925.38191	842.44451	16
K	18	989.42940	785.42305	15
F	19	1062.96360	721.37557	14
H	20	1131.49306	647.84136	13
T	21	1182.01690	579.31191	12
F	22	1255.55110	528.78807	11
P	23	1304.07749	455.25386	10
Q	24	1368.10678	406.72748	9
T	25	1418.63061	342.69819	8
A	26	1454.14917	292.17435	7
I	27	1510.69120	256.65579	6
G	28	1539.20193	200.11376	5
V	29	1588.73614	171.60303	4
G	30	1617.24687	122.06882	3
A	31	1652.76543	93.55809	2
P	32	1700.79181	58.03953	1

Seq	#	B	Y	# (+3)
C	1	35.34427	1140.20069	32
G	2	54.35142	1105.86429	31
N	3	92.36573	1086.85714	30
L	4	130.06042	1048.84283	29
S	5	159.07109	1011.14814	28
T	6	192.75365	982.13746	27
C	7	227.09005	948.45490	26
M	8	270.77021	914.11851	25
L	9	308.46490	870.43835	24
G	10	327.47205	832.74366	23
T	11	361.15461	813.73650	22
Y	12	415.50905	780.05395	21
T	13	449.19161	725.69950	20
Q	14	491.87781	692.01694	19
D	15	530.22012	649.33075	18
F	16	579.24292	610.98844	17
N	17	617.25723	561.96563	16
K	18	659.95555	523.95132	15
F	19	708.97836	481.25300	14
H	20	754.66466	432.23020	13
T	21	788.34722	386.54389	12
F	22	837.37003	352.86133	11
P	23	869.72095	303.83853	10
Q	24	912.40714	271.48761	9
T	25	946.08970	228.80142	8
A	26	969.76874	195.11886	7
I	27	1007.46343	171.43982	6
G	28	1026.47058	133.74513	5
V	29	1059.49338	114.73798	4
G	30	1078.50054	81.71517	3
A	31	1102.17958	62.70802	2
P	32	1134.19716	39.02898	1

Figure 3-55. Fragment ion tables of hCT: theoretical monoisotopic mass values of singly-, doubly- and triply-charged b and y ions. From http://db.systemsbiology.net/proteomicsToolkit/

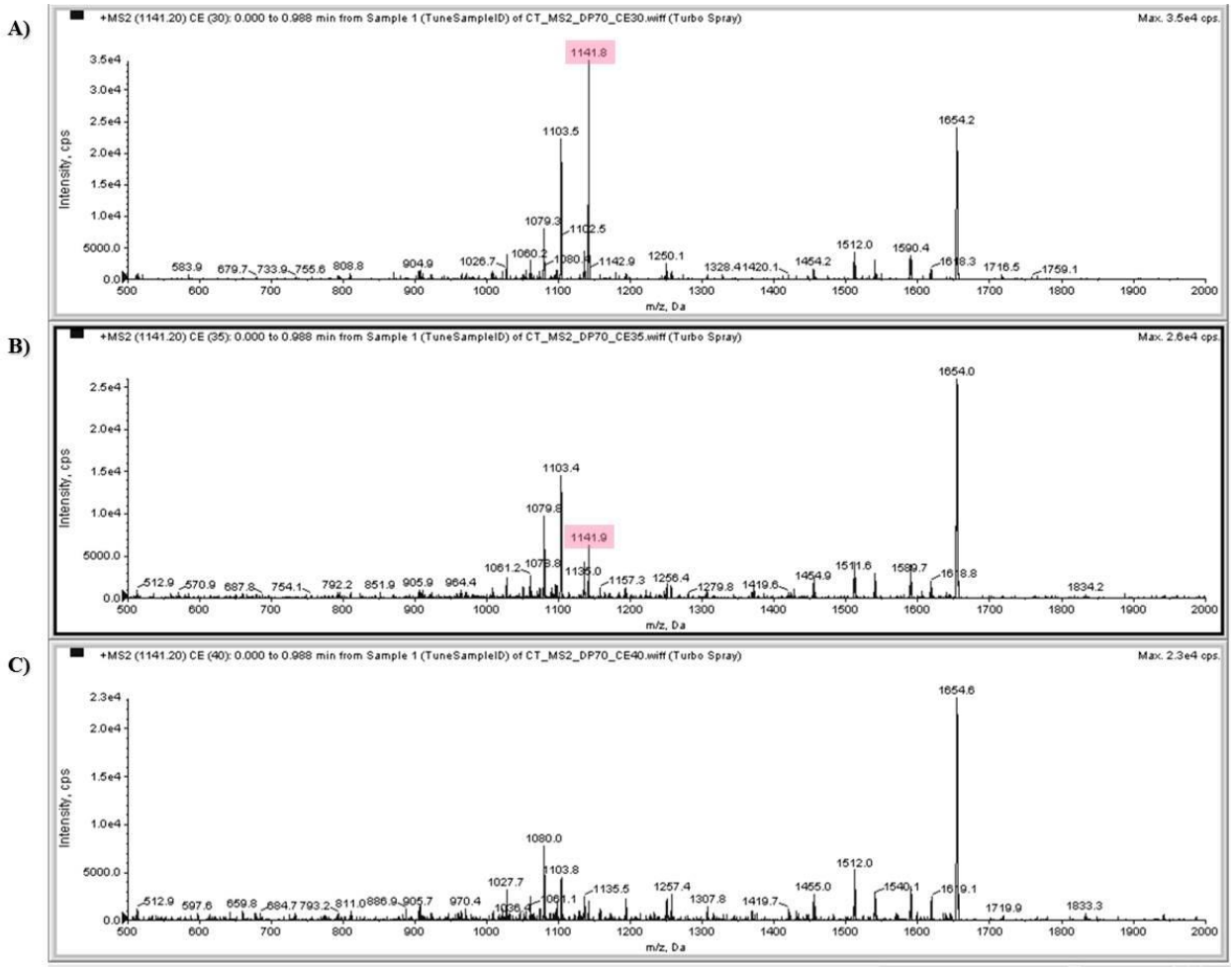

Figure 3-56. MS2 fragmentation spectra of hCT. Increasing CE values were applied: 30 (A), 35 (B) and 40 (C). The precursor ion is highlighted in pink.

MRM ANALYSIS

The following transitions were analyzed:

m/z precursor ion (Q1)	m/z fragment ion (Q3)	Fragment ion
1141.2	**1654.0**	b31(2+)
1141.2	**1103.4**	b31(3+)
1141.2	**1079.8**	b30(3+)

Linearity in the theoretical range of concentrations 0.1 – 12.5 µg/ml was tested and calibration curves were obtained (Figure 3-57).

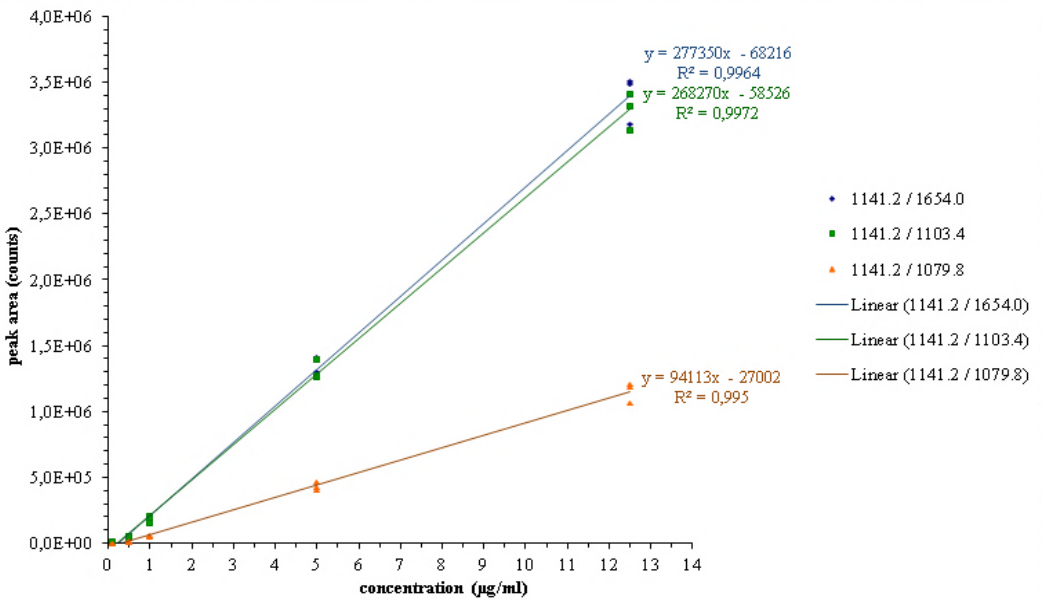

Figure 3-57. Calibration curves obtained for intact hCT.

The transition 1141.2/1103.4 featured the best linearity (R^2 = 0.997).

Human procalcitonin

Digestion in 60% ACN

Digestion of hPCT was performed in 60% ACN / 40% 50 mM ammonium bicarbonate, which represented the best choice among the mixed organic-aqueous solvent systems tested for hCT.
Abrupt digestion in the above mentioned reaction solution with trypsin to protein ratio 1:5, without previous reduction of disulfide bonds and alkylation of Cys residues, was monitored over time (15 – 90 minutes) (Figure 3-58).
Sample preparation:

- solubilization of the protein standard (10 µg) in 50 mM ammonium bicarbonate: 100 µl of stock solution 0.1 mg/ml
- 2.5x dilution of 50 µl of the stock solution with ACN: PCT 40 µg/ml in 60% ACN / 40% 50 mM ammonium bicarbonate
- in-solution digestion with trypsin 1:5 (w/w) at 37 °C
- quenching of digestion by addition of 0.1% formic acid after 15, 30, 60 and 90 minutes.

MALDI-TOF ANALYSIS

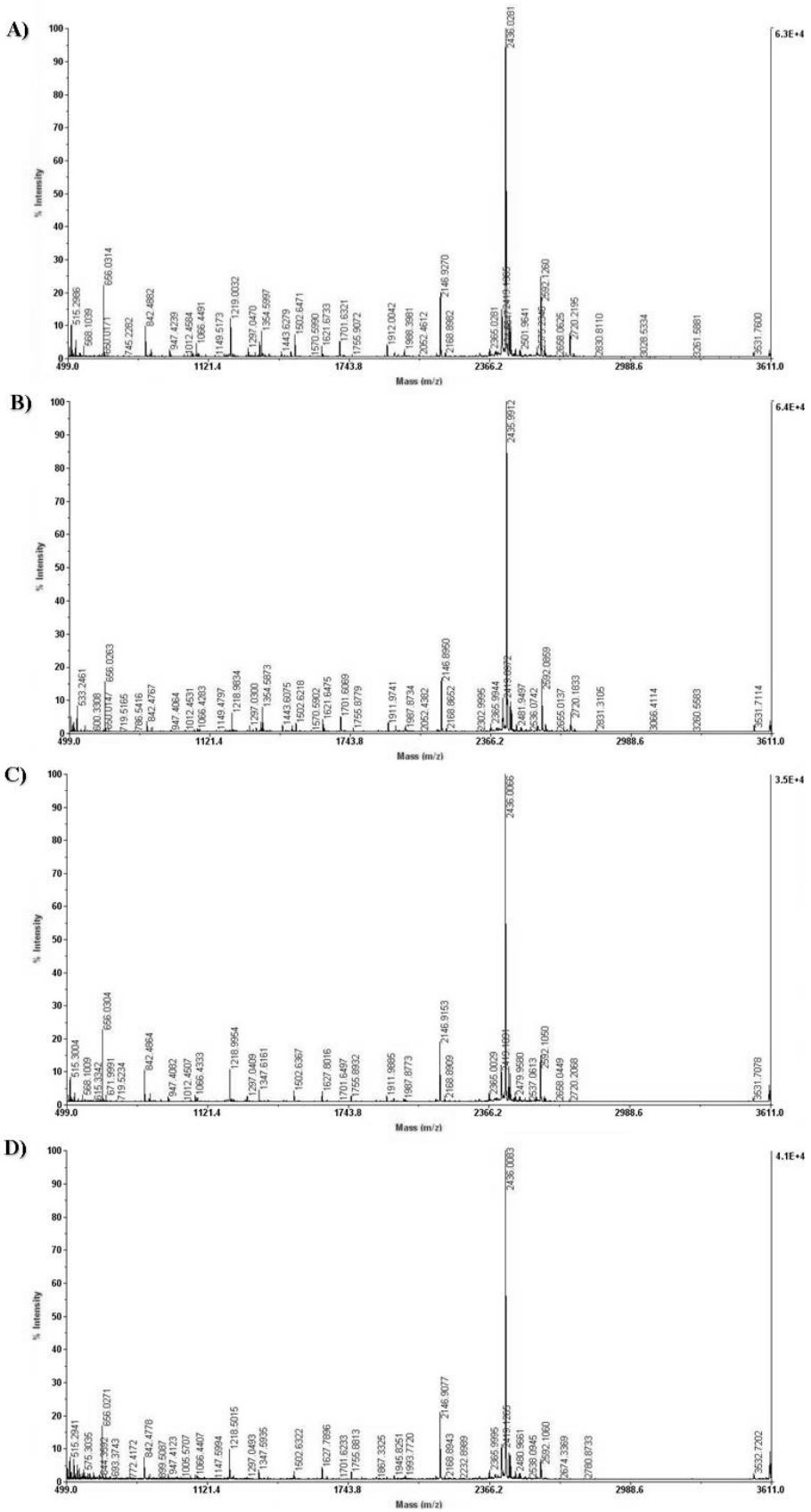

Figure 3-58. MALDI-TOF spectra of the digestion solution of hPCT after 15 minutes (A), 30 minutes (B), 60 minutes (C) and 90 minutes (D).

The MALDI-TOF spectrum after 1 hour of reaction was analyzed looking for signals which could be attributed to the tryptic digestion of hPCT (Figure 3-59).

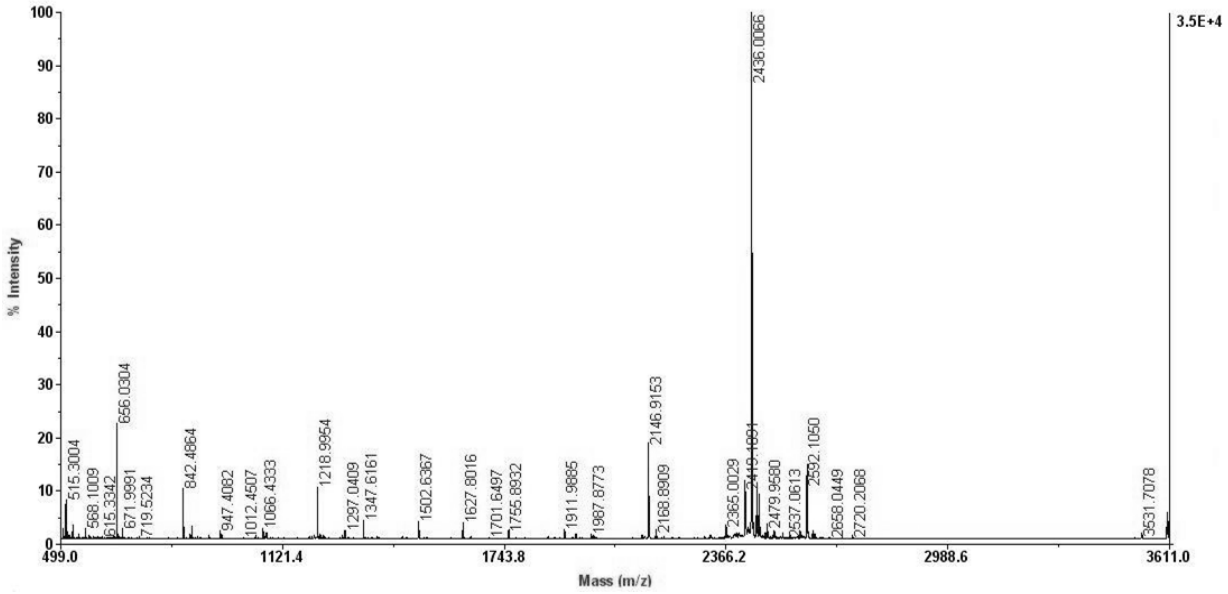

Figure 3-59. MALDI-TOF spectrum of digestion solution of hPCT in 60% ACN after 1 hour of reaction.

Peptide sequence	Length (aa)	Position	Missed cleavages	Theoretical monoisotopic molecular weight	Experimental monoisotopic $[M+H]^+$
EGSSLDSPR	9	48 – 56	-	946.44	947.4082
ASELEQEQER	10	38 – 47	-	1217.55	1218.9954
DH*R*PHVSMPQNAN	13	104 – 116	1	1501.68	1502.6367
FHTFPQTAIGVGAPGK	16	78 – 93	-	1626.85	1627.8016
FHTFPQTAIGVGAPG*K*K	17	78 – 94	1	1754.95	1755.9832
FHTFPQTAIGVGAPG*KK*R	18	78 – 95	2	1911.05	1911.9885
ASELEQEQE*R*EGSSLDSPR	19	38 – 56	1	2145.98	2146.9153
DMSSDLE*R*DH*R*PHVSMPQNAN	21	96 – 116	2	2435.07	2436.0066
*R*DMSSDLE*R*DH*R*PHVSMPQNAN	22	95 – 116	3	2591.17	2592.1050
*KR*DMSSDLE*R*DH*R*PHVSMPQNAN	23	94 – 116	4	2719.20	2720.2068

Sequence coverage = 50%

The peptides of interest are present even after just 15 minutes of reaction.

Q TRAP INFUSION ANALYSIS

Desalting of the digestion solution of hPCT prior to Q TRAP infusion analysis was performed using Pierce C18 Spin Columns, Thermo Scientific. The sample was analyzed in Q1 and EMS mode (data not shown). The m/z value of the most abundant ion in the full scan spectra was compatible with the one expected for the triply-charged ion of C-terminal peptide DMSSDLERDHRPHVSMPQNAN. Therefore an ER spectrum was acquired, which confirmed the triply-charged state of the ion of interest (Figure 3-60).

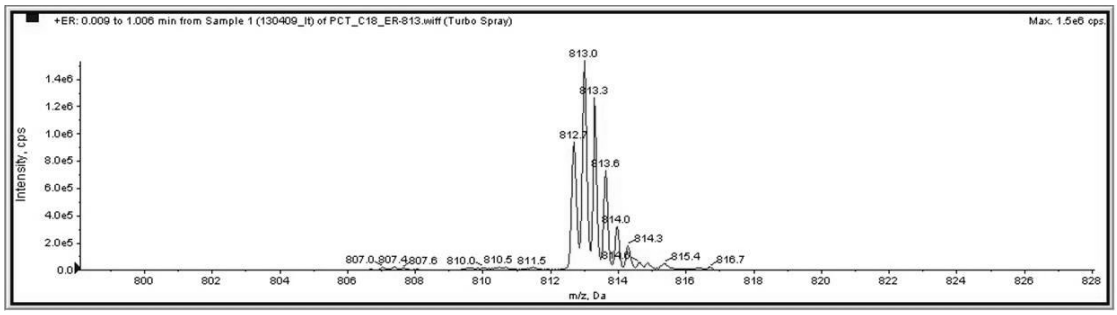

Figure 3-60. ER spectrum of the triply-charged ion of peptide DMSSDLERDHRPHVSMPQNAN.

MS/MS ANALYSIS

MS/MS analyses were performed to confirm the identity of the ion of interest as the C-terminal peptide DMSSDLERDHRPHVSMPQNAN. MALDI-TOF/TOF, MS^E, EPI and MS2 spectra were acquired (Figure 3-61, Figure 3-62, Figure 3-63, Figure 3-65).

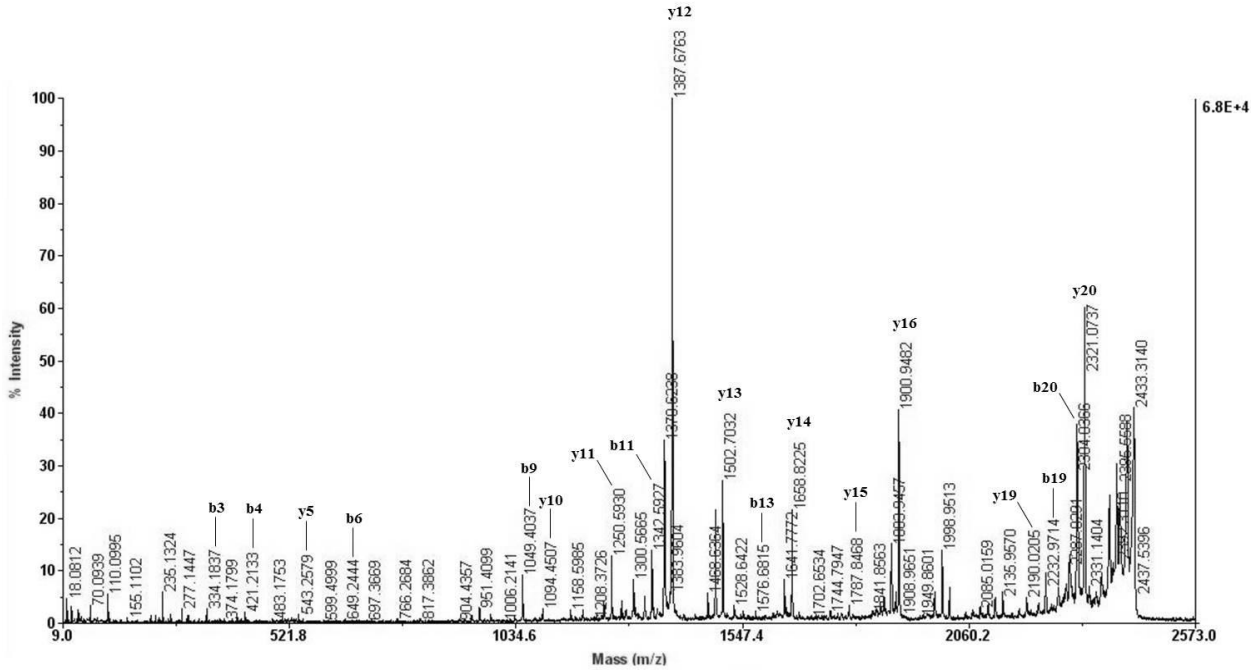

Figure 3-61. MALDI-TOF/TOF spectrum of peptide DMSSDLERDHRPHVSMPQNAN.

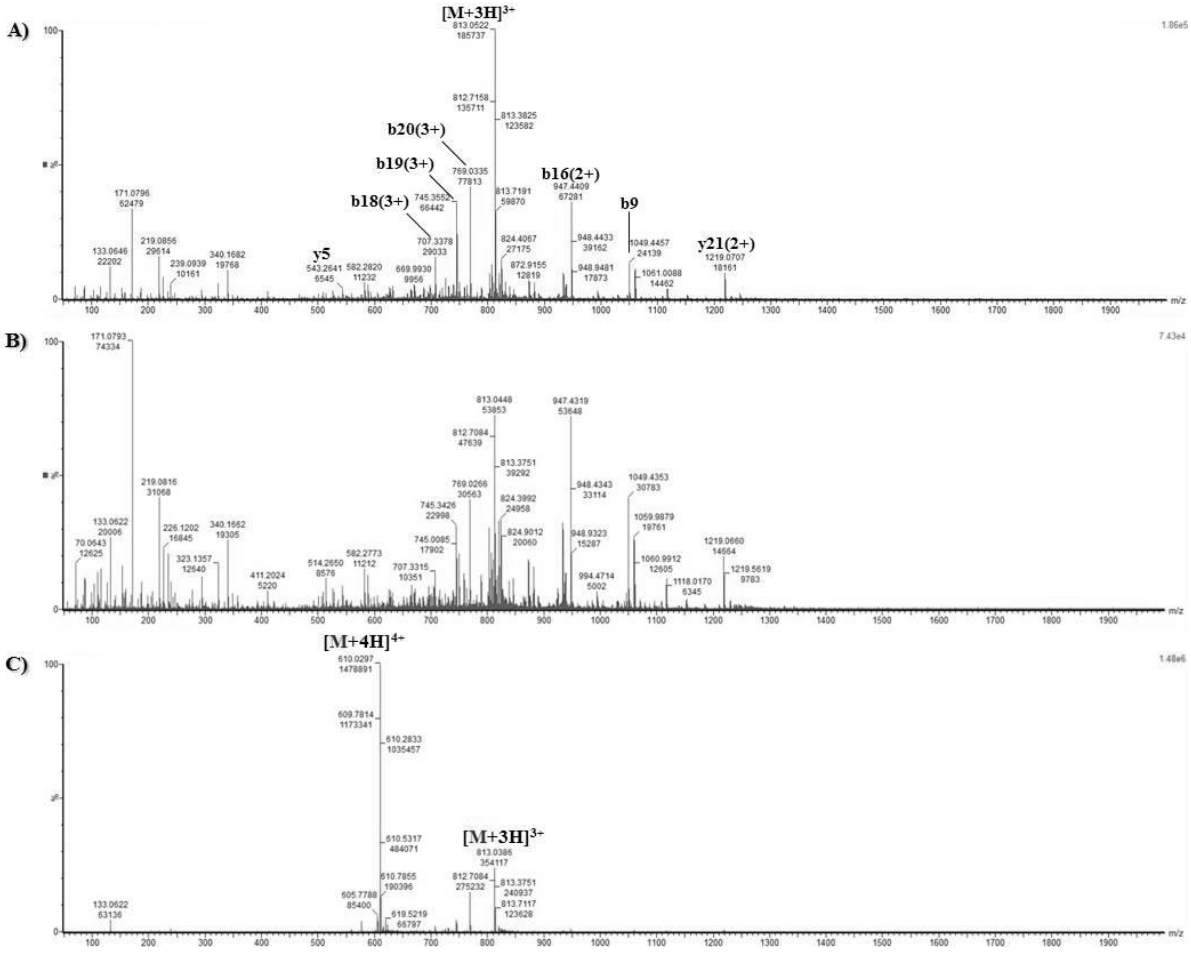

Figure 3-62. MS^{E} spectra of peptide DMSSDLERDHRPHVSMPQNAN. The low energy function is reported in (C). Different ranges of CE values have been tested: 15 – 30 (A) and 20 – 35 (B).

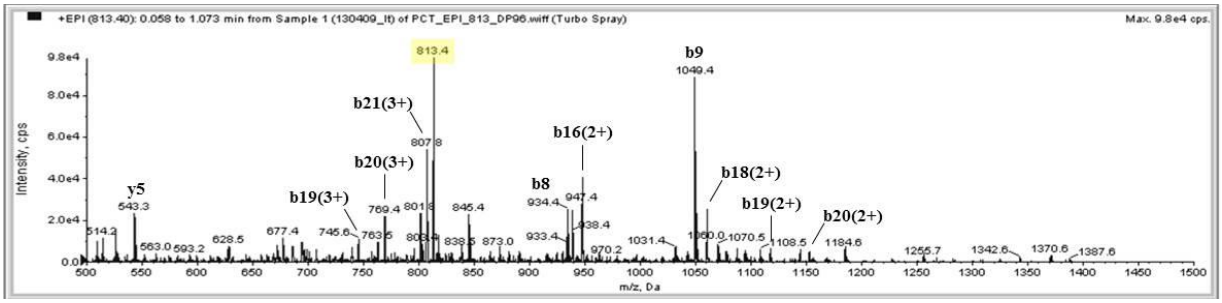

Figure 3-63. EPI fragmentation spectrum of C-terminal peptide DMSSDLERDHRPHVSMPQNAN. The precursor ion is highlighted in yellow.

Seq	#	B	Y	# (+1)
D	1	116.03481	2436.07851	21
M	2	247.07530	2321.05156	20
S	3	334.10733	2190.01108	19
S	4	421.13935	2102.97905	18
D	5	536.16630	2015.94702	17
L	6	649.25036	1900.92008	16
E	7	778.29295	1787.83601	15
R	8	934.39406	1658.79342	14
D	9	1049.42101	1502.69231	13
H	10	1186.47992	1387.66537	12
R	11	1342.58103	1250.60646	11
P	12	1439.63379	1094.50535	10
H	13	1576.69270	997.45258	9
V	14	1675.76112	860.39367	8
S	15	1762.79315	761.32526	7
M	16	1893.83363	674.29323	6
P	17	1990.88640	543.25274	5
Q	18	2118.94497	446.19998	4
N	19	2232.98790	318.14140	3
A	20	2304.02501	204.09848	2
N	21	2418.06794	133.06136	1

Seq	#	B	Y	# (+2)
D	1	58.52134	1218.54319	21
M	2	124.04158	1161.02972	20
S	3	167.55760	1095.50947	19
S	4	211.07361	1051.99346	18
D	5	268.58708	1008.47745	17
L	6	325.12912	950.96397	16
E	7	389.65041	894.42194	15
R	8	467.70097	829.90065	14
D	9	525.21444	751.85009	13
H	10	593.74389	694.33662	12
R	11	671.79445	625.80716	11
P	12	720.32083	547.75661	10
H	13	788.85029	499.23023	9
V	14	838.38449	430.70077	8
S	15	881.90051	381.16656	7
M	16	947.42075	337.65055	6
P	17	995.94713	272.13031	5
Q	18	1059.97642	223.60392	4
N	19	1116.99788	159.57464	3
A	20	1152.51644	102.55317	2
N	21	1209.53791	67.03462	1

Seq	#	B	Y	# (+3)
D	1	39.35018	812.69808	21
M	2	83.03035	774.35577	20
S	3	112.04102	730.67561	19
S	4	141.05170	701.66493	18
D	5	179.39401	672.65425	17
L	6	217.08870	634.31194	16
E	7	260.10290	596.61725	15
R	8	312.13660	553.60305	14
D	9	350.47892	501.56935	13
H	10	396.16522	463.22704	12
R	11	448.19892	417.54073	11
P	12	480.54984	365.50703	10
H	13	526.23615	333.15611	9
V	14	559.25895	287.46980	8
S	15	588.26963	254.44700	7
M	16	631.94979	225.43632	6
P	17	664.30071	181.75616	5
Q	18	706.98690	149.40524	4
N	19	745.00121	106.71905	3
A	20	768.68025	68.70474	2
N	21	806.69456	45.02570	1

Figure 3-64. Fragment ion tables of C-terminal peptide DMSSDLERDHRPHVSMPQNAN: theoretical monoisotopic mass values of singly-, doubly- and triply-charged b and y ions. From http://db.systemsbiology.net/proteomicsToolkit/

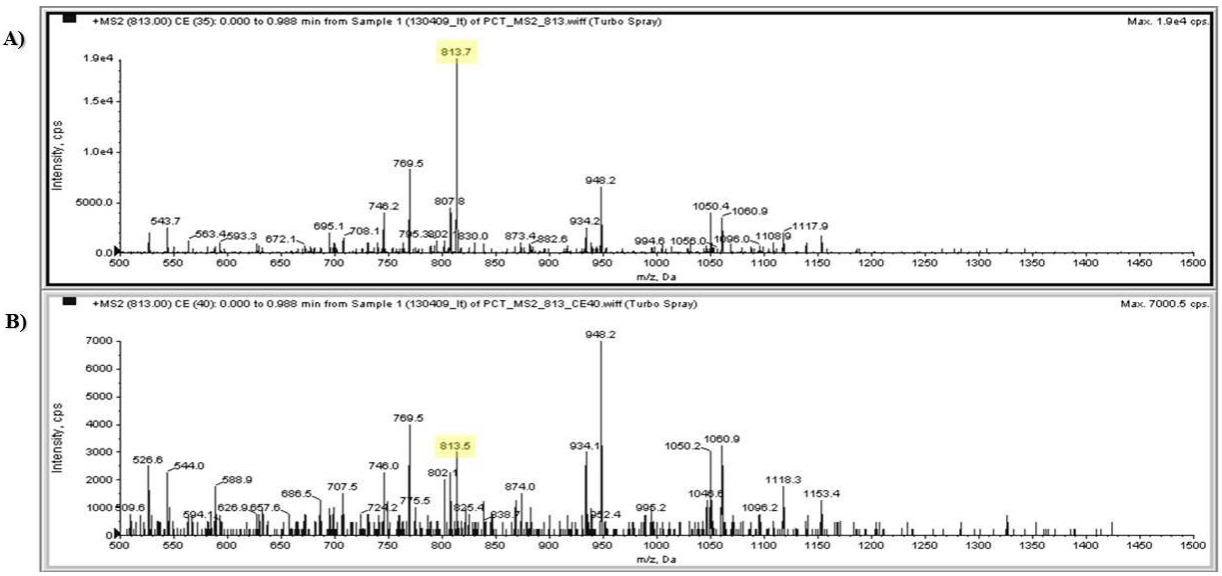

Figure 3-65. MS2 fragmentation spectra of C-terminal peptide DMSSDLERDHRPHVSMPQNAN. The applied CE values are 35 (A) and 40 (B). The precursor ion is highlighted in yellow.

Human C-reactive protein

Digestion of hCRP was performed in 60% ACN / 40% 50 mM ammonium bicarbonate, which represented the best choice among the mixed organic-aqueous solvent systems tested for hCT. Two different trypsin to protein ratios were tested, 1:20 and 1:5 (Figure 3-66).

Digestion of the reduced and alkylated protein in 60% ACN

Sample preparation:

- 20x dilution of the stock solution of CRP 1 mg/ml with 60% ACN / 40% 50 mM ammonium bicarbonate
- reduction in 5 mM TCEP, 5 minutes at 25 °C in the dark
- alkylation in 17 mM IAA, 30 minutes at 25°C in the dark
- quenching of alkylation by addition of 5 mM DTT, 15 minutes at 25 °C
- split the solution in two aliquots
- in-solution digestion: 1 hour at 37 °C with trypsin 1:20 and 1:5 (w/w)
- quenching of digestion by addition of 0.1% formic acid.

MALDI-TOF ANALYSIS

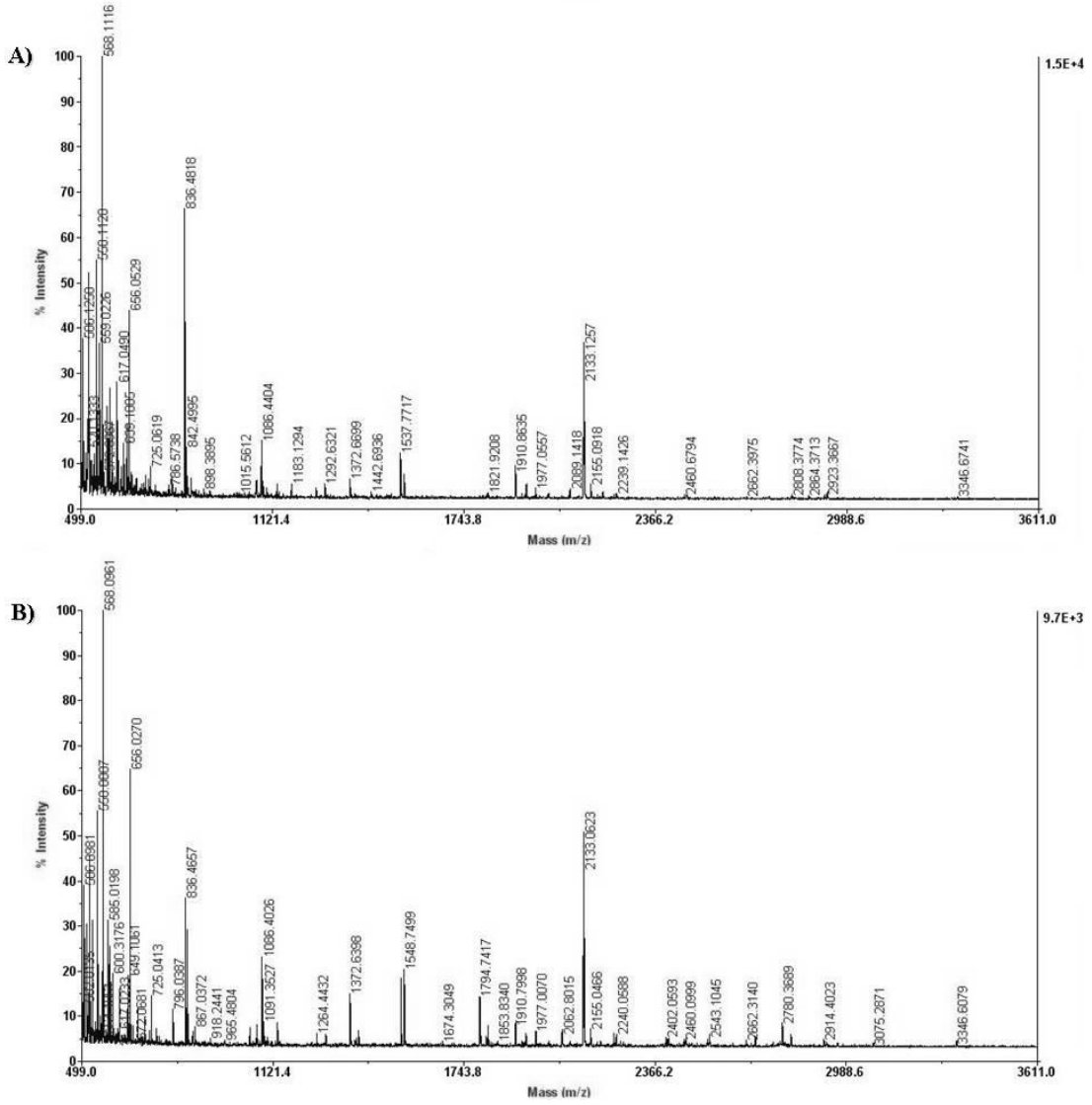

Figure 3-66. MALDI-TOF spectra of the digestion solutions of hCRP in 60% ACN with trypsin to protein ratio 1:20 (A) and 1:5 (B).

The MALDI-TOF spectra of the digestion solutions were analyzed to look for the presence of signals which can be attributed to hCRP peptides:

Peptide sequence	Length (aa)	Position	Missed cleavages	Theoretical monoisotopic molecular weight	Experimental monoisotopic $[M+H]^+$
*K*AFVFPK	7	7 – 13	1	835.50	836.4657
GYSIFSYATK	10	48 – 57	-	1135.55	1136.5061
GYSIFSYAT*K*R	11	48 – 58	1	1291.66	1292.6123
QDNEILIFWSK	11	59 – 69	-	1391.71	1392.6337
*R*QDNEILIFWSK	12	58 – 69	1	1547.81	1548.7499
YEVQGEVFT*K*PQLWP	15	192 – 206	1	1819.91	1820.8497
ESDTSYVSL*K*APLT*K*PLK	18	14 – 31	2	1976.08	1977.0070
AL*K*YEVQGEVFT*K*PQLWP	18	181 – 206	2	2132.13	2133.0623

Sequence coverage = 31.6%

The lower the trypsin to protein ratio is, the poorer the digestion yield of peptides RQDNEILIFWSK (m/z 1548.8) and ALKYEVQGEVFTKPQLWP (m/z 2133.1).

Digestion of hCRP in 60% ACN / 40% 50 mM ammonium bicarbonate with trypsin to protein ratio 1:5, with previous reduction of disulfide bonds and alkylation of Cys residues, was monitored over time (15 – 90 minutes) (Figure 3-67).

MALDI-TOF ANALYSIS

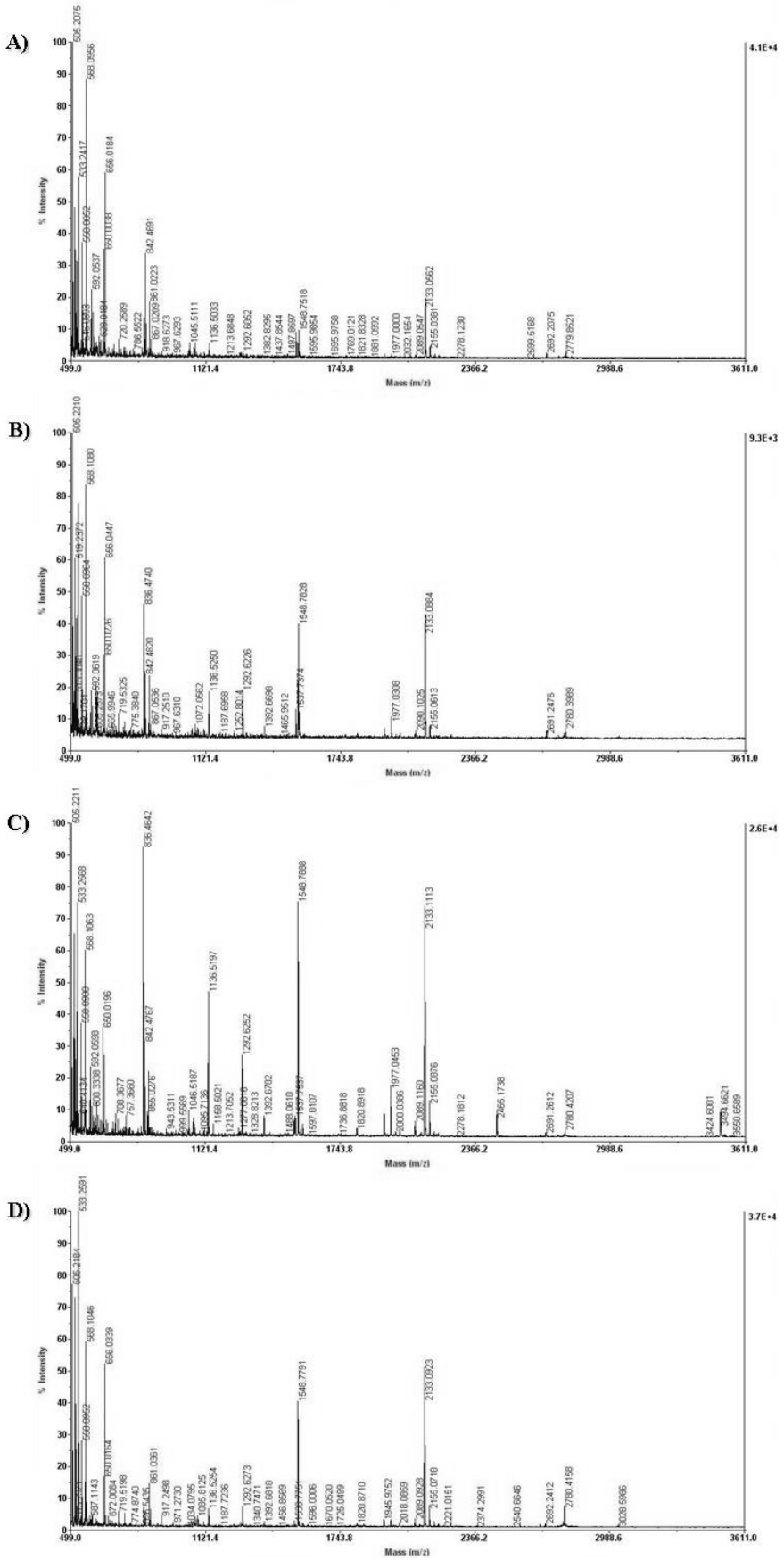

Figure 3-67. MALDI-TOF spectra of the digestion solution of hCRP after 15 minutes (A), 30 minutes (B), 60 minutes (C) and 90 minutes (D).

Digestion in 60% ACN

Digestion of hCRP in 60% ACN / 40% 50 mM ammonium bicarbonate with trypsin to protein ratio 1:5, without previous reduction of disulfide bonds and alkylation of Cys residues, was monitored over time (15 – 90 minutes) (Figure 3-68).

Sample preparation:

- 20x dilution of the stock solution of CRP 1 mg/ml with 60% CAN / 40% 50 mM ammonium bicarbonate, pH 8
- in-solution digestion with trypsin 1:5 (w/w) at 37 °C
- quenching of digestion by addition of 0.1% formic acid after 15, 30, 60 and 90 minutes.

MALDI-TOF ANALYSIS

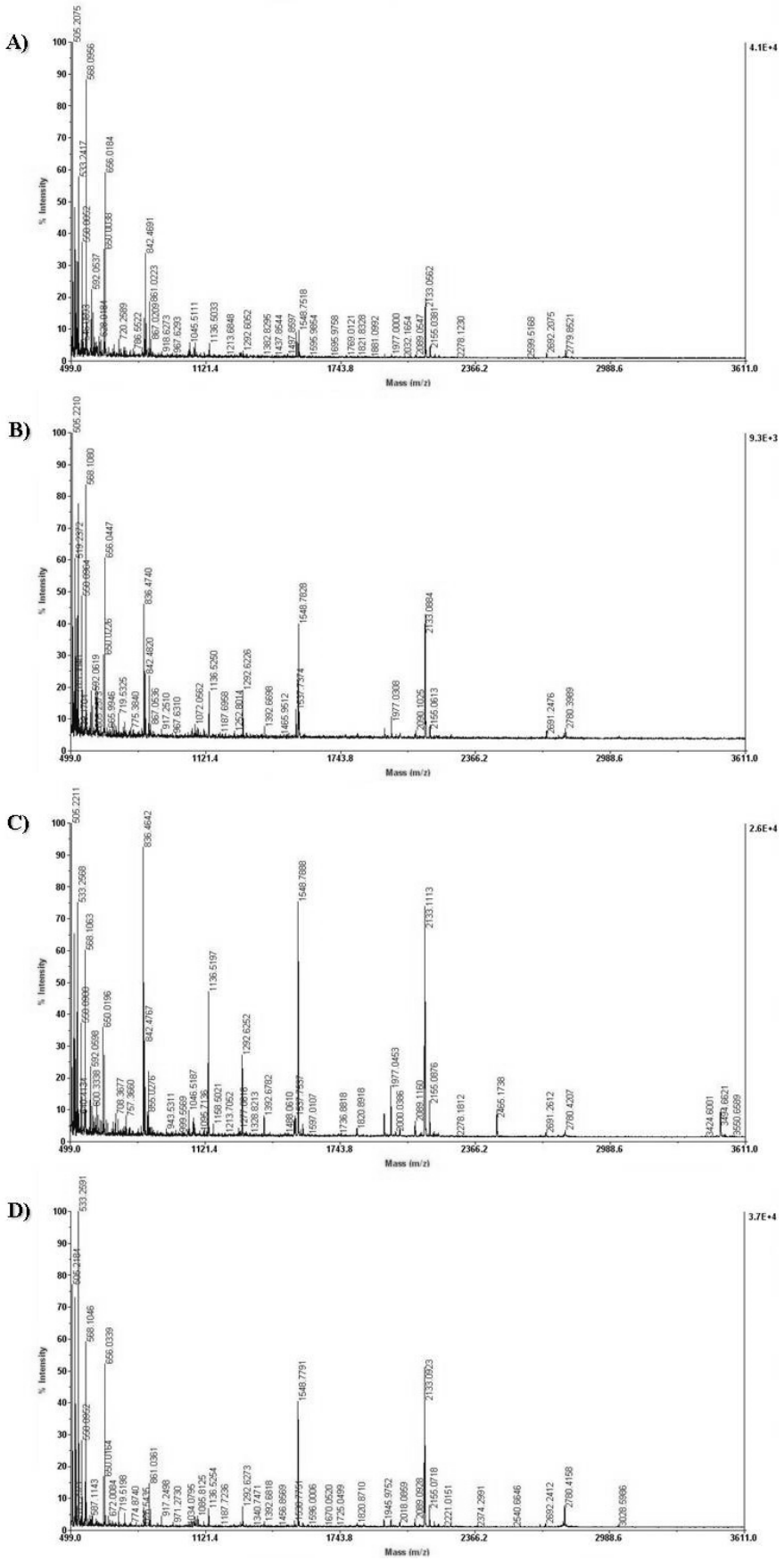

Figure 3-68. MALDI-TOF spectra of the digestion solution of hCRP in 60% ACN after 15 minutes (A), 30 minutes (B), 60 minutes (C) and 90 minutes (D).

The MALDI-TOF spectrum of the digestion solution after one hour of reaction was analyzed (Figure 3-69) and compared to the spectra acquired at different reaction times.

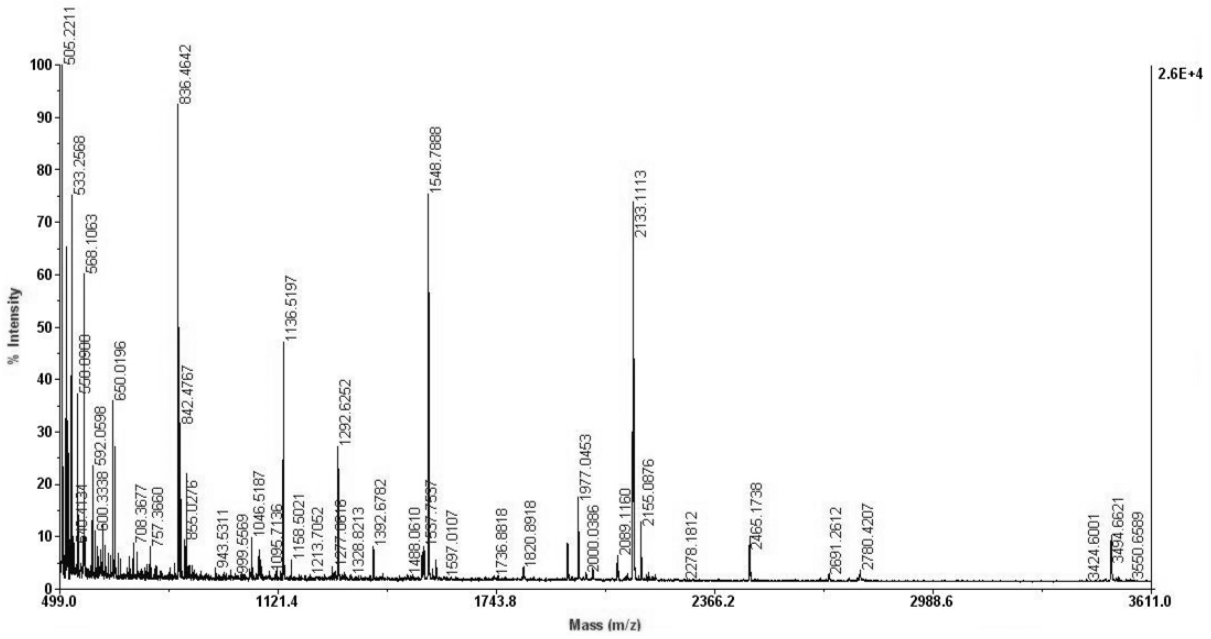

Figure 3-69. MALDI-TOF spectrum of digestion solution of hCRP in 60% ACN after 1 hour of reaction.

Peptide sequence	Length (aa)	Position	Missed cleavages	Theoretical monoisotopic molecular weight	Experimental monoisotopic $[M+H]^+$
*K*AFVFPK	7	7 – 13	1	835.50	836.4642
GYSIFSYATK	10	48 – 57	-	1135.55	1136.5197
GYSIFSYAT*K*R	11	48 – 58	1	1291.66	1292.6254
QDNEILIFWSK	11	59 – 69	-	1391.71	1392.6782
*R*QDNEILIFWSK	12	58 – 69	1	1547.81	1548.7888
YEVQGEVFT*K*PQLWP	15	192 – 206	1	1819.91	1820.8918
ESDTSYVSL*K*APLT*K*PLK	18	14 – 31	2	1976.08	1977.0453
AL*K*YEVQGEVFT*K*PQLWP	18	181 – 206	2	2132.13	2133.1113

Sequence coverage = 31.6%

The peptides of interest, RQDNEILIFWSK and ALKYEVQGEVFTKPQLWP, are present even after just 15 minutes of reaction.

MS/MS ANALYSIS

MS/MS analyses were performed to confirm the identity of the ions of interest as the peptides RQDNEILIFWSK and ALKYEVQGEVFTKPQLWP. MALDI-TOF/TOF and MS^E spectra were acquired (Figure 3-70, Figure 3-72, Figure 3-71, Figure 3-74).

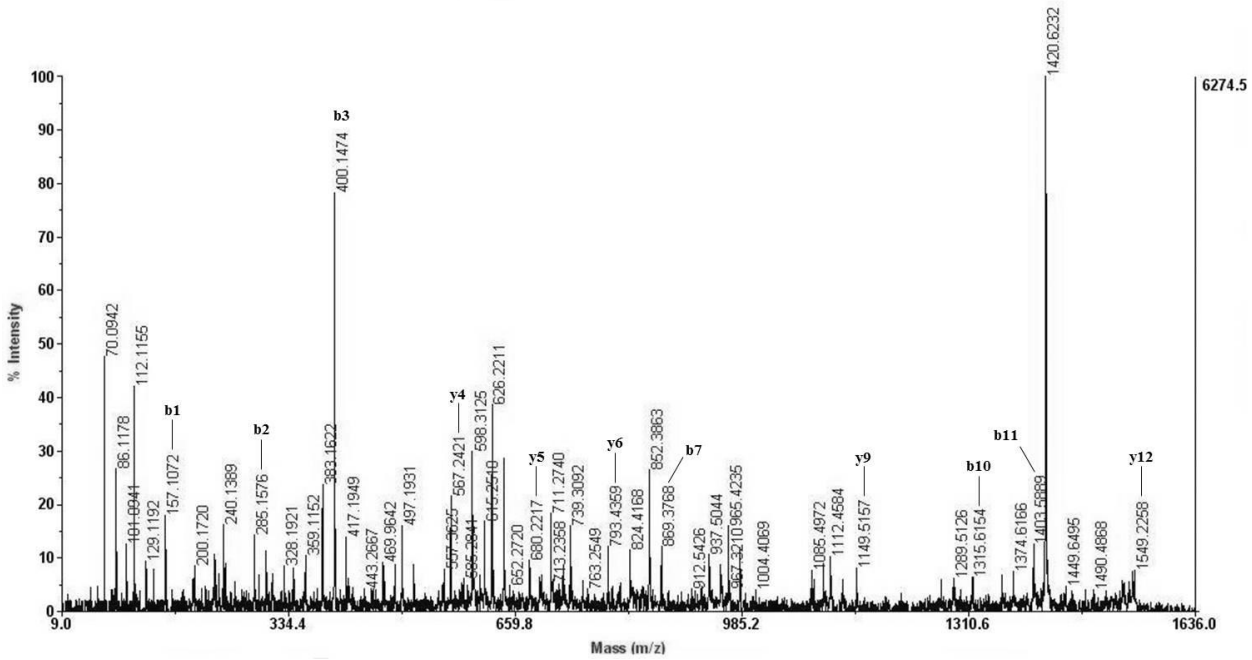

Figure 3-70. MALDI-TOF/TOF spectrum of peptide RQDNEILIFWSK.

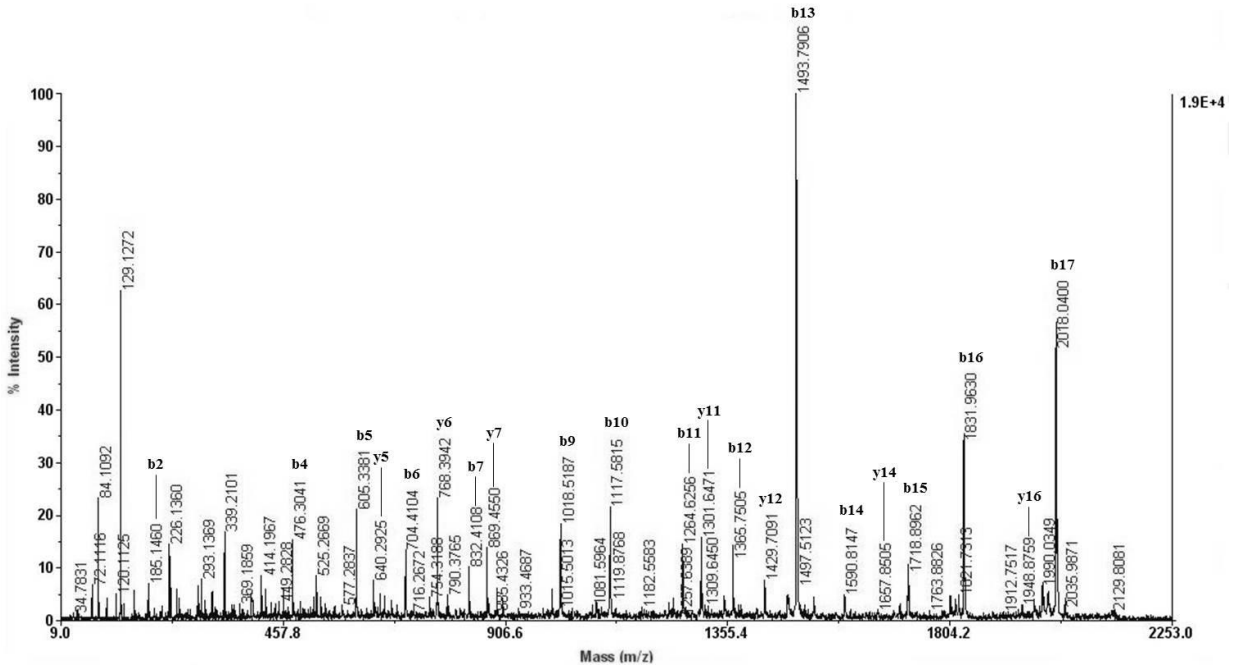

Figure 3-71. MALDI-TOF/TOF spectrum of C-terminal peptide ALKYEVQGEVFTKPQLWP.

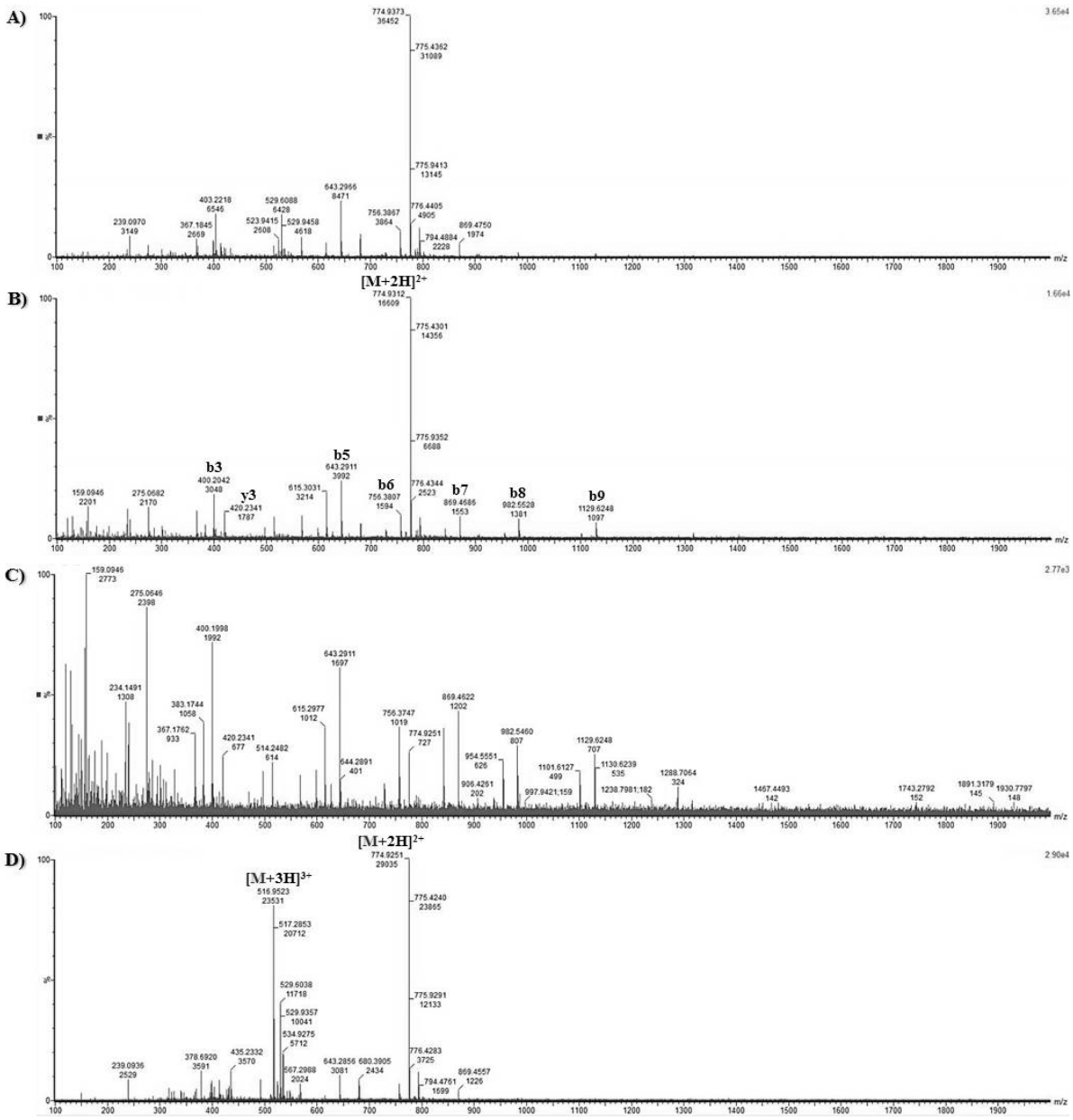

Figure 3-72. MS^E spectra of peptide RQDNEILIFWSK. The low energy function is reported in (D). A wide range of CE values have been tested: 15 – 30 (A), 25 – 40 (B) and 30 – 45 (C).

Seq	#	B	Y	# (+1)
R	1	157.10898	1548.81749	12
Q	2	285.16756	1392.71638	11
D	3	400.19450	1264.65781	10
N	4	514.23743	1149.63086	9
E	5	643.28002	1035.58794	8
I	6	756.36408	906.54534	7
L	7	869.44815	793.46128	6
I	8	982.53221	680.37722	5
F	9	1129.60063	567.29315	4
W	10	1315.67994	420.22474	3
S	11	1402.71197	234.14543	2
K	12	1530.80693	147.11340	1

Seq	#	B	Y	# (+2)
R	1	79.05843	774.91268	12
Q	2	143.08771	696.86213	11
D	3	200.60119	632.83284	10
N	4	257.62265	575.31937	9
E	5	322.14395	518.29790	8
I	6	378.68598	453.77661	7
L	7	435.22801	397.23457	6
I	8	491.77004	340.69254	5
F	9	565.30425	284.15051	4
W	10	658.34390	210.61630	3
S	11	701.85992	117.57665	2
K	12	765.90740	74.06063	1

Seq	#	B	Y	# (+3)
R	1	53.04157	516.94441	12
Q	2	95.72777	464.91071	11
D	3	134.07008	422.22452	10
N	4	172.08439	383.88220	9
E	5	215.09859	345.86789	8
I	6	252.79327	302.85369	7
L	7	290.48796	265.15901	6
I	8	328.18265	227.46432	5
F	9	377.20546	189.76963	4
W	10	439.23189	140.74683	3
S	11	468.24257	78.72039	2
K	12	510.94089	49.70971	1

Figure 3-73. Fragment ion tables of peptide RQDNEILIFWSK: theoretical monoisotopic mass values of singly-, doubly- and triply-charged b and y ions. From http://db.systemsbiology.net/proteomicsToolkit/

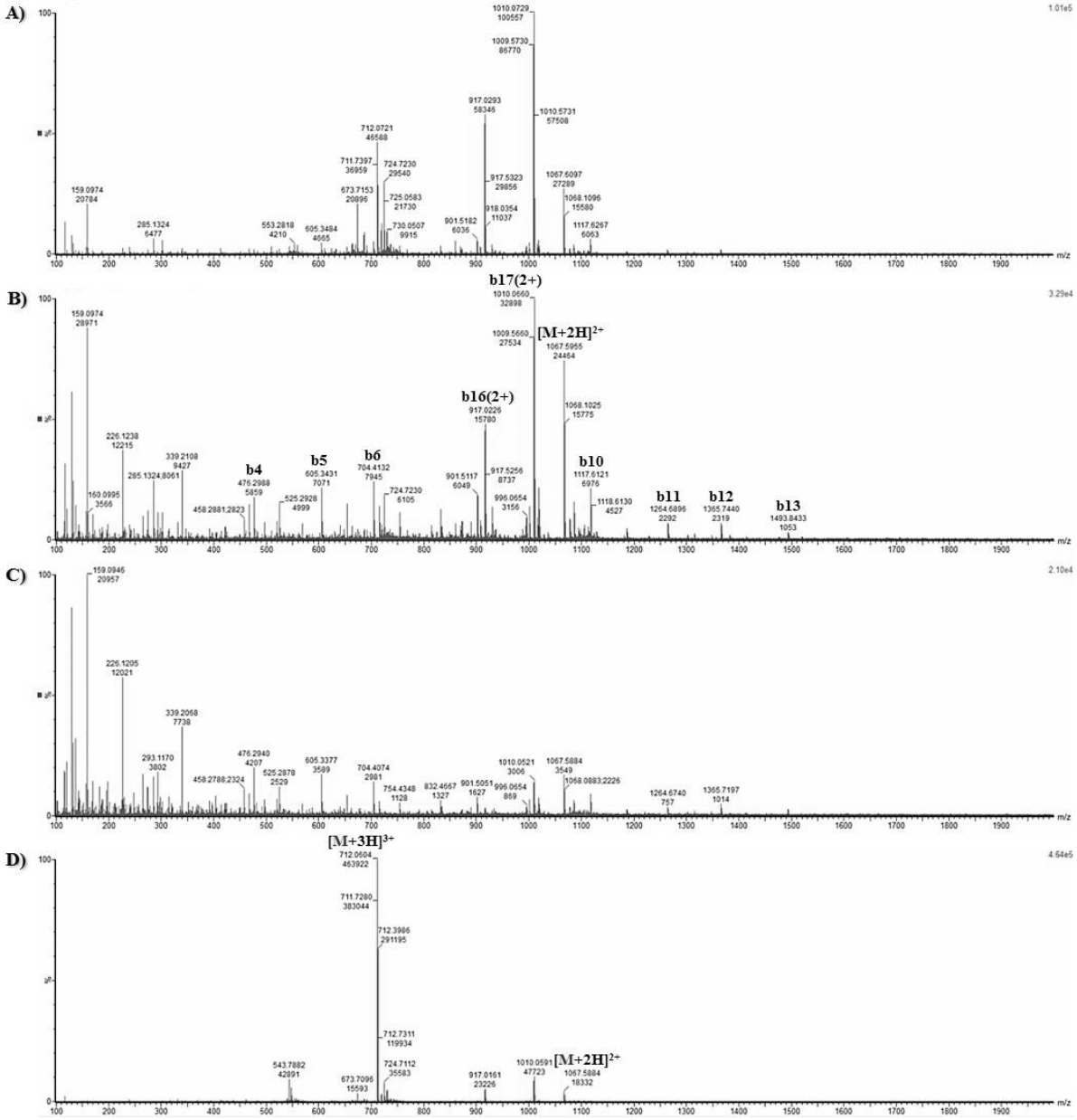

Figure 3-74. MS^E spectra of C-terminal peptide ALKYEVQGEVFTKPQLWP. The low energy function is reported in (D). A wide range of CE values have been tested: 10 – 25 (A), 20 – 35 (B) and 30 – 45 (C).

Seq	#	B	Y	# (+1)
A	1	72.04498	2133.13849	18
L	2	185.12905	2062.10138	17
K	3	313.22401	1949.01731	16
Y	4	476.28734	1820.92235	15
E	5	605.32993	1657.85902	14
V	6	704.39834	1528.81643	13
Q	7	832.45692	1429.74802	12
G	8	889.47839	1301.68944	11
E	9	1018.52098	1244.66798	10
V	10	1117.58939	1115.62538	9
F	11	1264.65781	1016.55697	8
T	12	1365.70548	869.48856	7
K	13	1493.80045	768.44088	6
P	14	1590.85321	640.34592	5
Q	15	1718.91179	543.29315	4
L	16	1831.99585	415.23457	3
W	17	2018.07516	302.15051	2
P	18	2115.12793	116.07120	1

Seq	#	B	Y	# (+2)
A	1	36.52643	1067.07318	18
L	2	93.06846	1031.55462	17
K	3	157.11594	975.01259	16
Y	4	238.64760	910.96511	15
E	5	303.16890	829.43345	14
V	6	352.70311	764.91215	13
Q	7	416.73240	715.37794	12
G	8	445.24313	651.34865	11
E	9	509.76442	622.83792	10
V	10	559.29863	558.31663	9
F	11	632.83284	508.78242	8
T	12	683.35668	435.24821	7
K	13	747.40416	384.72437	6
P	14	795.93054	320.67689	5
Q	15	859.95983	272.15051	4
L	16	916.50186	208.12122	3
W	17	1009.54152	151.57919	2
P	18	1058.06790	58.53953	1

Seq	#	B	Y	# (+3)
A	1	24.68691	711.71808	18
L	2	62.38160	688.03904	17
K	3	105.07992	650.34435	16
Y	4	159.43436	607.64603	15
E	5	202.44856	553.29159	14
V	6	235.47136	510.27739	13
Q	7	278.15755	477.25459	12
G	8	297.16471	434.56839	11
E	9	340.17891	415.56124	10
V	10	373.20171	372.54704	9
F	11	422.22452	339.52424	8
T	12	455.90707	290.50143	7
K	13	498.60540	256.81887	6
P	14	530.95632	214.12055	5
Q	15	573.64251	181.76963	4
L	16	611.33720	139.08344	3
W	17	673.36363	101.38875	2
P	18	705.71456	39.36231	1

Figure 3-75. Fragment ion tables of C-terminal peptide ALKYEVQGEVFTKPQLWP: theoretical monoisotopic mass values of singly-, doubly- and triply-charged b and y ions. From http://db.systemsbiology.net/proteomicsToolkit/

Q TRAP INFUSION ANALYSIS

Peptides RQDNEILIFWSK and ALKYEVQGEVFTKPQLWP were also fragmented in MS2 mode (data not shown):

- fragmentation of peptide RQDNEILIFWSK produced b7, b8 and b9 fragment ions, listed in decreasing order of signal intensity;
- fragmentation of peptide ALKYEVQGEVFTKPQLWP produced b17(2+), b10 and b16(2+) fragment ions, listed in decreasing order of signal intensity.

MRM ANALYSIS

The following transitions were analyzed:

m/z precursor ion (Q1)	m/z fragment ion (Q3)	Fragment ion
776.7	**1130.4**	b9(1+)
776.7	**870.1**	b7(1+)
776.7	**983.3**	b8(1+)
712.9	**917.5**	b16(2+)
712.9	**1010.7**	b17(2+)
712.9	**1118.1**	b10(1+)

Linearity in the theoretical range of concentrations 2.5 – 50 µg/ml was tested and calibration curves were obtained (Figure 3-76).

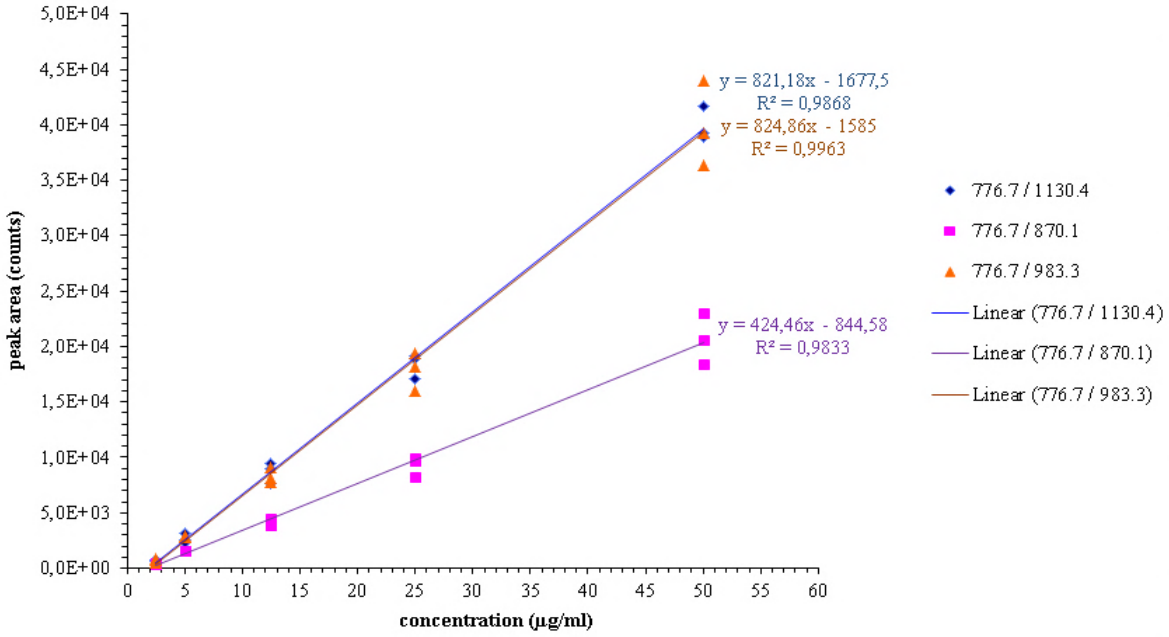

Figure 3-76. Calibration curves obtained for hCRP peptide RQDNEILIFWSK.

The transition of peptide RQDNEILIFWSK 776.7/983.3 featured the best linearity (R^2 = 0.996).

3.3. ANALYSIS OF PEPTIDES

The main characteristics of peptides originated by tryptic digestion of human calcitonin, human procalcitonin and human C-reactive protein in aqueous and organic-aqueous solutions were analyzed. Table 3-9 shows for each peptide its amino acidic sequence and its length, the theoretical monoisotopic molecular weight, the isoelectric point, the aliphatic index and the composition in hydrophobic/polar/basic/acidic residues.

PROTEIN	PEPTIDE	aa	MW (monoisotopic)	pI	aliphatic index	RESIDUES (%)			
						hydrophobic	polar	basic	acidic
CT	**CGNLSTCMLGTYTQDFNK**	18	1994.85	5.82	43.33	22.2	**66.7**	5.6	5.6
	FHTFPQTAIGVGAP	14	1441.74	6.74	62.86	**57.1**	35.7	7.1	-
	CGNLSTCMLGTYTQDFNKFHTFPQTAIGVGAP	**32**	3418.58	**6.72**	51.88	37.5	**53.1**	6.3	3.1
PCT	**ASELEQEQER**	10	1217.55	4.09	49.00	20.0	**30.0**	10.0	40.0
	DHRPHVSMPQNAN	13	1501.68	6.92	30.00	30.8	**38.5**	23.1	7.7
	LLLAALVQDYVQMK	14	1603.90	5.83	167.14	64.3	21.4	7.1	7.1
	FHTFPQTAIGVGAPGK	16	1626.85	8.76	55.00	50.0	37.5	12.5	-
	FHTFPQTAIGVGAPGKK	17	1754.95	10.00	51.76	47.1	35.3	17.6	-
	FHTFPQTAIGVGAPGKKR	18	1911.05	11.17	48.89	44.4	33.3	22.2	-
	SALESSPADPATLSEDEAR	19	1944.89	3.83	32.11	42.1	26.3	5.3	26.3
	ASELEQEQEREGSSLDSPR	19	2145.98	4.14	46.32	15.8	**36.8**	15.8	31.6
	DMSSDLERDHRPHVSMPQNAN	**21**	2435.07	5.26	37.14	**33.3**	28.6	19.0	19.0
	RDMSSDLERDHRPHVSMPQNAN	**22**	2591.17	**6.01**	33.45	**31.8**	27.3	22.7	18.2
	KRDMSSDLERDHRPHVSMPQNAN	23	2719.27	6.93	33.91	30.4	26.1	26.1	17.4
CRP	**ESDTSYVSLK**	10	1127.53	4.37	68.00	20.0	**50.0**	10.0	20.0
	GYSIFSYATK	10	1135.55	8.50	49.00	30.0	**60.0**	10.0	-
	GYSIFSYATKR	11	1291.66	9.70	44.55	27.3	54.5	18.2	-
	QDNEILIFWSK	11	1391.71	4.37	106.36	45.5	27.3	9.1	18.2
	RQDNEILIFWSK	12	1547.81	**6.07**	**97.50**	**41.7**	25.0	16.7	16.7
	YEVQGEVFTKPQLWP	15	1819.91	4.53	64.67	46.7	33.3	6.7	13.3
	AFTVCLHFYTELSSTR	16	1873.90	6.78	73.12	37.5	43.8	12.5	6.3
	ESDTSYVSLKAPLTKPLK	18	1976.08	8.53	86.67	38.9	33.3	16.7	11.1
	ALKYEVQGEVFTKPQLWP	**18**	2132.13	**6.19**	**81.11**	**50.0**	27.8	11.1	11.1

Table 3-9. Table showing the main characteristics of peptides originated by tryptic digestion of human calcitonin, human procalcitonin and human C-reactive protein. The peptides whose cleavage is particularly favored in aqueous solution or in mixed organic-aqueous solvent system are reported in blue and green respectively.

3.4. CHOICE OF THE STATIONARY PHASE

LC-MS analyses of the protein standards digested in mixed organic-aqueous solutions were performed after having tested a selection of columns, specific for peptide mixtures and suitable for both HPLC and UHPLC instrumentation, looking for the most fit for purpose stationary phase: three are based on the fused-core technology (Aeris Peptide XB-C18, Ascentis Express Peptide ES-C18, Halo Peptide ES-C18), whereas one is characterized by the Charged-Surface Hybrid technology (XSelect CSH 130) (Table 3-9).

Table 3-10. Table reporting the main features of the LC columns tested.

Column name	SP	Particle size (µm)	Pore size (Å)	Length (mm)	I. D. (mm)	Brand
Aeris Peptide	C18	3.6	100	150	2.1	Phenomenex
Ascentis Express	C18	2.7	160	150	4.6	SIGMA
HALO ES-C18	C18	2.7	160	150	2.1	CPS
XSelect CSH 130	C18	2.5	130	150	4.6	Waters

Digestion solutions of hCRP and hCT in 60% ACN / 40% 50 mM ammonium bicarbonate were injected and analyzed in methanol gradient.

Retention times and peak areas of the tryptic peptides of interest were monitored and compared (Table 3-11, Figure 3-77 and Figure 3-78).

PROTEIN	PEPTIDE	code	MW (monoisotopic)	m/z	RT (minutes)			
					Halo Peptide	XSelect CSH	Aeris Peptide	Ascentis Express
CRP	ESDTSYVSLK	1	1127.53	564.78	15.82	22.17	14.64	24.16
	GYSIFSYATK	2	1135.55	568.78	19.52	25.49	18.02	-
	RQDNEILIFWSK	3	1547.81	774.92	21.8	27.35	19.97	-
	ESDTSYVSLKAPLTKPLK	4	1976.08	495.05	18.61	23.21	17.06	-
	ALKYEVQGEVFTKPQLWP	5	2132.13	711.73	22.02	26.84	20.34	29.87
CT	CGNLSTCMLGTYTQDFNKFHTFPQTAIGVGAP	-	3418.58	1140.25	25.07	29.62	23.46	32.72

Table 3-11. Table reporting the retention times of hCT and hCRP peptides. Peptides are listed in increasing order of monoisotopic molecular weight.

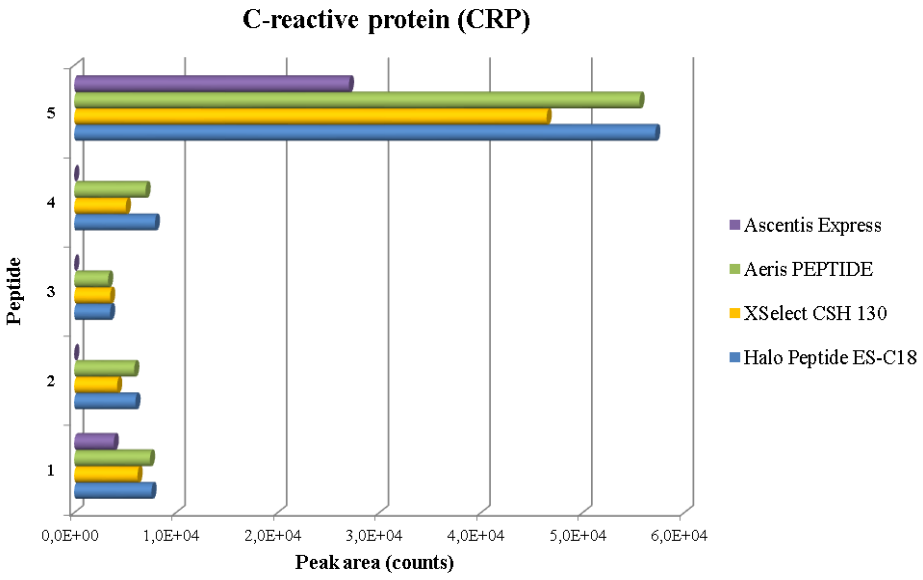

Figure 3-77. LC-MS^E analysis of hCRP peptides with various C18 stationary phases. The stationary phases tested are Halo Peptide ES-C18 (CPS), XSelect CSH 130 (Waters), Aeris PEPTIDE (Phenomenex) and Ascentis Express (SIGMA). Peptide 1 = ESDTSYVSLK, peptide 2 = GYSIFSYATK, peptide 3 = RQDNEILIFWSK, peptide 4 = ESDTSYVSLKAPLTKPLK and peptide 5 = ALKYEVQGEVFTKPQLWP.

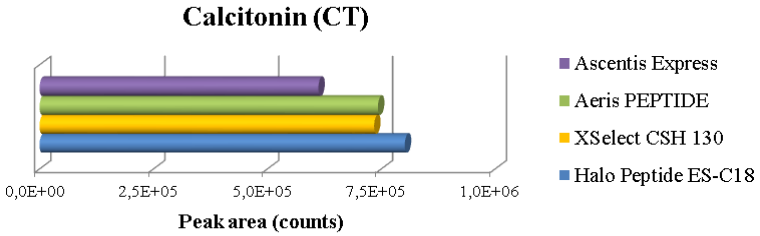

Figure 3-78. LC-MS^E analysis of intact hCT with various C18 stationary phases. The stationary phases tested are Halo Peptide ES-C18 (CPS), XSelect CSH 130 (Waters), Aeris PEPTIDE (Phenomenex) and Ascentis Express (SIGMA).

3.5. ANALYSIS OF THE MATRIX EFFECT

The general term matrix refers to the components of a sample other than the analyte. Evaluation of the matrix effect, that is the change (suppression or enhancement) in the LC-MS response of a specific analyte compared to the analysis of the pure standard, is a necessary stage in the process of validation of bioanalytical methods.
In this thesis a preliminary investigation of the matrix effect was performed using a pooled sample. The pool was created merging the extraction solutions of samples collected from five healthy newborns on their second day after birth (Table 3-12).

Table 3-12. Clinical data of five healthy newborns. The extraction solutions of the samples collected on their second day after birth were merged to create a pool.

NEWBORN	RACE	SEX	WEIGHT (g)	AGE (weeks)	DELIVERY	samplings	
						I	II
3953/2013	Caucasian	M	3000	38	caesarean section	2 hours	30 hours
4111/2013	Caucasian	F	3220	39	spontaneous	19 hours	38 hours
4141/2013	Caucasian	M	3600	40	spontaneous	22 hours	40 hours
4901/2013	Caucasian	F	3020	39	caesarean section	6 hours	30 hours
4905/2013	Caucasian	F	3120	39	spontaneous	6 hours	30 hours

The pool, representative of an healthy state, was digested in aqueous solution and analyzed: calcitonin, procalcitonin and C-reactive protein, if present, were not detectable. Therefore the digested pooled sample was spiked with hCT or hCRP protein standards, both separately digested in 60% ACN / 40% 50 mM ammonium bicarbonate, to verify how the matrix influences the detection and quantitation of the analytes of interest. The pooled sample digested in aqueous solution was at first diluted with ACN, so that the solution reached the final composition of 60% ACN / 40% 50 mM ammonium bicarbonate, and then separately spiked with digested hCT or hCRP at different concentrations while keeping constant its concentration (60 µg/ml). The upper limits of the calibration curves previously obtained in the analyses of the protein standards alone were taken as the maximum concentrations ([hCT] = 12.5 µg/ml and [hCRP] = 50 µg/ml) and considered equal to 120%. The two successive dilutions represented the 100% and 80% solutions (Figure 3-79 and Figure 3-80).

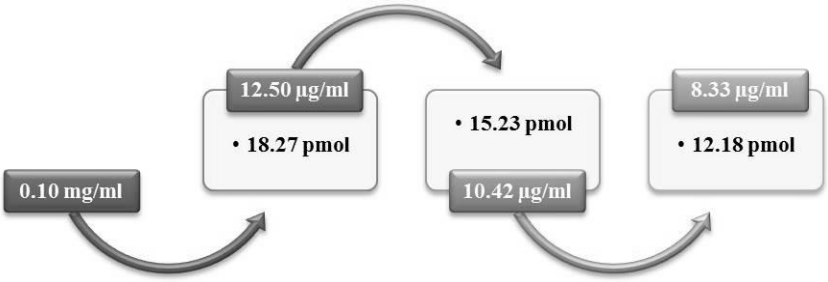

Figure 3-79. Scheme of the successive dilutions of hCT digestion solution, reporting the injected protein quantities.

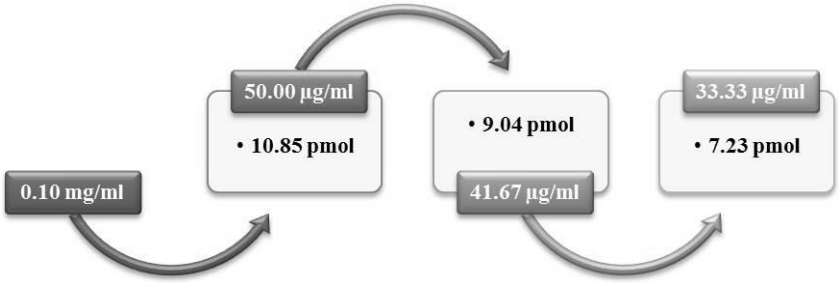

Figure 3-80. Scheme of the successive dilutions of hCRP digestion solution, reporting the injected protein quantities.

Retention times and peak areas of the proteotypic peptides were monitored.

Calcitonin

The retention time of intact hCT was increased of one minute. Furthermore, the peaks appeared broadened and pronged (Figure 3-81). This may be due to a combination of both matrix effect and column carryover.

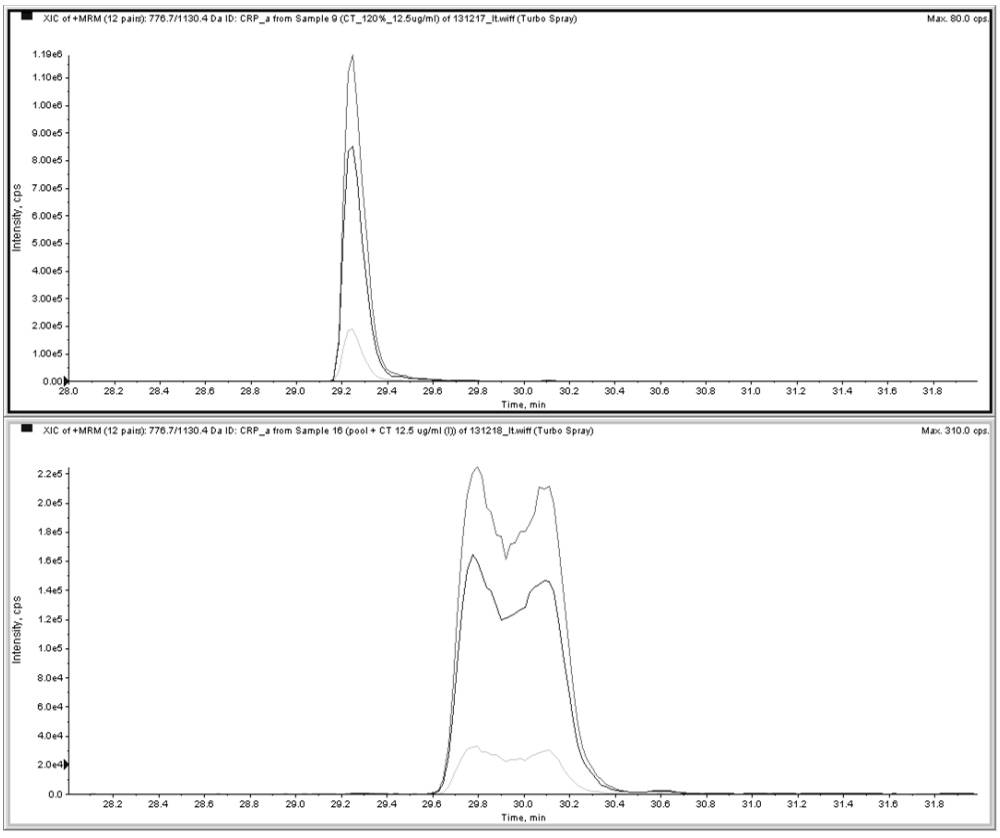

Figure 3-81. Comparison between hCT control (upper box) and the sample spiked at the maximum concentration (bottom box).

The matrix factor and the variation in hCT peak area values observed between the control and the spiked sample are reported in Table 3-13.

Table 3-13. Table reporting the matrix factor (MF) and the variation in hCT peak area values observed between the control and the spiked sample.

Transition	Concentration (µg/ml)	MF	Δ area (%)*
1141.2 / 1654.0	8.33	0.8	20.1
	10.42	0.9	7.7
	12.50	0.8	15.1
1141.2 / 1103.4	8.33	0.8	22.7
	10.42	0.9	10.8
	12.50	0.8	16.0
1141.2 / 1079.8	8.33	0.7	25.8
	10.42	0.9	9.5
	12.50	0.8	17.8

* (control-spiked)/control

C-reactive protein

The retention time of both hCRP proteotypic peptides was increased of 1.2 minutes. The matrix factor and the variation in peak area values observed between the control and the spiked sample are reported in Table 3-14.

Table 3-14. Table reporting the matrix factor (MF) and the variation in the peak area values observed between the control and the spiked sample for the two hCRP proteotypic peptides RQDNEILIFWSK (m/z 776.7) and ALKYEVQGEVFTKPQLWP (m/z 712.9).

Transition	Concentration (µg/ml)	MF	Δ area (%)*
776.7 / 1130.4	33.33	1.1	-9.5
	41.67	1.2	-16.9
	50.00	1.2	-24.0
776.7 / 870.1	33.33	1.1	-13.3
	41.67	1.1	-14.6
	50.00	1.2	-22.2
776.7 / 983.3	33.33	1.1	-6.8
	41.67	1.2	-19.9
	50.00	1.2	-19.1
712.9 / 917.5	33.33	0.7	31.1
	41.67	0.7	26.8
	50.00	0.8	18.2
712.9 / 1010.7	33.33	0.7	28.3
	41.67	0.7	25.3
	50.00	0.8	17.7
712.9 / 1118.1	33.33	0.7	32.1
	41.67	0.7	26.1
	50.00	0.8	22.4

* (control-spiked)/control

4. DISCUSSION

4.1. GEL-BASED APPROACHES

Early-onset sepsis (EOS), defined as a septic state manifested in the first three days of life, is one of the major causes of neonatal mortality and surviving infants are at increased risk for developing morbidities, including bronchopulmonary dysplasia, prolonged hospital stay, and neurodevelopmental impairment [56]. Therefore, the availability of diagnostic tools allowing the early detection of an ongoing infective state represents an urgency in neonatal clinical care units.

In this thesis, untargeted gel-based approaches were explored to conduct qualitative investigation of the salivary proteins in samples collected from healthy newborns in their early 48 hours after birth. This investigation is instrumental to the comparison between healthy newborns and newborns affected by bacterial infection. In particular the aims of this phase of the study were the description of the overall protein profile and the identification of the most abundant proteins, as well as the clarification of the differences, if present, occurring between samples collected in the first and in the second day of life. Both 2D-PAGE – MALDI-TOF/TOF and SDS-PAGE – LC-(HR)MS/MS analyses were performed in order to collect complementary information. The investigation proceeded through several steps.

Initially 2-DE analyses were performed on single newborns in the pH range 4 – 7. As expected, the comparison between images acquired after Coomassie and Silver staining revealed that the latter is characterized by greater sensitivity, since on average it helped to visualize more than 60% of the number of spots detected with Coomassie. The MALDI-TOF analyses of the digestion solutions of the excised spots led to define the identity of the most abundant proteins in the oral fluid samples: polymeric immunoglobulin receptor (PIGR), serum albumin, keratin and actin, all present in multiple isoforms (Figure 3-3). Due to the low amount of sample at our disposal (15 µg loaded per gel), a special care was put on the definition of protein identification guidelines: protein score (C. I. %) when different from zero, peptide count preferably greater than three, agreement between experimental and theoretical molecular weight and isoelectric point, as well as reproducibility of outcome between replicate spots, between different sample preparations and between different databases (Swiss-Prot and NCBI).

2-DE analyses of pools were later performed. This produced a few advantages: pool analyses give a simplified picture of general conditions (e. g. healthy or pathological states); the higher total protein amount not only enables to use longer IPG strips, characterized by higher resolution of protein spots on the gel, but also leads to an increase in the number of Coomassie detectable spots and better chance of identification (avoiding the use of Silver staining). Furthermore, the depletion of the most abundant proteins prior to 2-DE (e. g. keratins) becomes an attractive chance.

Feasibility of a SDS-PAGE – LC-(HR)MS/MS approach was verified analyzing a single saliva sample. Protein identifications were based on high resolution MS/MS data and agreement between the theoretical and the experimental molecular weight, the latter being not a necessary condition. The approach combining SDS-PAGE and LC-(HR)MS/MS analysis proved to be useful in supplying complementary

information compared to the designed 2-DE – MALDI-TOF/TOF approach. In particular, a large number of the identified proteins features basic pI and high molecular weight (Figure 3-10 and Figure 3-13).

As a whole, the gel-based analyses of the salivary samples of healthy newborns led to the identification of a number of proteins linked to epidermal tissue functions and, more interestingly, some proteins involved in inflammatory processes (in particular annexin A1, glutathione S-transferase P, heat shock proteins, protein S100-A8 and -A9), evidence of a stressed condition in the early 48 hours after birth (Table 3-4 and Table 3-5).

4.2. TARGETED ANALYSIS

SAMPLE PREPARATION

The most important step in the sample preparation for bottom-up proteomics studies is the efficient and reproducible cleavage of proteins into their constituent peptides. In most cases trypsin is the preferred proteolytic enzyme, thanks mainly to its high specificity.
The most common steps in classical sample preparation protocols are schematized in Figure 4-1. Prior to protein digestion proteins need to be denatured, reduced and alkylated using various chemical reagents that are usually neither trypsin-tolerated nor MS-compatible, therefore sample purification procedures are required. Moreover, protein digestion is a time-consuming step in the sample preparation workflow since it typically consists in an overnight reaction at 37 °C with a trypsin to protein ratio between 1:100 and 1:10.

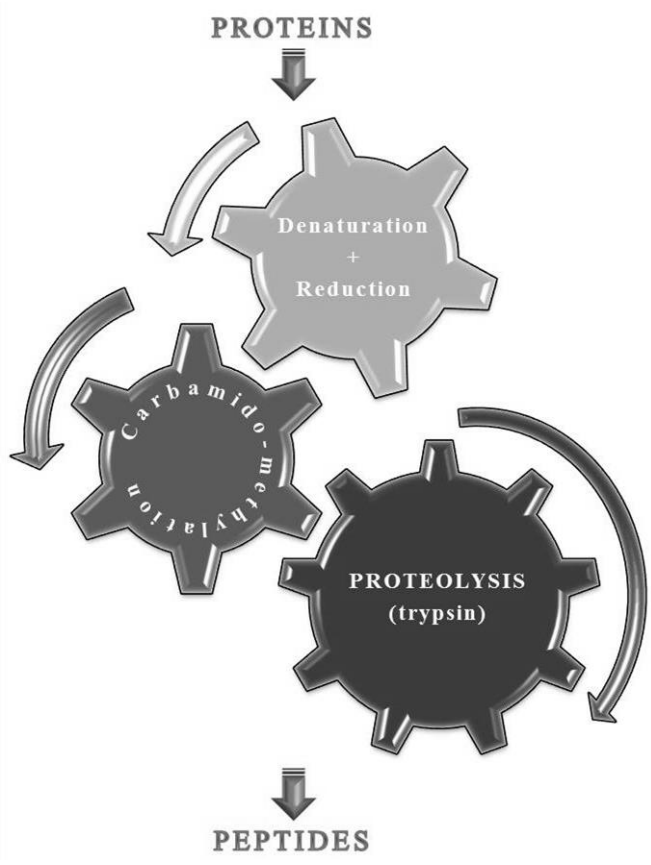

Figure 4-1. Scheme of the most common steps in sample preparation protocols. Denaturation and reduction can often be carried out simultaneously (e.g.: a combination of heat and a reducing reagent) and the following alkylation of cysteine residues is necessary to prevent re-oxidation of sulfhydryl groups. The protein, blocked in its denatured state, is exposed to the action of the proteolytic enzyme.

Among the different techniques developed with the aim to accelerate sample preparations and maximize the yield in proteotypic peptides there is the use of mixed organic-aqueous solutions. It has been demonstrated that solvent-assisted digestions often improve protein sequence coverage at shorter digestion times, due to an enhanced enzymatic activity of trypsin. Even though 20% is usually the maximum concentration recommended by the manufacturers in the product information sheets, trypsin is active even in 80% organic solvent (ACN or others). However, it has been reported that at solvent concentrations higher than 40% the risk of enzyme autolysis progressively increases, protein solubility generally decreases and multiple missed cleavages are more frequently observed [27, 30, 31, 57, 58].
A sample preparation protocol based on solvent-assisted protein digestion is schematized in Figure 4-2.

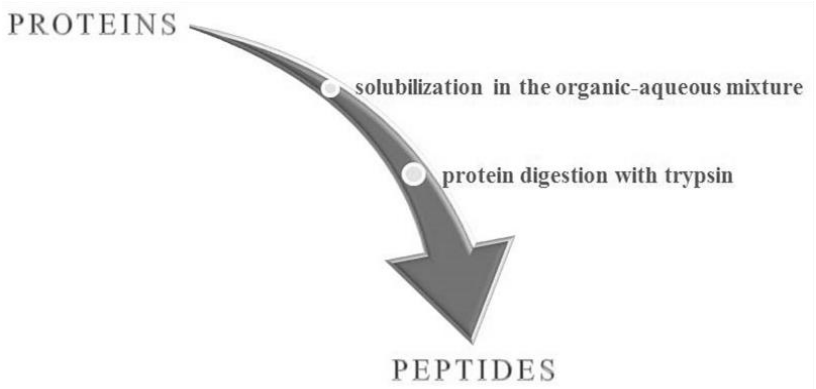

Figure 4-2. Schematic of the main steps in accelerated sample preparation protocols. The choice of organic solvent and its concentration, the proper buffer, the adequate trypsin to protein ratio and the optimal duration of the digestion reaction, have to be experimentally determined for the target protein.

Sample preparation in mixed organic-aqueous solution presents some relevant advantages:

- ☆ it's clean (the organic solvent represents a MS-compatible denaturing agent);
- ☆ it's fast (one hour of reaction is usually sufficient);
- ☆ it's cheap (use of chemical denaturing reagents and sample purification procedures is not required).

In this work of thesis both the classical and the solvent-assisted digestion protocols were tested for the preparation of the three target acute-phase proteins calcitonin, procalcitonin and C-reactive protein.

Digestions in aqueous solution

Various sample preparations of the protein standards were tested, essentially differing in the denaturing step: the use of SDS and thermal denaturation was compared to the combination of urea and thiourea.

Calcitonin

Disruption of human calcitonin α-helical structure was possible only using the combination of urea and thiourea. The successive reduction and alkylation of the two Cys residues (disulfide bond between C1 and C7) in this reaction mixture resulted almost complete: only a small fraction of molecules was in the mono-alkylated state and there was no evidence of non-alkylated protein (Figure 3-17). The following

overnight digestion produced the two hCT constituent peptides leading to a sequence coverage of 100% (Figure 3-24).

Procalcitonin

Given the small quantity of protein standard at our disposal, only a protocol based on SDS and thermal denaturation was tested for human procalcitonin. A sequence coverage of 62.9% was obtained and the observed peptides are relative to the N- and C- terminal portions of the protein, whereas there is no trace of the two peptides in the central immature calcitonin region (Figure 3-34). It may be that, as previously noticed in the analysis of hCT standard, in the presence of SDS this region remains folded and the cleavage site is not accessible to the proteolytic enzyme.

C-reactive protein

Both the protocol of digestion based on urea denaturation and the one based on SDS and thermal denaturation produced the same sequence coverage (39.3%) in the analysis of human C-reactive protein (Figure 3-37 and Figure 3-47). The low coverage is mainly due to the presence of two long central portions of the protein (residues 70 – 114 and 124 – 188) lacking tryptic cleavage sites.

Digestions in mixed organic-aqueous solvent systems

Different protocols of digestion in mixed organic-aqueous solvent system were tested varying:

- type and concentration of organic solvent:
  - 60% acetonitrile / 40% 50 mM ammonium bicarbonate
  - 80% acetonitrile / 20% 50 mM ammonium bicarbonate
  - 60% methanol / 40% 50 mM ammonium bicarbonate
  - 80% methanol / 20% 50 mM ammonium bicarbonate
- trypsin to protein ratio: between 1:20 and 1:5
- time: reactions were conducted for 15 – 90 minutes
- alkylation of Cys residues: performed or not prior to digestion.

Temperature (37 °C) and pH (8) were kept constant.

Calcitonin

In each of the solvent systems tested hCT essentially remained intact. Reduction of disulfide bonds and alkylation of Cys residues occurred to a variable extent depending on the type of organic solvent used and its concentration in the reaction mixture (Figure 3-49). The best results were obtained in the solvent system 60% ACN / 40% 50 mM ammonium bicarbonate, where hCT apparently adopts a conformation in which the Cys residues (N-terminal portion of the protein) are exposed to the solvent, whereas the unique cleavage site (Lys18) is hindered. The reduction of the ACN concentration to 20%, prior to the addition of trypsin in the reaction mixture, is likely to cause a change in hCT conformation since the cleavage site appears more exposed to the action of the proteolytic enzyme, but times longer than one hour are necessary for the reaction to be complete (Figure 3-50).

Digestion of hCT in 60% ACN / 40% 50 mM ammonium bicarbonate with trypsin to protein ratio 1:5, without previous reduction of disulfide bonds and alkylation of Cys residues, was tested and monitored

over time: the protein remained essentially intact even after one hour of reaction, however little digestion was observed after 90 minutes (Figure 3-51).

Procalcitonin

Given the small quantity of protein standard at our disposal, only a protocol of abrupt digestion with trypsin to protein ratio 1:5 in 60% ACN / 40% 50 mM ammonium bicarbonate was tested for hPCT and monitored over time (Figure 3-58). A sequence coverage of 50% was obtained after one hour of reaction (Figure 3-59). The cleavage of the C-terminal peptide DMSSDLERDHRPHVSMPQNAN is particularly favored. Moreover it is interesting to note that the MALDI-TOF spectrum of the digestion solution reveals the presence of peptides belonging to the central portion of the protein, the calcitonin region, whereas it was previously demonstrated that in the same reaction solution hCT remains intact.

C-reactive protein

Since the solvent system 60% ACN / 40% 50 mM ammonium bicarbonate resulted to be the best suited for the analysis of hCT after reduction of disulfide bonds and alkylation of Cys residues, the same reaction mixture constituted the first choice for the analysis of hCRP. A sequence coverage of 31.6% was obtained after one hour of digestion with trypsin added in 1:5 ratio (Figure 3-66). As previously mentioned, the low sequence coverage obtained in the analysis of hCRP is mainly attributable to the presence of two long central portions of the protein (residues 70 – 114 and 124 – 188) lacking tryptic cleavage sites. Peptides RQDNEILIFWSK and ALKYEVQGEVFTKPQLWP, whose cleavage is particularly favored, are present even after just 15 minutes of reaction (Figure 3-67).
Digestion of hCRP in 60% ACN / 40% 50 mM ammonium bicarbonate, without previous reduction of disulfide bonds and alkylation of Cys residues, was tested and monitored over time (Figure 3-68). Once again, a sequence coverage of 31.6% was obtained after one hour of reaction with trypsin added in 1:5 ratio and the peptides of interest are present even after just 15 minutes of reaction.

To sum up, digestion in the mixed organic-aqueous solvent system 60% ACN / 40% 50 mM ammonium bicarbonate with trypsin to protein ratio 1:5, one hour at 37 °C, without previous reduction of disulfide bonds and alkylation of Cys residues, appears suitable for the simultaneous analysis of the three proteins of interest: calcitonin can be detected as intact protein, whereas procalcitonin and C-reactive protein are cleaved into their constituent peptides, even after just 15 minutes of reaction.

CHARACTERISTICS OF THE PEPTIDES

The peptides that are particularly favored in the aqueous solution are:

- ✓ both N-terminal and C-terminal hCT constituent peptides C[alk]GNLSTC[alk]MLGTYTQDFNK (1 – 18) and FHTFPQTAIGVGAP (19 – 32);
- ✓ hPCT peptide ASELEQEQER (38 – 47), C-terminal peptide DHRPHVSMPQNAN (104 – 116) and peptide SALESSPADPATLSEDEAR (5 – 23);
- ✓ hCRP peptides ESDTSYVSLK (14 – 23) and GYSIFSYATK (48 – 57).

On the other hand, the peptides that are particularly favored in the mixed organic-aqueous solvent system 60% ACN / 40% 50 mM ammonium bicarbonate are:

- ✓ intact hCT peptide CGNLSTCMLGTYTQDFNKFHTFPQTAIGVGAP (1 – 32);
- ✓ hPCT C-terminal peptide DMSSDLERDHRPHVSMPQNAN (96 – 116);
- ✓ hCRP C-terminal peptide ALKYEVQGEVFTKPQLWP (181 – 206);
- ✓ hCRP peptide RQDNEILIFWSK (58 – 69).

Analyzing the major physicochemical characteristics of the previously mentioned peptides, some general considerations can be inferred (Table 3-9). Missed cleavages are more frequently observed in the mixed organic-aqueous reaction mixture (up to two), therefore peptides are generally longer. Furthermore, peptides very often represent the C-terminal portion of the protein. hCRP peptides also present higher aliphatic indexes than the other peptides. The aliphatic index of a peptide is defined as the relative volume occupied by aliphatic side chains (alanine, valine, isoleucine and leucine) and may be regarded as a positive factor for the increase of thermostability.

EVALUATION OF STATIONARY AND MOBILE PHASES

Human calcitonin, procalcitonin and C-reactive protein standards digested in aqueous solutions were analyzed with a traditional HPLC fully porous column (BioBasic 18, 5 µm, 300 Å, 250 x 4.6 mm, Thermo Scientific).

Later analyses of the same protein standards digested in mixed organic-aqueous solutions were performed after having tested a selection of new columns, suitable for both HPLC and UHPLC analyses, looking for the most fit for purpose stationary phase: three are based on the fused-core technology (Aeris Peptide XB-C18, Ascentis Express Peptide ES-C18, Halo Peptide ES-C18), whereas one is characterized by the Charged-Surface Hybrid technology (XSelect CSH 130).

The above-mentioned HPLC – UHPLC columns tested also feature smaller pore size (100 – 160 Å), optimized for the separation of peptides or small proteins up to 10 kDa. To allow fast and high-resolution separation of peptides, the pores must be large enough to permit efficient diffusion of peptide molecules in and out of the pores where they can fully interact with the bonded-phase. If the pore size is too small, there will be limited diffusion and the peptides will elute from the column with broad peaks, whereas, if the pore size is too large, there will be less surface area for peptides to interact with the bonded-phase, thus negatively affecting retention time, resolution, and sample capacity.

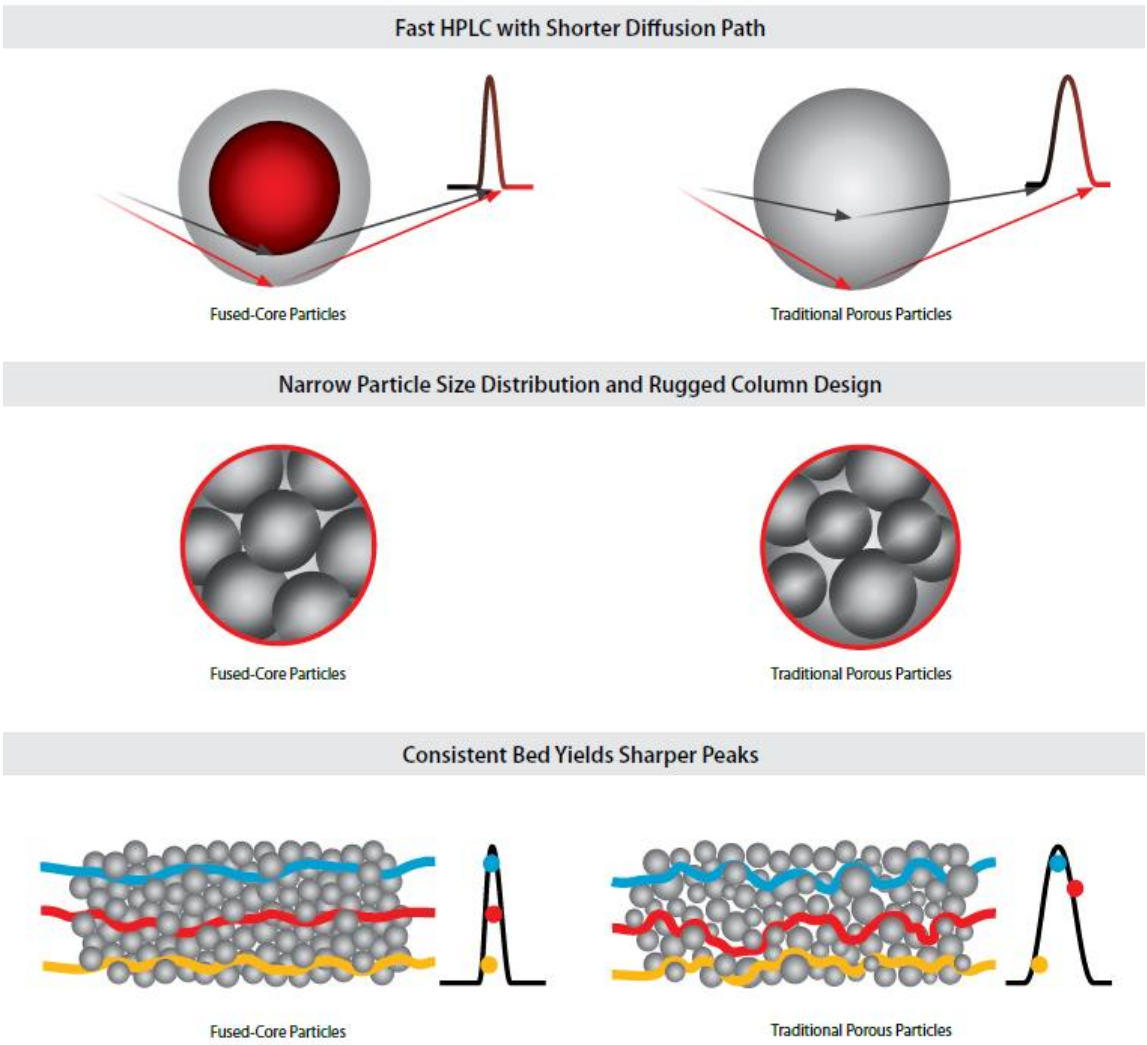

Figure 4-3. Comparison between fused-core and fully porous stationary phase particles. The most striking differences include: shorter diffusion path, narrower particle size distribution and therefore more consistent chromatographic bed. All these features lead to sharper peaks. From Ascentis Express HPLC columns brochure (Supelco).

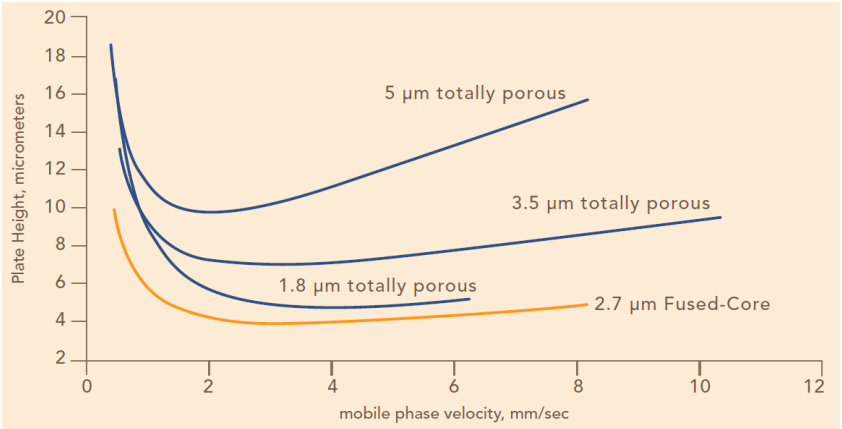

Figure 4-4. Comparison of Van Deemter plots of different HPLC columns. Fused-core HPLC – UHPLC columns are more efficient than columns packed with totally porous particles and that they can be run at higher mobile phase linear velocity and still maintain their resolving power.

With respect to the mobile phase, a methanol gradient was preferred to the acetonitrile gradient previously employed. Mobile phases were added with FA instead of TFA as modifier, since it facilitates more sensitive detection of peptides in ESI-MS peptide mapping analyses.

Aeris Peptide XB-C18 (C18, 3.6 µm, 100 Å, 150 x 2.1 mm), Phenomenex.

The stationary phase of this column is constituted by Core-Shell particles, that are characterized by the presence of a uniform porous silica layer, the 0.5 µm "shell", grown around a solid silica sphere, the "core" of 2.6 µm of diameter (Figure 4-5). The thin porous layer is designed to decrease the diffusion path length compared to fully porous particles, thus reducing the time it takes for biomolecules to adsorb and desorb into and out of the particle and therefore minimizing band broadening. The dimension of the pores is optimized for the diffusion of peptides. Also the uniform size and shape of the particles, along with tight packing specifications, oppose to losses in efficiency and performance due to band broadening.

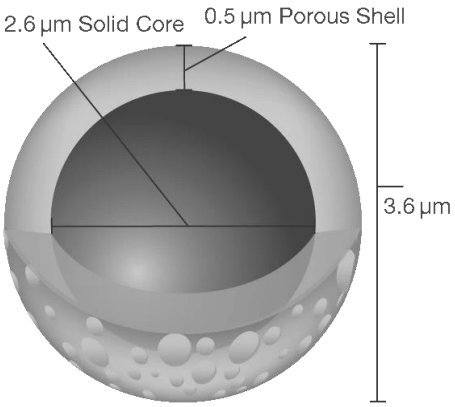

Figure 4-5. Schematic picture of a Core-Shell stationary phase particle of Aeris Peptide column.

Ascentis Express Peptide ES-C18 (C18, 2.7 µm, 160 Å, 150 x 4.6 mm), Sigma-Aldrich.

The stationary phase of this column is constituted by Fused-Core particles (Figure 4-6). The short diffusion path (0.5 µm), the narrow particle size distribution and the homogeneity of the packed bed, aim at yielding sharp peaks and allowing high flow rates with reduced back pressure compared to the columns constituted by fully porous particles. Moreover, the extra stable (ES) C18 bonded-phase is sterically protected to guarantee high resistance to acid-catalyzed hydrolysis of the siloxane bond that attaches the C18 chain to the surface. Thus, the combination of low pH and elevated temperature of operation is well tolerated.

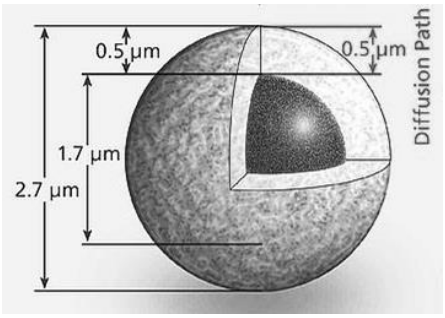

Figure 4-6. Schematic picture of a stationary phase particle of Ascentis Express column.

Halo Peptide ES-C18 (C18, 2.7 µm, 160 Å, 150 x 2.1 mm), CPS Analitica.
The stationary phase of this column is constituted by Fused-Core particles (Figure 4-7).

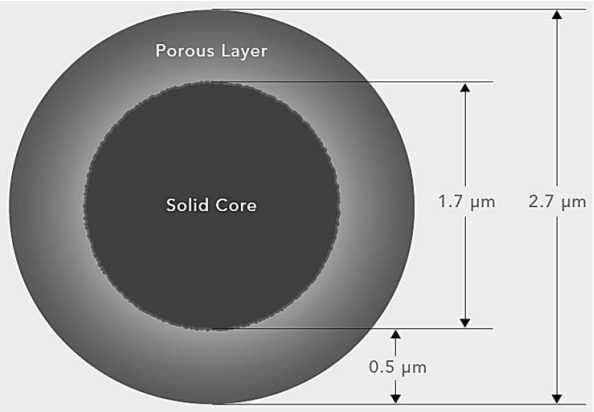

Figure 4-7. Schematic picture of a stationary phase particle of Halo ES-C18 column.

Halo columns generate fast separations with high resolving power thanks to the Fused-Core technology that creates a 0.5 µm porous shell fused to a solid core particle, which represents a small path for diffusion of solutes into and out of the stationary phase. The packing process of Fused-Core particles is facilitated for two reasons: particles have extremely narrow size distribution and, since those particles are significantly more dense than conventional totally porous particles, they are more easily packed into stable and efficient columns.
The bonded C18 phase is extra stable (ES): the bulky side groups of organosilanes sterically protect the siloxane bond from acid hydrolysis and yield a stationary phase that is especially stable to the conditions typically used for the separation of peptides (Figure 4-8).

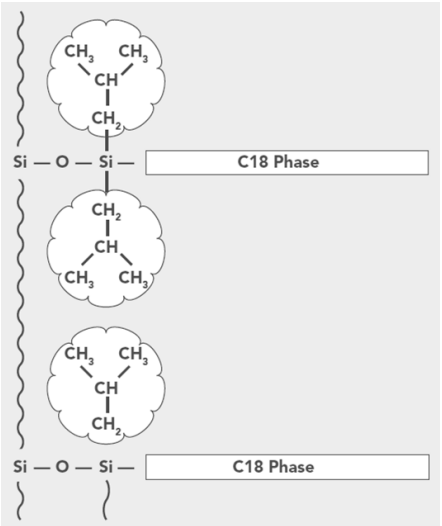

Figure 4-8. Schematic illustration of the extra stable (ES) bonded phase.

Moreover Halo columns are endowed with an inlet frit with a porosity that is significantly larger than other UHPLC columns (2 µm versus 0.5 µm) to prevent inlet plugging.

XSelect CSH 130 (C18, 2.5 µm, 130 Å, 150 x 4.6 mm), Waters.

The stationary phase of this column is constituted by Charged Surface Hybrid (CSH) particles. CSH particles are generated via chemical bonding of a low-level charge to the surface of Ethylene-Bridged Hybrid (BEH) particles and successive C18 functionalization (end-capping) (Figure 4-9).

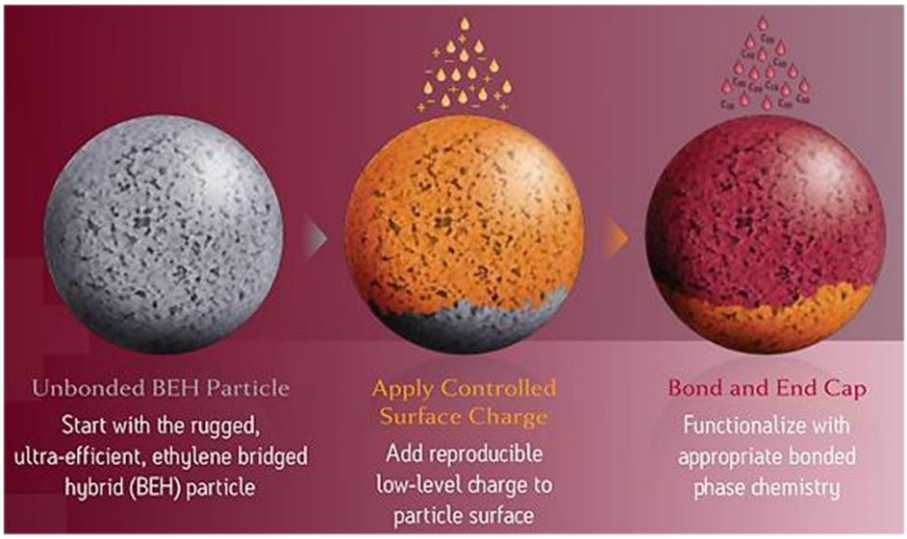

Figure 4-9. Picture illustrating the sequential stages of production of stationary phase particles of CSH columns.

The retention of peptides on XSelect CSH 130 C18 columns seems to be influenced by their charge (or charge density). Most tryptic peptides contain only two basic functional groups, one at the N-terminus and the other at the side chain of the C-terminal Lys/Arg residue. Peptides containing histidine residues or missed cleavage sites present additional positive charges and this causes shifts in retention times if compared to non-CSH columns.

The evaluation of the four different HPLC – UHPLC columns was based on full scan analyses of hCT and hCRP digestion solutions on Synapt G2-S. Retention times and peak areas of the tryptic peptides of interest were monitored and compared. Given the small quantity of protein standard at our disposal, hPCT was later analyzed only with the column that gave the best results.

The retentivity of peptides in the different columns varied (Table 3-11). The most retentive column was the Ascentis Express. For the rest, XSelect CSH 130 was more retentive than both the Halo and Aeris Peptide stationary phases. Also the elution order of two hCRP peptides changed in the XSelect column compared to the Halo and Aeris Peptide columns: peptide RQDNEILIFWSK eluted earlier than peptide ALKYEVQGEVFTKPQLWP.

Regarding the peak areas of the peptides of interest, Halo Peptide and Aeris Peptide columns gave the best results for both hCRP C-terminal peptide ALKYEVQGEVFTKPQLWP and intact hCT (Figure 3-77 and Figure 3-78).

MS/MS ANALYSES

The type and relative abundance of different fragment ions in MS/MS spectra of a peptide depend on many factors, including the features of the peptide itself (presence/absence of basic amino acids, size, charge state), instrumentation and collision energy. Sequence ions *b* and *y* (also with loss of water or ammonia), internal ions and immonium ions are the most frequently observed in lower-energy collision-induced dissociation (CID) spectra [59].

The mechanism proposed to explain the relationship between location of charges and fragmentation of protonated peptides is called "mobile proton model" (Figure 4-10). The model assumes that protons are initially localized at the most basic sites in the peptide, that is the N-terminus and the side chains of basic amino acid residues, particularly the C-terminal Arg/Lys in peptides originated by trypsin digestions. However, following activation, those protons show a high degree of internal solvation by the heteroatoms in the peptide, such as carbonyl oxygen and amino nitrogen, and proton transfer events may become possible, leading to a heterogeneous population of structures that fragment, finally generating the MS/MS spectra of the peptide [59, 60].

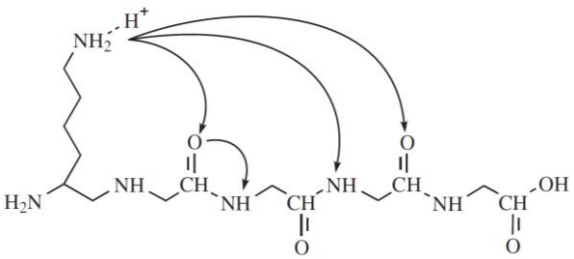

Figure 4-10. The mobile proton model. From Wysocki *et al.* [61].

In this work of thesis MS/MS analyses of the peptides of interest, originated by aqueous or mixed organic-aqueous digestions, were performed using one or more of the available mass spectrometers:

- Q TRAP (LINAC Collision Cell and LIT);
- Synapt G2-S (Trap/Transfer Cell);
- MALDI-TOF/TOF (CID Cell).

In ESI analyses fragmentation of peptides generated by digestions in aqueous solutions produced mainly *y* ions, whereas *b* ions were produced in MS/MS analyses of peptides whose cleavage is particularly favored in mixed organic-aqueous solutions. Both *b* and *y* ions were observed in MALDI-TOF/TOF analyses of the main hPCT and hCRP peptides generated in 60% ACN (Table 4-1).

PROTEIN	PEPTIDE	FRAGMENTS		
		Q TRAP	SYNAPT G2-S	MALDI-TOF/TOF
CT	C[alk]GNLSTC[alk]MLGTYTQDFNK	y	-	-
	FHTFPQTAIGVGAP	b	-	-
	CGNLSTCMLGTYTQDFNKFHTFPQTAIGVGAP	b	b	-
PCT	ASELEQEQER	y	-	-
	SALESSPADPATLSEDEAR	y	-	-
	DMSSDLERDHRPHVSMPQNAN	b	b	b, y
CRP	ESDTSYVSLK	y	y	-
	GYSIFSYATK	y	y	-
	RQDNEILIFWSK	b	b	b, y
	ALKYEVQGEVFTKPQLWP	b	b	b, y

Table 4-1. Table reporting the main type of fragments observed for each peptide in MS/MS analyses performed on different instruments. The peptides whose cleavage is particularly favored in aqueous solution or in mixed organic-aqueous solvent system are reported in blue and green respectively.

Calibration curves

Digestions in aqueous solution

Table 4-2 summarizes the main features of the analyses of protein standards digested in aqueous solution in agreement to classical sample preparation protocols.

PROTEIN	concentration range (µg/ml)	lowest quantity injected (pmol)	best R^2	transition
CT	0.5 – 50	2.92	0.989	721.9/629.4
CRP	2.5 – 50	4.34	0.998	565.0/696.8

Table 4-2. Table summarizing the main features of the calibration curves obtained for hCT and hCRP digested in aqueous solution.

Tryptic digestion of hCT produces two peptides that mainly ionize in ESI as doubly-charged ions: the N-terminal peptide C[alk]GNLSTC[alk]MLGTYTQDFNK and the C-terminal peptide FHTFPQTAIGVGAP (Figure 3-25). Linearity in the theoretical range of concentrations 0.5 – 50 µg/ml was tested and calibration curves were obtained (Figure 3-32 and Figure 3-33).
Tryptic digestion of hCRP produces peptides that ionize in ESI as doubly-charged ions. The transitions of C-terminal peptide featured better linearity than those of the N-terminal peptide in the analyzed range most intense signals in Q1 full scan spectra are those of peptides ESDTSYVSLK and GYSIFSYATK (Figure 3-38). Linearity in the theoretical range of concentrations 2.5 – 50 µg/ml was tested and calibration curves were obtained (Figure 3-46). R^2 values are ≥ 0.995 for each of the analyzed transitions of peptide ESDTSYVSLK.

Digestions in mixed organic-aqueous solvent systems

The main features of the analyses of protein standards digested in organic-aqueous solution, without previous reduction of disulfide bonds and alkylation of Cys residues, are summarized in Table 4-3.

PROTEIN	concentration range (µg/ml)	lowest quantity injected (pmol)	best R^2	transition
CT	0.1 – 12.5	0.15	0.997	1141.2/1103.4
CRP	2.5 – 50	0.54	0.996	776.7/983.3

Table 4-3. Table summarizing the main features of the calibration curves obtained for hCT and hCRP digested in 60% ACN.

Tryptic digestion of hCT in 60% ACN actually leaves the protein undigested at least until after one hour of reaction (Figure 3-51), whereas the same sample preparation procedure applied to hCRP produces cleavage of the protein into its constituent peptides (Figure 3-69).

Intact hCT mainly ionizes in ESI as triply-charged ion. Linearity in the theoretical range of concentrations 0.1 – 12.5 µg/ml was tested and a calibration curve was obtained (Figure 3-57). R^2 values are ≥ 0.995 for each of the analyzed transitions.

Tryptic digestion of hCRP produces peptides that ionize in ESI as doubly-charged ions. The most intense signals in Q1 full scan spectra are those of peptides ALKYEVQGEVFTKPQLWP and RQDNEILIFWSK (data not shown). Linearity in the theoretical range of concentrations 2.5 – 50 µg/ml was tested and calibration curves were obtained (Figure 3-76Figure 3-46). The transitions of peptide RQDNEILIFWSK featured better linearity than those of peptide ALKYEVQGEVFTKPQLWP in the analyzed range.

ANALYSIS OF THE MATRIX EFFECT

The general term matrix refers to the components of a sample other than the analyte. The matrix effect may be defined as the change (suppression or enhancement) in the LC-MS response of a specific analyte caused by co-eluting matrix compounds, compared to the analysis of the pure standard. The quantitative measure of matrix effects is the matrix factor (MF), defined as the ratio between the analyte peak response in the presence and in the absence of the matrix: MF = 1 indicates that there are no matrix effects, whereas MF < 1 indicates ion suppression and MF > 1 indicates ion enhancement. If matrix effects occur, they may affect the analytical method performance parameters such as limit of detection (LOD), limit of quantification (LOQ), linearity, accuracy and precision [62, 63].

Although the European Medicines Agency (EMEA) guidelines on bioanalytical method validation suggest the use of six lots of matrix from individual donors to investigate the matrix effect [64], in this work of thesis the preliminary experiments were carried out on a pooled matrix.
Since proteins may act differently in different environments and less effective digestions are frequently observed when target proteins are digested in a mixture as compared to being digested separately [27], the evaluation of the matrix effect on the detection of the proteotypic peptides of hCT and hCRP was conducted by spiking a digested pooled sample with organic-aqueous digestion solutions of the protein standards.
The pool, representative of healthy state, was analyzed soon after digestion in aqueous solution: calcitonin, procalcitonin and C-reactive protein, if present, were not detectable. Therefore the pool was separately spiked with the organic-aqueous digestion solutions of hPCT or hCRP, each at three concentration levels set in the medium-high range of the relative calibration curves (Figure 3-79 and Figure 3-80). MRM analyses followed and retention times and peak areas of the proteotypic peptides were monitored.

The retention time of both intact hCT and the two hCRP peptides was increased in the spiked samples as compared with the reference values of the standards. Furthermore, the peaks relative to hCT appear broadened and pronged (Figure 3-81). This may be due to a combination of both matrix effect and column carryover. The latter represents a drawback affecting the Halo column, especially at the high analyte concentrations chosen in this test.
The matrix factor (MF) was calculated for the analytes of interest: intact hCT and hCRP peptide ALKYEVQGEVFTKPQLWP showed a MF < 1 (suppression of analyte response) whereas hCRP peptide RQDNEILIFWSK showed a MF >1 (enhancement of analyte response) (Table 3-13 and Table 3-14).

5. CONCLUSIONS

In this work of thesis two gel-based bottom-up approaches were explored to characterize the protein content of whole saliva samples collected from healthy newborns in their early 48 hours after birth: 2D-PAGE – MALDI-TOF/TOF and SDS-PAGE – LC-(HR)MS/MS. The two approaches proved to be feasible, considering the low amount of protein within the collected samples, and the results obtained were complementary. As a whole, the gel-based analyses of the salivary samples of healthy newborns led to the identification of a number of proteins linked to epidermal tissue functions, whose presence appears justified considering the sample collection procedure. More interestingly, some identifications were related to common proteins usually highly expressed and involved in inflammatory processes (in particular annexin A1, glutathione S-transferase P, heat shock proteins, protein S100-A8 and -A9), probable evidence of a stressed condition already detectable in the early 48 hours after birth. Future comparison between healthy newborns and newborns affected by bacterial infection will eventually highlight the differential expression of proteins and this will give new inputs to the development of innovative and noninvasive diagnostic methods for the early detection of EOS in newborns.

Targeted analyses were focused on the development of an analytical method based on liquid chromatography coupled to mass spectrometry to qualitatively and quantitatively assay C-reactive protein, procalcitonin and calcitonin within salivary samples. Analytical MS-based methods present some undeniable advantages over immunochemical methods: high specificity, throughput multiplex analysis capable to monitor several analytes at the same time, investigation of structural modifications of proteins (e. g. post-translational modifications), fast method development and cheaper analyses. This study also enables to investigate the properties of newborn whole saliva samples as biological matrix for quantitative MS-based assays. Preliminary experiments on salivary samples showed the presence of a matrix factor in the determination of the proteins of interest. After having clarified the matrix effect, biological samples of newborns affected by bacterial infections will be analyzed to verify whether C-reactive protein and procalcitonin access to the oral fluid at detectable concentrations.
The quantitative platform will be also applied to the determination of proteins highlighted as potential inflammatory markers depending upon the results of the untargeted analyses.

Even though the bioanalytical platform has been applied to saliva samples, the developed methods and strategies can be adapted to other biological fluids.

6. EXPERIMENTAL SECTION

6.1. GEL-BASED APPROACHES

REAGENTS AND TOOLS

Chemicals

Acetic acid
Agarose
Ammonium bicarbonate (ABC)
3-[(3-cholamidopropyl)dimethylammonium]-1-propanesulfonate (CHAPS)
Formic acid (FA)
Iodoacetamide (IAA)
Dithioerythritol (DTE)
Dithiothreitol (DTT)
Glycerol
Sodium dodecyl sulfate (SDS)
Thiourea
Trifluoroacetic acid (TFA)
Tris•HCl
Tris(2-carboxyethyl)phosphine hydrochloride (TCEP•HCl)
Urea
Water, LC-MS Ultra CHROMASOLV, tested for UHPLC-MS.
All reagents are from SIGMA-ALDRICH.

Preparative tools and devices

ZipTip C18 Pipette Tips, Millipore
Centrifuge 5430 R, Eppendorf
CentriVap concentrator, Labconco
Pipettes, Gilson
Thermomixer comfort, Eppendorf
Misonix Ultrasonic Processor XL-2020, Gilson Italia
Ultrasonic Cleaner 5510, Branson
Vortex, VWR International
XP56 and XP205 balances, Mettler Toledo

Solvents

Acetone
Acetonitrile
Methanol
All the solvents are from SIGMA-ALDRICH.

1D- and 2D-PAGE

ReadyStrip ampholytes pH 3.9 – 5.1, pH 4.7 – 5.9 and pH 5.5 – 6.7
Mineral oil
2X Laemmli Sample Buffer
10X Tris/Glycine Buffer
Bio-Safe Coomassie Stain
Silver Stain Plus kit
7 cm Focusing Tray
ReadyStrip IPG Strips, 7 cm, pH 4 – 7
Protean IEF Cell
Mini-PROTEAN TGX Precast Gels
Mini-PROTEAN Tetra Cell
11 cm Focusing Tray
ReadyStrip IPG Strips, 11 cm, pH 4 – 7
PROTEAN i12 IEF System
Criterion TGX Precast Gels
Criterion Electrophoresis Cell
GS-800 densitometer
ChemiDoc MP System
All the 1D- and 2D-PAGE consumables and devices are from BIO-RAD.

MALDI-TOF/TOF

4800 MALDI-TOF/TOF, AB Sciex
α-cyano-4-hydroxycinnamic acid, LaserBio Labs
PepMix4, LaserBio Labs
ProteoMass Peptide MALDI-MS Calibration Kit, SIGMA

LTQ-Orbitrap XL

LTQ-Orbitrap XL, Thermo Scientific
UltiMate 3000 nano LC, Dionex
Jupiter Proteo 4 µm, 90 Å, 250 x 0.30 mm, Phenomenex
LC Packings, 30 µm (desalting), Dionex

Software

4000 Series Explorer, AB SCIEX
GPS Explorer, AB Sciex
Chromeleon, Thermo Scientific
Xcalibur, Thermo Scientific
Proteome Discoverer, Thermo Scientific

Online software

Matrix Science: http://www.matrixscience.com/search_form_select.html

COLLECTION OF BIOLOGICAL SAMPLES

The collection of whole unstimulated saliva is carried out by highly specialized staff of the Neonatology Unit at the Vaio Hospital in Fidenza (Parma). Gentle touches are applied with a sterile cotton swab, proven to be protein-free, inserted between the external surface of gingival walls and the cheek. Altogether, four swabs are collected for each newborn: the first pair of samples is collected within 24 hours from birth and the second pair within the next 24 hours, at least two hours far from the meals.
The freshly collected samples are stored at 4 °C in a Dewar for a maximum of 15' and then frozen at -80 °C. The samples are transferred to Chiesi Farmaceutici using dry ice and stored at -20 °C prior to analysis.

Permission of the Ethical Committee ("Comitato Etico Unico per la Provincia di Parma") was obtained for the collection of salivary samples with unanimous favorable opinion (Protocol 35269, 24 September 2012). Furthermore, written informed consent was obtained from parents.

EXTRACTION OF PROTEINS FROM SWABS

Extraction of proteins from swabs

Extraction of proteins to be analyzed in 2D-PAGE was performed with the following protocol:

a) cut away the rod and put the swab into a 2 ml tube
b) add 700 µl of freshly prepared extraction solution to completely cover the swab: 40 mM Tris•HCl, 1% SDS, pH 7.4
c) vortex for a few seconds
d) submit to 3' of sonication (6 cycles of 30" ON and 1' OFF) in an ultrasonic bath at 4 °C
e) remove the swab and centrifuge the solution for 15' at 13,200 rpm and 4 °C
f) separate the supernatant from the pellet and discard the latter
g) add ice-cold acetone in 5:1 ratio and keep overnight at -20 °C
h) centrifuge for 30' at 13,200 rpm and 4 °C to pellet the precipitated proteins
i) discard the supernatant, then let the pellet dry out at room temperature
j) re-solubilize the pellet in 100 µl of 2D-PAGE buffer: 7 M urea, 2 M thiourea, 4% CHAPS
k) quantitate the protein amount in the extracted samples.

Quantitation of the extracted protein amount

The extracted protein amount was quantified before 2-DE analysis:

a) dilute an aliquot of each sample in SDS-PAGE sample buffer
b) SDS-PAGE: load the samples and PrecisionPlus Protein Standards (duplicate)
c) ImageLab analysis of the gel and quantification of the extracted proteins.

2-DE – MALDI-TOF/TOF ANALYSES

Single newborn analyses

Sample preparation

ReadyStrip IPG Strips, 7 cm, pH 4 – 7

Total loading volume = 125 µl
Protein quantity = 15 µg Rehydration buffer 65 mM DTE 0.5% ampholytes

Isoelectric focusing

Sample loading on IPG strip with active rehydration method (12 hours at 50 V).
Isoelectric focusing process at 20 °C:

Step	Voltage (V)	Time	Mode
1	250	15 minutes	Rapid
2	4000	1 hour	Slow
3	4000 V until 11000 V/h		Rapid
4	500	72 hours	Rapid

Equilibration

The equilibration of the IPG strip prior to SDS-PAGE consisted of two steps:

1) reduction in equilibration buffer with 1% DTE, 15 minutes at room temperature;
2) alkylation in equilibration buffer with 4% IAA. 15 minutes in the dark at room temperature.

SDS-PAGE

The second dimension was carried out using Mini-PROTEAN TGX precast gels run at constant voltage (200 V).

2-DE analyses of pools

Sample preparation

ReadyStrip IPG Strips, 11 cm, pH 4 – 7.

Total loading volume = 200 µl
Protein quantity = 40 µg Rehydration buffer 65 mM DTE 0.5% ampholytes

Pools were created collecting the same amount of protein from each single sample.

Isoelectric focusing

Sample loading on IPG strip with passive rehydration method.
Isoelectric focusing process at 20 °C:

Step	Voltage (V)	Time (hours)	Mode
1	0	16	Passive rehydration
2	300	1	Rapid
3	600	1	Rapid
4	1000	1	Rapid
5	4000	1	Rapid
6	8000	1	Gradual
7	8000 V until 26000 V/h		
8	500	72	Rapid

Equilibration

The equilibration of the IPG strip prior to SDS-PAGE consisted of two steps:

1) reduction in equilibration buffer with 1% DTE, 15 minutes at room temperature;
2) alkylation in equilibration buffer with 4% IAA. 15 minutes in the dark at room temperature.

SDS-PAGE

The second dimension was carried out using Criterion TGX precast gels run at constant voltage (200 V).

Visualization of proteins

Visualization of proteins on the 2-DE was carried out in 3 steps:

3) Bio-Safe Coomassie staining
4) destaining
5) Silver staining.

Spot excision and tryptic digestion

The following digestion procedure was applied to the excised spots:

a) gel destaining with a mixed solution of 30 mM potassium ferricyanide and 100 mM sodium thiosulfate in 1:1 ratio
b) wash thoroughly with water to remove the destaining solution

c) add a mixed solution of ACN and 20 mM ammonium bicarbonate in 1:1 ratio and incubate for 20 minutes
d) remove the solution
e) add 100% ACN and incubate for 5 minutes, then dry out the spot in a speed-vac for 5 minutes
f) gel rehydration with trypsin solution for in-gel digestions, 15 minutes at room temperature
g) remove the excess of trypsin solution
h) addition of 20 mM ammonium bicarbonate to completely cover the spot
i) in-gel digestion: 16 hours at 37 °C
j) recovery of peptides:
   - recover the digestion solution
   - add 0.1% TFA and incubate at 37 °C for 45 minutes, then recover the solution
   - add ACN – 0.1% TFA in 1:1 ratio and incubate at 37 °C for 45 minutes, then recover the solution
k) dry out the solution in a speed-vac
l) solubilize the peptides just prior to MALDI-TOF/TOF analysis.

MALDI-TOF/TOF analyses

All of the samples were analyzed using an Applied Biosystems/MDS SCIEX 4800 MALDI TOF/TOF Analyzer.
Peptide ion masses were measured with manual acquisition in the positive reflectron mode.
Matrix: α-cyano-4-hydroxycinnamic acid (CHCA), 10 mg/ml in ACN – 0.1% TFA mixed 1:1.
Sample preparation: dried droplet.
External calibration was performed with either PepMix4 (500 – 3500 Da) or ProteoMass Peptide (700 – 3500 Da) (Table 6-1 and Table 6-2).

Table 6-1. PepMix4 calibration mixture.

Standard	Sequence	Theoretical monoisotopic molecular weight
Bradykinin fragment 1-5	RPPGF	572.31
Human Angiotensin II	DRVYIHPF	1045.53
Neurotensin	ZLYENKPRRPYIL	1672.92
ACTH fragment 18-39	RPVKVYPNGAEDESAEAFPLEF	2464.19
Insulin Chain B oxidized	FVNQHLCGSHLVEALYLVCGERGFFYTPKA	3493.65

Table 6-2. ProteoMass Peptide MALDI calibration mixture.

Standard	Sequence	Theoretical monoisotopic molecular weight
Bradykinin fragment 1-7	RPPGFSP	756.3997
Human Angiotensin II	DRVYIHPF	1045.5423
$P_{14}R$	PPPPPPPPPPPPPR	1532.8582
ACTH fragment 18-39	RPVKVYPNGAEDESAEAFPLEF	2464.1989
Insulin Chain B oxidized	FVNQHLCGSHLVEALYLVCGERGFFYTPKA	3493.6513

Calibrations were accepted when they satisfied the following conditions:

min S/N:	10
mass tolerance:	± 10 ppm
min peaks to match:	4
max outlier error:	± 10 ppm

SDS-PAGE – LC-(HR)MS/MS ANALYSES

SDS-PAGE analysis

12% acrylamide gel run at constant voltage (200 V).
Loaded sample quantity per lane = 10 µg.
Bio-Safe Coomassie staining.

Band excision and tryptic digestion

Band excision and analysis:

a) destaining with a solution 50% ethanol, 10% acetic acid
b) wash: 10 minutes in water
c) reduction in 1% DTE, 15 minutes
d) alkylation in 4% IAA, 15 minutes in the dark
e) 20 minutes in 80% ACN / 20% 20 mM ammonium bicarbonate
f) 5 minutes in 100% ACN and then dry out the band in a speed-vac for 5 minutes
g) gel rehydration with trypsin solution for in-gel digestions, 15 minutes at room temperature
h) removal of the excess of trypsin solution
i) addition of 20 mM ammonium bicarbonate to completely cover the band
j) in-gel digestion: 16 hours at 37 °C
k) recovery of peptides:
   - recover the digestion solution
   - add 0.1% TFA and incubate at 37 °C for 45 minutes, then recover the solution
   - add ACN – 0.1% TFA in 1:1 ratio and incubate at 37 °C for 15 minutes, then recover the solution.

LC-(HR)MS/MS analyses

Mass spectrometer: LTQ-Orbitrap XL.

LC pump: Dionex UltiMate 3000 nano LC.
Micro pump column: Jupiter Proteo 4 µm, 90 Å, 250 x 0.30 mm – Flow rate 5 µl/min.
Loading pump column: LC Packings, 30 µm (desalting) – Flow rate 30 µl/min.

Column oven: 45 °C.

Mobile phases:

A) 5% ACN, 0.1% FA, 0.01% TFA in H_2O
B) 5% H_2O, 0.1% FA, 0.02% TFA in ACN

Mobile phase gradient (Figure 6-1):

Time (min)	% A	% B
0	95	5
4	95	5
34	50	50
45	50	50
62	5	95
72	5	95
84	95	5
90	95	5

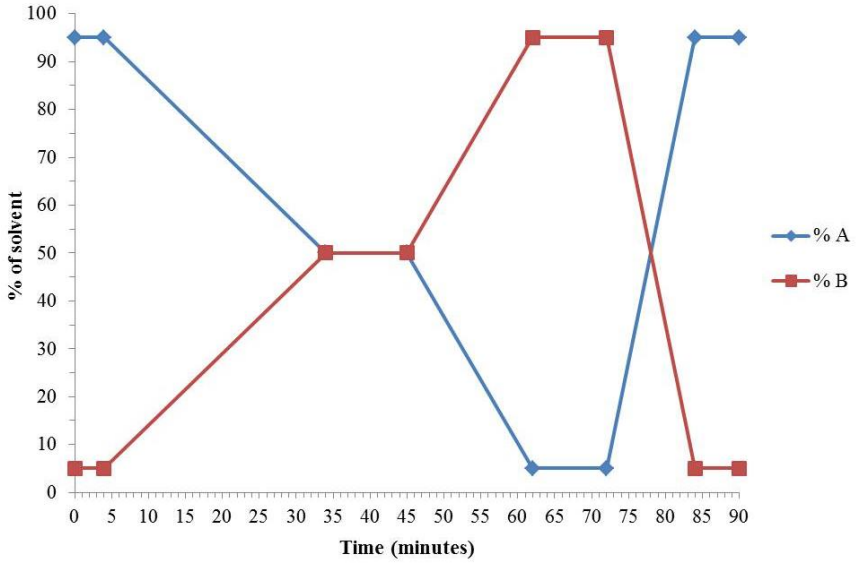

Figure 6-1. Graph of the mobile phase gradient applied.

6.2. TARGETED ANALYSES

REAGENTS AND TOOLS

Proteins

Human calcitonin, Sigma T3535
Human procalcitonin, recombinant, expressed in *E. coli*, Sigma SRP6003
Human C-reactive protein, recombinant, expressed in E. coli, Merck 236608
Human C-reactive protein, RayBiotech, Inc. 228-10278-1
Trypsin proteomics grade, Sigma T6567

Chemicals

Acetic acid
Ammonium bicarbonate (ABC)
Formic acid (FA)
Iodoacetamide (IAA)
Dithioerythritol (DTE)
Dithiothreitol (DTT)
Glycerol
Sodium dodecyl sulfate (SDS)
Thiourea
Trifluoroacetic acid (TFA)
Tris•HCl
Tris(2-carboxyethyl)phosphine hydrochloride (TCEP•HCl)
Urea
Water, LC-MS Ultra CHROMASOLV, tested for UHPLC-MS.
All reagents are from SIGMA-ALDRICH.

Preparative tools and devices

ZipTip C18 Pipette Tips, Millipore
Pierce C18 Spin Columns, Thermo Scientific
Micro Bio-Spin Chromatography Columns, BIO-RAD
PD MiniTrap G-10, GE Healthcare
Pierce Detergent Removal Spin Columns, Thermo Scientific
Pipettes, Gilson
Centrifuge 5430 R, Eppendorf
CentriVap concentrator, Labconco
Thermomixer comfort, Eppendorf
Ultrasonic Cleaner 5510, Branson

Vortex, VWR International
XP56 and XP205 balances, Mettler Toledo

Solvents

Acetone
Acetonitrile
Methanol
All the solvents are from SIGMA-ALDRICH.

MALDI-TOF/TOF

4800 MALDI-TOF/TOF, AB Sciex
α-cyano-4-hydroxycinnamic acid, LaserBio Labs
PepMix3, LaserBio Labs
PepMix4, LaserBio Labs
ProteoMass Peptide MALDI-MS Calibration Kit, SIGMA

LC columns

BioBasic 18 column, 5 µm, 250 x 4.6 mm, Thermo Scientific
Aeris Peptide UHPLC/HPLC column, 3.6 µm, 150 x 2.1 mm, Phenomenex
Ascentis Express C18 HPLC column, 2.7 µm, 150 x 4.6 mm, SIGMA
HALO ES-C18 UHPLC column, 2.7 µm, 150 x 2.1 mm, Bruker-Michrom
XSelect CSH 130 column, 2.5 µm, 150 x 4.6 mm, Waters

LC-MS instruments

HPLC HP1100, Agilent
4000 QTRAP, AB Sciex
UPLC Acquity, Waters
Synapt G2-S, Waters

Software

4000 Series Explorer, AB SCIEX
Analyst 1.5, AB Sciex
MRM Pilot, AB Sciex
MultiQuant, AB Sciex
MassLynx, Waters
BiopharmaLynx, Waters

Online software

ExPASy Compute pI/Mw: http://web.expasy.org/compute_pi/
ExPASy FindPept: http://web.expasy.org/findpept/

ExPASy Peptide Cutter: http://web.expasy.org/peptide_cutter/
ExPASy ProtParam: http://web.expasy.org/protparam/
Fragment ion calculator: http://db.systemsbiology.net/proteomicsToolkit/FragIonServlet.html

PURIFICATION PROCEDURES

Reverse-phase chromatography

ZipTip C18 Pipette Tips (Millipore)

1) prepare the following solutions:

Solution	Composition
Wetting	100% ACN
Equilibration	0.1% TFA in H_2O
Wash	0.1% TFA in H_2O
Elution	100% ACN – 0.1% TFA in H_2O mixed 1:1

2) add 0.1% TFA to the sample solution
3) equilibration of the ZipTip Pipette Tip for sample binding:
   a) aspirate 10 µl of wetting solution and dispense to waste
   b) repeat
   c) aspirate equilibration solution and dispense to waste
   d) repeat
4) binding of the peptides/protein to the resin: aspirate and dispense the sample (7 – 10 cycles)
5) sample wash: aspirate the wash solution and dispense to waste, then repeat at least once
6) sample elution:
   a) dispense a desired volume of elution solution into a clean vial
   b) aspirate and dispense the elution solution through the ZipTip within the vial
   c) repeat at least three times.

Pierce C18 Spin Columns (Thermo Scientific)

1) prepare the following solutions:

solution	composition	total volume (µl)
Activation	50% methanol	400
Equilibration	0.5% TFA in 5% ACN	400
Sample	0.5% TFA in 5% ACN	10 – 150
Wash	0.5% TFA in 5% ACN	800 – 1200
Elution	0.1% FA in 70% ACN	40

2) column preparation:
   a) tap the column to settle the resin
   b) remove top e and bottom cap and place the column in a 1.5ml tube
   c) add 200 µl of activation solution to rinse the walls of the column and wet the resin
   d) centrifuge at 1,500 x g for 1', then discard the flow-through
   e) repeat once
3) column equilibration:
   a) add 200 µl of equilibration solution
   b) centrifuge at 1,500 x g for 1', then discard the flow-through
   c) repeat once
4) sample binding:

a) load sample on top of the resin bed
b) place the column in a receiver tube
c) centrifuge at 1,500 x g for 1'
d) recover the flow-through, reload it and centrifuge again at 1,500 x g for 1'

5) sample wash:
   a) place the column in a receiver tube
   a) add 200 µl of wash solution, then centrifuge at 1,500 x g for 1'
   b) repeat once or twice
6) sample elution:
   a) place the column in a new receiver tube
   b) add 20 µl of elution solution, then centrifuge at 1,500 x g for 1'
   c) repeat once using the same receiver tube.

Size exclusion chromatography

Micro Bio-Spin Chromatography Columns (BIO-RAD)

1) prepare the column:
   a) resuspend the gel and remove air bubbles by inverting the column sharply several times
   b) snap off the tip and place the column in a 2 ml tube, then remove the top cap
   c) allow the excess packing buffer to drain by gravity and discard it
   d) centrifuge for 2' at 1,000 x (g) to remove the remaining buffer and discard it
2) column equilibration:
   a) apply 500 µl of the desired buffer, centrifuge for 1' at 1,000 x (g) and discard the flow-through
   b) repeat the previous step for at least three times
3) sample application and elution:
   a) place the column in a clean 1.5 or 2 ml tube and apply the sample (20 – 75 µl)
   b) centrifuge for 4' at 1,000 x (g) to recover the sample in the new buffer.

PD MiniTrap G-10 columns (GE Healthcare)

1) prepare the column:
   a) invert the column several times to resuspend the medium in the storage solution
   b) allow the medium to settle
   c) remove the top and bottom caps and allow the storage solution to drain by gravity
2) column equilibration:
   a) fill the column with the desired equilibration buffer and allow it to flow out
   b) repeat at least twice
3) sample application:
   a) add maximum 0.3 ml of sample and let it enter the packed bed completely
   b) add a stacker volume of equilibration buffer so that the total volume of sample and buffer equals 0.7 ml and let it enter the packed bed completely
4) sample elution:
   a) place a clean tube under the column

b) add 0.5 ml of buffer and collect the eluate.

Others

Pierce Detergent Removal Spin Columns (Thermo Scientific)

1) column preparation:
   a) remove the bottom cap and loosen the top one
   b) place the column into a 2 ml tube
   c) centrifuge at the speed and time indicated to remove the storage solution
2) column equilibration:
   a) add the equilibration buffer and centrifuge
   b) repeat at least twice
3) sample application:
   a) place the column in a clean 1.5 ml collection tube
   b) slowly apply the sample to the top of the compact resin bed
   c) incubate for 2' at room temperature
4) sample elution: centrifuge for 2' at the indicated speed.

			Column size (µl)	
			125	**500**
solutions	Sample volume range (µl)		10 – 25	25 – 100
	Equilibration solution (µl)		100	400
centrifuge	Speed (g)		1000	1500
	Time (min):	- storage solution removal	1	1
		- washes	1	1
		- sample recovery	2	2

MALDI-TOF/TOF

All of the samples were analyzed using an Applied Biosystems/MDS SCIEX 4800 MALDI TOF/TOF Analyzer.

Peptide ion masses were measured with manual acquisition in the positive reflectron mode.

Matrix: α-cyano-4-hydroxycinnamic acid (CHCA), 10 mg/ml in ACN – 0.1% TFA mixed 1:1.

Sample preparation: dried droplet.

External calibration was performed with one of the following calibration mixtures, depending on the expected mass of the analytes: PepMix3 (3000 – 9000 Da), PepMix4 (500 – 3500 Da) or ProteoMass Peptide (700 – 3500 Da) (Table 6-3, Table 6-4, Table 6-5).

Table 6-3. PepMix3 calibration mixture.

Standard	Sequence	Theoretical monoisotopic molecular weight
Insulin Chain B oxidized	FVNQHLCGSHLVEALYLVCGERGFFYTPKA	3493.65
Insulin (bovine)	GIVEQCCASVCSLYQLENYCN-FVNQHLCGSHLVEALYLVCGERGFFYTPKA	5733.49
Aprotinin	RPDFCLEPPYTGPCKARIIRYFYNAKAGLCQTFVYGGC RAKRNNFKSAEDCMRTCGGA	6511.44
Ubiquitin (bovine)	MQIFVKTLTGKTITLEVEPSDTIENVKGKIQEKEGIPPD QQRLIFAGKQLEDGRTLSDYNIQKESTLHLVLRLRGG	8559.62

Table 6-4. PepMix4 calibration mixture.

Standard	Sequence	Theoretical monoisotopic molecular weight
Bradykinin fragment 1-5	RPPGF	572.31
Human Angiotensin II	DRVYIHPF	1045.53
Neurotensin	ZLYENKPRRPYIL	1672.92
ACTH fragment 18-39	RPVKVYPNGAEDESAEAFPLEF	2464.19
Insulin Chain B oxidized	FVNQHLCGSHLVEALYLVCGERGFFYTPKA	3493.65

Table 6-5. ProteoMass Peptide MALDI calibration mixture.

Standard	Sequence	Theoretical monoisotopic molecular weight
Bradykinin fragment 1-7	RPPGFSP	756.3997
Human Angiotensin II	DRVYIHPF	1045.5423
$P_{14}R$	PPPPPPPPPPPPPR	1532.8582
ACTH fragment 18-39	RPVKVYPNGAEDESAEAFPLEF	2464.1989
Insulin Chain B oxidized	FVNQHLCGSHLVEALYLVCGERGFFYTPKA	3493.6513

Calibrations were accepted when they satisfied the following conditions:

min S/N:	10
mass tolerance:	± 10 ppm
min peaks to match:	4
max outlier error:	± 10 ppm

HPLC – Q TRAP

Analyses of protein standards digested in aqueous solution

HPLC pump: Agilent 1100.

HPLC column: BioBasic 18 (Thermo Scientific), 250 x 4.6 mm, 5 µm.
Column oven: 45 °C.

Mobile phases:

A) 5% ACN, 0.1% FA, 0.02% TFA in H_2O

B) 5% H_2O, 0.1% FA, 0.02% TFA in ACN

Mobile phase flux = 250 µl/min.

Mobile phase gradient "Biobasic_2" (Figure 6-2):

Time (min)	% A	% B
0	95	5
8	95	5
15	50	50
25	50	50
35	5	95
40	5	95
46	95	5
65	95	5

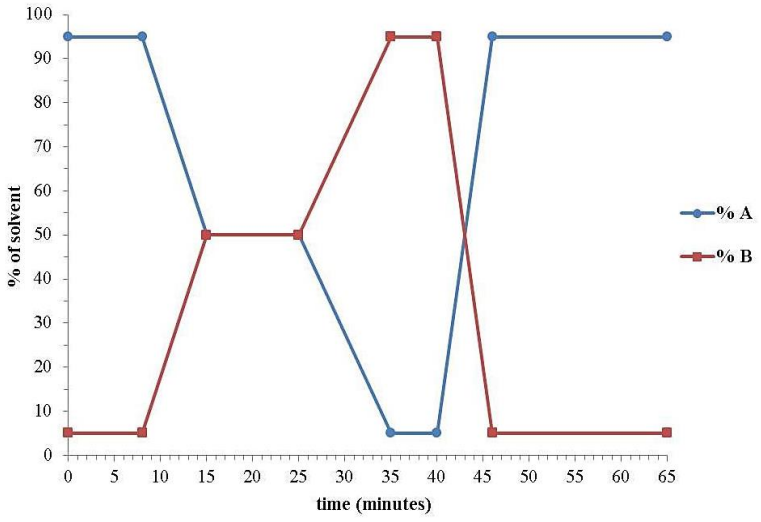

Figure 6-2. Mobile phase gradient "Biobasic_2".

Mobile phase gradient “Biobasic_3” (Figure 6-3):

Time (min)	% A	% B
0	95	5
8	95	5
15	50	50
20	50	50
40	5	95
45	5	95
50	95	5
65	95	5

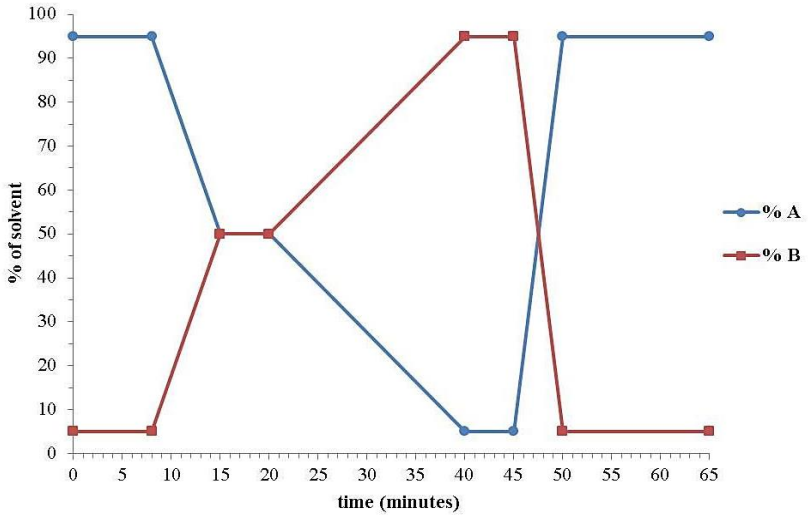

Figure 6-3. Mobile phase gradient “Biobasic_3”.

Ion source: Turbo V Ion Source.
y-axis probe position = 2
Source parameters:

Curtain gas (CUR):	30
CAD:	High
Ion Spray Voltage (IS):	5500
Temperature (TEM):	550
Gas 1 (GS1):	50
Gas 2 (GS2):	40

Injection volume = 20 µl

Analyses of protein standards digested in organic-aqueous solutions

HPLC pump: Agilent 1100
HPLC column: HALO ES-C18 UHPLC column, 2.7 µm, 150 x 2.1 mm, Bruker-Michrom
Column oven: 65 °C

Mobile phases:

A) 0.1% FA in H_2O

B) 0.1% FA in MeOH

Mobile phase flux = 250 µl/min

Mobile phase gradient (Figure 6-4):

Time (min)	% A	% B
0	99	1
5	99	1
15	69	31
15.2	68	32
35	10	90
50	99	1
75	99	1

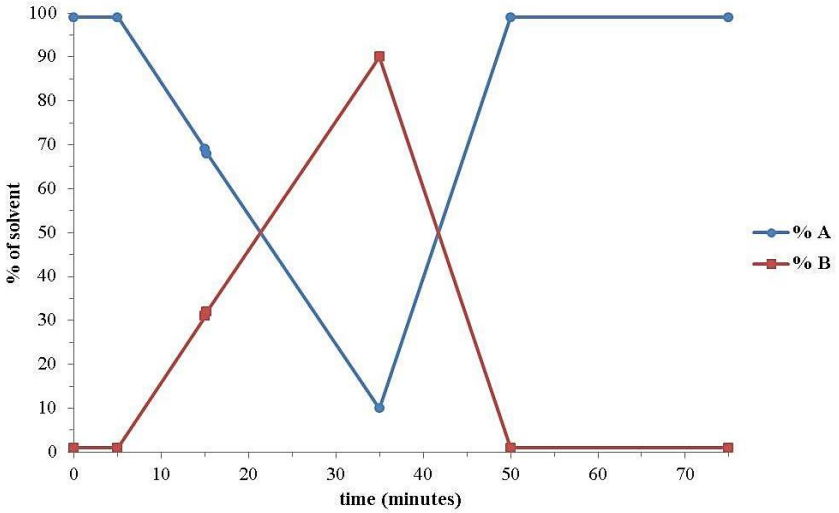

Figure 6-4. Mobile phase gradient applied in the analyses of protein standards digested in organic-aqueous solutions.

Ion source: Turbo V Ion Source

y-axis probe position = 2

Source parameters:

Curtain gas (CUR):	30
CAD:	High
Ion Spray Voltage (IS):	5500
Temperature (TEM):	550
Gas 1 (GS1):	50
Gas 2 (GS2):	40

Injection volume = 5 µl

UPLC – SYNAPT

UPLC pump: Waters Acquity

UPLC columns tested:

Column name	SP	Particle size (µm)	Pore size (Å)	Length (mm)	I. D. (mm)	Brand
Aeris Peptide	C18	3.6	100	150	2.1	Phenomenex
Ascentis Express	C18	2.7	160	150	4.6	SIGMA
HALO ES-C18	C18	2.7	160	150	2.1	CPS
XSelect CSH 130	C18	2.5	130	150	4.6	Waters

Column oven: 65 °C

Mobile phases:

A) 0.1% FA in H_2O

B) 0.1% FA in methanol

Mobile phase flux = 200 µl/min

Mobile phase gradient (Figure 6-4):

Time (min)	% A	% B
0	99	1
5	99	1
15	69	31
15.2	68	32
35	10	90
50	99	1
75	99	1

MRM ANALYSES

Protein standards digested in aqueous solution

Intact calcitonin

The transitions analyzed are reported in Table 6-6.

Table 6-6. MRM transitions of intact hCT.

m/z precursor ion (Q1)	m/z fragment ion (Q3)	Fragment ion	DP	CE	Time (msec)
1179.0	**1711.0**	y32(2+)	80	50	100
1179.0	**1569.0**	y15(1+)	80	50	100
1179.0	**1141.0**	y32(3+)	80	50	100
1179.0	**1249.0**	y23(2+)	80	50	100
1179.0	**910.0**	y10(1+)	80	50	100

Linearity in the theoretical range of concentrations 0.4 – 50 µg/ml was tested (HPLC gradient "biobasic_2") using four solutions generated through successive dilutions of the digestion solution (Figure 6-5).

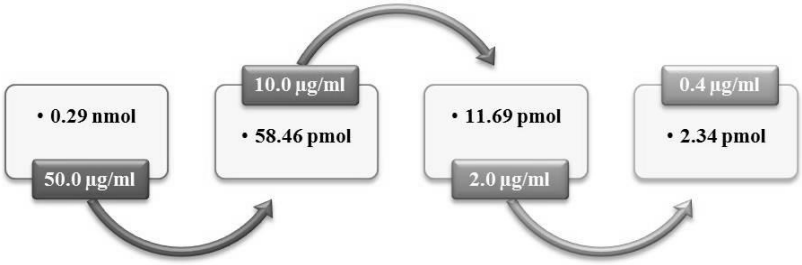

Figure 6-5. Scheme of the successive dilutions of the digestion solution, reporting the injected protein quantities.

Digested calcitonin

The transitions analyzed are reported in Table 6-7.

Table 6-7. MRM transitions of digested hCT.

m/z precursor ion (Q1)	m/z fragment ion (Q3)	Fragment ion	DP	CE	Time (msec)
721.9	**1328.2**	b13(1+)	70	30	100
721.9	**665.0**	b13(2+)	70	30	100
721.9	**629.4**	b5(1+)	70	30	100
1056.0	**1074.3**	y9(1+)	70	50	100
1056.0	**1187.2**	y10(1+)	70	50	100
1056.0	**753.2**	y6(1+)	70	50	100

Linearity in the theoretical range of concentrations 0.5 – 50 µg/ml was tested (HPLC gradient "biobasic_2") using five solutions generated through successive dilutions of the digestion solution (Figure 6-6).

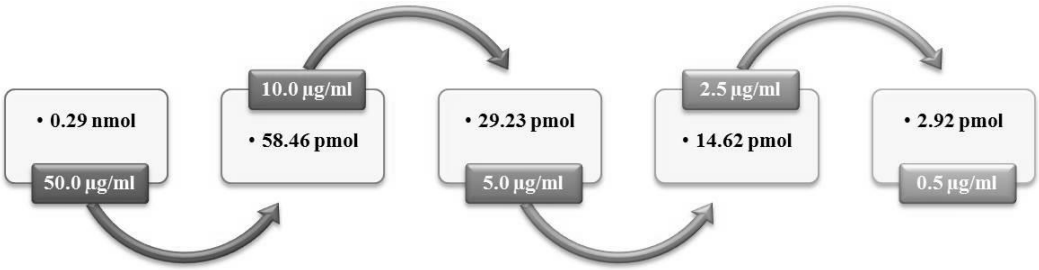

Figure 6-6. Scheme of the successive dilutions of the digestion solution, reporting the injected protein quantities.

Three independent replicas for each concentration were generated and then analyzed.

C-reactive protein

The transitions analyzed are reported in Table 6-8.

Table 6-8. MRM transitions of digested hCRP.

m/z precursor ion (Q1)	m/z fragment ion (Q3)	Fragment ion	DP	CE	Time (msec)
565.0	**609.8**	y5(1+)	70	25	100
565.0	**696.8**	y6(1+)	70	25	100
565.0	**913.0**	y8(1+)	70	25	100
565.0	**797.9**	y7(1+)	70	25	100
569.8	**918.1**	y8(1+)	60	30	100
569.8	**717.1**	y6(1+)	60	30	100
569.8	**831.0**	y7(1+)	60	30	100

Linearity in the theoretical range of concentrations 2.5 – 50 µg/ml was tested (HPLC gradient "biobasic_3") using five solutions generated through successive dilutions of the digestion solution (Figure 6-7).

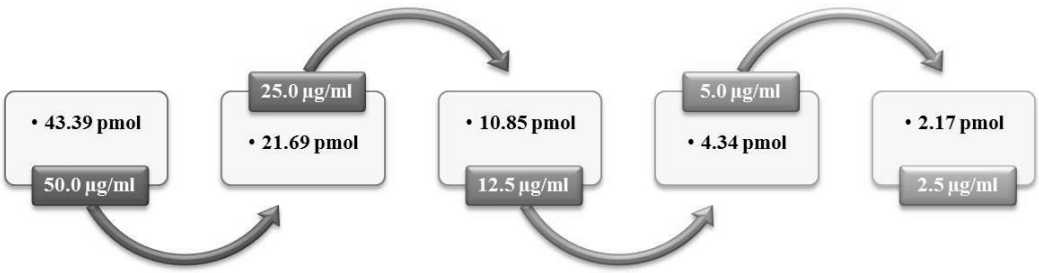

Figure 6-7. Scheme of the successive dilutions of the digestion solution, reporting the injected protein quantities.

Protein standards digested in mixed organic-aqueous solvent system

Intact calcitonin

The transitions analyzed are reported in Table 6-9.

Table 6-9. MRM transitions of intact hCT.

m/z precursor ion (Q1)	m/z fragment ion (Q3)	Fragment ion	DP	CE	Time (msec)
1141.2	**1654.0**	b31(2+)	70	35	100
1141.2	**1103.4**	b31(3+)	70	35	100
1141.2	**1079.8**	b30(3+)	70	35	100

Linearity in the theoretical range of concentrations 0.1 – 12.5 µg/ml were tested using five solutions generated through successive dilutions of the digestion solution (Figure 6-8).

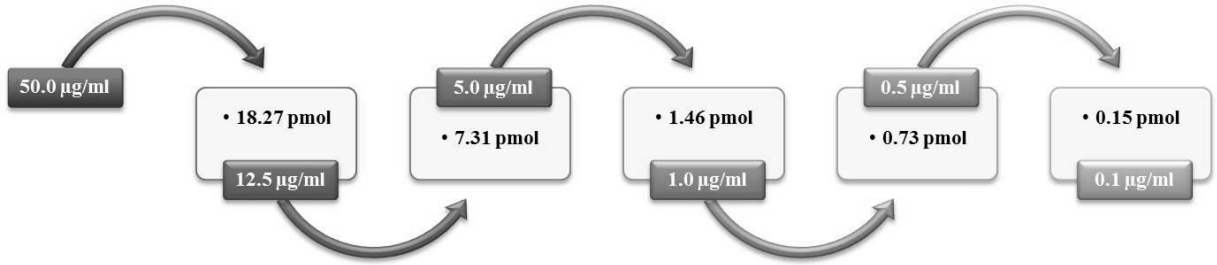

Figure 6-8. Scheme of the successive dilutions of the digestion solution, reporting the injected protein quantities.

Three independent replicas for each concentration were generated and then analyzed.

C-reactive protein

The transitions analyzed are reported in Table 6-10.

Table 6-10- MRM transitions of digested hCRP.

m/z precursor ion (Q1)	m/z fragment ion (Q3)	Fragment ion	DP	CE	Time (msec)
776.7	**1130.4**	b9(1+)	100	43	100
776.7	**870.1**	b7(1+)	100	43	100
776.7	**983.3**	b8(1+)	100	43	100
712.9	**917.5**	b16(2+)	75	27	100
712.9	**1010.7**	b17(2+)	75	27	100
712.9	**1118.1**	b10(1+)	75	27	100

Linearity in the theoretical range of concentrations 2.5 – 50 µg/ml were tested using five solutions generated through successive dilutions of the digestion solution (Figure 6-9).

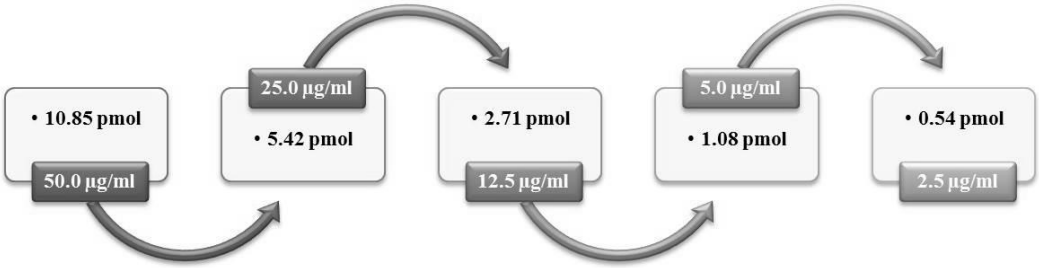

Figure 6-9. Scheme of the successive dilutions of the digestion solution, reporting the injected protein quantities.

Three independent replicas for each concentration were generated and then analyzed.

COLLECTION OF BIOLOGICAL SAMPLES

The collection of whole unstimulated saliva is carried out by highly specialized staff of the Neonatology Unit at the Vaio Hospital in Fidenza (Parma). Gentle touches are applied with a sterile cotton swab, proven to be protein-free, inserted between the external surface of gingival walls and the cheek. Altogether, four swabs are collected for each newborn: the first pair of samples is collected within 24 hours from birth and the second pair within the next 24 hours, at least two hours far from the meals.
The freshly collected samples are stored at 4 °C in a Dewar for a maximum of 15' and then frozen at -80 °C.
The samples are transferred to Chiesi Farmaceutici using dry ice and stored at -20 °C prior to analysis.

Permission of the Ethical Committee ("Comitato Etico Unico per la Provincia di Parma") was obtained for the collection of salivary samples with unanimous favorable opinion (Protocol 35269, 24 September 2012). Furthermore, written informed consent was obtained from parents.

SAMPLE PREPARATION AND LC-MS/MS ANALYSIS

Extraction of proteins from swabs and creation of a pooled sample

Extraction of proteins to be pooled and analyzed in LC-MS/MS was performed with the following protocol:

a) cut away the rods and put the swabs into 2 ml tubes
b) add 700 µl of freshly prepared extraction solution in each tube to completely cover the swab: 40 mM Tris•HCl, 1% SDS, pH 7.4
c) vortex the tubes for a few seconds
d) submit to 3' of sonication (6 cycles of 30" ON and 1' OFF) in an ultrasonic bath at 4 °C
e) remove the swabs and centrifuge the extraction solutions for 15' at 13,200 rpm and 4 °C
f) separate the supernatant from the pellet and discard the latter
g) merge the extraction solutions and then divide in aliquots
h) add ice-cold acetone in 5:1 ratio and keep overnight at -20 °C
i) centrifuge for 30' at 13,200 rpm and 4 °C to pellet the precipitated proteins
j) discard the supernatant, then let the pellets dry out at room temperature
k) store the pellets at -20 °C.

Quantitation of the extracted protein amount

The extracted protein amount was quantified before digestion:

a) re-solubilize an aliquot in SDS-PAGE sample buffer
b) SDS-PAGE: load the pooled sample and PrecisionPlus Protein Standards (duplicate)
c) ImageLab analysis of the gel for the quantification of the extracted proteins.

Digestion of the pooled sample for LC-MS/MS analysis

Protocol for the digestion of the pooled sample prior to LC-MS/MS analysis:

- thaw the pelleted sample stored at -20 °C
- solubilize the pellet in 50 mM ammonium bicarbonate, 0.1% SDS
- in-solution digestion: 16 hours at 37 °C with trypsin 1:20 (w/w)
- quenching of digestion by addition of 0.1% formic acid.

Digestion of the protein standards in organic-aqueous solution

Human calcitonin and human C-reactive protein were digested separately:

- dilution of the stock solution to 0.1 mg/ml with 60% ACN / 40% ammonium bicarbonate
- in-solution digestion: 1 hour at 37 °C with trypsin 1:5 (w/w)
- quenching of digestion by addition of 0.1% formic acid.

MRM analyses

The pool created from five healthy newborns on their second day after birth and digested in aqueous solution was analyzed to verify if the proteins of interest, calcitonin, procalcitonin and C-reactive protein, were present and detectable. The transitions monitored are reported in Table 6-11.

Table 6-11. Transitions monitored in the analysis of the pool representative of healthy state.

PROTEIN	m/z precursor ion (Q1)	m/z fragment ion (Q3)	Fragment ion	DP	CE	Time (msec)
hCT	**1179.0**	**1711.0**	y32(2+)	80	50	100
	1179.0	**1569.0**	y15(1+)	80	50	100
	1179.0	**1141.0**	y32(3+)	80	50	100
	721.9	**1328.2**	b13(1+)	70	30	100
	721.9	**665.0**	b13(2+)	70	30	100
	721.9	**629.4**	b5(1+)	70	30	100
hPCT	**609.9**	**818.9**	y6(1+)	60	35	100
	609.9	**690.0**	y5(1+)	60	35	100
	974.5	**1089.4**	y10(1+)	60	40	100
	974.5	**1372.8**	y13(1+)	60	40	100
hCRP	**565.0**	**609.8**	y5(1+)	70	25	100
	565.0	**696.8**	y6(1+)	70	25	100
	565.0	**797.9**	y7(1+)	70	25	100
	569.8	**918.1**	y8(1+)	60	30	100
	569.8	**717.1**	y6(1+)	60	30	100
	569.8	**831.0**	y7(1+)	60	30	100

The pool was separately spiked with the organic-aqueous digestion solutions of hPCT or hCRP and MRM analyses followed. The transitions monitored are reported in Table 6-12.

Table 6-12. Transitions monitored in the analysis of the pool representative of healthy state.

PROTEIN	m/z precursor ion (Q1)	m/z fragment ion (Q3)	Fragment ion	DP	CE	Time (msec)
hCT	**1141.2**	**1654.0**	b31(2+)	70	35	100
	1141.2	**1103.4**	b31(3+)	70	35	100
	1141.2	**1079.8**	b30(3+)	70	35	100
hPCT	**813.0**	**769.5**	b20(3+)	90	35	100
	813.0	**948.2**	b16(2+)	90	35	100
	813.0	**1050.4**	b9(1+)	90	35	100
hCRP	**776.7**	**1130.4**	b9(1+)	100	43	100
	776.7	**870.1**	b7(1+)	100	43	100
	776.7	**983.3**	b8(1+)	100	43	100
	712.9	**917.5**	b16(2+)	75	27	100
	712.9	**1010.7**	b17(2+)	75	27	100
	712.9	**1118.1**	b10(1+)	75	27	100

BIBLIOGRAPHY

1. Pfaffe, T., *et al., Diagnostic potential of saliva: current state and future applications.* Clin Chem, 2011. 57(5): p. 675-87.
2. Uitto, V.J., *Gingival crevice fluid--an introduction.* Periodontol 2000, 2003. 31: p. 9-11.
3. Humphrey, S.P. and R.T. Williamson, *A review of saliva: normal composition, flow, and function.* J Prosthet Dent, 2001. 85(2): p. 162-9.
4. Standring, S., *Oral cavity,* in *Gray's anatomy: the anatomical basis of clinical practice*, S. Standring, Editor. 2008, Churchill Livingstone.
5. Genco, R.J., *Salivary diagnostic tests.* J Am Dent Assoc, 2012. 143(10 Suppl): p. 3S-5S.
6. Lee, J.M., E. Garon, and D.T. Wong, *Salivary diagnostics.* Orthod Craniofac Res, 2009. 12(3): p. 206-11.
7. Wong, D.T., *Salivary diagnostics.* J Calif Dent Assoc, 2006. 34(4): p. 283-5.
8. Kaufman, E. and I.B. Lamster, *The diagnostic applications of saliva--a review.* Crit Rev Oral Biol Med, 2002. 13(2): p. 197-212.
9. Miller, C.S., *et al., Current developments in salivary diagnostics.* Biomark Med, 2010. 4(1): p. 171-89.
10. Schapher, M., O. Wendler, and M. Groschl, *Salivary cytokines in cell proliferation and cancer.* Clin Chim Acta, 2011. 412(19-20): p. 1740-8.
11. Lima, D.P., *et al., Saliva: reflection of the body.* Int J Infect Dis, 2010. 14(3): p. e184-8.
12. Becker, K.L., *et al., Clinical review 167: Procalcitonin and the calcitonin gene family of peptides in inflammation, infection, and sepsis: a journey from calcitonin back to its precursors.* J Clin Endocrinol Metab, 2004. 89(4): p. 1512-25.
13. Gabay, C. and I. Kushner, *Acute-phase proteins and other systemic responses to inflammation.* N Engl J Med, 1999. 340(6): p. 448-54.
14. Pepys, M.B. and G.M. Hirschfield, *C-reactive protein: a critical update.* J Clin Invest, 2003. 111(12): p. 1805-12.
15. Ittner, L., *et al., Circulating procalcitonin and cleavage products in septicaemia compared with medullary thyroid carcinoma.* Eur J Endocrinol, 2002. 147(6): p. 727-31.
16. Jin, M. and A.I. Khan, *Procalcitonin: uses in the clinical laboratory for the diagnosis of sepsis.* LabMedicine, 2010. 41(3): p. 173-177.
17. Riedel, S., *et al., Procalcitonin as a marker for the detection of bacteremia and sepsis in the emergency department.* Am J Clin Pathol, 2011. 135(2): p. 182-9.
18. Schuetz, P., W. Albrich, and B. Mueller, *Procalcitonin for diagnosis of infection and guide to antibiotic decisions: past, present and future.* BMC Med, 2011. 9: p. 107.
19. Baruti Gafurri, Z., *et al., The importance of determining procalcitonin and C reactive protein in different stages of sepsis.* Bosn J Basic Med Sci, 2010. 10(1): p. 60-4.

20. Maruna, P., K. Nedelnikova, and R. Gurlich, *Physiology and genetics of procalcitonin.* Physiol Res, 2000. 49 Suppl 1: p. S57-61.

21. Meisner, M., *Pathobiochemistry and clinical use of procalcitonin.* Clin Chim Acta, 2002. 323(1-2): p. 17-29.

22. Matera, G., *et al.*, *Procalcitonin neutralizes bacterial LPS and reduces LPS-induced cytokine release in human peripheral blood mononuclear cells.* BMC Microbiol, 2012. 12: p. 68.

23. Black, S., I. Kushner, and D. Samols, *C-reactive Protein.* J Biol Chem, 2004. 279(47): p. 48487-90.

24. Thompson, D., M.B. Pepys, and S.P. Wood, *The physiological structure of human C-reactive protein and its complex with phosphocholine.* Structure, 1999. 7(2): p. 169-77.

25. Volanakis, J.E., *Human C-reactive protein: expression, structure, and function.* Mol Immunol, 2001. 38(2-3): p. 189-97.

26. Han, X., A. Aslanian, and J.R. Yates, 3rd, *Mass spectrometry for proteomics.* Curr Opin Chem Biol, 2008. 12(5): p. 483-90.

27. Hustoft, H.K., *et al.*, *A critical review of trypsin digestion for LC-MS based proteomics*, in *Integrative proteomics*, H.-C.E. Leung, Editor. 2012, InTech.

28. Berg, J.M., J.L. Tymoczko, and L. Stryer, *Catalytic strategies*, in *Biochemistry*. 2007, W. H. Freeman and Company.

29. Simon, L.M., *et al.*, *Stability of hydrolytic enzymes in water-organic solvent systems.* Journal of Molecular Catalysis B, 1998. 4: p. 41-45.

30. Russell, W.K., Z.Y. Park, and D.H. Russell, *Proteolysis in mixed organic-aqueous solvent systems: applications for peptide mass mapping using mass spectrometry.* Anal Chem, 2001. 73(11): p. 2682-5.

31. Strader, M.B., *et al.*, *Efficient and specific trypsin digestion of microgram to nanogram quantities of proteins in organic-aqueous solvent systems.* Anal Chem, 2006. 78(1): p. 125-34.

32. Berkelman, T. and T. Stenstedt, *2-D electrophoresis using immobilized pH gradients: principles and methods*, 2002, Amersham Bioscences.

33. Canas, B., *et al.*, *Mass spectrometry technologies for proteomics.* Brief Funct Genomic Proteomic, 2006. 4(4): p. 295-320.

34. Dass, C., *Modes of ionization*, in *Fundamentals of contemporary mass spectrometry*. 2007, Wiley. p. 15-65.

35. de Hoffmann, E. and V. Stroobant, *Ion sources*, in *Mass spectrometry. Principles and applications*. 2007, Wiley. p. 15-83.

36. Karas, M. and R. Kruger, *Ion formation in MALDI: the cluster ionization mechanism.* Chem Rev, 2003. 103(2): p. 427-40.

37. Knochenmuss, R., *Ion formation mechanisms in UV-MALDI.* Analyst, 2006. 131(9): p. 966-86.

38. Padliya, N.D. and T.D. Wood, *Improved peptide mass fingerprinting matches via optimized sample preparation in MALDI mass spectrometry.* Anal Chim Acta, 2008. 627(1): p. 162-8.

39. Cohen, S.L. and B.T. Chait, *Influence of matrix solution conditions on the MALDI-MS analysis of peptides and proteins.* Anal Chem, 1996. 68(1): p. 31-7.

40. Kebarle, P. and U.H. Verkerk, *Electrospray: from ions in solution to ions in the gas phase, what we know now.* Mass Spectrom Rev, 2009. 28(6): p. 898-917.

41. Wilm, M., *Principles of electrospray ionization.* Mol Cell Proteomics, 2011. 10(7): p. M111 009407.

42. Westman-Brinkmalm, A. and G. Brinkmalm, *A mass spectrometer's building blocks*, in *Mass spectrometry. Instrumentation, interpretation and applications*, R. Ekman, et al., Editors. 2009, Wiley. p. 15-87.

43. Dass, C., *Mass analysis and ion detection*, in *Fundamentals of contemporary mass spectrometry*. 2007, Wiley. p. 67-117.

44. de Hoffmann, E. and V. Stroobant, *Mass analysers*, in *Mass spectrometry. Principles and applications*. 2007, Wiley. p. 85-173.

45. Thiede, B., *et al.*, *Peptide mass fingerprinting.* Methods, 2005. 35(3): p. 237-47.

46. Rubakhin, S.S. and J.V. Sweedler, *A mass spectrometry primer for mass spectrometry imaging*, in *Mass spectrometry imaging. Principles and protocols*. 2010, Humana Press. p. 21-49.

47. Hopfgartner, G., *et al.*, *Triple quadrupole linear ion trap mass spectrometer for the analysis of small molecules and macromolecules.* J Mass Spectrom, 2004. 39(8): p. 845-55.

48. Hu, Q., *et al.*, *The Orbitrap: a new mass spectrometer.* J Mass Spectrom, 2005. 40(4): p. 430-43.

49. Perry, R.H., R.G. Cooks, and R.J. Noll, *Orbitrap mass spectrometry: instrumentation, ion motion and applications.* Mass Spectrom Rev, 2008. 27(6): p. 661-99.

50. Dass, C., *Tandem mass spectrometry*, in *Fundamentals of contemporary mass spectrometry*. 2007, Wiley. p. 119-150.

51. de Hoffmann, E. and V. Stroobant, *Tandem mass spectrometry*, in *Mass spectrometry. Principles and applications*. 2007, Wiley. p. 189-215.

52. Domon, B. and R. Aebersold, *Mass spectrometry and protein analysis.* Science, 2006. 312(5771): p. 212-7.

53. Gerdes, J.S., *Diagnosis and management of bacterial infections in the neonate.* Pediatr Clin North Am, 2004. 51(4): p. 939-59, viii-ix.

54. Lever, A. and I. Mackenzie, *Sepsis: definition, epidemiology, and diagnosis.* BMJ, 2007. 335(7625): p. 879-83.

55. Volante, E., et al., *Early diagnosis of bacterial infection in the neonate.* J Matern Fetal Neonatal Med, 2004. 16 Suppl 2: p. 13-6.

56. Hornik, C.P., *et al.*, *Early and late onset sepsis in very-low-birth-weight infants from a large group of neonatal intensive care units.* Early Hum Dev, 2012. 88 Suppl 2: p. S69-74.

57. Hervey, M.B. Strader, and G.B. Hurst, *Comparison of digestion protocols for microgram quantities of enriched protein samples.* J Proteome Res, 2007. 6(8): p. 3054-61.

58. Wall, M.J., *et al.*, *Implications of partial tryptic digestion in organic-aqueous solvent systems for bottom-up proteome analysis.* Anal Chim Acta, 2011. 703(2): p. 194-203.

59. Paizs, B. and S. Suhai, *Fragmentation pathways of protonated peptides.* Mass Spectrom Rev, 2005. 24(4): p. 508-48.

60. Boyd, R. and A. Somogyi, *The mobile proton hypothesis in fragmentation of protonated peptides: a perspective.* J Am Soc Mass Spectrom, 2010. 21(8): p. 1275-8.

61. Wysocki, V.H., *et al.*, *Peptide fragmentation overview*, in *Principles of mass spectrometry applied to biomolecules*, J. Laskin and C. Lifshitz, Editors. 2006, Wiley-Interscience.

62. Liang, H.R., *et al.*, *Ionization enhancement in atmospheric pressure chemical ionization and suppression in electrospray ionization between target drugs and stable-isotope-labeled internal standards in quantitative liquid chromatography/tandem mass spectrometry.* Rapid Commun Mass Spectrom, 2003. 17(24): p. 2815-21.

63. Wysocki, V.H., *et al.*, *Mass spectrometry of peptides and proteins.* Methods, 2005. 35(3): p. 211-22.

64. CHMP, *Guideline on bioanalytical method validation*, 2011, European Medicines Agency.